

AD-A067 177

SYSTEMS TECHNOLOGY INC HAWTHORNE CALIF

F/G 1/3

ANALYSIS OF DIGITAL FLIGHT CONTROL SYSTEMS WITH FLYING QUALITIE--ETC(U)

SEP 78 R F WHITBECK, L G HOFMANN

F33615-77-C-3026

UNCLASSIFIED

STI-TR-1101-1-VOL-2

AFFDL-TR-78-115-VOL-2

NL

1 OF 3

AD
A067177



7

AFFDL-TR-78-115
Volume II

LEVEL

4066809

1

AFFDL-TR-78-115

AD A0 671 77

ANALYSIS OF DIGITAL FLIGHT CONTROL SYSTEMS WITH FLYING QUALITIES APPLICATIONS

Volume II — Technical Report

RICHARD F. WHITBECK

L. G. HOFMANN

SYSTEMS TECHNOLOGY, INC.
HAWTHORNE, CALIFORNIA 90250

DDC
RECEIVED
APR 10 1979
C

SEPTEMBER 1978

TECHNICAL REPORT AFFDL-TR-78-115, Volume II
Final Report — March 1977 - September 1978 Jun 78

Approved for public release; distribution unlimited.

AIR FORCE FLIGHT DYNAMICS LABORATORY
AIR FORCE WRIGHT AERONAUTICAL LABORATORIES
AIR FORCE SYSTEMS COMMAND
WRIGHT-PATTERSON AIR FORCE BASE, OHIO 45433

79 04 05 05 4

ANALYSIS OF DIGITAL FLIGHT CONTROL SYSTEMS
WITH FLYING QUALITIES APPLICATIONS

DDC FILE COPY

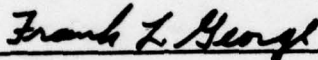
R. F. WHITBECK
L. G. HOFMANN

NOTICE

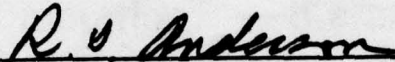
When Government drawings, specifications, or other data are used for any purpose other than in connection with a definitely related Government procurement operation, the United States Government thereby incurs no responsibility nor any obligation whatsoever; and the fact that the government may have formulated, furnished, or in any way supplied the said drawings, specifications, or other data, is not to be regarded by implication or otherwise as in any manner licensing the holder or any other person or corporation, or conveying any rights or permission to manufacture, use, or sell any patented invention that may in any way be related thereto.

This report has been reviewed by the Information Office (OI) and is releasable to the National Technical Information Service (NTIS). At NTIS, it will be available to the general public, including foreign nations.

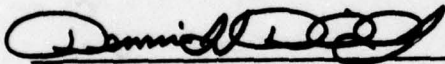
This technical report has been reviewed and is approved for publication.



Frank L. George, Project Engineer
Control Dynamics Branch
Flight Control Division

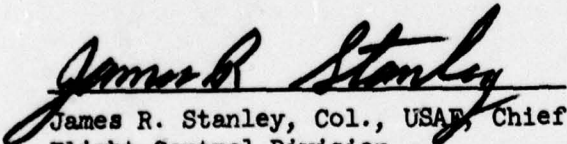


R. O. Anderson, Chief
Control Dynamics Branch
Flight Control Division



Dennis G. J. Didaleusky, Capt., USAF
Project Engineer
Control Dynamics Branch
Flight Control Division

FOR THE COMMANDER



James R. Stanley, Col., USAF, Chief
Flight Control Division

"If your address has changed, if you wish to be removed from our mailing list, or if the addressee is no longer employed by your organization please notify AFFDL/FGC, WPAFB, OH 45433 to help us maintain a current mailing list."

Copies of this report should not be returned unless return is required by security considerations, contractual obligations, or notice on a specific document.

Unclassified

SECURITY CLASSIFICATION OF THIS PAGE (When Data Entered)

REPORT DOCUMENTATION PAGE		READ INSTRUCTIONS BEFORE COMPLETING FORM
1. REPORT NUMBER (18) AFFDL-TR-78-115, Volume II	2. GOVT ACCESSION NO. (19) TR-78-425-VOL-2	3. REPORTING CATALOG NUMBER
4. TITLE (and Subtitle) (6) ANALYSIS OF DIGITAL FLIGHT CONTROL SYSTEMS WITH FLYING QUALITIES APPLICATIONS Volume II: Technical Report	5. TYPE OF REPORT & PERIOD COVERED (9) Final Report, Mar 77-Jun 78	
7. AUTHOR(s) R. F. Whitbeck L. G. Hofmann	6. PERFORMING ORG. REPORT NUMBER TR-1101-1	8. CONTRACT OR GRANT NUMBER(s) (15) F33615-77-C-3026
9. PERFORMING ORGANIZATION NAME AND ADDRESS Systems Technology, Inc. 13766 South Hawthorne Boulevard Hawthorne, California 90250 340 425	10. PROGRAM ELEMENT, PROJECT, TASK AREA & WORK UNIT NUMBERS Program Element 61102F, Project 2307, Mechanics, Task 03, Flight Control Res.	
11. CONTROLLING OFFICE NAME AND ADDRESS Air Force Flight Dynamics Laboratory Air Force Systems Command Wright-Patterson Air Force Base, Ohio 45433	12. REPORT DATE (10) September 1978	
14. MONITORING AGENCY NAME & ADDRESS (if different from Controlling Office) (14) STI-TR-77-01-1-VOL-2	13. NUMBER OF PAGES	
16. DISTRIBUTION STATEMENT (of this Report) Approved for public release; distribution unlimited. (16) 2307 (17) 03	15. SECURITY CLASS. (of this report) Unclassified	
15a. DECLASSIFICATION/DOWNGRADING SCHEDULE		
17. DISTRIBUTION STATEMENT (of the abstract entered in Block 20, if different from Report)		
18. SUPPLEMENTARY NOTES (10) Richard F. Whitbeck L. G. Hofmann	DDC RECEIVED APR 10 1979 C	
19. KEY WORDS (Continue on reverse side if necessary and identify by block number)		
Digital Control Systems	Frequency Response	Inter-Sample Ripple
Sampled Data	Switch Decomposition	Computational Delays
z-Transforms	Closed-Loop Systems	Flying Qualities
w-Domain	Linear Systems	Tustin Transform
Multi-Rate Sampling	Data Holds	Alias Response
Servo Analysis	Closed-Loop Analysis	Root Locus
20. ABSTRACT (Continue on reverse side if necessary and identify by block number)		
<p>Revisitation and extension of classical sampled data approaches for the analysis of discretely controlled continuous systems is the focus of this report. A review of basic linear analysis topics required to support later developments is given. These topics include Laplace, z- and advanced z-transform facts; partial fraction expansion; data holds and the switch decomposition technique. Extension of switch decomposition for the vector signal case is given. → next page (Continued)</p>		

DD FORM 1 JAN 73 1473

EDITION OF 1 NOV 65 IS OBSOLETE

Unclassified

SECURITY CLASSIFICATION OF THIS PAGE (When Data Entered)

340 425

alt

Unclassified

SECURITY CLASSIFICATION OF THIS PAGE(When Data Entered)

20. ABSTRACT (Continued)

cont. The w' -domain is defined by a bilinear transformation of the z -domain. Properties of the w' -domain are developed. It is demonstrated that all analysis and synthesis techniques of the frequency and s -domains carry over directly for the w' -domain. This is with the one exception that the imaginary axis of the w' -plane is in terms of $(2/T) \tan (\omega T/2)$ rather than angular frequency, ω , as in the s -plane. (T is the sampling period.) Effects of sampling rate and data hold and algorithm-induced delays are readily assessed in the w' -domain.

→ A new direct transform domain approach for analyzing two-rate sampled systems is developed. This approach also applies for multi-rate sampled systems in restricted circumstances. Utility of this approach resides in its operator notation and conventions for manipulation in connection with vector block diagram algebra. This, in turn, expedites development of pulse transfer functions and of response recursion relations for multivariable, closed-loop systems. This is accomplished without resorting to the more complicated switch decomposition method.

→ Multi-rate sampling analysis procedures are used to sharpen the concept of "frequency response" for discretely excited, continuous systems. Frequency response, in this case, pertains to steady-state responses at the input frequency and its positive aliases. Simple expressions are developed for computing the amplitude ratios and phase angles as a function of these frequencies. Results are presented in terms of the familiar Bode plot. This Bode plot must be interpreted in a novel way, however. Similar expressions, appropriate for interpreting "frequency response" data obtained from sampled records of continuous responses, are also developed. These frequency response methods apply for analysis of both open-loop and closed-loop discretely controlled continuous system responses, and are useful for assessing intersample ripple effects.

→ All methods of analysis presented in this report are closed-form and exact in that no approximation is required in the mathematical development of any result.

Unclassified

SECURITY CLASSIFICATION OF THIS PAGE(When Data Entered)

FOREWORD

The research described in this report was performed by Systems Technology, Inc., Hawthorne, California, under Air Force Contract F33615-77-C-3026. The AFFDL Task Number 03, Flight Control Research, was under Project Number 2307, Mechanics. This work was directed by the Control Criteria Branch, Flight Control Division, Air Force Flight Dynamics Laboratory, Air Force Systems Command, Wright-Patterson Air Force Base, Ohio. The work was administered by Frank L. George and Capt. Dennis G. J. Didaleusky.

Richard F. Whitbeck was the Systems Technology, Inc., Project Engineer under the direction of Duane McRuer. The Project Engineer was assisted by L. G. Hofmann.

The authors wish to express their appreciation to the Systems Technology publication staff for their efforts in preparing both this lengthy report and the notes for the short course (based on the material herein) given at WPAFB in June 1978.

The authors also wish to express their thanks to Mr. George for his appreciable efforts on this program. Captain Didaleusky's considerable facility with the technical concepts set forth in this report provided a significant impetus to the overall effort. In addition, he has authored Subsection V.K and Appendix G.

This report covers work performed from March 1977 through June 1978. The report was submitted by the authors in October 1978.

ACCESS		
NTIS	Version	<input checked="" type="checkbox"/>
DOC	Dist. Section	<input type="checkbox"/>
UNANNOUNCED		<input type="checkbox"/>
JUSTIFICATION		
BY		
DISTRIBUTION/AVAILABILITY CODES		
Dist. Avail. and/or SPECIAL		
A		

TABLE OF CONTENTS

SECTION	PAGE
I. INTRODUCTION	1
II. MATHEMATICAL PRELIMINARIES.	6
A. Problem Scope	6
B. s-Domain Preliminaries	6
C. z-Domain Preliminaries	16
D. Pulse Transfer Functions and Data Holds	20
E. An Introduction to Multi-Rate Sampling	24
F. Slow Input/Fast Output Sampling with Data Hold	29
G. Fast Input/Slow Output Sampling	31
H. Vector Block Diagrams	34
I. Switch Decomposition Concept	37
J. Vector Switch Decomposition	38
K. Advanced z-Transforms	46
L. A Comparison of Vector Switch Decomposition and the Phantom Sampler	48
M. Section Summary	55
III. ANALYSIS IN THE w' -DOMAIN	56
A. Introduction	56
B. Relationships Between z , w , and w'	57
C. Illustrative Design Problem — Short-Period Aircraft Model	63
D. Short-Period Aircraft with Bending Mode	70
E. Section Summary	76
IV. MULTI-RATE TRANSFORM DOMAIN APPROACH	77
A. Introduction	77
B. Use of Zero-Order Holds as Couplers	79
C. Multi-Rate Formulation	84
D. A Closed-Loop Multi-Rate Application	86
E. The Slew Rate Data Hold	88
F. Illustrative Example	93
G. A Motivating Example	96
H. Section Summary	98

SECTION	PAGE
V. FREQUENCY RESPONSE OF A DIGITALLY CONTROLLED CONTINUOUS SYSTEM	99
A. Introduction	99
B. Continuous System Bode Plots	100
C. Mathematical Preliminaries	101
D. Open-Loop Frequency Response — Finite N	104
E. Open-Loop Frequency Response — Continuous Output	111
F. Input Signal with Phase Shift	115
G. Single-Rate Closed-Loop Frequency Response	115
H. The "Motivating" Example Revisited	119
I. A Particular Multi-Rate Configuration	124
J. A Fast Inner-Loop, Slow Outer-Loop Problem	131
K. General Results	142
L. Section Summary	146
VI. FLYING QUALITIES APPLICATIONS	151
A. Introduction	151
B. Tactical Fighter — Analog Controller	153
C. Tactical Fighter — Digital Controller	157
D. Lower-Order Models	164
E. Control Roughness	164
F. Section Summary	164
VII. SUMMARY, CONCLUSIONS, AND RECOMMENDATIONS	166
A. Summary and Conclusions	166
B. Recommendations	168
REFERENCES	169
APPENDICES	
A. Properties of the Laplace Transform	171
B. The Pulse Transfer Function	186
C. Illustrative Example — Methods for Finding the Continuous Responses of Discretely Excited Systems	194
D. Partial Fraction Coefficients for Second-Order Real Poles	204
E. Sine Wave Input of Arbitrary Phase	207

APPENDICES (Continued)

PAGE

F. Non-Synchronous Sampling	210
G. Conversion from Analog to Discrete State Equations	212
H. A Particular Design Procedure	215
I. The Limiting Form for a Particular Example	216

LIST OF FIGURES

FIGURE	PAGE
1. Correspondence Between Transfer Function and Pulse Transfer Function	20
2. Typical Data Hold Configuration	22
3. Slow Input/Fast Output Sampling	25
4. Equivalent Model for Fig. 3	25
5. Step Response	28
6. Slow Input/Fast Output Sampling with Data Hold	29
7. Fast Input/Slow Output Sampling	31
8. Equivalent System	31
9. Simple Closed-Loop Configuration	35
10. A Representative Closed-Loop System	36
11. Decomposition of a Sample Sequence	39
12. Vector Block Diagrams for Multi-Rate Sampling Operations	43
13. A Multi-Rate Closed-Loop System	44
14. A Scalar Two-Rate Example	45
15. Slow-Input/Fast-Output Sampling	50
16. Fast-Input/Slow-Output Sampling	50
17. Vector Switch Decomposition Model; Fast-Input/Slow-Output Sampling	51
18. Vector Switch Decomposition; Slow-Input/Fast-Output Sampling	51
19. Illustrative Example	53
20. Block Diagram, Illustrative Example	64
21. Digital Control Block Diagram	67
22. Bode Plots q/a_g , q/R	72
23. Bode Plots a/a_g , a/R	73

FIGURE	PAGE
24. Bode Plots x_b/a_g , x_b/R	74
25. q Transient Responses of Continuous and Digitally Controlled Systems	75
26. A Basic Multi-Rate Configuration	77
27. Zero-Order Hold Case	79
28. Response to a Cosine Wave Input	84
29. An Open-Loop Multi-Rate System	85
30. Multi-Rate Example	86
31. Transient Response, Cosine Wave Input	87
32. Impulse Response of Triangular Data Hold	88
33. Reconstruction Via the Slewler	89
34. Slewler Sampling Logic	92
35. Comparison Between Slewler and ZOH	95
36. A Closed-Loop Single-Rate System	96
37. Closed-Loop Step Responses	98
38. Continuous System	100
39. Open-Loop Case	104
40. Magnitude Plot for $N = 1, 2, 4$	108
41. Two Continuous Sine Waves which Match the Sample Points	109
42. Frequency Response and Spectral Components of Output	113
43. "Steady-State" Transient Response	114
44. A More Complex Case	114
45. Illustrative Vector Closed-Loop Configuration	116
46. Closed-Loop Step Response	119
47. Magnitude Plot for Single-Rate Closed-Loop System	120
48. Transient Response, $a = 10$, ZOH, $\sin(\pi/2)t$ Input	121

FIGURE	PAGE
49. Steady-State Sinusoidal Components, $N = 1$	121
50. Steady-State Sinusoidal Components, $N = 2$	122
51. Steady-State Sinusoidal Components, $N = 10$, Half Period	123
52. A Specific Two-Rate Closed-Loop Configuration	125
53. Magnitude Plot $T/4$, T , Closed-Loop System	132
54. Magnitude Plot T , Closed-Loop System	132
55. Fast Inner-Loop, Slow Outer-Loop Example	133
56. Bode Plot for Illustrative Example	141
57. FCS Loop Closure for Typical Fighter Aircraft in Power Approach	155
58. Comparison of Augmented and Effective Short-Period Roots (Pitch Rate FCS)	156
59. Comparison of Exact and Effective Time Responses	156
60. Digital Implementation of FCS for Tactical Fighter	158
61. Digital FCS Timing Diagram	158
62. Model of a Non-Synchronous Sampling Operation	158
63. Fighter Attitude Dynamics (Digital Controller)	163
A-1. A Periodic Function	177
A-2. The Dirac Delta Comb Function.	179
A-3. Product of e^{-at} with Comb Function	181
A-4. Representation of Impulse Modulation	182
A-5. The Complex p Plane	183
B-1. An Open-Loop Two-Rate System	186
C-1. Illustrative Example.	195
C-2. Illustrative Example Relabeled	197
E-1. Open-Loop System	207

FIGURE	PAGE
F-1. A Set of Non-Synchronously Sampled Signals	210
F-2. Sampling Notation.	211
F-3. Advance, Sample, Delay	211

LIST OF TABLES

TABLE	PAGE
1. An Abbreviated Transform Table	10
2. An Abbreviated Table, $F(z)$ Added	21
3. Some Representative Data Holds	24
4. Transform Table	49
5. Representative s , z , and w' Plane Transfer Functions	62
6. Compensation Networks	97
7. Component Coefficients $N = 1, 2, 4$	124
8. An Open-Loop Configuration	147
9. A Single-Rate Closed-Loop Configuration	148
10. A Particular Multi-Rate Configuration	149
11. A Fast Inner-Loop, Slow Outer-Loop Configuration	150
12. Coefficients of $(GME^{-sT_0})^T$	160
C-1. Discrete Transient Response.	200
C-2. Continuous Response	201
C-3. Continuous Response — "Jumping Ahead"	202

SECTION I

INTRODUCTION

Widening flight envelopes coupled with increasingly stringent operational demands on military aircraft have forced the use of more complex stability and control augmentation systems. It is recognized (Refs. 1 and 2) that this trend has created problems in interpreting the applicable military specification for the flying qualities of piloted aircraft, MIL-F-8785B(ASG) (Ref. 3). For example, Section 3.2.2.1, which relates to the short-period response, makes no provision for the dynamics of the aircraft plus flight control system (FCS) if these are different in dynamic form from those for an unaugmented aircraft. The specification assumes, in essence, that the longitudinal dynamic response will have only two modes (phugoid and short period) in the low and mid frequency regions, when in practice there may be additional significant modes in these frequency regions due to equalization of the FCS feedbacks. Because of these additional modes, an augmented aircraft may appear quite different to the pilot than an unaugmented aircraft which appears to have the same short-period dynamics (Ref. 4). That is, it may develop that the short-period mode characteristics meet the specification and yet the aircraft actually responds as if it had short-period characteristics which do not meet the specification. This opens the possibility that it will receive low ratings from evaluation pilots.

How should this situation be treated? Are new requirements needed which account directly for the additional dynamics, or is it possible to develop lower-order mathematical models of the higher-order system that can be reliably compared against the MIL-F-8785 requirements as presently stated? Moreover, the criteria of MIL-F-8785 presume an analog augmentation system. There is now an additional concern for response characteristics which are unique to use of digital augmentation systems. It is the purpose of this study to identify those characteristics which are unique to the digitally controlled system, and to review the quantitative tools

available which permit an assessment of the effects of these unique characteristics relative to the MIL-F-8785 requirements. The larger issue of what additional flying qualities criteria are required is outside the scope of this research.

The results of this study indicate that two important characteristics are introduced by digital control laws. They are:

- The effective delay introduced by the A/D and D/A process and the delay introduced by the digital algorithms and computational frame time of the computer cycle.
- The "control roughness" or inter-sample ripple introduced when the digital computer is coupled to the control actuators using data holds.

The first characteristic is of great concern to the flying qualities community since even relatively small delays are potentially important in certain closed-loop piloting tasks involving motion cues and pilot-induced oscillation possibilities. Measures of the effective time delay introduced by the A/D, computation, D/A conversion process can be computed using a variety of analytical techniques that apply at the sampling instants. For example, w' -, w -, or z -domain analyses and discrete frequency response techniques can be applied effectively to obtain both a quantitative and qualitative evaluation of the delay introduced.

The second characteristic is of concern since aircraft response resulting from control roughness is in effect an additional disturbance source. Moreover, the step-like control deflections caused by the use of zero-order data holds can produce excessive actuator wear and fatigue damage, reducing service life and/or reliability of the aircraft system. This second characteristic is more difficult to assess since it involves the response of the continuous system during the inter-sample interval. Therefore, analysis tools such as the "sampled spectrum" (sampled frequency response) are of little value. It is this observation which prompted the development, during this study, of a basic analysis tool for computing the spectral content of the continuous responses of a discretely controlled system. We are tempted to describe this method of analysis as "frequency

response" evaluation since it applies equally for continuously controlled systems as well as multi-rate discretely controlled systems. However, this must be further qualified. This is necessary because of possible confusion with the concept of the "sampled spectrum." In computing the sampled spectrum one finds the lowest frequency sine wave that fits the sampled response at the sampling instants. The sampled spectrum is commonly, but incorrectly, understood to be the frequency response of a discretely controlled system. For this reason it is preferable to describe the new method more precisely as the "continuous frequency response of a discretely excited system." Once a method is in hand for computing the spectral content of the continuous response, then one has the means for assessing both of the digital characteristics discussed above. The frequency response magnitude data can be used to quantify control roughness, while the phase data can be used to quantify the effective time delay.

There is another main objective of this study effort — that of giving the practicing engineer working familiarity with three analytical tools we consider to be well suited for the analysis of digitally controlled systems:

- 1) Analysis (and synthesis) in the w' -domain.
- 2) Multi-rate transform domain approaches.
- 3) The continuous frequency response of a discretely excited system.

The w' -domain is related to the well-known w -domain by a scalar transformation and to the z -domain by a bilinear algebraic transformation. We believe that those engineers skilled in frequency domain design procedures will immediately feel at home with analysis in the w' -domain, since all analog control system design technology transfers completely for digital control system design.

The second item deals with a multi-rate transform domain approach that has been developed into an effective tool for analyzing the transient inter-sample response of discretely excited systems. That is, it yields recursion equations describing the inter-sample performance to any degree of fineness desired without increasing computer storage requirements. A basic understanding of this approach leads to the development of the third tool

which gives the continuous spectrum of a discretely controlled system. It is this third tool which we perceive as being of the greatest value to those engineers working at the flying qualities, digital flight control system interface.

In Section II, we will first review the fundamentals of sampled data control theory to the extent necessary to "refamiliarize" the engineer with its terminology and background mathematics. No proofs will be given; we will simply state results and give illustrative examples to demonstrate viewpoints which will be needed at a later point in order to develop an understanding of the three analytical tools mentioned above. This section will also serve to introduce a multi-rate terminology and give the reader a chance to gain familiarity with the notation (always a crucial factor in how easily a report reads).

Section III is devoted to modest extensions of classical analysis and synthesis techniques for digitally controlled systems. Emphasis is upon analyses conducted in the w' -domain. The w' -domain offers the advantage that non-minimum phase effects of the sampling and data-hold operations and of sampling rate can be directly accounted for without approximation while using conventional frequency domain design tools such as root locus and Bode plots. These conventional frequency domain design tools can be used to considerably greater advantage in the w' -domain than in the w - and z -domain, because several more powerful analogies between the s -domain and the w' -domain exist. These analogies are, in a sense, the key to exploiting the w' -domain for design purposes, making direct design in the w' -domain more attractive than either optimal procedures or the numerous approximate methods. First, the basic properties which make the w' -domain preferable to the z -domain or w -domain are reviewed. Following this, illustrative examples are used to highlight the analogies between s and w' . Finally, we demonstrate the clear manner in which the nonminimum-phase effects of sampling, data-hold operations, and sample rate are evident in the w' -domain analyses.

Almost all existing or contemplated digital flight control systems are multi-rate in nature. The predominant reason for this is the necessity to work within the basic restrictions imposed by computer word length, memory

capacity, frame time, etc. Thus, it is typical, for example, to update inner loops at a faster rate than the "slower" outer loops.

A basic transform domain approach, the "T/N method," which eliminates a variety of dimensional and indexing problems associated with state transition (Ref. 5) and switch decomposition (e.g., see Refs. 6-8) methods, is developed in Section IV. The approach is very efficient for computing the response of discretely controlled continuous systems at both sampling instants and at equally spaced times during the inter-sample interval. The methods also requires a minimum of information to define the system for the computer program.*

The T/N method discussed in Section IV is used as a departure point in Section V to extend frequency response concepts to include the continuous frequency response of a discretely controlled system. The discrete frequency response concept (e.g., Ref. 7) has not been particularly productive for the analysis of discretely controlled systems, since it is limited to determining the amplitude and phase of the single sinusoid that fits the output samples of a single-rate system at the sampling instants. Development proceeds by first removing this restriction for open-loop systems and then extending the results to single-rate closed-loop systems. Finally, the solution for the multi-rate closed-loop case is developed using the results of Section IV.

Although each section contains a representative number of illustrative examples, an application pertinent to the flying qualities/flight control system interface is not taken up until Section VI.

Section VII contains the conclusions and recommendations. The appendices contain support material, much of which will be familiar to practicing engineers.

*But the computer program is somewhat restricted as to the form of the problem that can be accommodated.

SECTION II

MATHEMATICAL PRELIMINARIES

A. PROBLEM SCOPE

Systems governed by linear differential and difference equations with constant coefficients are reviewed. This is a framework which can adequately deal with aircraft nonlinear equations linearized about an operating point. In the treatment of discretely controlled systems, "impulsive" sampling operations are assumed. All developments will use vector notation, although scalar examples will be used frequently for illustrative purposes. In the interests of brevity we will, wherever possible, pursue the direct and remarkably effective methods of Aseltine (Ref. 9) in bringing the basic issues to the fore.

B. s-DOMAIN PRELIMINARIES

The partial fraction expansion table-lookup approach for transferring information from one domain to another will be used frequently in subsequent mathematical developments. Although this is a familiar topic, our viewpoint and approach is sufficiently different to warrant a careful review.

A main objective of this section is to produce a table of abbreviated transforms that will permit one to transfer between the t , s , z , and w domains in a relatively easy and straightforward manner.

We start by developing a transform table (from the time domain to the s -domain) using the Laplace transform of an exponential time function and several properties of the Laplace transform. We will then mimic this procedure in order to augment the table with z -transform and time-advanced z -transform entries.

To begin, compute $\mathcal{L}[e^{-at}]$:

$$\begin{aligned}\mathcal{L}[e^{-at}] &\triangleq \int_0^{\infty} e^{-at} e^{-st} dt = \int_0^{\infty} e^{-(s+a)t} dt \\ &= \left. \frac{e^{-(s+a)t}}{-(s+a)} \right|_0^{\infty} = \frac{1}{s+a}\end{aligned}$$

It is convenient to use the notation

$$e^{-at} \iff \frac{1}{s+a} \quad (1)$$

to indicate that e^{-at} corresponds to $1/(s+a)$ and vice versa. This transform pair, coupled with two other properties of Laplace transforms, provides the basic information needed to develop a table of transform pairs. The first (trivial) property is:

$$f_1(t) + kf_2(t) \iff F_1(s) + kF_2(s) \quad (2)$$

The second property of interest is:

$$tf(t) \iff -\frac{d}{ds} F(s) \quad (3)$$

Note further that "a" in Eq. 1 is a parameter which is not restricted to have real values. For example, let

$$a \rightarrow a + jb \quad (4)$$

in Eq. 1 and obtain

$$e^{-(a+jb)t} = e^{-at} [\cos bt - j \sin bt] \iff \frac{1}{(s+a) + jb} \quad (5)$$

Rationalize the right-hand side of Eq. 5 to obtain:

$$e^{-at} \cos bt - je^{-at} \sin bt \iff \frac{(s + a) - jb}{(s + a)^2 + b^2} \quad (6)$$

Using the property of Eq. 2 now gives two additional transform pairs (one for the damped cosine wave, the other a damped sine wave):

$$e^{-at} \cos bt \iff \frac{s + a}{(s + a)^2 + b^2} \quad (7)$$

$$e^{-at} \sin bt \iff \frac{b}{(s + a)^2 + b^2} \quad (8)$$

This approach for developing the table leads to a frequency domain description of a damped sine or cosine wave which describes the poles in terms of the wave damped natural frequency and an exponential damping envelope rather than damping ratio and undamped natural frequency. That is, the description is in terms of $[(s + a)^2 + b^2]$ rather than $[s^2 + 2\zeta\omega_0 s + \omega_0^2]$. For the purposes of this report, the form given in Eqs. 7 and 8 will prove more useful than the alternative description.

We may set $a = 0$ in Eqs. 7 and 8 to obtain the transform of sine and cosine waves.

$$\cos bt \iff \frac{s}{s^2 + b^2} \quad (9)$$

$$\sin bt \iff \frac{b}{s^2 + b^2} \quad (10)$$

To continue, setting $a = 0$ in Eq. 1 produces the transform pair for the unit step function.

$$u(t) \iff \frac{1}{s} \quad (11)$$

Applying the property given in Eq. 3 to Eq. 11 yields the transform pair for a ramp function:

$$t \iff -\frac{d}{ds} \left(\frac{1}{s} \right) = \frac{1}{s^2} \quad (12)$$

Repeat the application, this time to Eq. 12, and obtain the transform pair for t^2 :

$$t^2 \iff -\frac{d}{ds} \left(\frac{1}{s^2} \right) = \frac{2s}{s^4} = \frac{2}{s^3} \quad (13)$$

In a like manner, the application of this property to Eq. 1 gives:

$$te^{-at} \iff -\frac{d}{ds} \left(\frac{1}{s+a} \right) = \frac{1}{(s+a)^2} \quad (14)$$

By proceeding in this fashion we have now built up Table 1. This abbreviated table is sufficient for most of our needs since the occurrence of multiple poles in aircraft stability and control work is somewhat rare. Later we will use the same approach to develop a table of z-transforms. This will result in a third column for Table 1.

Consider next an efficient method for expanding a given rational polynomial function $F(s)$ in terms of the entries of Table 1. Since the entries of Table 1 constitute the set of elementary time functions of interest, it makes good sense to expand $F(s)$ in terms of these time functions. To illustrate, given the proper rational $F(s)$,

$$F(s) = \frac{3s^3 + 15s^2 + 35s + 13}{s^4 + 5s^3 + 17s^2 + 13s} \quad (15)$$

then it is convenient to expand the right-hand side in terms of partial fractions, viz.,

TABLE 1

AN ABBREVIATED TRANSFORM TABLE

$f(t)$	$F(s) = \mathcal{L}[f(t)]$
$u(t)$	$\frac{1}{s}$
t	$\frac{1}{s^2}$
t^2	$\frac{2}{s^3}$
e^{-at}	$\frac{1}{s + a}$
te^{-at}	$\frac{1}{(s + a)^2}$
$\sin bt$	$\frac{b}{s^2 + b^2}$
$\cos bt$	$\frac{s}{s^2 + b^2}$
$e^{-at} \sin bt$	$\frac{b}{(s + a)^2 + b^2}$
$e^{-at} \cos bt$	$\frac{s + a}{(s + a)^2 + b^2}$

$$F(s) = \frac{3s^3 + 15s^2 + 35s + 13}{(s)(s+1)(s^2+4s+13)} = \frac{A}{s} + \frac{B}{s+1} + \frac{C(s+2) + D(3)}{(s+2)^2 + (3)^2} \quad (16)$$

since

$$s^2 + 4s + 13 \equiv (s+2)^2 + (3)^2 \quad (17)$$

Once the partial fraction coefficients A, B, C, and D are known, the time function can be written immediately as:

$$f(t) = Au(t) + Be^{-t} + e^{-2t}(C \cos 3t + D \sin 3t) \quad (18)$$

There is a variety of ways to find A, B, C, and D. For example, multiply each side of Eq. 16 by s and let s = 0 to find A = 1. Next, multiply each side by (s + 1) and let s = -1 to find B = 1. Next, multiply each side of the equation by s and let s = ∞ to find out that A + B + C = 3, and therefore C = 1. Finally, pick any convenient value of s and evaluate Eq. 16 for the remaining unknown, D (D = 1 also). This approach is neat but not very general. We need a method better suited for machine computation. Such a method is described next.

Let F(s) be a proper rational function of the form

$$F(s) = \frac{N(s)}{D(s)} = \frac{A}{s+a} + \dots \quad (19)$$

with a simple pole, (s + a). Obviously,

$$A = \left. \frac{(s+a)N(s)}{D(s)} \right|_{s=-a} \quad (20)$$

However, if (s + a) is not explicitly factored out of the denominator, an indeterminate form will result when s is set equal to -a (0/0). To resolve

this difficulty, without explicitly dividing out $(s + a)$, use L'Hôpital's rule:

$$A = \frac{(s + a)N' + N}{D'(s)} \Big|_{s = -a} = \frac{N}{D'} \Big|_{s = -a} \quad (21)$$

where $D' = dD/ds$. Equation 21 treats all simple real poles and, since only polynomials are involved, is ideally suited to machine computation using "nesting procedures." Moreover, the same polynomials are used for all partial fraction coefficient evaluations involving simple roots.

Next, suppose $F(s)$ has a complex conjugate root at $s = -a + jb$. That is,

$$F(s) = \frac{N(s)}{D(s)} = \frac{Ab + B(s + a)}{(s + a)^2 + b^2} + \dots \quad (22)$$

Clearly,

$$[(s + a)^2 + b^2] \frac{N(s)}{D(s)} \Big|_{s = -a + jb} = Ab + jBb. \quad (23)$$

Again, an indeterminate form results if $[(s + a)^2 + b^2]$ is not explicitly divided out. L'Hôpital's rule permits one to avoid the division step:

$$\frac{2(s + a)N + [(s + a)^2 + b^2]N'(s)}{D'(s)} \Big|_{s = -a + jb} = Ab + jBb \quad (24)$$

or

$$\frac{2j\cancel{b}N}{D'} \Big|_{s = -a + jb} = A\cancel{b} + jB\cancel{b} \quad (25)$$

This simplifies to

$$B - jA = \left. \frac{2N}{D'} \right|_{s = -a+jb} \quad (26)$$

and clearly

$$B = 2 \operatorname{Re} \left. \frac{N}{D'} \right|_{s = -a+jb} \quad (27)$$

$$A = -2 \operatorname{Im} \left. \frac{N}{D'} \right|_{s = -a+jb} \quad (28)$$

Other expressions can be obtained for multiple roots. For example, if:

$$F(s) = \frac{N}{D} = \frac{A}{(s+a)^2} + \frac{B}{(s+a)} + \dots \quad (29)$$

One can show (see Appendix D):

$$A = \left. \frac{2N}{D''} \right|_{s = -a}, \quad B = \left. \frac{2N'}{D''} - \frac{AD'''}{3D''} \right|_{s = -a} \quad (30)$$

Some illustrative examples demonstrate the simplicity of the process.
First, let:

$$F(s) = \frac{3s^2 + 2s + 1}{s(s+1)^2} = \frac{3s^2 + 2s + 1}{s^3 + 2s^2 + s} \quad (31)$$

Therefore,

$$\frac{3s^2 + 2s + 1}{s^3 + 2s^2 + s} = \frac{A}{(s+1)^2} + \frac{B}{(s+1)} + \frac{C}{s} \quad (32)$$

Since $D' = 3s^2 + 4s + 1$ and $D'' = 6s + 4$, $D''' = 6$.

$$C = \left. \frac{N}{D'} \right|_{s=0} = 1 \quad (33)$$

$$A = \left. \frac{2N}{D''} \right|_{s=-1} = \left. \frac{2(3s^2 + 2s + 1)}{6s + 4} \right|_{s=-1} = \frac{2(2)}{-2} = -2 \quad (34)$$

and

$$B = \left. \frac{2N'}{D''} - \frac{AD'''}{3D''} \right|_{s=-1} = \left. \frac{2(6s + 2)}{6s + 4} \right|_{s=-1} - \frac{(-2)6}{(3)(6s + 4)} \bigg|_{s=-1} = 2 \quad (35)$$

As a second example,

$$F(s) = \frac{s^2 - 5}{s^3 + 3s^2 + 7s + 5} = \frac{s^2 - 5}{(s + 1)(s^2 + 2s + 5)} = \frac{s^2 - 5}{(s + 1)[(s + 1)^2 + (2)^2]} \quad (36)$$

$$= \frac{A}{s + 1} + \frac{B(2) + C(s + 1)}{(s + 1)^2 + (2)^2} \quad (37)$$

Since $D' = 3s^2 + 6s + 7$,

$$A = \left. \frac{N}{D'} \right|_{s=-1} = \left. \frac{s^2 - 5}{3s^2 + 6s + 7} \right|_{s=-1} = \frac{-4}{3 - 6 + 7} = -1 \quad (38)$$

and

$$C = 2 \operatorname{Re} \left. \frac{s^2 - 5}{(3s + 6)s + 7} \right|_{s=-1+j2} = 2 \quad (39)$$

$$B = -2 \operatorname{Im} \left. \frac{s^2 - 5}{(3s + 6)s + 7} \right|_{s=-1+j2} = -1 \quad (40)$$

Those readers with pocket calculators having rectangular to polar conversion features will have little problem in verifying the coefficient values for C and B.

Thus far we have dealt only with "proper" rational functions wherein the order of the numerator polynomials is at least one order less than the denominator polynomials. In the event $F(s)$ is not proper, it can be converted (using synthetic division) into two parts — the first is a polynomial in s , the second part a proper rational function. For example,

$$F(s) = \frac{s^4 + 3s^3 + 5s^2 + 5s + 4}{s^2 + 2s + 2} = s^2 + s + 1 + \frac{s + 2}{(s + 1)^2 + (1)^2} \quad (41)$$

Therefore,

$$f(t) = \delta''(t) + \delta'(t) + \delta(t) + e^{-t}[\sin t + \cos t] \quad (42)$$

We assume the reader is familiar with Laplace transform of impulse functions to the extent that $\delta(t)$ is recognized as an impulse in time, $\delta(t)$; s is recognized as a "doublet," $\delta'(t)$; and s^2 is recognized as a "triplet," $\delta''(t)$.

Before proceeding to the development of a table of z-transforms (in the next section), we pause to review the concept of the system transfer function. Given

$$f(t) \Leftrightarrow F(s) \quad (43)$$

we presume familiarity with the transform pair (or refer to Appendix A)

$$\frac{df(t)}{dt} \Leftrightarrow sF(s) - f(0) \quad (44)$$

which, through repeated application, enables us to transform the differential system

$$\ddot{x} + 2\dot{x} + 2x = f(t) \quad (45)$$

in time to an algebraic system in s :

$$\overbrace{[s^2 + 2s + 2]}^A \overbrace{X(s)}^B = \overbrace{[F(s) + 2x(0) + sx(0) + \dot{x}(0)]}^C \quad (46)$$

This equation highlights three basic parts characteristic of all linear systems:

- A: The part related to the system
- B: The part related to the response
- C The part related to the input and initial conditions

Dividing through by Part A gives

$$X(s) = \frac{F(s)}{s^2 + 2s + 2} + \frac{(s + 2)x(0)}{s^2 + 2s + 2} + \frac{\dot{x}(0)}{s^2 + 2s + 2} \quad (47)$$

or

$$X(s) = W_1(s)F(s) + W_2(s)x(0) + W_3(s)\dot{x}(0) \quad (48)$$

W_1 , W_2 , and W_3 are the "transfer functions" (or system functions) which relate the transforms of the output components to the transform of the input components. For example, let the initial conditions $x(0)$ and $\dot{x}(0)$ be zero. Then $W_1(s)$ can be written as:

$$W_1 = \frac{\mathcal{L}[x(t)]}{\mathcal{L}[f(t)]} = \frac{X(s)}{F(s)} \quad (49)$$

It is in this sense that transfer functions characterize the system independently of the input. The Laplace transform of the system time response, on the other hand, can always be expressed as a sum of products of system transfer functions with the Laplace transforms of the various corresponding input time functions and initial conditions.

C. z-DOMAIN PRELIMINARIES

An abbreviated table of transforms was built up in the previous section, starting with an exponential transform pair. Here a similar approach is taken with z-transform pairs. Let $z \triangleq e^{sT}$ for the purpose of constructing

this table. Then the following equation may be regarded as the definition of the z-transform:

$$f^T(t) = f(0)\delta_+(t) + f(T)\delta_+(t-T) + f(2T)\delta_+(t-2T) + \dots \quad (50)$$

The Laplace transform for delayed time functions (refer to Appendix A) can be used to transform Eq. 50 into the frequency domain.

$$F^T(s) = F^*(s) = \sum_{n=0}^{\infty} f(nT)e^{-snT} = \sum_{n=0}^{\infty} f(nT)z^{-n} = F(z) \quad (51)$$

where $z = e^{sT}$.

Some comments on notation are in order. We use $f^T(t) \Leftrightarrow F^T(s)$ to denote that the time function $f(t)$ is sampled at $1/T$ samples per second. $F^T(s)$ denotes the Laplace transform of the sampled continuous time function, given that the continuous time function has the transform $F(s)$. While the traditional notation for $F^T(s)$, which is $F^*(s)$, is perhaps better established, we have elected to use the superscript notation because it permits an explicit statement of the sampling rates involved in multi-rate systems (the main concern of this report). This point is discussed further in Appendix B.

Let us now proceed to develop an abbreviated table of z-transforms. Let $f(t) = e^{-at}$, so that Eq. 51 becomes

$$f^T(t) \Leftrightarrow F(z) = \sum_{n=0}^{\infty} e^{-anT} z^{-n} \quad (52)$$

$$= 1 + e^{-aT} z^{-1} + e^{-2aT} z^{-2} + \dots$$

$$\equiv 1 + \left(\frac{e^{-aT}}{z}\right) + \left(\frac{e^{-aT}}{z}\right)^2 + \dots$$

$$= \frac{1}{1 - (e^{-aT}/z)} \Leftrightarrow \frac{z}{z - e^{-aT}} \quad (53)$$

We now know that this continuous time function sampled at $1/T$ samples/second gives the transform pair

$$(e^{-at})^T \Leftrightarrow \frac{z}{z - e^{-aT}} \quad (54)$$

Just as in the case of the Laplace transform we can let "a" take on convenient complex values. For example, let $a \rightarrow a + jb$,

$$[e^{-(a+jb)t}]^T \Leftrightarrow \frac{z}{z - e^{-aT} e^{-jbT}} \quad (55)$$

or

$$(e^{-at} \cos bt - j e^{-at} \sin bt)^T \Leftrightarrow \frac{z}{z - e^{-aT} (\cos bT - j \sin bT)} \quad (56)$$

Rationalization of the right-hand side of Eq. 56 results in:

$$(e^{-at} \cos bt - j e^{-at} \sin bt)^T \Leftrightarrow \frac{z(z - e^{-aT} \cos bT) - j z e^{-aT} \sin bT}{(z - e^{-aT} \cos bT)^2 + (e^{-aT} \sin bT)^2}$$

Therefore

$$(e^{-at} \cos bt)^T \Leftrightarrow \frac{z(z - e^{-aT} \cos bT)}{z^2 - 2e^{-aT} \cos bTz + e^{-2aT}} \quad (57)$$

and

$$(e^{-aT} \sin bT)^T \Leftrightarrow \frac{z e^{-aT} \sin bT}{z^2 - 2e^{-aT} \cos bTz + e^{-2aT}} \quad (58)$$

We now have the transform for the sampled damped sine and cosine pair. Continuing, let $a = 0$ in Eqs. 57 and 58 to obtain the transform for sampled sine wave and cosine waves.

$$(\cos bt)^T \Leftrightarrow \frac{z(z - \cos bT)}{z^2 - 2 \cos bTz + 1} \quad (59)$$

$$(\sin bt)^T \Leftrightarrow \frac{z \sin bT}{z^2 - 2 \cos bTz + 1} \quad (60)$$

Further, let $a = 0$ in Eq. 54 to obtain the z -transform for a sampled-unit step.

$$\left(e^{-at} \Big|_{a \rightarrow 0} \right)^T = [u(t)]^T \Leftrightarrow \frac{z}{z - 1} \quad (61)$$

To complete the table, first find the transform of $tf(t)$:

$$\begin{aligned} [tf(t)]^T &\equiv [nTf(nT)] \Leftrightarrow \sum_{n=0}^{\infty} (nT)f(nT)z^{-n} \\ &= -zT \sum_{n=0}^{\infty} f(nT) [-(n)z^{(-n-1)}] \end{aligned}$$

We recognize the term in brackets as the derivative of z^{-n} with respect to z . Therefore:

$$[tf(t)]^T \Leftrightarrow -zT \frac{d}{dz} \sum_{n=0}^{\infty} f(nT)z^{-n} = -zT \frac{d}{dz} F(z) \quad (62)$$

Equation 62 is completely analogous to the s -domain result (Eq. 3). With it, we can complete our abbreviated table of z -transforms, since

$$\begin{aligned} [te^{-at}]^T &= -zT \frac{d}{dz} \left(\frac{z}{z - e^{-aT}} \right) \\ &= -zT \frac{z - e^{-aT} - z}{(z - e^{-aT})^2} = \frac{zTe^{-aT}}{(z - e^{-aT})^2} \end{aligned} \quad (63)$$

Setting $a = 0$, the z -transform of a ramp is obtained:

$$[t]^T = \frac{Tz}{(z-1)^2} \quad (64)$$

We may now complete Table 2, showing the relationship between time and the s - and z -domains. Strictly speaking there should be a " $f(nT)$ " column as well, but the manner in which the table is presented is sufficient. It forces us to remember that $f(nT)$ can be thought of as the continuous $f(t)$ sampled at intervals of T seconds starting at $t = 0$.

Given an $F(z)$, one can expand in partial fractions in exactly the same manner as was done for $F(s)$. We will defer demonstrating the process until the additional considerations introduced by data holds have been reviewed.

D. PULSE TRANSFER FUNCTIONS AND DATA HOLDS

The correspondence between a given $F(s)$ and the associated $F(z)$ from the transform table is depicted in Fig. 1 from the transfer function point of view. From Fig. 1 and the results of Appendix B:

$$C(z) = \left[C^T(s) \right]_{z=e^{sT}} = \left[G^T(s) R^T(s) \right]_{z=e^{sT}} = G(z) R(z) \quad (65)$$

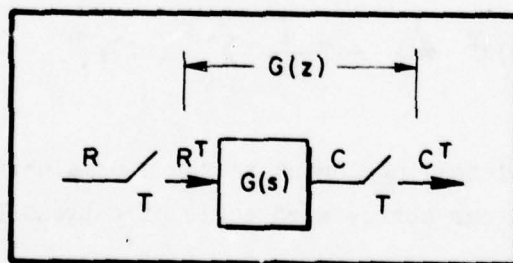


Figure 1. Correspondence Between Transfer Function and Pulse Transfer Function

TABLE 2

AN ABBREVIATED TABLE, $F(z)$ ADDED

$f(t)$	$F(s) = \mathcal{L}[f(t)]$	$F(z) = \mathcal{Z}[f^T(t)], z \triangleq e^{sT}$
$u(t)$	$\frac{1}{s}$	$\frac{z}{z-1}$
t	$\frac{1}{s^2}$	$\frac{Tz}{(z-1)^2}$
t^2	$\frac{2}{s^3}$	$\frac{T^2 z(z+1)}{(z-1)^3}$
e^{-at}	$\frac{1}{s+a}$	$\frac{z}{z-e^{-aT}}$
te^{-at}	$\frac{1}{(s+a)^2}$	$\frac{Tze^{-aT}}{(z-e^{-aT})^2}$
$\sin bt$	$\frac{b}{s^2+b^2}$	$\frac{z \sin bT}{(z - \cos bT)^2 + (\sin bT)^2}$
$\cos bt$	$\frac{s}{s^2+b^2}$	$\frac{z(z - \cos bT)}{(z - \cos bT)^2 + (\sin bT)^2}$
$e^{-at} \sin bt$	$\frac{b}{(s+a)^2+b^2}$	$\frac{ze^{-aT} \sin bT}{(z - e^{-aT} \cos bT)^2 + (e^{-aT} \sin bT)^2}$
$e^{-at} \cos bt$	$\frac{s+a}{(s+a)^2+b^2}$	$\frac{z(z - e^{-aT} \cos bT)}{(z - e^{-aT} \cos bT)^2 + (e^{-aT} \sin bT)^2}$

Note:

$$(z - e^{-aT} \cos bT)^2 + (e^{-aT} \sin bT)^2 \equiv z^2 - 2e^{-aT} \cos bTz + e^{-2aT}$$

That is, given that $G(s)$ is isolated by samplers (and it is in Table 2), then $G(z)$ can be written directly. However, if $G(s)$ is the product of several of the tabulated functions of s , then a partial fraction expansion of $G(s)$ must be made before $G(z)$ can be found. For example, if $G(s) = 1/s^2$, then

$$G(z) = \frac{Tz}{(z-1)^2} \quad (66)$$

However, if $G(s) = 1/[s^2(s+a)]$, then

$$G(z) = \left[\frac{A}{s^2} + \frac{B}{s} + \frac{C}{s+a} \right]^T \quad (67)$$

or

$$G(z) = \frac{ATz}{(z-1)^2} + \frac{Bz}{z-1} + \frac{Cz}{z-e^{-aT}} \quad (68)$$

Moreover, the situation depicted in Fig. 1 does not represent the form of the problem which is usually of interest since no data hold is included. The form of interest is shown in Fig. 2.

In Fig. 2, $M(s)$ represents the transfer function of a data hold. Using the results of Appendix B, we can write

$$C^T = (GM)^T R^T \quad (69)$$

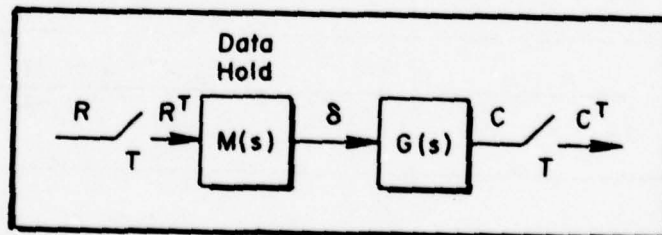


Figure 2. Typical Data Hold Configuration

The data hold is a physical device that takes the samples of the signal, R^T , and constructs a continuous signal which in turn forces the continuous system represented by $G(s)$. It is convenient to think of the data hold as a coupler between the digital computer and the control actuator input. This coupler is usually inherent in the digital-to-analog (D/A) converter device.

We will assume that the reader is familiar with the characteristics of various data holds. (Their properties can be reviewed in Refs. 7 and 8.)

The presence of the data hold in a single-rate system is only a mildly complicating factor. This is especially so if we are using a zero-order hold which has the transfer function:

$$M = \frac{1 - e^{-sT}}{s} \quad (70)$$

For example, let $G(s) = a/(s+a)$, $M = (1 - e^{-sT})/s$, then

$$(GM)^T = \left[\frac{(1 - e^{-sT})a}{s(s+a)} \right]^T = \left[(1 - e^{-sT}) \left(\frac{1}{s} - \frac{1}{s+a} \right) \right]^T \quad (71)$$

But, $1 - e^{-sT} \equiv (z - 1)/z$ and is unaffected by the sampling operator. Therefore,

$$\begin{aligned} (GM)^T &= \frac{z-1}{z} \left[\left(\frac{1}{s} \right)^T - \left(\frac{1}{s+a} \right)^T \right] \\ &= \frac{z-1}{z} \left(\frac{z}{z-1} - \frac{z}{z - e^{-aT}} \right) \\ &= \frac{1 - e^{-aT}}{(z - e^{-aT})} \end{aligned} \quad (72)$$

As we shall see, this simple computation becomes more complicated when the data hold and input sampler are working at a different sampling period than is the output sampler. This situation will be encountered later in the analyses of multi-rate sampled systems. For single-rate sampled systems

it can be appreciated that the partial fraction technique is quite adequate for computing overall pulse transfer functions (from the output of a sampler to the output of the previous one). This result pertains whether or not there is a data hold involved, even though the data hold alters the form of the answer dramatically.

Transfer functions for representative data holds are given in Table 3. The data holds of greatest interest are the zero-order hold and the slewer data hold. Their characteristics will be discussed at appropriate points in the text.

TABLE 3. SOME REPRESENTATIVE DATA HOLDS

DATA HOLD	TRANSFER FUNCTION
Zero-Order Hold	$M_0 = \frac{1 - e^{-sT}}{s}$
First-Order Hold	$M_1 = M_0^2 \left(s + \frac{1}{T} \right)$
Second-Order Hold	$M_2 = M_0^3 \left(s^2 + \frac{3}{2T} s + \frac{1}{T^2} \right)$
Triangular Data Hold	$M_{\Delta} = \frac{M_0^2}{T} e^{sT}$
Slewer Data Hold	$M_{\text{slew}} = \frac{M_0^2}{T}$

E. AN INTRODUCTION TO MULTI-RATE SAMPLING

Sufficient aspects of single-rate sampled systems have been reviewed to this point that we may now consider analysis of a restricted class of multi-rate sampled systems. A basic multi-rate sampled system element of interest is shown in Fig. 3.

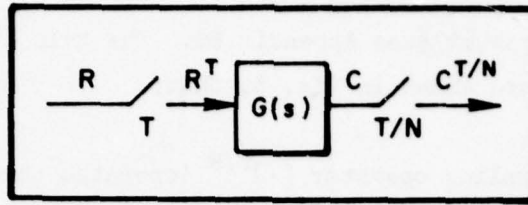


Figure 3. Slow Input/Fast Output Sampling

It is required, in Fig. 3, that N be an integer so that the output sample rate is N times the input sample rate. Write the output equation for the continuous variable C as

$$C = GR^T \quad (73)$$

so that

$$C^{T/N} = [GR^T]^{T/N} \quad (74)$$

To further reduce Eq. 74, we merely notice that Fig. 4 is equivalent in an input-output sense to Fig. 3. The T input sampling operation in Fig. 3 is replaced by two sampling operations which are equivalent to the

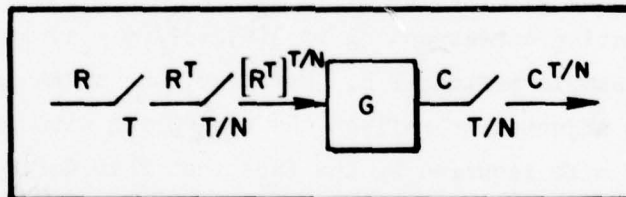


Figure 4. Equivalent Model for Fig. 3

original one. The time functions $[R^T]^{T/N}$ and R^T are obviously equivalent, since the intermediate samples of the new, but fictitious, input $[R^T]^{T/N}$ are zero. This "trick" does show that we may write

$$C^{T/N} = [GR^T]^{T/N} = G^{T/N} [R^T]^{T/N} = G^{T/N} R^T \quad (75)$$

which is the correct result (see Appendix B). The rule is, for sampling operations such as those shown in Fig. 3, that:

"The outer sampling operator $[\cdot]^{T/N}$ 'operates through' the inner ones if the ratios of the inner sampling periods to the outer sampling period, T/N , are integers."

Consider an example application. Let

$$r(t) = u(t) \quad , \quad G = \frac{1}{s + a} \quad , \quad z = e^{sT/N} \quad (76)$$

Therefore

$$C^{T/N} = \left(\frac{1}{s + a} \right)^{T/N} [u^T(t)]^{T/N} \quad (77)$$

Referring to Table 2, write

$$C^{T/N} = \left(\frac{z}{z - e^{-aT/N}} \right) \left(\frac{z^N}{z^N - 1} \right) \quad (78)$$

Note the important points. Since z has been defined as $z \triangleq e^{sT/N}$, the pulse transfer function corresponding to $G(s) = 1/(s + a)$ must represent the newly defined sample period, T/N . Moreover, the z -transform for $R^T = u^T(t)$ must be adjusted to reflect the resampling with period T/N . This adjustment is also required by the fact that z is defined as $e^{sT/N}$ as a result of the resampling.* The z -transform for $[R^T]^{T/N} = R^T$ is obtained in two steps:

- Obtain the z -transform for R^T in the usual manner with $z \triangleq e^{sT}$.
- Replace $z \triangleq e^{sT}$ everywhere it occurs in $R^T(z)$ by $z^N \triangleq (e^{sT/N})^N$.

*In this regard, some readers might find it helpful to read the review material of Appendices A and B.

Suppose the problem is to find a continuous time response which when sampled results in $C^{T/N}$ for the previous examples. The use of partial fractions now requires an expansion of the right-hand side of Eq. 78 into $N+1$ terms, since the denominator now has $N+1$ roots. This is not a pleasant prospect, especially if N is large, say on the order of 100 or more. When N is large, partial fraction expansion is not the best way to proceed. A recursion equation approach is preferable. Rewrite Eq. 78 in terms of the input R^T :

$$C^{T/N} = \frac{z}{z - e^{-aT/N}} R^T, \quad z = e^{sT/N} \quad (79)$$

Divide Eq. 79 by z and write the corresponding recursion equation.

$$C_n = e^{-aT/N} C_{n-1} + R_{n,N}^T \quad (80)$$

where

$$R_{n,N}^T = \begin{cases} 0 & \text{if } \text{Frac}(n/N) \neq 0 \\ R(nT/N) & \text{if } \text{Frac}(n/N) = 0 \end{cases} \quad (81)$$

The notation $R_{n,N}^T$ is interpreted as follows. Form the ratio of the index of the recursion equation, n , to N ; and take the fractional part of the number that results. If this is zero, then nT/N is a point in time for which an input sample is taken. However, if the fractional part of this ratio is non-zero, we are at an inter-sample time point for the input. Consequently, no input sample is taken, giving a zero input value for this sample point in time.

To illustrate, let $T = 1$, $e^{-aT} = 0.5$ ($a \doteq 0.6932$), and compute the transient response to a unit step input using

$$C_n = e^{-aT/N} C_{n-1} + R_{n,N}^T \quad (82)$$

where

$$R_{n,N}^T = \begin{cases} 0 & \text{Frac}(n/N) \neq 0 \\ 1 & \text{Frac}(n/N) = 0 \end{cases} \quad (83)$$

The transient response is shown in Fig. 5. Notice that the absence of a data-hold circuit forces the continuous output to be comprised of the summation of a train of weighted impulse responses of the first-order system $1/(s + a)$.

The following is accomplished by implementation in terms of this recursion equation:

- The inter-sample response can be computed with any desired degree of time resolution desired by increasing N .
- Computer storage requirements are unchanged as N is increased. The order of the recursion equation (i.e., the number of states) is not affected by N .

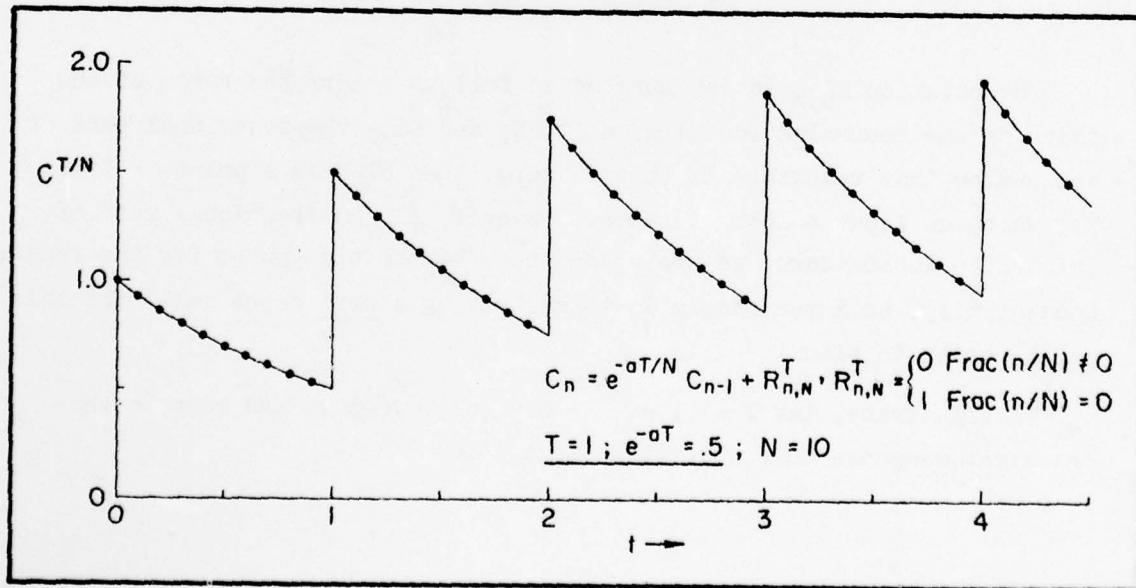


Figure 5. Step Response

F. SLOW INPUT/FAST OUTPUT SAMPLING WITH DATA HOLD

The inclusion of a data hold in the slow input/fast output sampling problem introduces an additional consideration. Adding a data hold to the block diagram of Fig. 3 gives Fig. 6. The output equation is

$$C^{T/N} = (GM)^{T/N} R^T \quad (84)$$

where M represents the transfer function of the data hold. It is important to notice that the data hold is configured for a T second sampling period, whereas the sampling operation on GM is for a T/N second sampling period. An example will demonstrate the nature of the problem.

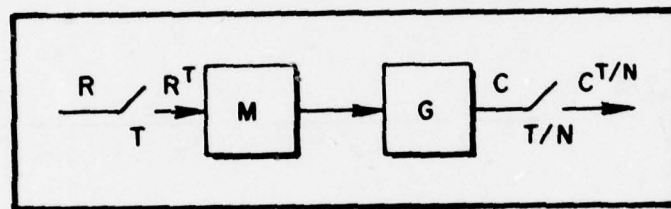


Figure 6. Slow Input/Fast Output Sampling
with Data Hold

Let

$$M = \frac{1 - e^{-sT}}{s}, \quad G = \frac{a}{s + a}, \quad z = e^{sT/N} \quad (85)$$

Therefore,

$$(GM)^{T/N} = \left[\frac{(1 - e^{-sT})a}{s(s + a)} \right]^{T/N} \quad (86)$$

Since $z = e^{sT/N}$, it follows that

$$e^{-sT} = e^{-(sT/N)N} = z^{-N} \quad (87)$$

and

$$1 - e^{-sT} \equiv \frac{z^N - 1}{z^N} \quad (88)$$

Moreover,

$$\frac{a}{s(s+a)} = \frac{1}{s} - \frac{1}{s+a} \quad (89)$$

so that the transform table gives

$$\left(\frac{1}{s} - \frac{1}{s+a}\right)^{T/N} = \frac{z}{z-1} - \frac{z}{z - e^{-aT/N}} \equiv \frac{z(1 - e^{-aT/N})}{(z-1)(z - e^{-aT/N})}$$

Therefore,

$$C^{T/N} = \left[\frac{z^N - 1}{z^N} \cdot \frac{z(1 - e^{-aT/N})}{(z-1)(z - e^{-aT/N})} \right] R^T \quad (90)$$

or

$$C^{T/N} = \left[\frac{1 - e^{-aT/N}}{z - e^{-aT/N}} \left(1 + z^{-1} + \dots + z^{-(N-1)} \right) \right] R^T \quad (91)$$

Comparing Eq. 91 with Eq. 79, it is seen that the inclusion of the zero-order hold has introduced an additional multiplicative function:

$$(1 - e^{-aT/N}) \frac{z^N - 1}{z^N(z-1)} = \frac{(1 - e^{-aT/N})}{z} [1 + z^{-1} + \dots + z^{-(N-1)}]$$

Methods for treating this additional complication when N is a given large number will be discussed in Section IV.

G. FAST INPUT/SLOW OUTPUT SAMPLING

The next fundamental multi-rate configuration of interest is the fast input/slow output sampling configuration of Fig. 7. This presents a more involved situation from a computational viewpoint than does the slow input/fast output case studied previously.

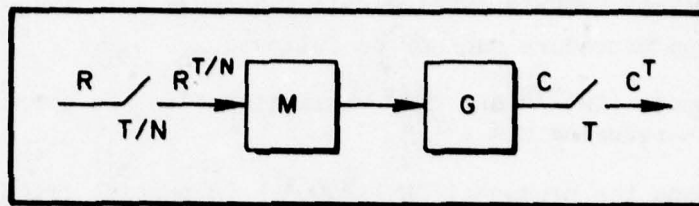


Figure 7. Fast Input/Slow Output Sampling

As always,

$$C = GMR^{T/N} \quad (92)$$

so that

$$C^T = [GMR^{T/N}]^T \quad (93)$$

In Eq. 93, the T operator can no longer "operate through" since the ratio of the inner sampling period to the outer is not an integer. However, it is legitimate to replace Fig. 7 with the equivalent block diagram shown in Fig. 8.

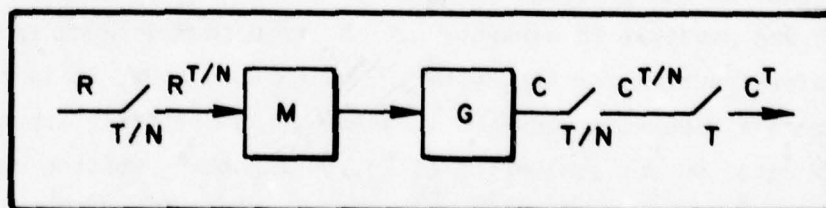


Figure 8. Equivalent System

It is readily apparent that the output C^T is not affected by introduction of the "phantom" T/N sampler, since the T output sampler rejects all the unwanted samples of C^T/N . One can write the following equation directly, from Fig. 8,

$$C^T = [GMR^T/N]^T = [(GM)^T/N R^T/N]^T \quad (94)$$

On the surface, this exercise does not appear to have been too fruitful, since the T operator still cannot operate through. Nevertheless, Eq. 94 offers a significant computational simplification. This is so because the following routine procedure can now be followed:

- Compute $(GM)^T/N$ and R^T/N z -transforms in the normal manner, using $z \triangleq e^{sT/N}$.
- Expand the product $[(GM)^T/N R^T/N]$ in partial fractions and use the transform table to find the continuous time function which, when sampled with period T/N , results in $[(GM)^T/N R^T/N]$.
- Find the z -transform of this sampled continuous generating function, for a sampling period, T , and $z \triangleq e^{sT}$ to obtain:

$$[(GM)^T/N R^T/N]^T = [GMR^T/N]^T$$

This process is in the spirit of the convolution approach described in Appendix B. The main difference is that we avoid the use of a complex inversion integral by substituting the procedure of going from the z -domain for a T/N sampling period (i.e., with $z \triangleq e^{sT/N}$) to the time domain and then back to the z -domain for a T sampling period (i.e., with $z \triangleq e^{sT}$).

Notice that in the previous section for the slow input/fast output problem, it was possible to separate out the transformed input from the pulse transfer function for the system. Having done this, it is then possible to write a recursion equation in terms of an arbitrary input. Here, a recursion equation for evaluation of Eq. 94 cannot be written until a specific R is given. That is, the recursion equation for C^T must be found on a case-by-case basis. Nevertheless, the basic method described in this

subsection will be valuable later for analysis of multi-rate closed-loop systems.

An example illustrates the computational method. Let

$$G = \frac{a}{s+a}, \quad M = \frac{1 - e^{-sT/N}}{s}, \quad R = \sin bt \quad (95)$$

First, compute $(GM)^{T/N}$ z-transform. This is straightforward, since the sampling operation on GM and the data hold are for the same sampling period, T/N . Then obtain $R^{T/N}(z)$ from the z-transform table, and form the product $[(GM)^{T/N} R^{T/N}]^{T/N}$.

$$(GM)^{T/N} = \left[\frac{(1 - e^{-sT/N})a}{s(s+a)} \right]^{T/N} = \frac{1 - e^{-aT/N}}{z - e^{-aT/N}}, \quad z \triangleq e^{sT/N} \quad (96)$$

Therefore,

$$(GM)^{T/N} R^{T/N} = \frac{1 - e^{-aT/N}}{z - e^{-aT/N}} \cdot \frac{z \sin bT/N}{(z - \cos bT/N)^2 + (\sin bT/N)^2} \quad (97)$$

Expand in partial fractions:

$$\begin{aligned} F^{T/N} &= (GM)^{T/N} R^{T/N} \\ &= \frac{Az}{z - e^{-aT/N}} + \frac{Bz \sin bT/N + Cz(z - \cos bT/N)}{(z - \cos bT/N)^2 + (\sin bT/N)^2}, \quad z = e^{sT/N} \end{aligned} \quad (98)$$

Compute $f(t)$ such that $f^{T/N} \Leftrightarrow F^{T/N}$

$$f(t) = Ae^{-at} + B \sin bt + C \cos bt \quad (99)$$

Compute F^T

$$F^T = [(GM)^T/N \ R^T/N]^T = \frac{Az}{z - e^{-aT}} + \frac{Bz \sin bT + Cz(z - \cos bT)}{(z - \cos bT)^2 + (\sin bT)^2}, \quad z = e^{sT} \quad (100)$$

Notice the clear resemblance of Eq. 98 to Eq. 100. The only difference is that T/N in Eq. 98 is replaced by T in Eq. 100. This emphasizes that the intermediate step of computing the generating time function is merely a convenient conceptual step which may usually be skipped in the analysis of single-rate systems. However, in a later section we shall see that execution of this step can be quite useful in sorting out delayed time functions arising in the analysis of closed-loop multi-rate systems.

To complete the example, it may be verified that:

$$A = -C = A_0 \sin bT/N \quad (101)$$

$$B = -A_0(e^{-aT/N} - \cos bT/N) \quad (102)$$

where

$$A_0 = \frac{1 - e^{-aT/N}}{(e^{-aT/N} - \cos bT/N)^2 + (\sin bT/N)^2} \quad (103)$$

H. VECTOR BLOCK DIAGRAMS

As noted in the introduction, one objective is to present all results in a vector notation which is compatible with either degree-of-freedom or state variable problem formulations. For example, consider the block diagram of Fig. 9 wherein the dimension of the G and H matrices are compatible with the dimensions of the C and E vectors. One can now develop equations and pulse transfer functions for this closed-loop system in an orderly manner.

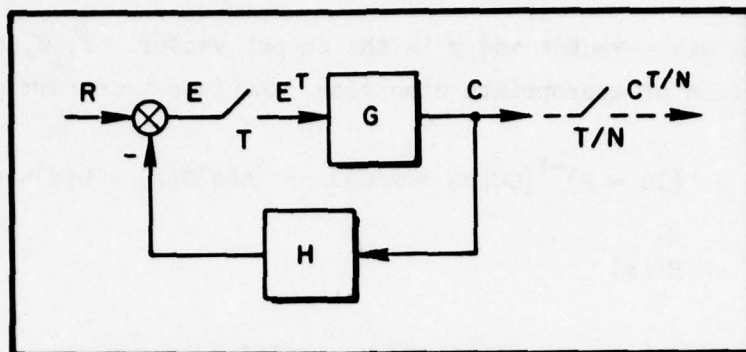


Figure 9. Simple Closed-Loop Configuration

$$E = R - HGE^T \quad (104)$$

so that

$$E^T = R^T - (HG)^T E^T \quad (105)$$

Thus,

$$E^T = [I + (HG)^T]^{-1} R^T \quad (106)$$

Using Eq. 106, write an equation for the continuous output vector C:

$$C = G[I + (HG)^T]^{-1} R^T \quad (107)$$

One can now conceptually add a "phantom sampler" at the output C and obtain

$$C^{T/N} = G^{T/N}[I + (HG)^T]^{-1} R^T \quad (108)$$

by using the results of Section II-E. Thus, values for the continuous output C can be calculated at as many inter-sample points as desired.

Consider another example. Suppose the open-loop plant is formulated in the first-order state variable form

$$\dot{x} = Fx + Gu \quad (109)$$

$$y = Hx \quad (110)$$

where x is the state vector and y is the output vector. F , G , and H are constant matrices of appropriate dimension. Laplace transforming, we obtain

$$X(s) = (Is - F)^{-1}[GU(s) + x(0)] = A(s)U(s) + B(s)x(0) \quad (111)$$

$$Y(s) = HX(s) \quad (112)$$

In Eq. 111, $x(0)$ represents the initial condition vector.

The open-loop plant, given by Eqs. 111 and 112, might then be embedded in the closed-loop configuration of Fig. 10 wherein W_1 and W_2 represent compensation matrices which may be selected to achieve closed-loop design objectives.

Suppose the objective is to find an expression for the (continuous) state vector x . First, write

$$U_1^T = W_1^T R^T - W_1^T W_2^T [HBx(0) + HAMU_1^T]^T \quad (113)$$

or

$$U_1^T = W_1^T R^T - W_1^T W_2^T (HB)^T x(0) - W_1^T W_2^T (HAM)^T U_1^T \quad (114)$$

Therefore,

$$U_1^T = [I + (W_1^T W_2^T)(HAM)^T]^{-1} [W_1^T R^T - W_1^T W_2^T (HB)^T x(0)] \quad (115)$$

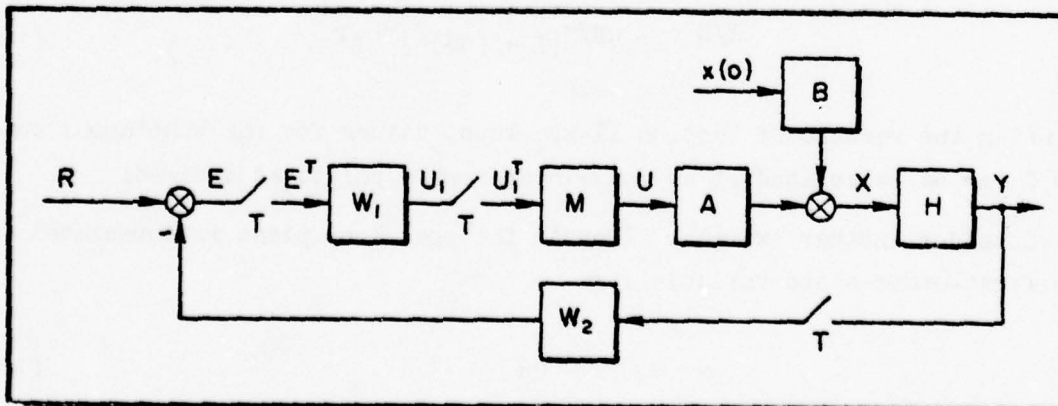


Figure 10. A Representative Closed-Loop System

Thus, U_1^T is a function of the input vector R and the initial condition vector $x(0)$.

To find the continuous state and output variables, x and y ,

$$X = Bx(0) + AMU_1^T \quad (116)$$

$$Y = HBx(0) + HAMU_1^T = Hx \quad (117)$$

The inter-sample response can be determined to any desired resolution:

$$\begin{aligned} X^{T/N} &= B^{T/N} x(0) + (AM)^{T/N} U_1^T \\ X^{T/N} &= B^{T/N} x(0) + (AM)^{T/N} \left\{ [I + (W_1^T W_2^T)(HAM)^T]^{-1} [W_1^T R^T - W_1^T W_2^T (HB)^T x(0)] \right\} \end{aligned} \quad (118)$$

In general, throughout the text care has been taken to develop all equations in vector notation, even though most of the illustrative examples are scalar. Note that this transform domain notation is applied just as easily to state vector problem formulations as it is to degree-of-freedom formulations.

I. SWITCH DECOMPOSITION CONCEPT

The phantom sampler approach was introduced in Section II-G in connection with the fast input/slow output sampling format. Now that vector notation has been discussed (Section II-H), we are able to present an alternative description that includes the phantom sampler as well as the "T/N" approach treated earlier in Section II-F. This alternative approach is called "switch decomposition" (Ref. 6).

In essence, switch decomposition is a procedure wherein systems having multiple sampling operations (occurring at fixed but unequal sampling intervals, but with a sampling pattern which is repeated over a fixed, finite time interval) are converted into an equivalent single sample rate form. As originally introduced by Kranc, the method used a summing point methodology

which proved to be extremely cumbersome when the ratios of the sampling periods become high. For this reason and also because evolving state transition methods were tending to push transform methods into the background, the method fell into disuse. However, there is much to recommend the switch decomposition concept for use in both time domain and transform domain analyses. In the subsections that follow we will review the basic concept and remove some earlier restrictions by recasting it in vector form. The vector form simplifies matrix block diagram manipulation for multiloop, multi-rate sampled systems; but, as we shall see, the dimensionality of problems formulated using this approach can present a practical limitation.

J. VECTOR SWITCH DECOMPOSITION

Consider the continuous signal shown in Fig. 11a to be sampled at $3/T$ samples/second. This results in the sample sequence shown in Fig. 11b. The sampled values have been numbered for easy reference. Suppose now we sample the continuous signal with a sampling period, T . This results in the sample sequence consisting of 1, 4, 7, 10, 13, ... shown in Fig. 11c. Define this sample sequence to be R^T .

Next, advance the continuous signal R by $T/3$. Then sample the advanced signal with a sampling period, T . This results in a sample sequence consisting of 2, 5, 8, 11, 14, ... shown in Fig. 11d. Define this sample sequence to be $(e^{sT/3} R)^T$. Finally, advance the continuous signal R by $2T/3$, and sample it with a sampling period, T . This results in the sequence consisting of 3, 6, 9, 12, 15, ... shown in Fig. 11e. Define this signal sequence to be $(e^{2sT/3} R)^T$.

The significance of the switch decomposition concept resides in its ability to provide an alternative expression for the original sequence, $R^{T/3}$. This alternative expression for $R^{T/3}$ consists of the sum of R^T , $(e^{sT/3} R)^T$, and $(e^{2sT/3} R)^T$ each delayed by a time interval corresponding to the advance.

$$R^{T/3} = R^T + (e^{sT/3} R)^T e^{-sT/3} + (e^{2sT/3} R)^T e^{-2sT/3} \quad (119)$$

Equation 119 has a simple factored equivalent which is the product of two vectors and the scalar, R ,

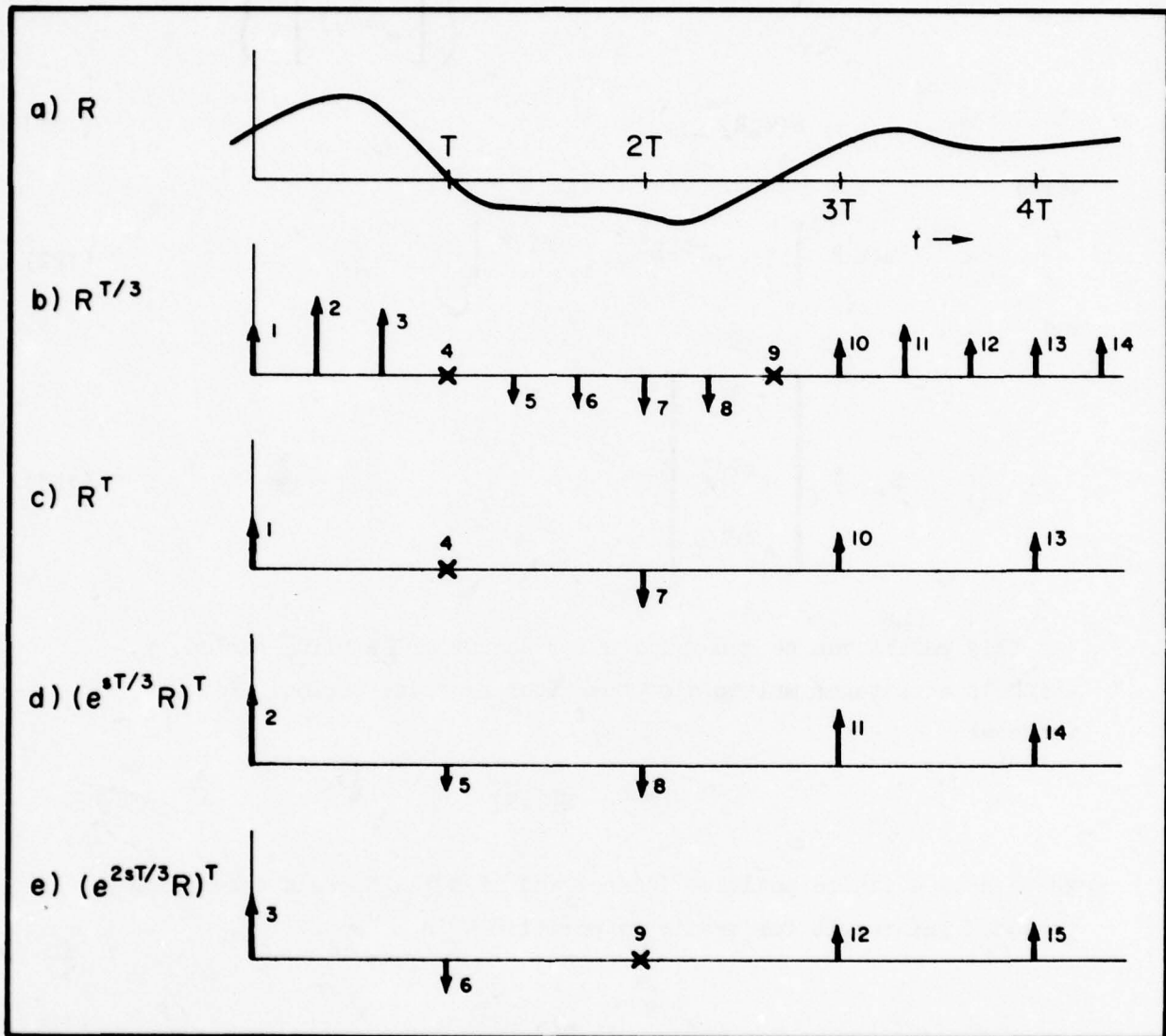


Figure 11. Decomposition of a Sample Sequence

$$R^{T/3} = \begin{bmatrix} 1 & e^{-sT/3} & e^{-2sT/3} \end{bmatrix} \left\{ \begin{bmatrix} 1 \\ e^{sT/3} \\ e^{2sT/3} \end{bmatrix} R \right\}^T \quad (120)$$

$$= W(W_*R)^T \quad (121)$$

where

$$W \triangleq \begin{bmatrix} 1 & e^{-sT/3} & e^{-2sT/3} \end{bmatrix} \quad (122)$$

and

$$W_* \triangleq \begin{bmatrix} 1 \\ e^{sT/3} \\ e^{2sT/3} \end{bmatrix} \quad (123)$$

This result can be generalized for any major sampling period, T , which is an integer multiple of the minor sampling period. That is, whenever

$$T = N(T/N)$$

where N is a finite positive integer and (T/N) is the minor sampling period. The result for arbitrary positive N is

$$R^{T/N} = W(W_*R)^T \quad (124)$$

where

$$W = W(s) \triangleq \begin{bmatrix} 1, e^{-sT/N}, e^{-2sT/N}, \dots, e^{-(N-1)sT/N} \end{bmatrix} \quad (125)$$

and

$$W_* = W_*(s) \triangleq W'(-s) \quad (126)$$

In Eq. 126, the prime denotes a transpose.

Further generalization allows R to be a vector of continuous signals. Equations 124 and 125 continue to apply. It is necessary to define a least common sampling period, T , and a greatest common subinterval, T_0 , with respect to the R vector. The p elements of R may be sampled at different minor sampling periods: $T_1, \dots, T_2, \dots, T_p$, respectively. It is further assumed that the minor sampling periods are such that a finite positive T exists such that

$$T = N_1 T_1 \dots = N_i T_i \dots = N_p T_p \quad (127)$$

holds for a set of finite positive integers:

$$N_1, \dots, N_i, \dots, N_p$$

The minimum T for which Eq. 127 holds is the least common sampling period (for R). A subinterval can be found for which

$$T = N T_0 \quad (128)$$

and N/N_i is an integer for all $i = 1, 2, \dots, p$. The largest value of T_0 satisfying these conditions is the greatest common subinterval (for R). Equation 128 defines N for the greatest common subinterval. Given values for N, N_i, p , and T , the $p \times \sum N_i$ block diagonal matrix, W , is

$$W = W(s) = \begin{bmatrix} W_1 & & & 0 \\ & W_2 & \dots & \\ & & W_i & \dots \\ 0 & & & W_p \end{bmatrix} \quad (129)$$

where

$$W_i = \begin{bmatrix} 1 & e^{-sT/N_i} & \dots & e^{-s(j-1)T/N_i} & \dots & e^{-s(N_i-1)T/N_i} \end{bmatrix} \quad (130)$$

The operator matrices W and W_* can be used to represent multi-rate sampling operations in terms of a single-rate sampling operation in vector block diagrams. This is illustrated in Fig. 12.

Consider an example. Let R be a vector with three components. Let the first component be sampled with period $T/6$, the second with period $T/3$, and the third with period $T/2$. That is,

$$R^* = \left[R_1^{T/6}, R_2^{T/3}, R_3^{T/2} \right]' \quad (131)$$

The objective is to compute W in order to obtain an explicit expression for R^* via Eqs. 129 and 124 (which is equivalent to Fig. 12b). For this example,

$$p = 3$$

T is the least common sampling period

$$T_1 = T/6, T_2 = T/3, T_3 = T/2$$

$$N_1 = 6, N_2 = 3, N_3 = 2$$

$T/6$ is the greatest common subinterval

$$N = 6$$

Therefore,

$$W = \begin{bmatrix} 1, e^{-sT/6}, e^{-2sT/6}, e^{-3sT/6}, e^{-4sT/6}, e^{-5sT/6} & 0 & 0 \\ 0 & 1, e^{-2sT/6}, e^{-4sT/6} & 0 \\ 0 & 0 & 1, e^{-3sT/6} \end{bmatrix} \quad (132)$$

This example gives us some insight as to how increased dimensionality can complicate problems in practical application. Consider the vectors R , R^* , and $(W_*R)^T$. These vectors have 3, 3, and 11 elements, respectively. The vector $(W_*R)^T$ will have $p \sum N_i$ elements in general; whereas R and R^* will only have p elements each. This is significant in that analyses will tend

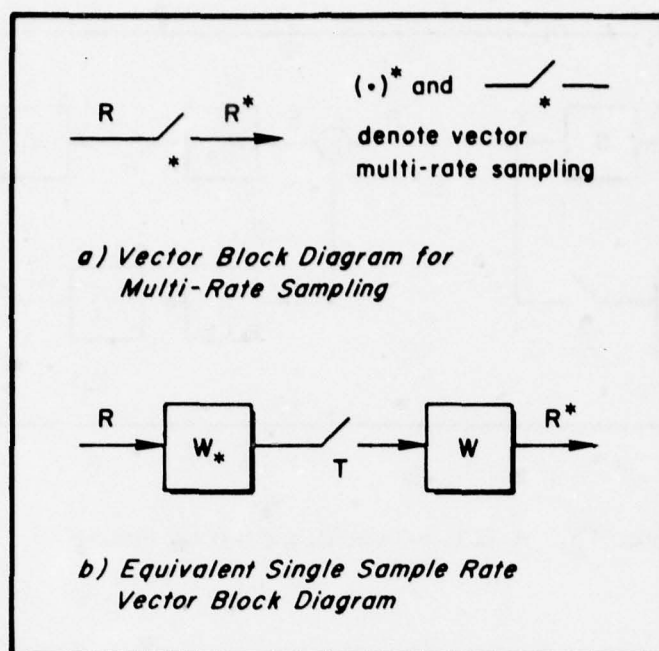


Figure 12. Vector Block Diagrams for Multi-Rate Sampling Operations

to be conducted in terms of vectors like $(W_*R)^T$ in distinction to vectors like R^* . Consequently, the potential for expanded dimensionality in connection with analyses of multi-rate sampled problems is great. For example, consider a problem wherein there are two minor sampling periods, 39 ms and 40 ms. It is easy to verify that the dimensionality expansion factor, N , is 1560.

Fortunately, minor sampling periods which are so little different are not usually of practical interest. Furthermore, it is important to stress the fact that the increase in dimensionality affects input and output vectors, but it does not affect the dimension of the system state vector.

On the more positive side, matrix operations are routine. Consider the system shown in Fig. 13. Once the vector multi-rate sampling operations in Fig. 13a have been replaced by the switch decomposition equivalent (Fig. 13b), analytical manipulations are routine:

$$E_1^T = (W_1 R)^T - (W_1 H W_2)^T (W_2 G W_1)^T E_1^T \quad (133)$$

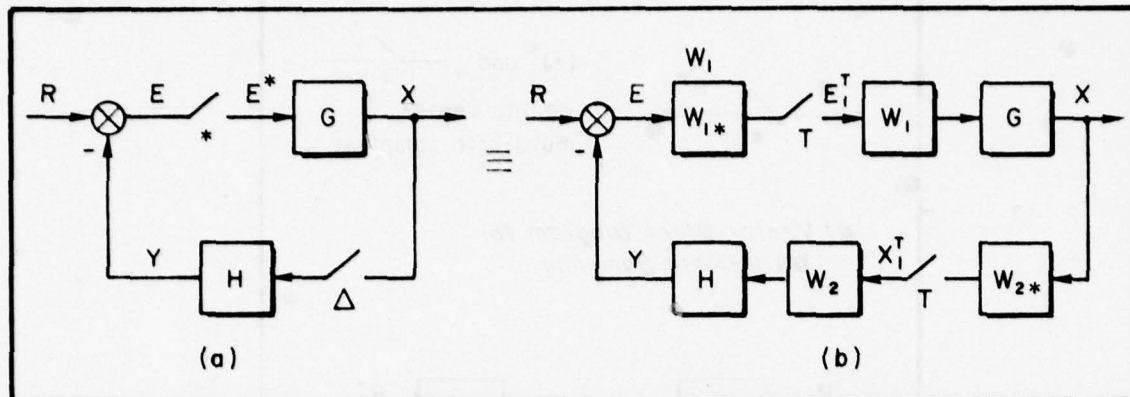


Figure 13. A Multi-Rate Closed-Loop System

Therefore

$$E_1^T = \left[I + (W_{1*} H W_2)^T (W_{2*} G W_1)^T \right]^{-1} (W_{1*} R)^T \quad (134)$$

and

$$X = G W_1 E_1^T \quad \text{or} \quad X^{T/N} = (G W_1)^{T/N} E_1^T \quad (135)$$

Notice that the dimension of the inverse in Eq. 134 is determined by the column dimension of W_1 . If this dimensionality is high, and if the column dimension of W_2 is lower, then we can develop an alternate equation having lower dimension. The alternative equation is in terms of the X_1^T vector. The dimension in this case is determined by the column dimension of W_2 .

$$X_1^T = \left[I + (W_{2*} G W_1)^T (W_{1*} H W_2)^T \right]^{-1} (W_{2*} G W_1)^T (W_{1*} R)^T \quad (136)$$

$$X = G W_1 \left[(W_{1*} R)^T - (W_{1*} H W_2)^T X_1^T \right] \quad (137)$$

or

$$X^{T/N} = (G W_1)^{T/N} \left[(W_{1*} R)^T - (W_{1*} H W_2)^T X_1^T \right] \quad (138)$$

A more concrete scalar example is shown in Fig. 14. The objective is to develop the pulse transfer function relating E^T and R^T .

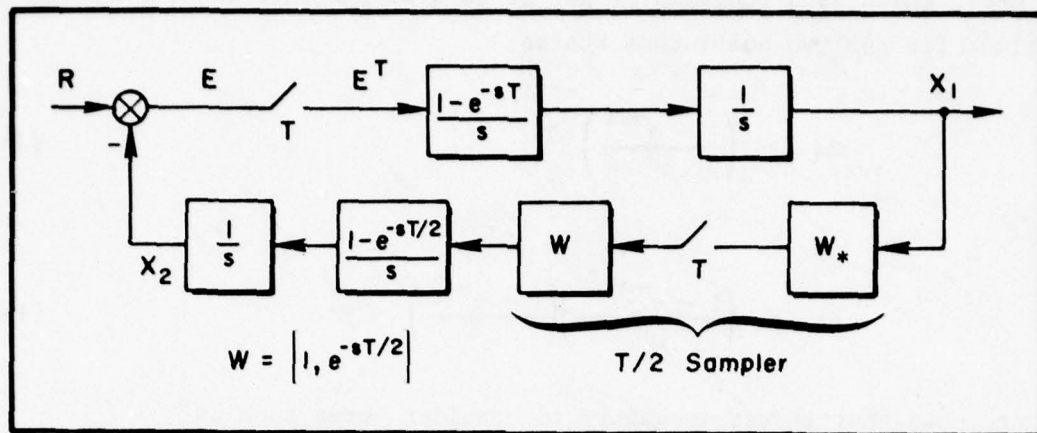


Figure 14. A Scalar Two-Rate Example

To develop this pulse transfer function, start by writing an equation for E^T in terms of R^T and E^T .

$$E^T = R^T - \left[\frac{1 - e^{-sT/2}}{s^2} \left(1, e^{-sT/2} \right) \right]^T \left[\begin{pmatrix} 1 \\ e^{sT/2} \end{pmatrix} \left(\frac{1 - e^{-sT}}{s^2} \right) \right]^T E^T \quad (139)$$

Coefficients of like terms in Eq. 139 are collected. Next, the various factors are expressed in terms of the z -transforms for sampled time functions which correspond to the Laplace transforms inside each of the sampling operators, $(\cdot)^T$. The result is then simplified to obtain

$$\left[1 + \frac{(T^2/4)z + (3/4)T^2}{(z - 1)^2} \right] E^T = R^T, \quad z \triangleq e^{sT} \quad (140)$$

Therefore,

$$E^T = \frac{(z - 1)^2}{z^2 + \left(\frac{T^2}{4} - 2 \right)z + \left(1 + \frac{3}{4}T^2 \right)} R^T \quad (141)$$

Once E^T is known as a function of R^T , it is a simple task to compute the equations for the two continuous states:

$$X_1 = \left(\frac{1 - e^{-sT}}{s^2} \right) E^T \quad (142)$$

and

$$X_2 = \left(\frac{1 - e^{-sT/2}}{s^2} \right) \left(\frac{1 - e^{-sT}}{s^2} \right)^{T/2} E^T \quad (143)$$

However, note that it was necessary to consider terms such as

$$F^T(s) = \left[\frac{1 - e^{-sT}}{s} \quad \frac{1}{s} e^{sT/2} \right]^T \quad (144)$$

in order to obtain the z-transformed functions required for Eq. 140. Thus, a method for obtaining z-transforms for functions of this form is needed at this point. An approach using the so-called advanced z-transform is presented in the next subsection.

K. ADVANCED z-TRANSFORMS

Matrix switch decomposition requires the z-transform of functions advanced in time by some fraction, Δ , of the least common sampling period, T . For example,

$$f(t) = e^{-a(t+\Delta T)} \quad , \quad 0 \leq (t+\Delta T) < (t+T) \quad (145)$$

By definition,

$$F(z) = \sum_{n=0}^{\infty} e^{-a(n+\Delta)T} z^{-n} \quad (146)$$

so we may write

$$F(z) = e^{-a\Delta T} \sum_{n=0}^{\infty} e^{-anT} z^{-n} \quad (147)$$

The infinite summation is recognized as a geometric progression which can be expressed in closed form. Therefore,

$$e^{-a(t+\Delta T)} \Leftrightarrow \frac{ze^{-a\Delta T}}{z - e^{-aT}} \quad \text{for } 0 \leq \Delta < 1 \quad (148)$$

Equation 148 can be used to generate a table of advanced z-transforms in the same manner as the z-transforms of e^{-at} were used to generate a table of ordinary z-transforms in Section II-C. Thus, we can let the parameter a in Eq. 148 take on new values to generate new entries for the table. Let $a \rightarrow a + jb$:

$$\frac{ze^{-(a+jb)\Delta T}}{z - e^{-(a+jb)T}} = \frac{ze^{-a\Delta T} (\cos b\Delta T - j \sin b\Delta T)}{z - e^{-aT} (\cos bT - j \sin bT)} \quad (149)$$

Rationalize Eq. 149 by multiplying numerator and denominator by the complex conjugate of the denominator to obtain the intermediate result, $F_1(z)$:

$$F_1(z) = \frac{ze^{-a\Delta T} [\cos b\Delta T - j \sin b\Delta T] [(z - e^{-aT} \cos bT) - je^{-aT} \sin bT]}{[z - e^{-aT} \cos bT + je^{-aT} \sin bT] [(z - e^{-aT} \cos bT) - je^{-aT} \sin bT]}$$

Multiplying out the factor and equating real and imaginary parts gives, after a small amount of trigonometric manipulation:

$$e^{-a(t+\Delta T)} [\cos b(t+\Delta T) - j \sin b(t+\Delta T)] \Leftrightarrow \frac{ze^{-a\Delta T} [\cos b\Delta T z - e^{-aT} \cos b(1-\Delta)T]}{z^2 - 2e^{-aT} \cos bT z + e^{-2aT}} - \frac{jze^{-a\Delta T} [\sin b\Delta T z + e^{-aT} \sin b(1-\Delta)T]}{z^2 - 2e^{-aT} \cos bT z + e^{-2aT}}$$

This is the advanced z-transform for the exponentially damped cosine and sine waves.

Next, let $a = 0$ in Eq. 148 to obtain the advanced z-transform for a unit step function:

$$\left. \frac{ze^{-a\Delta T}}{z - e^{-aT}} \right|_{a \rightarrow 0} = \frac{z}{z - 1} \quad (150)$$

This states the obvious fact that a unit step, advanced by ΔT seconds, has the same z-transform as the step function itself. Next, consider the z-transform of the time function:

$$(t + \Delta T)e^{-a(t+\Delta T)} = e^{-a\Delta T} \left[te^{-at} + \Delta Te^{-at} \right] \quad (151)$$

Since we already know the z-transform of each individual term, a straightforward computation results in:

$$e^{-a\Delta T} \left[\frac{zTe^{-aT}}{(z - e^{-aT})^2} + \frac{z\Delta T}{z - e^{-aT}} \right] \Leftrightarrow \frac{ze^{-a\Delta T} [z\Delta T + T(1 - \Delta)e^{-aT}]}{(z - e^{-aT})^2} \quad (152)$$

Similarly,

$$(t + \Delta T)^2 e^{-a(t+\Delta T)} = (t^2 + 2\Delta Tt + (\Delta T)^2) e^{-a\Delta T} [e^{-at}] \quad (153)$$

leads to the transform of the remaining terms needed in order to augment Table 2 with an additional column of advanced z-transforms. Table 4 is an abbreviated table that is sufficient for the purposes of this report.

L. A COMPARISON OF VECTOR SWITCH DECOMPOSITION AND THE PHANTOM SAMPLER

We are now in a position to compare vector switch decomposition and the phantom sampler. As already noted, the case of slow-input/fast-output sampling poses no conceptual difficulties (refer to Fig. 15), since

$$C^{T/N} = [GMR^T]^{T/N} = [GM]^{T/N} [R^T] \quad (154)$$

TABLE 4. TRANSFORM TABLE

$f(t)$	$F(s)$	$F(z)$	$F(z, \Delta) = Z[f(t + \Delta T)]$
$u(t)$	$\frac{1}{s}$	$\frac{z}{z-1}$	$\frac{z}{z-1}$
t	$\frac{1}{s^2}$	$\frac{Tz}{(z-1)^2}$	$\frac{z[\Delta Tz + T(1-\Delta)]}{(z-1)^2}$
$\frac{t^2}{2}$	$\frac{1}{s^3}$	$\frac{T^2 z(z+1)}{2(z-1)^3}$	$\frac{T^2 z \left[\frac{\Delta^2}{2} z^2 + \left(\frac{1}{2} - \Delta^2 + \Delta \right) z + \left(\frac{1}{2} - \Delta + \frac{\Delta^2}{2} \right) \right]}{(z-1)^3}$
e^{-at}	$\frac{1}{s+a}$	$\frac{z}{z-e^{-aT}}$	$\frac{ze^{-a\Delta T}}{z-e^{-aT}}$
te^{-at}	$\frac{1}{(s+a)^2}$	$\frac{Tze^{-aT}}{(z-e^{-aT})^2}$	$\frac{ze^{-a\Delta T} [\Delta Tz + T(1-\Delta)e^{-aT}]}{(z-e^{-aT})^2}$
$\sin bt$	$\frac{b}{s^2 + b^2}$	$\frac{z \sin bT}{(z - \cos bT)^2 + (\sin bT)^2}$	$\frac{z[(\sin b\Delta T)z + \sin b(1-\Delta)T]}{z^2 - 2 \cos bTz + 1}$
$\cos bt$	$\frac{s}{s^2 + b^2}$	$\frac{z(z - \cos bT)}{(z - \cos bT)^2 + (\sin bT)^2}$	$\frac{z[(\cos b\Delta T)z - \cos b(1-\Delta)T]}{z^2 - 2 \cos bTz + 1}$
$e^{-at} \sin bt$	$\frac{b}{(s+a)^2 + b^2}$	$\frac{ze^{-aT} \sin bT}{(z - e^{-aT} \cos bT)^2 + (e^{-aT} \sin bT)^2}$	$\frac{ze^{-a\Delta T} [(\sin b\Delta T)z + e^{-aT} \sin b(1-\Delta)T]}{z^2 - 2e^{-aT} \cos bTz + e^{-2aT}}$
$e^{-at} \cos bt$	$\frac{s+a}{(s+a)^2 + b^2}$	$\frac{z(z - e^{-aT} \cos bT)}{(z - e^{-aT} \cos bT)^2 + (e^{-aT} \sin bT)^2}$	$\frac{ze^{-a\Delta T} [(\cos b\Delta T)z - e^{-aT} \cos b(1-\Delta)T]}{z^2 - 2e^{-aT} \cos bTz + e^{-2aT}}$

Note: $(z - e^{-aT} \cos bT)^2 + (e^{-aT} \sin bT)^2 \equiv z^2 - 2e^{-aT} \cos bTz + e^{-2aT}$

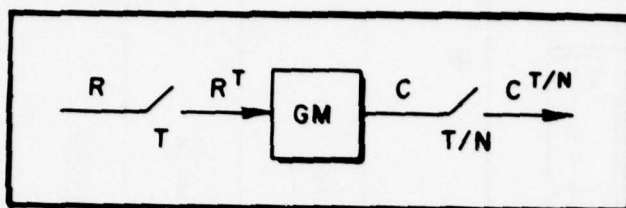


Figure 15. Slow-Input/Fast-Output Sampling

Thus, the output C^T/N is represented as a product of two factors, one of which describes the properties of the system and the other describes the input. Separation of system and input characteristics is crucial as far as conceptual closed-loop manipulations are concerned. For example, it is necessary for the use of signal flow graphs, block diagram algebra, etc. The state of affairs is somewhat different for the fast-input/slow-output sampling case shown in Fig. 16. The output in Fig. 16 is expressed as

$$C^T = [GMR^T/N]^T = [(GM)^T/N R^T/N]^T \quad (155)$$

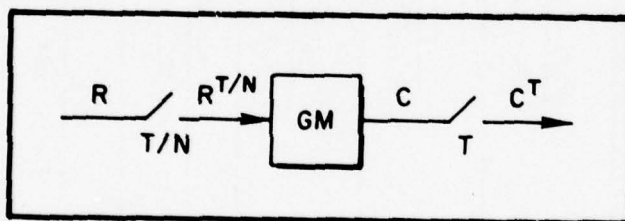


Figure 16. Fast-Input/Slow-Output Sampling

where the extreme right-hand side is obtained by using the phantom sampler concept (Eq. 94). No simple product factorization for Eq. 155 into a system pulse transfer function and a transform of the input signal is apparent. While vector switch decomposition, depicted in Fig. 17, provides the sought-after product factorization, this is at the expense of an increase in the dimensionality of the problem since

$$C^T = [GMW]^T [W_* R]^T \quad (156)$$

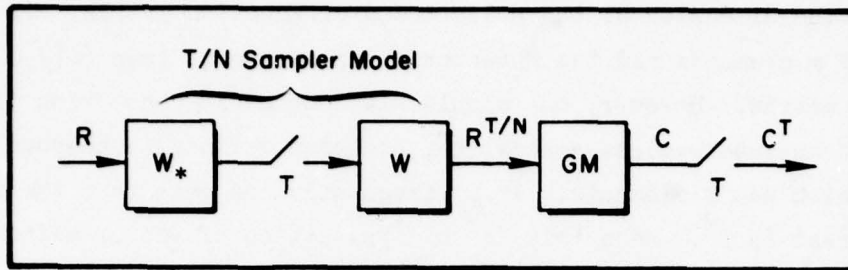


Figure 17. Vector Switch Decomposition Model;
Fast-Input/Slow-Output Sampling

Specifically, the row dimension of $[W_*R]^T$ and the column dimension of $[GM]^T$ are N for the fast-input/slow-output sampling case in Fig. 16.

On the other hand, if $G(s)$ and $R(s)$ are known prescribed functions, the evaluation of Eq. 155 can be carried to completion using either the vector switch decomposition or the phantom sampler concept.

Consider use of vector switch decomposition for analysis of the slow-input/fast-output sampling case (Eq. 154 and Fig. 15). The equivalent block diagram is shown in Fig. 18.

$$C^{T/N} = W[W_*GM]^T R^T = W[W_*GM]^T R^T \quad (157)$$

Notice that system properties are separable from the input as is always the case for the vector switch decomposition formulation. Also notice that from an input/output viewpoint [i.e., considering $(W[W_*GM]^T)$] there is no

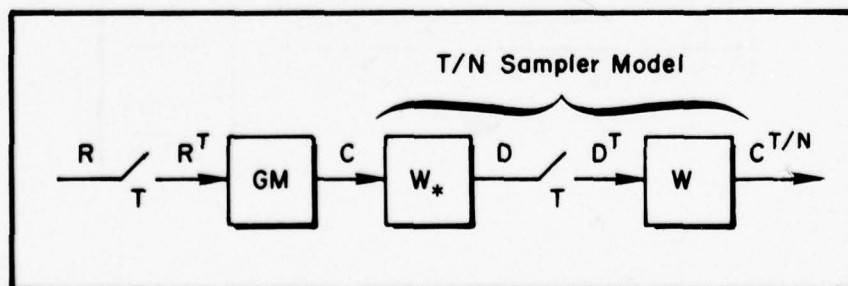


Figure 18. Vector Switch Decomposition; Slow-Input/
Fast-Output Sampling

increase in the dimension of the pulse transfer function matrix. If the C vector has m elements and the R vector has p elements, then $(W[W_*GM]^T)$ is an $m \times p$ matrix. However, one should also notice in connection with Eq. 157 that an intermediate vector, D^T , has been defined (conceptually, at least) which has N elements. It is frequently the case that the analyst has no interest in D^T . When this is so, application of vector switch decomposition does not result in increased dimensions for slow-input/fast-output sampling elements like that shown in Fig. 18.

We close with a specific numerical example to demonstrate the utility of advanced z-transforms in conjunction with switch decomposition. Consider Fig. 19, set up in a phantom sampler format.

By switch decomposition,

$$C^T = [GW]^T [W_*R]^T \quad (158)$$

$$= \left[\frac{1}{s+b} \left[1, e^{-sT/3}, e^{-(2sT/3)} \right] \right]^T \begin{bmatrix} \frac{1}{s+a} \\ \frac{e^{sT/3}}{s+a} \\ \frac{e^{2sT/3}}{s+a} \end{bmatrix}^T \quad (159)$$

$$= \left[\frac{1}{s+b}, \frac{e^{-sT} e^{2sT/3}}{s+b}, \frac{e^{-sT} e^{sT/3}}{s+b} \right]^T \begin{bmatrix} \frac{1}{s+a} \\ \frac{e^{sT/3}}{s+a} \\ \frac{e^{2sT/3}}{s+a} \end{bmatrix}^T \quad (160)$$

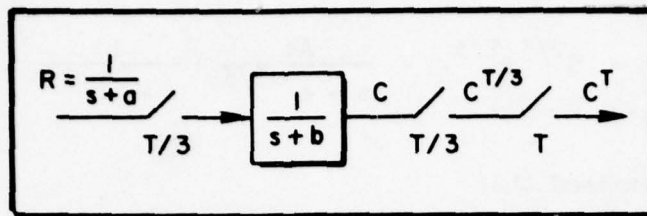


Figure 19. Illustrative Example

Note the manner in which w , written in terms of delay factors in Eq. 159 is converted to advanced factors in Eq. 160. Equation 160 is in a form suitable for the use of the advanced z -transform

$$\frac{e^{\Delta Ts}}{s+a} \rightarrow \frac{ze^{-a\Delta T}}{z - e^{-aT}}$$

Equation 160 becomes

$$C^T = \left[\frac{z}{z - e^{-bT}}, \frac{e^{-2bT/3}}{z - e^{-bT}}, \frac{e^{-bT/3}}{z - e^{-bT}} \right] \begin{bmatrix} \frac{z}{z - e^{-aT}} \\ \frac{ze^{-aT/3}}{z - e^{-aT}} \\ \frac{ze^{-2aT/3}}{z - e^{-aT}} \end{bmatrix} \quad (161)$$

Therefore,

$$C^T = \frac{z[z + e^{-2bT/3}e^{-aT/3} + e^{-bT/3}e^{-2aT/3}]}{(z - e^{-aT})(z - e^{-bT})} \quad (162)$$

Next, repeat the problem using the phantom sampler (Eq. 94):

$$R^{T/3} = \frac{z}{z - e^{-aT/3}}, \quad G^{T/3} = \frac{z}{z - e^{-bT/3}}, \quad z = e^{sT/3} \quad (163)$$

$$C^{T/3} = G^{T/3} R^{T/3} = \frac{Az}{z - e^{-aT/3}} + \frac{Bz}{z - e^{-bT/3}} \quad (164)$$

It is readily determined that

$$B = \frac{e^{-bT/3}}{e^{-bT/3} - e^{-aT/3}}, \quad A = \frac{-e^{-aT/3}}{e^{-bT/3} - e^{-aT/3}} \quad (165)$$

Equation 165 implies a continuous "generating" time function of the form

$$C(t) = Ae^{-at} + Be^{-bt} \quad (166)$$

so that upon resampling in the T frame time we obtain

$$C^T = \frac{Az}{z - e^{-aT}} + \frac{Bz}{z - e^{-bT}}, \quad z = e^{sT} \quad (167)$$

Substituting for A and B and then clearing gives

$$C^T = \frac{z[z + e^{-2bT/3}e^{-aT/3} + e^{-bT/3}e^{-2aT/3}]}{(z - e^{-aT})(z - e^{-bT})} \quad (168)$$

Equation 168 is in agreement with the switch decomposition result of Eq. 162.

One may conclude that the phantom sampler approach is more efficient than the vector switch decomposition approach when both approaches apply. On the other hand, vector switch decomposition always provides a means for analyzing system properties independently of system input signals which are unspecified or when various input signals are of interest. The computational approach one uses for any given problem should be selected on the basis of these considerations.

We may also note that the vector switch decomposition tool can be used to model the computational throughput delay of the computer. This topic is treated in Appendix F.

M. SECTION SUMMARY

A table of abbreviated transforms has been developed using the transform for an exponential function of time together with several transform domain properties. This table, coupled with partial fraction expansion, enables us to move back and forth between the t -, s -, and z -domains with relative ease. Basic background material for analysis of multi-rate sampled systems was also developed. Included were discussions of the "phantom sampler," vector switch decomposition, and the "T/N" transform approach. Examples have been used to demonstrate the strengths and weaknesses of each tool and to call attention to points which will be developed in greater depth in the text which follows.

SECTION III

ANALYSIS IN THE w' -DOMAIN

A. INTRODUCTION

During the 1950's and 1960's the need for simulating open- and closed-loop aircraft responses furnished an appreciable impetus for the development and refinement of discrete algorithms for the simulation of continuous systems using digital computers (e.g., Refs. 11-13). Thus, the Tustin transform method and other similar techniques for the approximate discretization of continuous systems made it feasible to replace analog computers with digital computers for the simulation phases of a design effort. Now, this approach is also commonly applied to design digital control laws for fly-by-wire aircraft. First a continuous control law is synthesized, and then it is adapted for digital implementation using one of the approximate discretization methods originally developed for simulation (e.g., Refs. 14-16). This procedure is called emulation.

This application of emulation for the design of a digital controller is motivated both by a fundamental reliance on system design criteria developed for analog systems and the justifiable desire to preserve the large body of design experience built up over the past twenty-five years. Emulation is an approximate procedure when the Tustin transform or other "direct substitution" methods are used. In general, emulation procedures fail to account for multiplexer/data bus effects and, more importantly, require use of high update rates (short computation frame times) in order that the inherent approximations be valid. Thus there is a need for a direct digital design procedure which is exact (in distinction to approximate), accounts for the effects of data holds, computational delays, etc., and yet preserves the experience and physical insight developed over the years using conventional design procedures. The main purpose of this section is to highlight the properties of a design domain wherein these objectives are realized.

Specifically, attention is focused on the w' -domain — a domain related to the well-known w -domain (Ref. 8) by an all-important scale factor. It

is a domain wherein the non-minimum phase effects of the sampling and data hold operations can be directly accounted for using conventional frequency domain design tools such as root locus and Bode plots. These conventional frequency domain design tools can be used to considerably greater advantage in the w' -domain than in the w - or z -domains because several more powerful analogies between the s -domain and the w' -domain exist. These analogies are, in a sense, the key to exploiting the w' -domain for design purposes, making direct design in the w' -domain an attractive alternative to design by emulation.

In the sections which follow, we first review basic properties which make the w' -domain preferable to the z -domain or w -domain. Following this, illustrative examples are used to highlight the analogies between s and w' . Next we demonstrate that satisfactory designs can be obtained using conventional design approaches even for low data rates where approximate discretization techniques are so seriously in error as to be invalid. Herein lies the main contribution: recognition that the w' -domain models the sampling and data hold operations exactly, regardless of the sampling rate employed, and that the w' -variable is analogous to the s -variable in the sense that all familiar frequency domain design concepts, procedures, and interpretations can be carried over directly.

B. RELATIONSHIPS BETWEEN z , w , AND w'

In the analysis of linear sampled data systems, use of $z \triangleq \exp(sT)$ results in transfer functions which are rational polynomial functions of z . This is in distinction to the corresponding transfer functions in s -domain terms which are transcendental functions of s . It is also the case that the left half of the s -plane is mapped into the interior of a unit circle in the z -plane. A drawback of the z -domain is that conventional design criteria, such as root locus and Bode plots, are more difficult to interpret. Moreover, at high sampling rates, the z -plane poles and zeros tend to cluster on the unit circle, creating numerical problems of a substantial magnitude. The region of the z -plane corresponding to stable system behavior is interior to the unit circle which prevents the direct application of Routh's stability criteria. Historically (e.g., see Ref. 8), this

fact prompted the application of an additional bilinear transformation which maps a function of z into a domain where the region of stability is once again the left half plane. This is the so-called w transformation defined by the equation:

$$w \triangleq \frac{z - 1}{z + 1} \quad (169)$$

One may use root locus and Bode plot methods in the w -domain with more facility and insight than would be possible in the z -domain, even though each domain contains exactly the same information.

However, the w -domain still lacks other desirable properties. Most important of these is the property that w approach s as the sampling interval approaches zero. This property is not provided since

$$w = \frac{z - 1}{z + 1} = \frac{e^{sT} - 1}{e^{sT} + 1} = \frac{sT + (sT)^2/2! + \dots}{2 + sT + (sT)^2/2! + \dots} \quad (170)$$

and in the limit, as $T \rightarrow 0$, w approaches zero rather than s . A simple scaling of the w -plane changes this situation dramatically. Define

$$w' \triangleq \frac{2}{T} w = \frac{2}{T} \frac{z - 1}{z + 1} \quad z = \frac{1 + (T/2)w'}{1 - (T/2)w'} \quad (171)$$

as the so-called " w -prime" transformation wherein

$$w' = \frac{2}{T} \frac{z - 1}{z + 1} = \frac{2}{T} \frac{e^{sT} - 1}{e^{sT} + 1} = \frac{2}{T} \frac{sT + (sT)^2/2! + \dots}{2 + sT + (sT)^2/2! + \dots} \quad (172)$$

In the limit as $T \rightarrow 0$ in Eq. 172, w' approaches s .

This property is significant in that it establishes the conceptual basis for defining a quantity in the w' -domain which is analogous to frequency in the s -domain. Furthermore, the analogy becomes an identity in the limiting case.

We are unable to cite a readily available reference for the transformation given in Eq. 172 even though the relationship is well known to many practicing control engineers.

One may, of course, use root locus and Bode plot methods in the w' -domain as well. However, the relationship between angular frequency, ω , and the imaginary part of w' , v , is

$$v = \frac{2}{T} \tan \omega T/2 \quad (v \doteq \omega \text{ for } |\omega| < \pi/2T) \quad (173)$$

The approximate relationship between v and ω is significant in that the designer/analyst may regard v as angular frequency (for $|v| < 2/T$) during qualitative phases of design development. Conversion to actual angular frequency units is almost always unnecessary. Moreover, $(w')^{-1}$ itself is the trapezoidal integration operator analogous to s^{-1} for continuous systems. Finally, the unit delay, z^{-1} , when expressed in the w' -domain, has break parameters which are a function of sampling period, T , and has the form of a first-order Pade approximation for a transport delay in the s -domain.

$$z^{-1} = -\frac{w' - 2/T}{w' + 2/T} \quad (174)$$

To illustrate another basic relationship which exists between the s -domain and the w' -domain, consider the z -transform for a continuous low-pass filter section

$$H(s) = \frac{a}{s + a} \quad (175)$$

obtained assuming the input signal to the filter has been reconstructed using a zero-order hold (ZOH). The result is

$$H(z) = \left[\frac{1 - e^{-sT}}{s} \frac{a}{s + a} \right]^T = \frac{1 - e^{-aT}}{z - e^{-aT}} \quad (176)$$

Applying Eq. 171 to Eq. 176 gives

$$H(w') = \frac{\frac{-(T/2)w' + 1}{\frac{T}{2} \frac{1 + e^{-aT}}{1 - e^{-aT}}} w' + 1}{\frac{2}{T} \frac{1 - e^{-aT}}{1 + e^{-aT}}} \frac{-(T/2)w' + 1}{w' + \frac{2}{T} \frac{1 - e^{-aT}}{1 + e^{-aT}}} \quad (177)$$

The equal-order over equal-order nature of Eq. 177 is, of course, a direct consequence of the use of Eq. 171. At first one may feel that the analogy between the s - and w' -domains is weak, since a proper rational function of s will always map into a rational equal-order over equal-order function of w' . However, this is not the case if zeros at infinity in the s -domain are considered, for then the s -domain zeros at infinity correspond to the "extra" finite zeros in the w' -plane. For example, Eq. 175 shows that $H(s)$ has a pole at $s = -a$ and a zero at infinity. In the w' -plane the pole at $s = -a$ is mapped into

$$w' = -\frac{2}{T} \frac{1 - e^{-aT}}{1 + e^{-aT}} \quad (w' \doteq -a \text{ for } |a| < \pi/2T) \quad (178)$$

while the zero at $s = \infty$ is mapped into a zero at $w' = 2/T$. Obviously, as $T \rightarrow 0$, $w' \rightarrow s$, the w' -domain pole goes to $-a$ and the w' -domain zero approaches infinity, its proper s -plane location. This is a general result; every pole and zero in the w' -plane has its counterpart in the s -plane, as long as the zeros at infinity in the s -plane are counted.

Notice now the clear resemblance of Eq. 177 to its s -domain counterpart. This is in distinction to the z -domain counterpart (Eq. 176) which has a pole that approaches the unit circle as $T \rightarrow 0$.

The zero at $w' = 2/T$ is especially significant. This zero is introduced by the ZOH used to reconstruct the input to $H(s)$. It provides a nonminimum-phase contribution which is the effect of the data hold sampling rate parameter. This provides another major advantage of the w' -domain in comparison to the z -domain since the effect of the data hold and sample rate will be quite apparent in root locus or Bode plots. To emphasize this point, let the input to the continuous filter be reconstructed with another type of

data hold called the "slewer data hold." The slewer data hold results in constant rate output between sampling instants and has no discontinuity at the sampling instant. Using the slewer, one computes

$$H(z) = \left[\frac{(1 - e^{-sT})^2}{Ts^2} \frac{a}{s + a} \right]^T \quad (179)$$

$$= \frac{\left[\left(T - \frac{1}{a} \right) + \frac{e^{-aT}}{a} \right] z + \left[\frac{1}{a} - \left(T + \frac{1}{a} \right) e^{-aT} \right]}{Tz(z - e^{-aT})} \quad (180)$$

Or, using Eq. 171,

$$H(w') = \frac{\left[\frac{(T - 2/a) + (T + 2/a)e^{-aT}}{2(1 - e^{-aT})} w' + 1 \right] \left[-\frac{T}{2} w' + 1 \right]}{\left[\frac{T}{2} \frac{1 + e^{-aT}}{1 - e^{-aT}} w' + 1 \right] \left[\frac{T}{2} w' + 1 \right]} \quad (181)$$

Observe that the slewer data hold has both a pole and zero in the w' -plane model. Thus it is seen that the use of a zero-order hold introduces a non-minimum phase zero at $w' = 2/T$ (refer to Eq. 177), whereas the slewer introduces both a pole and zero. Finally, note that Eq. 181 reduces to

$$\lim_{T \rightarrow 0} H(w') = \frac{a}{w' + a} \quad (182)$$

as was the case with the zero-order hold.

Table 5 summarizes the relationships between the various planes for three different filter sections assuming the use of a zero-order hold. One may evaluate these transfer functions, using T as a parameter, to obtain a feel for the relative positioning of poles and zeros in the three domains.

Thus far, three important properties of the w' -domain have been enumerated:

TABLE 5
REPRESENTATIVE s, z, AND w' PLANE TRANSFER FUNCTIONS

$H(s)$	$H(z)$	$H(w')$
$\frac{s}{s^2 + a^2}$	$\frac{1 - e^{-aT}}{z - e^{-aT}}$	$\frac{1 - (T/2)w'}{T \frac{1 + e^{-aT}}{2} w' + 1}$
$\frac{s^2 + a^2}{s^2 + a^2 + b^2}$	$\frac{1 - e^{-aT}}{z - 2e^{-aT} \cos bT + e^{-2aT}}$	$\frac{1 + \frac{1}{2} \frac{w'}{1 + e^{-aT}}}{1 + \frac{e^{-aT} \cos bT}{1 + e^{-2aT} - 2e^{-aT} \cos bT + 1}}$
$\frac{s^2 + b^2}{s^2 + a^2 + b^2}$	$\frac{1 - e^{-aT} \cos bT}{z - 2e^{-aT} \cos bT + e^{-2aT}}$	$\frac{\left[\frac{1 + \frac{1}{2} \frac{w'}{1 + e^{-aT}} \right] \left(\frac{1 - e^{-aT} \cos bT}{1 + e^{-2aT} - 2e^{-aT} \cos bT + 1} \right)}{\left[\frac{1 + \frac{1}{2} \frac{w'}{1 + e^{-aT}} \right] \left(\frac{1 - e^{-aT} \cos bT}{1 + e^{-2aT} - 2e^{-aT} \cos bT + 1} \right) + \frac{1}{2} \frac{w'}{1 + e^{-aT}}}$

Example: $\frac{s}{(s+1)^2 + 2^2} \longleftrightarrow \frac{5.004086913}{w'^2 + 2.018401616w' + 5.025028} \left[-\frac{w'}{2} + 1 \right]$

T = 0.1

Example: $\frac{5}{s^2 + 2s + 5} \longleftrightarrow \frac{5.025028}{w'^2 + 2.018401616w' + 5.045208} \left(\frac{1}{2} - \frac{w'}{2} + 1 \right)$

T = 0.1

Note: Input signal smoothed with zero-order hold.

- $w' \rightarrow s$ as $T \rightarrow 0$.
- The nonminimum-phase effects of data holds become clearly evident.
- Conventional methods for stability analyses continue to be applicable since the left half of the w' -plane corresponds to the left half of the s -plane.

A most important property of the w' -domain which remains to be shown is:

- Conventional frequency domain synthesis methods (both scalar and vector) continue to be applicable, even when the sampling rate is so low as to cause large differences between s -plane and w' -plane pole and zero locations for a given plant.

This property is the topic of the next two subsections.

C. ILLUSTRATIVE DESIGN PROBLEM — SHORT-PERIOD AIRCRAFT MODEL

Conventional frequency domain design methods are directly applicable in the w' -domain. This will be demonstrated in two stages. In this subsection we first consider the design of a stability augmentation system using a representative model of a short-period aircraft.* The use of the second-order model will allow us to illustrate clearly the manner in which the non-minimum phase contribution of the data hold affects closed-loop system properties and responses. (Furthermore, these effects are different for a disturbance input than they are for a command input.) The short-period model will, however, tend to have modal frequencies well below the folding frequency even for data rates as low as ten samples/second. Thus, the most dramatic effect that folding (or aliasing) may have upon the plant w' transfer functions will not be evident. Therefore, in the next subsection we consider a fourth-order aircraft model which includes a high frequency, lightly damped bending mode for which the effects of folding are dramatic. This will enable us to demonstrate that the w' -domain continues

*The technical details of the models used in this subsection and the next are contained in Ref. 17.

to yield satisfactory closed-loop designs even when the differences between the s-domain and w'-domain modal representations are large.

Consider first the simplified aircraft model of Eq. 183:

$$\begin{bmatrix} \dot{q} \\ \dot{\alpha} \end{bmatrix} = \begin{bmatrix} -1 & -37 \\ 1 & -3 \end{bmatrix} \begin{bmatrix} q \\ \alpha \end{bmatrix} + \begin{bmatrix} -50 \\ 0 \end{bmatrix} \delta_e + \begin{bmatrix} -37 \\ -3 \end{bmatrix} \alpha_g \quad (183)$$

In Eq. 183, δ_e is the control input, α_g is the gust disturbance input, and q (body axis pitch rate) and α (inertial angle-of-attack component) are the states of the system. Suppose the continuous controller is designed using the multiloop analysis technique of Refs. 18 and 19. The block diagram of Fig. 20 defines the closed-loop configuration with postulated compensation networks H_1 , H_2 , and H_3 . In Fig. 20, H_1 , H_2 , and H_3 are to be determined (designed), R is the command input, and x_1 and x_2 are used to represent the states q and α , respectively. Application of the multiloop analysis method

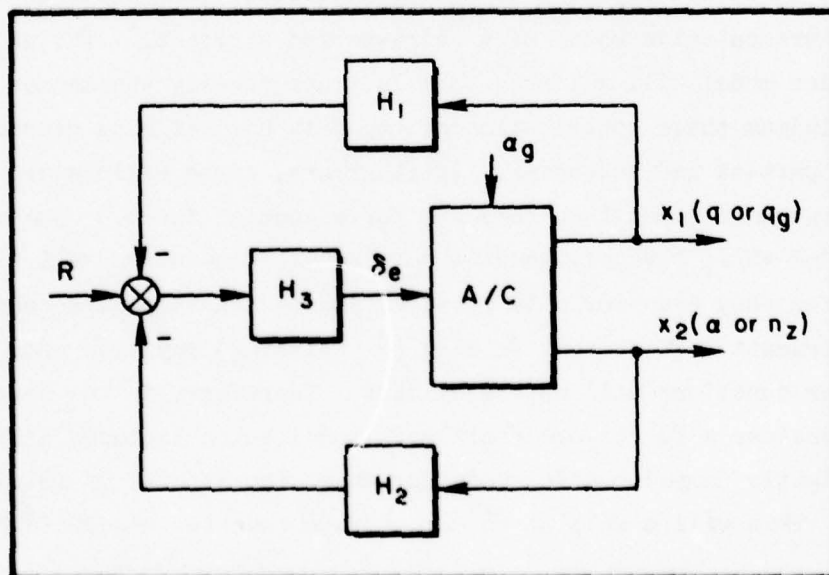


Figure 20. Block Diagram, Illustrative Example

yields the matrix of closed-loop transfer functions directly. The theoretical details of the multiloop analysis method are documented in Chapter 3 of Ref. 18.

$$\begin{bmatrix} x_1 \\ x_2 \end{bmatrix} = \frac{\begin{bmatrix} N_{\delta_e}^{x_1} H_3 & N_{\alpha_g}^{x_1} + H_2 H_3 N_{\alpha_g \delta_e}^{x_1 x_2} \\ N_{\delta_e}^{x_2} H_3 & N_{\alpha_g}^{x_2} + H_1 H_3 N_{\alpha_g \delta_e}^{x_2 x_1} \end{bmatrix} \begin{bmatrix} R \\ \alpha_g \end{bmatrix}}{\Delta + H_2 H_3 N_{\delta_e}^{x_2} + H_1 H_3 N_{\delta_e}^{x_1}} \quad (184)$$

The various numerators of Eq. 184 are found using Cramer's rule applied to the Laplace transform of Eq. 183 (see Eq. 185).

$$\begin{bmatrix} s + 1 & 37 \\ -1 & s + 3 \end{bmatrix} \begin{bmatrix} x_1 \\ x_2 \end{bmatrix} = \begin{bmatrix} -50 & -37 \\ 0 & -3 \end{bmatrix} \begin{bmatrix} \delta_e \\ \alpha_g \end{bmatrix} \quad (185)$$

$N_{\delta_e}^{x_2}$, for example, is found by substituting the δ_e column on the right-hand side of Eq. 185 into the x_2 column on the left-hand side of Eq. 185 and evaluating the determinant of the array that results. Δ is the characteristic open-loop polynomial and is the determinant of the left-hand matrix in Eq. 185. To illustrate

$$\Delta = \begin{vmatrix} s + 1 & 37 \\ -1 & s + 3 \end{vmatrix} = s^2 + 4s + 40 = (s + 2)^2 + (6)^2 \quad (186)$$

$$N_{\delta_e}^{x_2} = \begin{vmatrix} s + 1 & -50 \\ -1 & 0 \end{vmatrix} = -50 \quad (187)$$

$$N_{\delta_e}^{x_1} = -50(s + 3) \quad (188)$$

$$N_{ag}^{x_1} = -37s$$

(189)

$$N_{ag}^{x_2} = -(3s + 40)$$

(190)

The numerators of the "second kind" (coupling numerators), $N_{ag\delta e}^{x_1 x_2} = -N_{ag\delta e}^{x_1 x_2}$, are found by making two column substitutions and computing the determinant of the resulting array.

$$N_{ag\delta e}^{x_2 x_1} = \begin{vmatrix} -50 & -37 \\ 0 & -3 \end{vmatrix} = 150 = -N_{ag\delta e}^{x_1 x_2}$$

(191)

Substitution of these equations into Eq. 184 gives Eq. 192:

$$\begin{bmatrix} x_1 \\ x_2 \end{bmatrix} = \frac{\begin{bmatrix} -3.75[(s/3) + 1]H_3 & -0.925s - 3.75H_2H_3 \\ -1.25H_3 & -1[(s/13.33) + 1] + 3.75H_1H_3 \end{bmatrix} \begin{bmatrix} R \\ a_g \end{bmatrix}}{\left(\frac{s^2}{40} + \frac{4}{40}s + 1\right) - 1.25H_2H_3 - 3.75\left(\frac{s}{3} + 1\right)H_1H_3}$$

(192)

From this point on, the design effort for a continuous controller would focus on the specification of H_1 , H_2 , and H_3 in order to achieve desirable closed-loop characteristics. Bode plots, Nyquist diagrams, root loci, etc., could be used to achieve this goal. Rather than dwell on these well understood facets of the frequency domain synthesis, we turn our attention instead to the synthesis of a (single rate) digital controller for the plant described by Eq. 183.

Suppose Fig. 20 is modified to explicitly account for A/D and D/A conversions. A simplified representation of the digital control system is shown in Fig. 21, where the elements interior to the dotted box represent the continuous elements (plant and data hold) of the overall system. The input R is assumed to undergo an A/D conversion that is adequately modeled

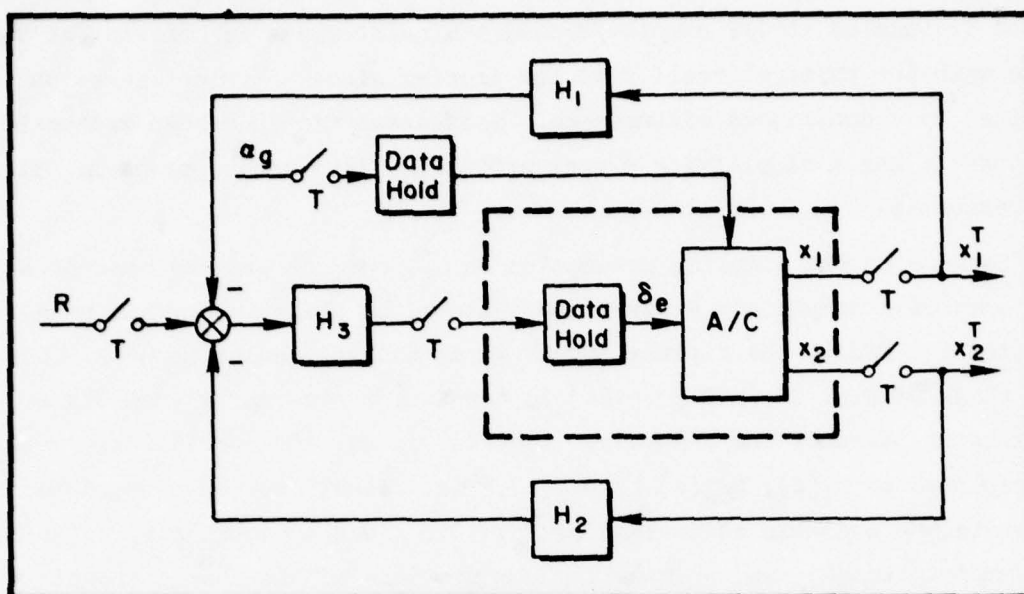


Figure 21. Digital Control Block Diagram

by a sampler. All the remaining elements of Fig. 21 are to be implemented on a digital computer. For simplicity of presentation, the data hold is assumed to be a zero-order hold; however, the synthesis procedure we are about to explore will be directly applicable for other types of data holds as well.

Taking the z -transform of the first-order set of differential equations given in Eq. 183 gives:

$$\begin{bmatrix} z - .752776009 & 2.850789304 \\ -.07704836 & z - .59867929 \end{bmatrix} \begin{bmatrix} x_1(z) \\ x_2(z) \end{bmatrix} = \begin{bmatrix} -4.490576597 & -2.850789304 \\ -.212719539 & -.401320710 \end{bmatrix} \begin{bmatrix} \delta_e \\ a_g \end{bmatrix} \quad (193)$$

Equation 193 may be developed from Eq. 183 using either time domain or frequency domain approaches (refer to Appendix F). We have assumed the gust

input is sampled at $1/T$ samples/second and held. This is somewhat at variance with the physical reality of the problem since the plant is actually excited by a continuous disturbance. This assumption has been made merely because it has a simplifying effect upon this illustrative problem. It is not essential.

Because of the sampling assumption on α_g , one can proceed conceptually in terms of a completely discretized system; the state vector has been sampled and fed to the digital computer, as has the scalar input R . One may think of Fig. 20 (and Eq. 184) in terms of the z - and w' -domains as well as in terms of the s -domain. That is, in Eq. 184 consider $x_1(s)$ to be replaced by $x_1(z)$, $N_{8e}^{x_2}(s)$ by $N_{8e}^{x_2}(z)$, etc. Thus, one can proceed to generate the z -domain equivalent of Eq. 192, given a sampling rate (assume 10 samples/second), and upon making computations of the characteristic polynomial and numerators of the first and second kinds.

z -Domain

$$\begin{bmatrix} x_1(z) \\ x_2(z) \end{bmatrix} = \frac{\begin{bmatrix} (-4.491z + 3.295)H_3 & | & (-2.851z + 2.851) + H_2H_3(-1.196) \\ (-.2127z - .1859)H_3 & | & (-.4013z + .0825) + H_1H_3(1.196) \end{bmatrix} \begin{bmatrix} R(z) \\ \alpha_g(z) \end{bmatrix}}{(z^2 - 1.352z + .6703) + H_2H_3(-.2127z - .1859) + H_1H_3(-4.491z + 3.295)}$$

(194)

The closed-loop z -domain equation is not easily interpreted by methods useful for interpreting the closed-loop s -domain equations. To facilitate interpretation; it is our assertion that the w' -transform should be applied to Eq. 194, i.e., $z = [1 + (T/2)w']/[1 - (T/2)w']$. The result is given in Eq. 195. The reader should compare the numerical values for the gains and break frequencies in Eq. 195 with the corresponding quantities in Eq. 192. Close correspondence for many of these numerical values should be noted.

w' -Domain

$$\begin{bmatrix} x_1 \\ x_2 \end{bmatrix} = \frac{\begin{bmatrix} -3.750000159\left(\frac{w'}{3.072} + 1\right)H_3\left(1 - \frac{w'}{20}\right) & | & -.89404w'\left(1 - \frac{w'}{20}\right) - 3.75H_2H_3\left(1 - \frac{w'}{20}\right)^2 \\ -1.250000067\left(\frac{w'}{296.81} + 1\right)H_3\left(1 - \frac{w'}{20}\right) & | & -1.000000051\left(\frac{w'}{13.1823}\right) + 3.75H_1H_3\left(1 - \frac{w'}{20}\right)^2 \end{bmatrix} \begin{bmatrix} R \\ \alpha_g \end{bmatrix}}{\left(\frac{w'^2}{42.2089} + \frac{4.3641}{42.2089}w' + 1\right) - 1.250000067\left(\frac{w'}{296.81} + 1\right)H_2H_3\left(1 - \frac{w'}{20}\right) - 3.750000159\left(\frac{w'}{3.0718} + 1\right)H_1H_3\left(1 - \frac{w'}{20}\right)}$$

(195)

It is our contention that the effects of the sample/hold operation, the data rate, etc., are readily apparent in Eq. 195. Comparing Eqs. 195 and 192 it is seen that:

- Numerators of the first kind pick up additional zeros at $2/T$ in such a way that they have the same degree as the characteristic polynomial.
- Numerators of the second kind pick up additional zeros at $2/T$ in such a way that they are equal in degree to the characteristic polynomial.
- Every entry in the s-domain equation can be considered to be equal-order over equal-order if the zeros at infinity are included.
- Every entry in the w'-plane equation is equal-order over equal-order. Zeros at infinity in the s-plane move to either $2/T$ or some other location, for example:

$$-1.25H_3(s) \rightarrow -1.25\left(\frac{w'}{297} + 1\right)\left(1 - \frac{w'}{20}\right)H_3(w') \quad (196)$$

- The numerical values of gains and time constants in the w'-plane are very similar to their s-plane counterparts. (Although not demonstrated in this example, this observation holds only for modes having an s-plane modal frequency which is well below the folding frequency ($2Ws$ equals $4\pi/T$). The fact that this observation holds true only under the stated conditions does not limit validity of the w'-plane analysis techniques in any way when the stated conditions are not satisfied. That this is so is demonstrated in the next subsection.)

Thus, one may proceed in the w'-domain using all the familiar synthesis tools of the s-domain. The direct digital design in the w'-domain, however, proceeds with additional explicit knowledge of the nonminimum-phase effects introduced by the A/D and D/A conversion through the zeros introduced at $2/T$ (equal to 20 rad/sec for this example). If these nonminimum-phase effects become significant (the zeros move closer to the origin as the sampling rate is decreased) then they can be regarded in exactly the same manner and treated using the same techniques as are used in the s-domain.

The actual synthesis will not be carried out since the prime objective was to highlight the analogy between the closed-loop transfer functions in

the s-, z-, and w'-domains. A synthesis will be carried to completion for the more complex aircraft model used in the next subsection.

D. SHORT-PERIOD AIRCRAFT WITH BENDING MODE

It remains to demonstrate the utility of the w'-domain in the face of substantial folding effects. This can be done by modifying the example of the previous section to present a more realistic design situation. Specifically, the aircraft model is modified to include a lightly damped bending mode at 25 rad/sec (this will be close to the 10 samples/second aliasing frequency of 31.4 rad/sec) and to include accelerometer and rate gyro output equations. Thus, we will have one control input, one disturbance input, four components in the state vector, and two components in the output vector. The details of the model are given in Ref. 17. For our present purposes, it is sufficient to modify our interpretation of the block diagram of Fig. 20. Let the bending mode state be called x_b , the output of the accelerometer (n_z) be x_1 , and the output of the rate gyro (q_g) be x_2 . The open-loop transfer functions are given in Eqs. 197 and 198:

s-Domain

$$\begin{bmatrix} x_1(s) \\ x_2(s) \end{bmatrix} = \begin{bmatrix} n_z \\ q_g \end{bmatrix} = \frac{\begin{bmatrix} -117.72[.141, 35.2][-.0314, 26.357] \\ -3.7975\left[\frac{s}{3.1045} + 1\right][.0152, 24.346] \end{bmatrix}}{[.355, 6.675][.01, 25]} \delta_e \quad (197)$$

w'-plane ($T = 0.1$)

$$\begin{bmatrix} x_1(w') \\ x_2(w') \end{bmatrix} = \begin{bmatrix} n_z \\ q_g \end{bmatrix} = \frac{\begin{bmatrix} -123.5\left(-\frac{w'}{27.53} + 1\right)\left(\frac{w'}{13020} + 1\right)[.1, 32.62] \\ -3.7974\left(\frac{w'}{3.22} + 1\right)\left(-\frac{w'}{20} + 1\right)[.069, 107.22] \end{bmatrix}}{[.3789, 6.864][.0417, 60.137]} \delta_e \quad (198)$$

In these equations quadratic factors $[s^2 + 2\zeta\omega_n s + \omega_n^2]$ have been shown in the shorthand form $[\zeta, \omega_n]$. Comparison of the corresponding numerator and characteristic polynomial roots in Eqs. 197 and 198 leads to the following observations:

- The short-period quadratic is essentially the same in either the s- or w'-domains.
- The bending mode at 25 rad/sec s-domain has been shifted upward to 60 rad/sec in the w'-domain. (A still lower sampling rate could shift it downward.)
- The n_z numerator, which is equal-order over equal-order in the s-domain does not have the zero at $w' = 2/T$.

Clearly, we now have a design problem where the folding effects are significant. However, the closed-loop design can still be synthesized using conventional multiloop frequency domain techniques. The following compensation was arrived at using mainly root locus techniques.

$$H_1 H_3 = 0.006 \quad (199)$$

$$H_2 H_3 = 0.0085 \frac{w' + 1.644}{w' + 3.273} \quad (200)$$

This translates back into the z-domain (and gives the required recursion equation for the discrete control law) as:

$$H_1 H_3 = 0.006 \quad (201)$$

$$H_2 H_3 = \frac{.0079z - .0067}{z - .71875} \quad (202)$$

The closed-loop relationships are given by Eq. 184, which is valid for both the s- or w'-domains. Rather than give numerical comparison between s and w' using Eq. 171 (as was done in the previous section), it is our preference to show Bode plots for the closed-loop system in the s- and w'-domains. The Bode plots for the transfer functions of interest are plotted in Figs. 22, 23, and 24. Notice in particular the effect of the nonminimum-phase zero on the magnitude and phase plots.

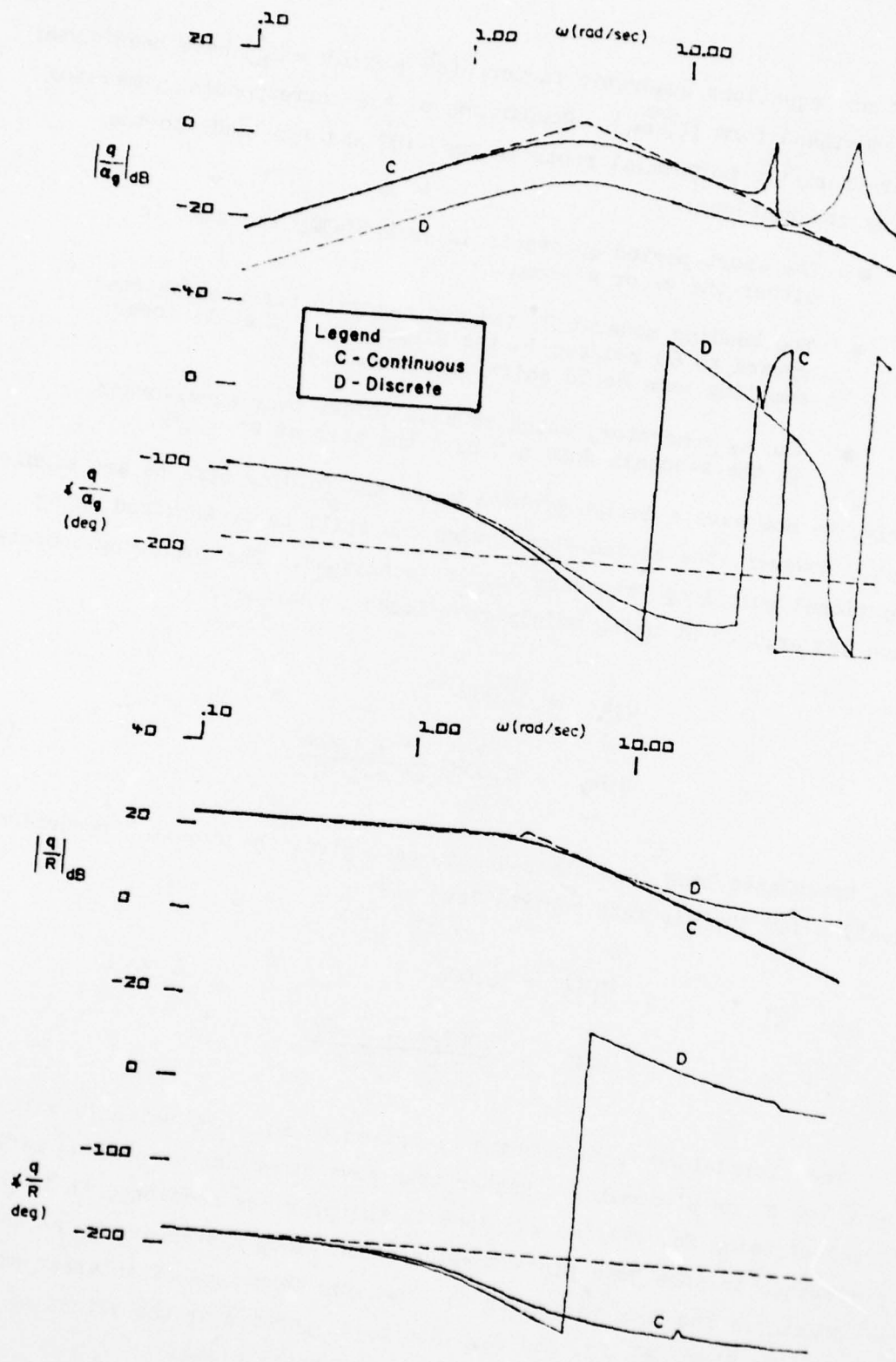


Figure 22. Bode Plots q/α_g , q/R

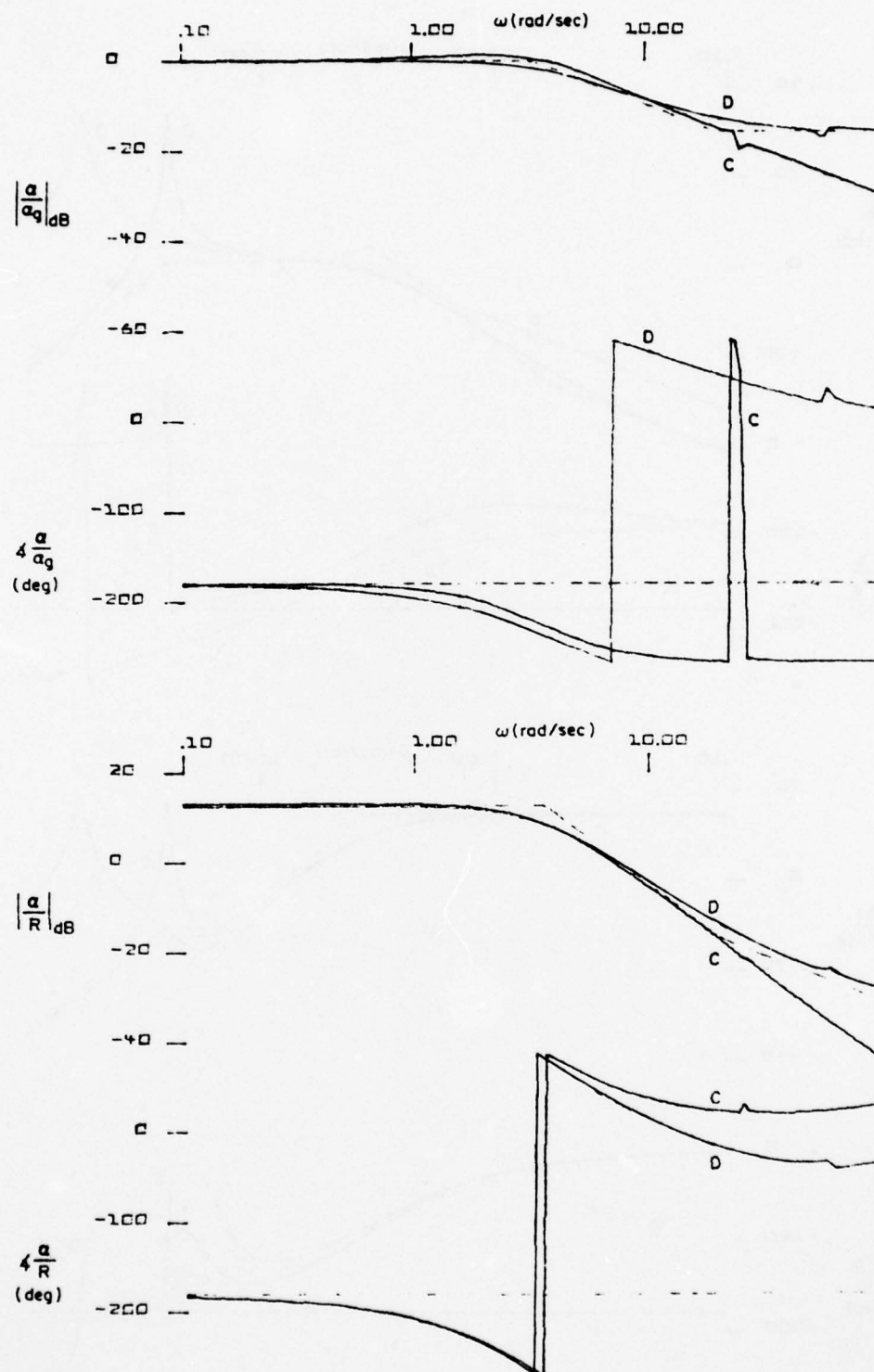


Figure 23. Bode Plots α/α_g , α/R

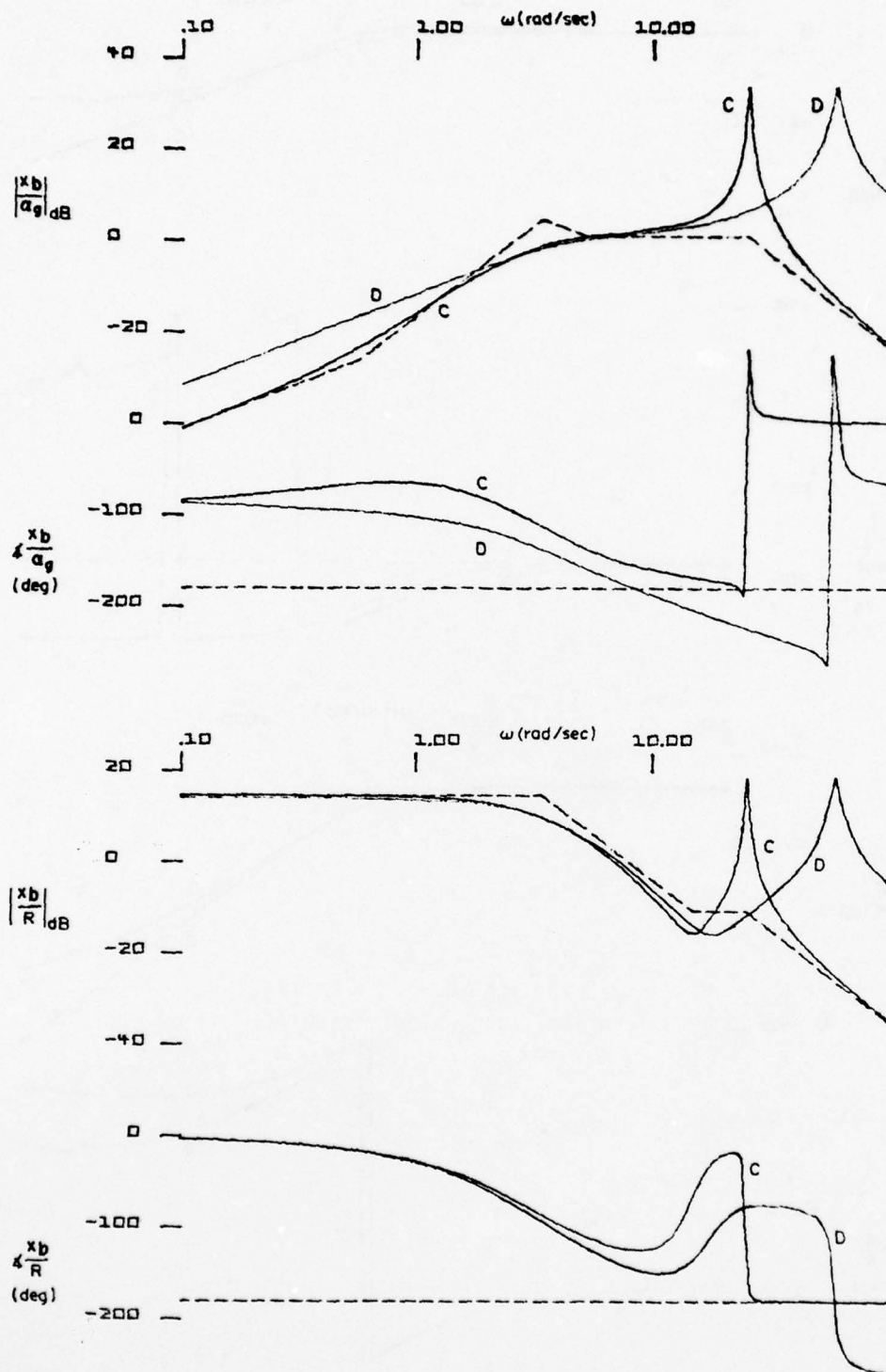


Figure 24. Bode Plots x_b/a_g , x_b/R

At this point we come face to face with the central question, "Are s-domain design procedures and concepts effective in the w'-domain?" We proceeded with the design in the w'-domain on the hypothesis that these design procedures and concepts are effective and with the knowledge that the w'-domain transfer functions for the plant properly and comprehensively incorporate all the effects of the data hold and sampling rate for all modes. To demonstrate that this hypothesis is correct we must check the time responses for the discrete controlled system to see if they are acceptable. This is done for the q variable in Fig. 25. Notice that there is no basis to conclude that the performance of the digitally controlled system is inferior to that of the continuously controlled one or vice versa. In fact, the use of an accelerometer feedback gain of 0.006 has resulted in a lower q/α_g amplitude ratio at lower frequencies for the digitally controlled system.

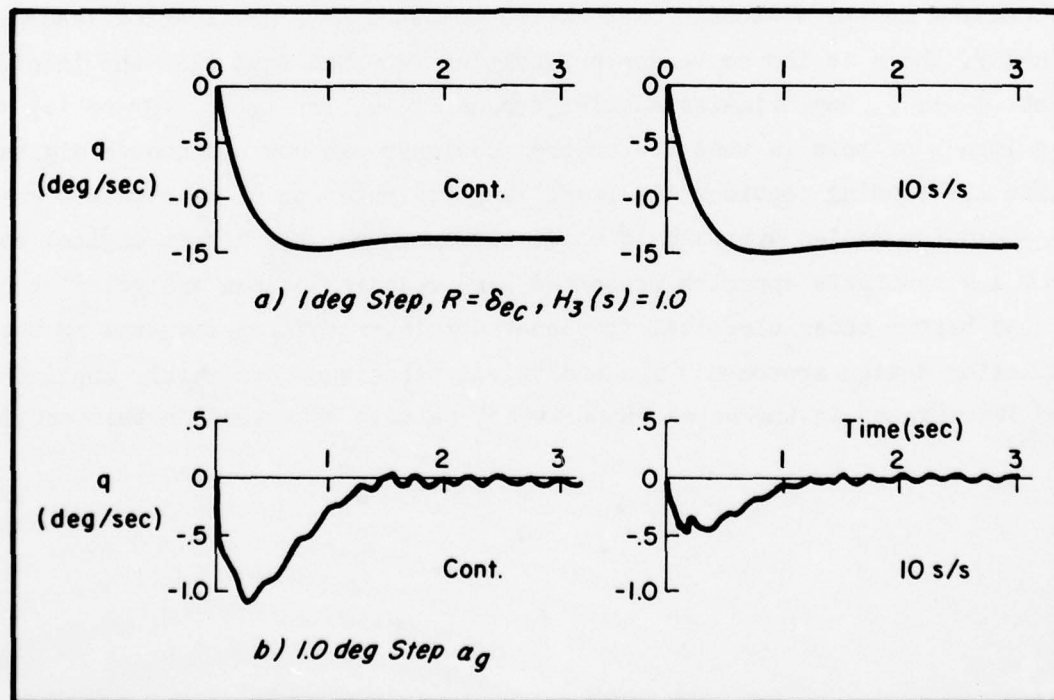


Figure 25. q Transient Responses of Continuous and Digitally Controlled Systems

E. SECTION SUMMARY

Analogies between system formulations in the s - and w' -domains have been drawn. To arrive at the w' -plane formulation one must first discretize the problem by means of a valid mathematical technique if the effects of data holds are to be represented exactly. This leads to a statement of the discretized problem in the z -domain. The z -domain statement of the problem is then converted to a w' -domain statement by means of a bilinear algebraic transformation.

It has been demonstrated that direct digital control law synthesis in the w' -domain is a viable and practical alternative to design by emulation of a continuous system. Key properties of the w' -domain have been stated, and the "visibility" of data hold and sampling rate non-minimum phase effects in the w' -domain has been demonstrated. Most importantly, it has been pointed out that conventional frequency domain design procedures, such as multiloop analysis, Bode plots, root locus, etc., are valid and useful procedures in the w' -domain even in the presence of significant aliasing. Finally, there is the convenience resulting from the fact that the imaginary part of w' , v , approximates angular frequency, ω , for $|\omega| < \pi/2T$ or $|v| < 2/T$. The impact of this is that the control designer can now synthesize digital controllers using considerably lower sampling rates than are required when an emulation design approach is used. Furthermore, the direct digital control law synthesis approach presented here requires no new analytical techniques beyond those classical frequency domain procedures required by the emulation design approach. The analytical techniques are merely applied and interpreted in the novel manner which we have described in this section.

SECTION IV

MULTI-RATE TRANSFORM DOMAIN APPROACH

A. INTRODUCTION

The existing state of affairs with regard to the multi-rate problem (introduced in Section II) can be reviewed with the aid of Fig. 26. It may well be that our major interest in Fig. 26 is the response of the continuous output C in response to the input $r(t)$. This can, of course, be computed, since

$$C(s) = G(s)R^T(s) \quad (203)$$

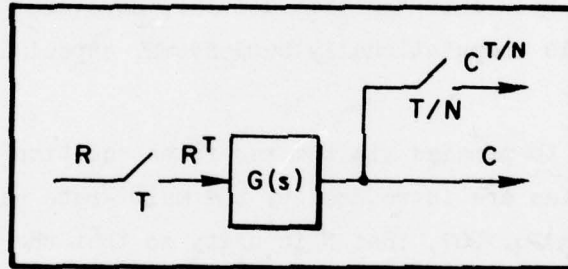


Figure 26. A Basic Multi-Rate Configuration

For example, if $G(s) = 1/(s+2)$ and $R(s) = 1/s$, then we may write, setting $z = e^{sT}$,

$$C(s) = \frac{1}{(s+2)} \frac{z}{(z-1)} = \left(\frac{1}{s+2} \right) (1 + z^{-1} + z^{-2} + \dots) \quad (204)$$

Therefore,

$$C(t) = e^{-2t} u(t) + e^{-2(t-T)} u(t-T) + e^{-2(t-2T)} u(t-2T) + \dots \quad (205)$$

Equation 205, while correct, is not very illuminating. We can gain more insight and increase computational efficiency by looking at the inter-sample

response at a finite number of points. This is indicated by the use of a sampler working in a T/N frame time. The basic property of the transform domain, discussed in Section II, can be invoked to give

$$C^{T/N} = [GR^T]^{T/N} = G^{T/N} R^T \quad (206)$$

Letting $z = e^{sT/N}$ gives, for our illustrative example,

$$C^{T/N} = \frac{z}{z - e^{-2T/N}} R^T = \left(\frac{z}{z - e^{-2T/N}} \right) \left(\frac{z^N}{z^N - 1} \right) \quad (207)$$

We could pursue a course of action that would yield a "closed form" answer by finding the $N+1$ poles of Eq. 207, expanding in partial fractions and inverting the result back into the time domain. However, this "increased dimension" approach is computationally burdensome, especially if the order of N is high.

Suppose we elect to proceed via the recursion equation route. What additional complexities are introduced by the multi-rate nature of the problem? Suppose, in Eq. 207, that N is unity so that the recursion equation becomes

$$C_{nT} = e^{-2T} C_{(n-1)T} + r_{nT} \quad (208)$$

In practice, one usually makes a mental note of the frame time and suppresses the use of it in the recursion equation:

$$C_n = e^{-2T} C_{n-1} + r_n \quad (209)$$

In general, the basic requirement is for four storage registers (r_n , C_{n-1} , e^{-2T} , C_n). Letting N be non-unity, define $z = e^{sT/N}$ and suppress the T/N frame time:

$$C_n = e^{-2T/N} C_{n-1} + r_{n,N}^T \quad (210)$$

But, $r_{n,N}^T$ merely indicates that $r(t)$ is being sampled every T seconds and therefore non-zero values result only for every N th occurrence. Therefore,

$$r_{n,N}^T = \begin{cases} 0 & n = 0, N, 2N, \dots \\ r(t) & \end{cases} \quad (211)$$

It is seen that the memory requirements of Eq. 210 are basically unchanged from Eq. 209. There is, of course, the calculational logic needed to implement Eq. 211. For the example,

$$C_n = e^{-nT/N} C_{n-1} + \begin{cases} 0 & n/N \neq \text{integer} \\ 1 & n/N = \text{integer} \end{cases} \quad (212)$$

While this pleasant state of affairs remains essentially unchanged when zero-order holds are used as couplers, the use of higher-order data holds (such as the slewer) does significantly increase the modeling complexity. These cases are discussed in succeeding sections.

B. USE OF ZERO-ORDER HOLDS AS COUPLERS

Modifying Fig. 26 to include a zero-order hold (ZOH) gives Fig. 27. As we shall see, the use of the zero-order hold will cause no increase in the dimensionality or storage requirements.

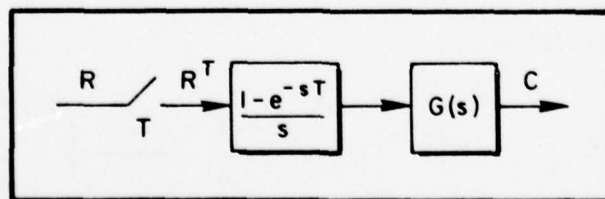


Figure 27. Zero-Order Hold Case

From Fig. 27,

$$C = G(s) \frac{(1 - e^{-sT})}{s} R^T \quad (213)$$

Evaluate Eq. 213 at a sampling interval of T/N :

$$C^{T/N} = \left[\frac{(1 - e^{-sT})}{s} [G(s)] \right]^{T/N} R^T \quad (214)$$

Let $z = e^{sT/N}$ so that Eq. 214 becomes

$$C^{T/N} = \frac{z^N - 1}{z^N} \left[\frac{G(s)}{s} \right]^{T/N} R^T$$

or

$$C^{T/N} = \frac{(z^N - 1)z}{z^N(z - 1)} \left[\frac{(1 - e^{-sT/N})}{s} [G(s)] \right]^{T/N} R^T \quad (215)$$

In Eq. 215 we have "inserted"

$$1 = \frac{z}{(z - 1)} \frac{(z - 1)}{z} = \frac{z}{z - 1} (1 - e^{-sT/N})$$

in order to give the bracketed term the same form as the single-rate case (see Eq. 214).

Equation 215 simplifies to:

$$C^{T/N} = [1 + z^{-1} + \dots + z^{-(N-1)}] \left[\frac{1 - e^{-sT/N}}{s} [G(s)] \right]^{T/N} R^T \quad (216)$$

Let the power series in z^{-1} operate on the input R^T :

$$c^{T/N} = \left[\frac{(1 - e^{-sT/N})[G(s)]}{s} \right]^{T/N} R^T[1 + z^{-1} + \dots + z^{-(N-1)}] \quad (217)$$

The first term in Eq. 217 is recognized as the z-transform of $G(s)$, on the assumption of smoothing by a zero-order hold, at the T/N sampling interval. Thus, it is computed in exactly the same manner that the T result is computed. Next, observe that $R^T[1 + z^{-1} + \dots + z^{-(n-1)}]$ has a particularly simple interpretation in the time domain:

$$R^T[1 + z^{-1} + \dots + z^{-(N-1)}] \rightarrow R_n^T + R_{n-1}^T + \dots + R_{n-(N-1)}^T \quad (218)$$

But R_n^T , for example, only has a non-zero value when the n index takes on a value which is a multiple of T . Thus, the T value is "held" N times before it is updated; this is the significance of Eq. 218. Therefore, we can note the following:

$$\left. \begin{aligned} R^T[1 + z^{-1} + \dots + z^{-(N-1)}] &= R[(n/N)_{INT}^T] = R_{n,N}^T \\ z^{-1}R^T[1 + z^{-1} + \dots + z^{-(N-1)}] &= R[(n-1/N)_{INT}^T] = R_{n-1,N}^T \\ &\vdots \\ z^{-m}R^T[1 + z^{-1} + \dots + z^{-(N-1)}] &= R[(n-m/N)_{INT}^T] = R_{n-m,N}^T \end{aligned} \right\} \quad (219)$$

In Eq. 219 the running index is divided by N and the integer value taken. The value of the argument is found by multiplying this number by T . Thus, to find the recursion equation for $c^{T/N}$, follow essentially the same procedure as when finding c^T . If one were seeking the T difference equation, $G(s)/s$ would be expanded in partial fractions, table look-up would give the individual components, and then these components would be placed in a rational format. The result would be of the form given in Eq. 220 (assume an m th order system).

$$C^T = \left[\frac{G(s)}{s} (1 - e^{-sT}) \right]^T R^T = \frac{a_0 z^m + a_1 z^{m-1} + \dots + a_m}{z^m + b_1 z^{m-1} + \dots + b_m} R(z) \quad (220)$$

From Eq. 220 the recursion equation is written directly (let nT , the time index, be represented by n):

$$C_n = -b_1 C_{n-1} - b_2 C_{n-2} - \dots - b_m C_{n-m} + a_0 R_n + a_1 R_{n-1} + \dots + a_m R_{n-m} \quad (221)$$

The recursion equation for $C^{T/N}$ has identically the same form as Eq. 221. Simply recompute the a 's and b 's (the coefficients) using a T/N sampling interval. Now let the index nT/N be n and write:

$$C_n = -b_1 C_{n-1} - b_2 C_{n-2} - \dots - b_m C_{n-m} + a_0 R_{n,N}^T + a_1 R_{n-1,N}^T + \dots + a_m R_{n-m,N}^T \quad (222)$$

In Eq. 222 the only noticeable change for the T/N case is the input notation (refer to Eq. 219).

We illustrate with several examples.

Example 1

Let

$$G(s) = \frac{a}{s + a} \quad (223)$$

The T recursion equation is

$$C_n = e^{-aT} C_{n-1} + (1 - e^{-aT}) R_{n-1}, \quad z = e^{sT} \quad (224)$$

whereas the T/N recursion equation is

$$C_n = e^{-aT/N} C_{n-1} + (1 - e^{-aT/N}) R_{n-1,N}^T, \quad z = e^{sT/N} \quad (225)$$

Example 2

Let

$$G(s) = \frac{s + b}{s + a} \quad (226)$$

so that

$$C^{T/N} = \frac{z - [1 - (b/a) + (b/a)e^{-aT/N}]}{z - e^{-aT/N}} R^T [1 + z^{-1} + \dots + z^{-(N-1)}] \quad (227)$$

The T recursion equation is

$$C_n = e^{-aT} C_{n-1} + R_n + \left(\frac{b}{a} - 1 - \frac{b}{a} e^{-aT} \right) R_{n-1}, \quad z = e^{sT} \quad (228)$$

whereas the T/N recursion equation is

$$C_n = e^{-aT/N} C_{n-1} + R_{n,N}^T + \left(\frac{b}{a} - 1 - \frac{b}{a} e^{-aT/N} \right) R_{n-1,N}^T, \quad z = e^{sT/N} \quad (229)$$

In the next section, these basic ideas will be extended in a manner that permits the analysis of multi-rate closed-loop systems containing zero-order holds. Before proceeding, it will be instructive to exercise Eq. 225 for a cosine wave input. This is done in Fig. 28 for the case where $T \equiv 1$, thus causing a sampling frequency of 2π rad/sec. The input frequency in Fig. 28a is $\pi/2$ rad/sec, which bears an integer relationship to the sampling frequency. On the other hand, the input frequency in Fig. 28b is 1.5 rad/sec, giving a ratio of the sampling frequency to the input frequency which is an irrational number. The effect of this on the "steady state" response is clear. In the steady state, Fig. 28a has acquired the additional attribute of periodicity, whereas Fig. 28b shows the modulation caused by the non-integer relationship between the input frequency and the sampling frequency.

The concept of the continuous frequency response of a discretely excited system will be developed in Section V. This will provide the tool for identifying the spectral components of waveforms such as those shown in Fig. 28.

AD-A067 177

SYSTEMS TECHNOLOGY INC HAWTHORNE CALIF

F/G 1/3

ANALYSIS OF DIGITAL FLIGHT CONTROL SYSTEMS WITH FLYING QUALITIE--ETC(U)

SEP 78 R F WHITBECK, L G HOFMANN

F33615-77-C-3026

UNCLASSIFIED

STI-TR-1101-1-VOL-2

AFFDL-TR-78-115-VOL-2

NL

2 OF 3

AD
A067177



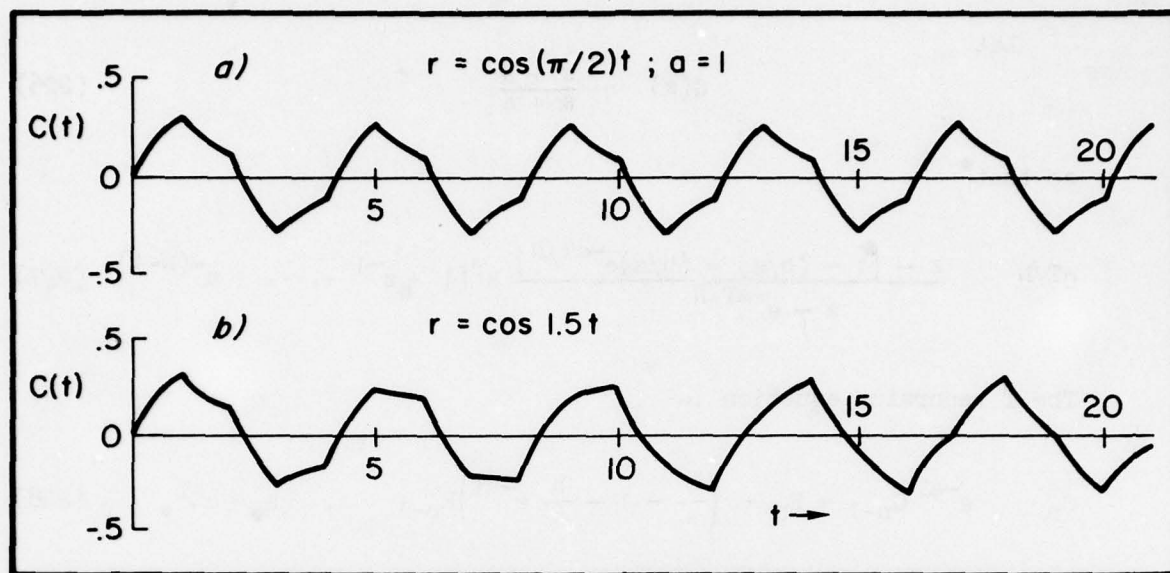


Figure 28. Response to a Cosine Wave Input

C. MULTI-RATE FORMULATION

The type of recursion equation developed in the previous section can be used to advantage in the analysis of closed-loop systems. To develop the basis ideas, we note that the transform approach states that if

$$C(s) = F_1(s) F_2^{T/M}(s) \quad (230)$$

then

$$C^{T/N} = F_1^{T/N} F_2^{T/M} \quad (231)$$

given N/M is an integer (see also Appendix B). The impact of this can be appreciated by considering Fig. 29.

The output equation is, letting $z = e^{sT/N}$,

$$C^{T/N} = \left[\frac{(1 - e^{-sT/M})}{s} G(s) \right]^{T/N} R^{T/M} \quad (232)$$

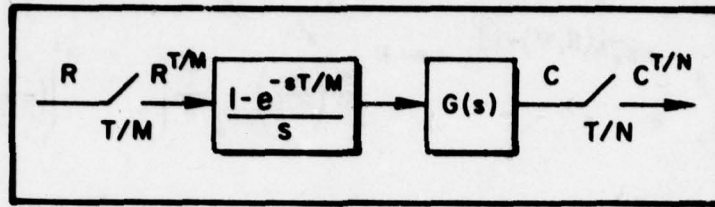


Figure 29. An Open-Loop Multi-Rate System

or

$$C^{T/N} = \left(\frac{z^{N/M} - 1}{z^{N/M}} \right) \left[\frac{G(s)}{s} \right]^{T/N} R^{T/M} \quad (233)$$

Rearranging gives

$$C^{T/N} = \frac{z^{N/M} - 1}{z^{N/M}} \cdot \frac{z}{z - 1} \left[\frac{1 - e^{-sT/N}}{s} G(s) \right]^{T/N} R^{T/M} \quad (234)$$

Again, let the power series in z^{-1} operate on the input $R^{T/M}$

$$C^{T/N} = \left[\frac{1 - e^{-sT/N}}{s} G(s) \right]^{T/N} R^{T/M} [1 + z^{-1} + \dots + z^{-(N/M)-1}] \quad (235)$$

and then interpret the time domain implications

$$R^{T/M} [1 + z^{-1} + \dots + z^{-(N/M)-1}] \rightarrow R_n^{T/M} + R_{n-1}^{T/M} + \dots + R_{n-(N/M)-1}^{T/M} \quad (236)$$

$R_n^{T/M}$, for example, only has a non-zero value when the n index takes on a value which is a multiple of T/M . Thus, the T/M value is "held" N/M times before it is updated. Therefore, we can write

$$R^{T/M} [1 + z^{-1} + \dots + z^{-(N/M)-1}] \rightarrow R \left[\frac{N}{M} \left(\frac{n}{N/M} \right)_{\text{INT}} \frac{T}{N} \right] = R \left[\left(\frac{n}{N/M} \right)_{\text{INT}} \frac{T}{M} \right]$$

$$= R_{n, N/M}^{T/M} \quad (237)$$

In Eq. 237, T/M is the sampling interval of the input, n is the running index of the recursion equation, N/M (which is an integer) is the number of indexing periods for which the input is held constant before updating.

D. A CLOSED-LOOP MULTI-RATE APPLICATION

The type of recursion equation developed in the previous section is very useful in the analysis of closed-loop systems. To illustrate, consider the problem given in Fig. 30. From Fig. 30 we can write the transformed equations

$$X = \frac{1 - e^{-sT/3}}{s^2} E^{T/3}, \quad Y = \frac{1 - e^{-sT/2}}{s(s+1)} X^{T/2} \quad (238)$$

Applying the results of the previous section:

$$X^{T/N} = \frac{T/N}{z-1} E^{T/3} \left[1 + z^{-1} + \dots + z^{-(N/3)-1} \right], \quad M = 3 \quad (239)$$

$$Y^{T/N} = \frac{1 - e^{-T/N}}{z - e^{-T/N}} X^{T/2} \left[1 + z^{-1} + \dots + z^{-(N/2)-1} \right], \quad M = 2 \quad (240)$$

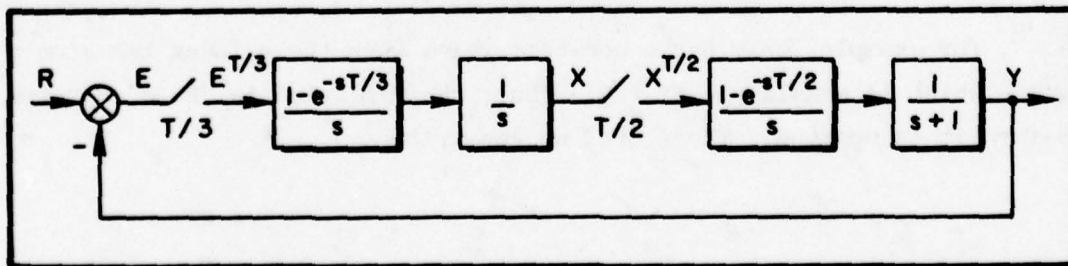


Figure 30. Multi-Rate Example

Any desired integer value of N can be used which is commensurate with 3 and 2 (for example, 6, 12, 18, ..., etc.). The difference equations can be written directly from Fig. 30. Noting that $z = e^{sT/N}$ and $E = R - Y$ gives

$$\left. \begin{aligned} X_n &= X_{n-1} - \frac{T}{N} Y_{n-1, N/3} + \frac{T}{N} R_{n-1, N/3} \\ Y_n &= e^{-T/N} Y_{n-1} + (1 - e^{-T/N}) X_{n-1, N/2}^{T/2} \end{aligned} \right\} \quad (241)$$

where, for example,

$$R_{n-1, N/3}^{T/3} = R \left[\frac{N(n-1)}{3(N/3)} \text{INT} \frac{T}{N} \right] = R \left[\left(\frac{n-1}{N/3} \right) \text{INT} \frac{T}{3} \right] \quad (242)$$

Note that these two recursion equations completely define the system no matter what value of N is selected. The response of this closed-loop system to a sine wave input is shown in Fig. 31. Since the sampling frequencies ($T = 1$) and the input frequency of π are commensurate, we see that the "steady state" in Fig. 31 takes on the additional property of periodicity. This would not be the case if the periods of the input wave were not commensurate with the sampling frequencies.

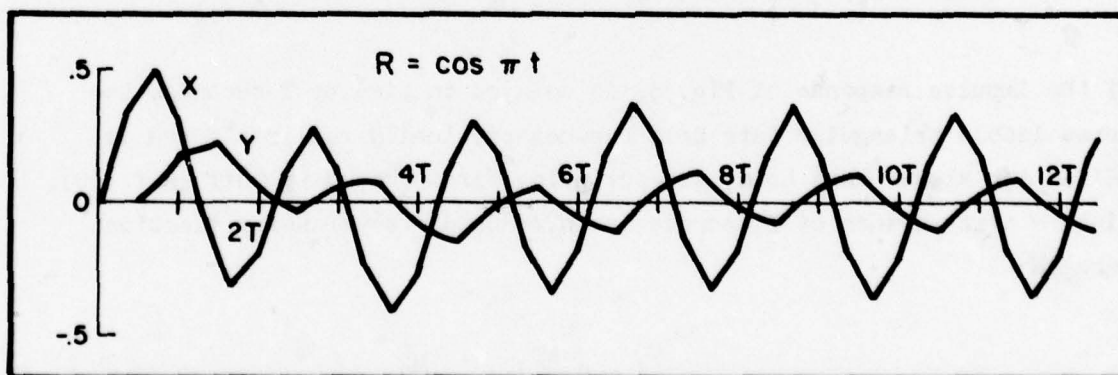


Figure 31. Transient Response, Cosine Wave Input

As mentioned previously, means for identifying the spectral content in response to sine and cosine wave inputs will be developed in Section V.

It is important to note that the basic simplicity of the multi-rate results is critically dependent on the use of zero-order holds. An indication of the type of complications which result from the use of more sophisticated couplers will be given in the next subsection, where we treat the slewer data hold.

E. THE SLEWER DATA HOLD

The impulse response of the familiar idealized triangular data hold is shown in Fig. 32. The transfer function, in the s-domain, is

$$M_{\Delta} = \frac{(1 - e^{-sT})^2}{Ts^2} e^{sT} \quad (243)$$

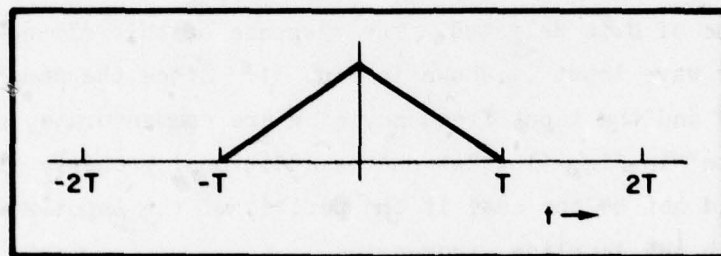


Figure 32. Impulse Response of Triangular Data Hold

If the impulse response of Fig. 32 is delayed in time by T seconds, the unrealizable triangular data hold becomes physically realizable and is called the slewer data hold, a description first coined by Goff (Ref. 10). Since a time advance of T seconds is introduced, the transfer function becomes

$$M_{\text{SLEW}} = \frac{(1 - e^{-sT})^2}{Ts^2} = \frac{M_{\Delta}^2}{T} \quad (244)$$

Thus, the transfer function of the slewer data hold is simply the square of the transfer function of the ZOH divided by T .

In the presence of no additional dynamics, the implications of Eq. 244 are clear — one simply samples the input waveform, advances this value T seconds, and ramps ("slews") to it (refer to Fig. 33). The basic property of the slewer is that it provides ramp-like waveforms, with no jump discontinuities at the sampling instants. An inherent lag of one frametime is introduced. This additional effective lag of one-half a period, when compared with the ZOH, must be taken into account in the synthesis of closed-loop control systems.

It will be helpful to review the development of the ZOH recursion equations in order to place the differences and similarities encountered in the use of the slewer into perspective. The basic open-loop equation

$$C^{T/N} = (GM)^{T/N} R^T \quad (245)$$

reduces to

$$C^T = \left(\frac{1 - e^{-sT}}{s} G \right)^T R^T \quad (246)$$

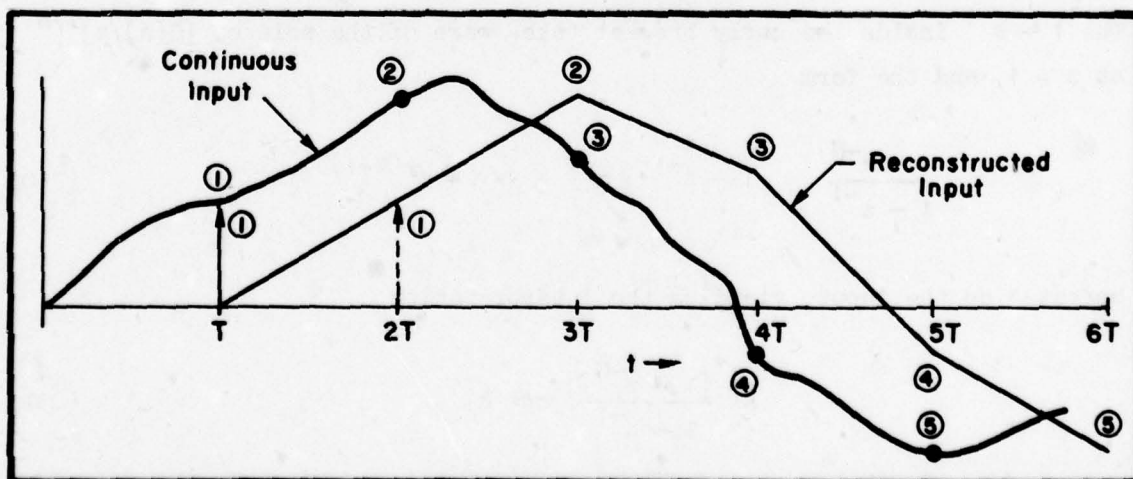


Figure 33. Reconstruction Via the Slewer

if M is permitted to be a ZOH and N is set equal to unity. More specifically, rewrite Eq. 246 as

$$C^T = \left\{ \left[\frac{G(s)}{s} \right]^T (1 - z^{-1}) \right\} R^T \quad (247)$$

where $1 - z^{-1}$ is constrained to operate within the "curly" brackets. This constraint is exercised because it is recognized that the $[G(s)/s]^T$ contains the pole $(1 - z^{-1})$. Failure to recognize this by implementing the recursion equation via

$$C^T = \left[\frac{G(s)}{s} \right]^T R^T (1 - z^{-1}) \quad (248)$$

adds an additional state which is (eventually) cancelled out by a "zero" operating on the input.

In the T/N case for the ZOH, set $z = e^{sT/N}$ and write

$$C^{T/N} = \left\{ \left[\frac{G(s)}{s} \right]^{T/N} (1 - z^{-1}) \right\} R^T \frac{1 - z^{-N}}{1 - z^{-1}} \quad (249)$$

The $1 - z^{-1}$ inside the curly bracket takes care of the pole of $[G(s)/s]^{T/N}$ at $z = 1$, and the term

$$\frac{1 - z^{-N}}{1 - z^{-1}} = 1 + z^{-1} + z^{-2} + \dots + z^{-(N-1)} \quad (250)$$

operates on the input, yielding the interpretation

$$R^T \frac{[1 - z^{-N}]}{1 - z^{-1}} \Rightarrow R_{n,N}^T \quad (251)$$

That is, the zero-order hold results in the " T " sampled function being held at a constant value over the entire " T " frame time.

Now consider the slewer where a similar situation pertains. Setting $M = M_s$ and $N = 1$ gives

$$c^T = \left\{ \left[\frac{G(s)}{Ts^2} \right]^T (1 - z^{-1})^2 \right\} R^T \quad (252)$$

In Eq. 252, the term $(1 - z^{-1})^2$ is constrained within the curly brackets because $[G(s)/Ts^2]^T$ will always produce a second-order pole at $z = 1$, and hence should be cancelled out at the onset. Letting N be non-unity gives

$$c^{T/N} = \left\{ \left[\frac{G(s)}{(T/N)s^2} \right]^{T/N} (1 - z^{-1})^2 \right\} R^T \frac{[1 - z^{-N}]^2}{N[1 - z^{-1}]^2}, \quad z = e^{sT/N} \quad (253)$$

Now the term in curly brackets is simply the "T" transform recomputed with a T/N frame time. That is, if we know how to compute the pulse transfer function using a slewer and a T frame time, then a recomputation for a T/N frame time is a straightforward operation. The term operating on the input can be rewritten as

$$\frac{1}{N} \frac{[1 - z^{-N}]^2}{[1 - z^{-1}]^2} = \frac{[1 + z^{-1} + \dots + z^{-(N-1)}]^2}{N} \quad (254)$$

The first $[1 + z^{-1} + \dots + z^{-(N-1)}]$ operates on the input creating the constant value over the T frametime. Now the additional $[1 + z^{-1} + \dots + z^{-(N-1)}]$ factor no longer operates on inter-sample points that are zero but rather sums the previous constant value with the present constant value. The only complication is that not all the previous $N-1$ constant values are in the same T frame; we now span values taken from two adjacent frames. The situation is depicted in Fig. 34 for the case where $N = 5$. Setting $z = e^{sT/5}$, we first construct $R_{n,5}^T$. Two cases will demonstrate the additional logic required. In Case 1 we add three constant values from the frame where $2T \leq t < 3T$ and two constant values from the frame where $T < t \leq 2T$. In Case 2, we add five values from the frame $4T \leq t < 5T$. Thus it is seen that

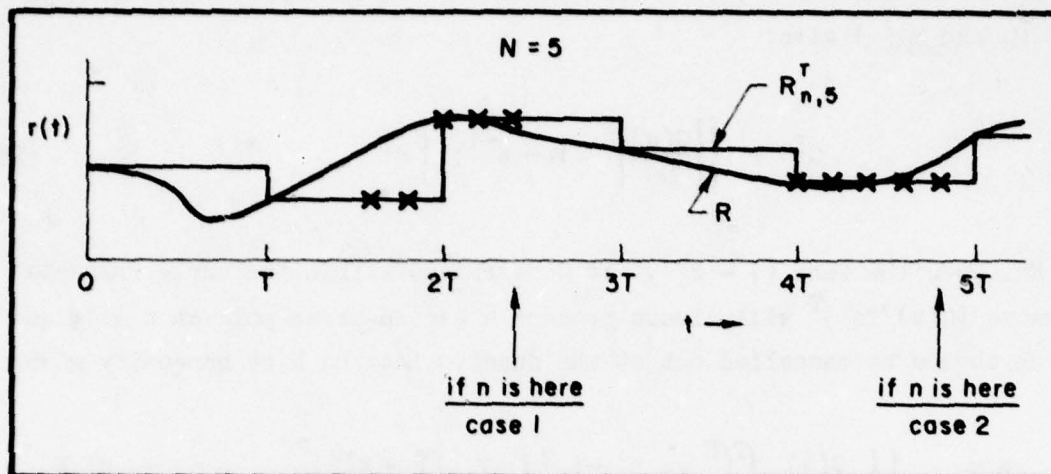


Figure 34. Slew Sampling Logic

the additional complication introduced is the need for an indexing register, call it k , which keeps track of numbers summed in the present frame and those summed from the past frame. We adopt the notation

$$\frac{R^T [1 + z^{-1} + \dots + z^{-(N-1)}]^2}{N} \Rightarrow R^T_{n-N,N} + \frac{k}{N} [R^T_{n,N} - R^T_{n-N,N}] \quad (255)$$

where

$$R^T_{n-N,N} + \frac{k}{N} [R^T_{n,N} - R^T_{n-N,N}] \triangleq R \left[N \left(\frac{n-N}{N} \right)_{\text{INT}} T \right] + \frac{k}{N} \left\{ R \left[N \left(\frac{n}{N} \right)_{\text{INT}} T \right] - R \left[N \left(\frac{n-N}{N} \right)_{\text{INT}} T \right] \right\} \quad (256)$$

The index k varies between 1 and N and increments in unison with n , the running index of the recursion equation. It is reset to unity whenever $R_{n,N}^T$ takes on a new value. That is,

$$k \rightarrow 1 \quad \text{if} \quad (n/N)_{\text{INT}} = \text{Integer} \quad (257)$$

or equivalently

$$k \rightarrow 1 \quad \text{if} \quad (n/N)_{\text{FRAC}} = 0 \quad (258)$$

In Eq. 255, $R_{n-N,N}^T$ is the first "back value", while $R_{n,N}^T - R_{n-N,N}^T$ represents the first back difference.

The reader should bear in mind that the pulse transfer obtained using the slower will always contain a free z in the denominator which will eventually end up operating on the input; hence, it is prudent to point out that

$$\frac{z^{-1} R^T [1 + z^{-1} + \dots + z^{-(N-1)}]^2}{N} \Rightarrow R_{n-(N+1),N}^T + \frac{k}{N} [R_{n-1,N}^T - R_{n-(N+1),N}^T] \quad (259)$$

F. ILLUSTRATIVE EXAMPLE

An example will serve to bring the details of the discussion into focus. Let

$$G(s) = \frac{1}{s+1}, \quad z = e^{sT/N}$$

so that

$$C^{T/N} = \left\{ \left[\frac{1}{\frac{T}{N} s^2(s+1)} \right]^{T/N} (1 - z^{-1})^2 \right\} R^T \frac{[1 + z^{-1} + \dots + z^{-(N-1)}]^2}{N} \quad (260)$$

Therefore,

$$\begin{aligned}
 G(z) &= \frac{1}{T/N} \left[\frac{1}{s^2} - \frac{1}{s} + \frac{1}{s+1} \right]^{T/N} (1 - z^{-1})^2 \\
 &= \frac{1}{T/N} \left[\frac{(T/N)z}{(z-1)^2} - \frac{z}{z-1} + \frac{z}{z - e^{-T/N}} \right] \frac{(z-1)^2}{z^2} \\
 &= \frac{\left(\frac{(T/N) - 1 + e^{-T/N}}{T/N} \right) z + \left(\frac{1 - e^{-T/N}[(T/N) + 1]}{T/N} \right)}{z(z - e^{-T/N})} \quad (261)
 \end{aligned}$$

or

$$G(z) = \frac{a_0 z + a_1}{z(z - a_2)} \quad (262)$$

The output, $c^{T/N}$, is then

$$c^{T/N} = \frac{a_0 z + a_1}{z - a_2} \cdot \frac{z^{-1} R^T [1 + z^{-1} + \dots + z^{-(N-1)}]^2}{N} \quad (263)$$

The recursion equation is written directly as

$$\begin{aligned}
 c_n &= a_2 c_{n-1} + a_0 \underbrace{\left[R_{n-(1+N),N}^T + \frac{k_1}{N} (R_{n-1,N}^T - R_{n-(1+N),N}^T) \right]}_A \\
 &\quad + a_1 \underbrace{\left[R_{n-(2+N),N}^T + \frac{k_2}{N} (R_{n-2,N}^T - R_{n-(2+N),N}^T) \right]}_B \quad (264)
 \end{aligned}$$

In Eq. 264, the indexes k_1 and k_2 vary between 1 and N :

$$\left. \begin{array}{ll} k_1 \rightarrow 1 & \text{when } [(n-1)/N]_{\text{FRAC}} = 0 \\ k_2 \rightarrow 1 & \text{when } [(n-2)/N]_{\text{FRAC}} = 0 \end{array} \right\} \quad (265)$$

An actual computation of the terms in Bracket B is unnecessary, since Bracket B is Bracket A delayed by the factor $e^{-sT/N}$. If N is set to unity (recall that a_0 , a_1 , and a_2 are functions of N), we obtain the "T" recursion equation as a check:

$$C_n = a_2 C_{n-1} + a_0 R_{n-1} + a_1 R_{n-2} \quad (266)$$

Using a sine wave input, the open-loop characteristic of the slewer can be contrasted against the ZOH. This is done in Fig. 35. Note the added attenuation and phase shift introduced by the slewer. On the other hand, the output is considerably smoother. We remark at this point that the "strength" of the slewer lies with its magnitude plot, whereas its weakness is linked with the phase characteristic. This point will become clearer in Section V.

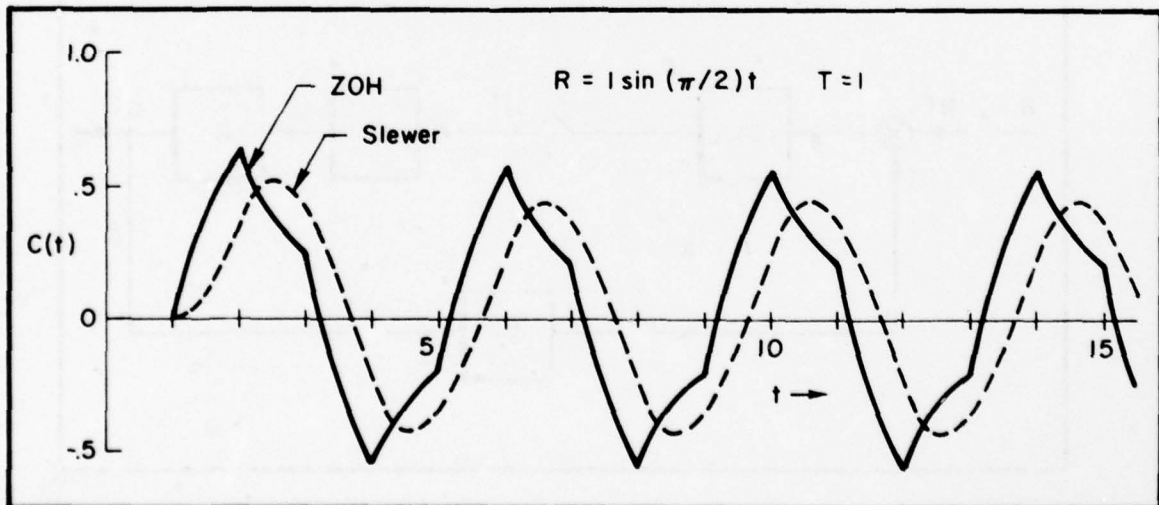


Figure 35. Comparison Between Slewer and ZOH

G. A MOTIVATING EXAMPLE

We have now demonstrated the application of the T/N approach both to open- and closed-loop systems and to multi-rate systems. The primary advantage of the technique is that the inter-sample response of multi-rate systems is obtained without a significant increase in the complexity of the defining recursion equations. The importance of being able to compute the inter-sample points will be demonstrated with the use of a "motivating" example. We use this particular adjective because, even though a step response is discussed, our true intent is to interest the reader in the idea of finding the "continuous" frequency response of a discretely controlled system.

Consider the block diagram of the single-rate closed-loop system shown in Fig. 36. In Fig. 36, let

$$G(s) = \frac{10}{s + 10} \quad \text{or} \quad G(s) = \frac{-4}{s - 4}$$

so that the open-loop plant is either strongly stable or unstable. Let M be either a slewer or a ZOH. As one of our design objectives we will

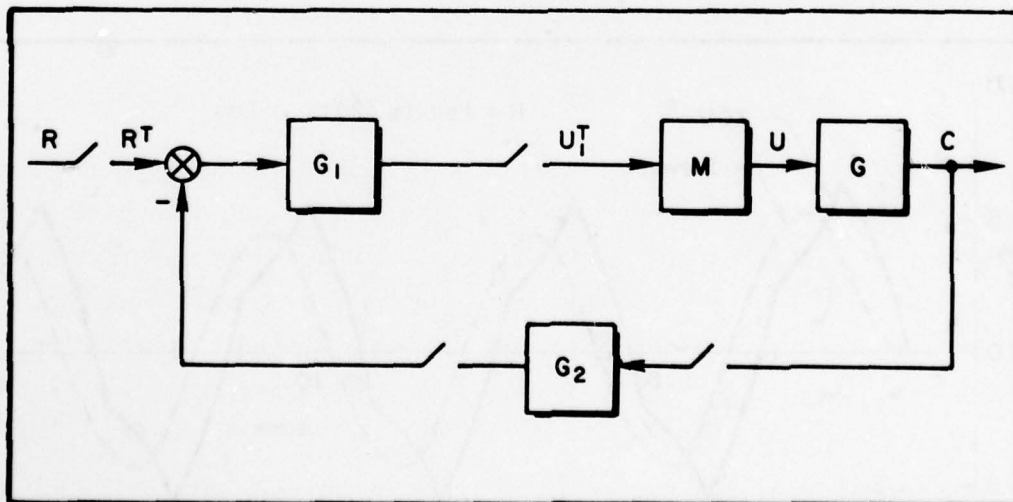


Figure 36. A Closed-Loop Single-Rate System

require a closed-loop pole in the z-plane that has $(s+0.5)$ as its s-plane counterpart. The other objective will be to force a unity steady-state step response. In addition, a 1 sec frame time will be utilized, forcing a sampling frequency of 2π rad/sec and a folding frequency of π rad/sec. Hence, the folding frequency will always be lower than the modulus of the open-loop characteristic equation.

The details of picking the compensation networks G_1 and G_2 which achieve these objectives are discussed in Appendix H. The actual design can be easily carried through in, among other domains, the w'-plane. The resultant compensation is given in Table 6. (Note that the slewer design was carried through for only one value of the open-loop root, since the inter-sample response is quite smooth and therefore very similar for either case.)

TABLE 6. COMPENSATION NETWORKS

DATA HOLD	OPEN-LOOP POLE	$G_1(z)$	$G_2(z)$
ZOH	$(s - 4)$	$-.00734$	137.2
ZOH	$(s + 10)$	$.393$	$- 1.541$
Slewer	$(s + 10)$	$\frac{.4372z}{z + .111}$	$- 1.541$

The step responses are shown in Fig. 37. Note that at the sampling instants all three closed-loop designs give exactly the same performance. However, the inter-sample responses present quite a different picture. There is a very noticeable roughness or "ripple" in the ZOH designs, whereas the slewer response is smooth and well behaved. In addition, notice that it was possible to overcome the additional phase lag, introduced by the slewer, through the use of a lead filter for $G_1(z)$.

Suppose this system was excited with a sinusoidal input signal. In the next section we will show that the classical sampled spectrum of z-transform theory would, like the step response evaluated at the sampling

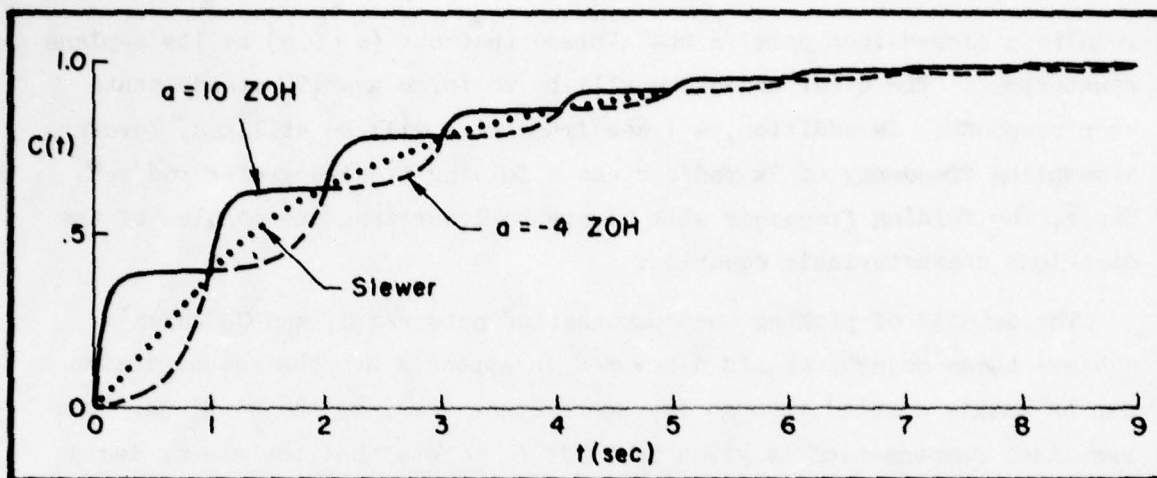


Figure 37. Closed-Loop Step Responses

instants, be unable to differentiate between the three designs. This is so because the sampled spectrum considers only the single sinusoid that matches the output at the sampling instants. Our objective in Section V will be to develop a tool that can define the spectral content for the continuous states of the system. Such a tool would have a capability to clearly differentiate between the three closed-loop systems of Fig. 37.

H. SECTION SUMMARY

A classical property of sampled data control theory has been exploited in order to develop a creditable tool for the analysis of the inter-sample responses of multi-rate systems under the influence of discrete controllers. In particular, it was shown that the use of ZOH's leads to recursion equations capable of defining the inter-sample response with any desired degree of fineness — yet the order of the recursion equation is not increased.

The characteristics of the slewer data hold were also developed. Here a noticeable increase in the logic requirements was needed, even though the order of the recursion equation is not increased (when compared to the single-rate recursion equation).

SECTION V

FREQUENCY RESPONSE OF A DIGITALLY CONTROLLED
CONTINUOUS SYSTEM

A. INTRODUCTION

When a continuous (stable) linear system is excited by a sine wave, the steady-state waveform is comprised of a single wave at the same frequency as the input. It differs from the input wave only by a phase angle and a magnitude factor. Moreover, it is unnecessary to compute the actual transient response of the system when the behavior for large values of time is of interest, since both the magnitude factor and phase angle can be read from a Bode plot.

As we shall see, a similar but more complex situation pertains to a discretely excited system. Given that the system is stable, the continuous output waveform will contain more than just a wave at the fundamental frequency; it will consist of the fundamental and all of its aliases. Thus, if the system is forced with $1 \sin bt$, $0 \leq b < 2\pi/T$; the output will contain terms at frequencies b , $b + (2\pi/T)$, $b + (4\pi/T)$, The relative amplitudes and phase angles will depend on the data hold employed as well as the system transfer function. Nevertheless, given a data hold and transfer function, the magnitude and phase angle of each and every component can be read from a particular "Bode plot." Note that this concept of frequency response is more comprehensive than the traditional concept of the "sampled spectrum," which is limited to determining the single sinusoid that fits the system output samples at the sampling instants.

In the subsections to follow we will first review the Bode plot concept for a continuous system and then proceed to the frequency response of a discretely excited open-loop system. We will conclude with demonstrations of the manner in which closed-loop systems (both single and multi-rate) are analyzed.

B. CONTINUOUS SYSTEM BODE PLOTS

It will be helpful to first review the Bode plot concept for continuous systems. Let R in Fig. 38 be a unit input sine wave with frequency ω_0 rad/sec. The output, in the frequency domain, is:

$$C(s) = G(s)R(s) = G(s) \frac{\omega_0}{s^2 + \omega_0^2} \quad (267)$$

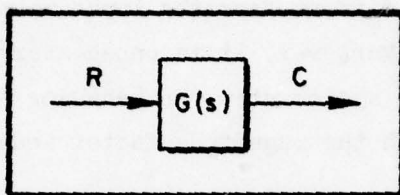


Figure 38. Continuous System

Equation 267 can be expanded in partial fractions as:

$$C(s) = \frac{A\omega_0}{s^2 + \omega_0^2} + \frac{Bs}{s^2 + \omega_0^2} + \left[\text{Terms associated with characteristic polynomial of } G(s) \right] \quad (268)$$

Given that all poles of $G(s)$ are in the left half plane, the bracketed term in Eq. 268 represents time functions that vanish as $t \rightarrow \infty$. Thus, the steady-state behavior is completely determined by the partial fraction coefficients A and B , since once they are known the steady-state time response can be written directly as:

$$\left. \begin{aligned} C(t) \Big|_{\lim_{t \rightarrow \infty}} &= A \sin \omega_0 t + B \cos \omega_0 t \\ &= \sqrt{A^2 + B^2} \sin (\omega_0 t + \varphi) \end{aligned} \right\} \quad (269)$$

where $\varphi = \tan^{-1} (B/A)$.

The details of solving for A and B clearly show the relationship between the Bode plot and the steady-state waveform. To solve for A and B, one multiplies Eq. 268 by $[s^2 + \omega_0^2]$ and evaluates the result for $s = j\omega_0$:

$$G(s)\omega_0 \Big|_{s=j\omega_0} = (A\omega_0 + Bs) \Big|_{s=j\omega_0} + \left[\begin{array}{c} \text{Terms associated} \\ \text{with characteristic} \\ \text{polynomial of } G(s) \end{array} \right] (s^2 + \omega_0^2) \Big|_{s=j\omega_0} \quad (270)$$

or

$$G(s) \Big|_{s=j\omega_0} = A + Bj = \sqrt{A^2 + B^2} e^{j \tan^{-1} B/A} \quad (271)$$

To summarize, we see that a sinusoidal input at frequency ω_0 produces a steady-state waveform of the same frequency. It differs from the input only by a magnitude factor and a phase shift. Both the magnitude factor and phase shift for any given input frequency, ω_0 , can be read directly from the Bode plot for $G(j\omega)$. That is, for any given input frequency ω_0 ,

$$A + jB = G(s) \Big|_{s=j\omega_0} \quad (272)$$

In the subsections that follow we will expand this "frequency response" viewpoint to encompass discretely excited systems.

C. MATHEMATICAL PRELIMINARIES

Let R be a sinusoid of unit amplitude with frequency b rad/sec. If R is sampled at $1/T$ samples/sec and then described in terms of a N/T samples/sec model, we obtain

$$R^T = \frac{z^N \sin bT}{z^{2N} - (2 \cos bT)z^N + 1} \quad ; \quad z = e^{sT/N} \quad (273)$$

For later use, it is necessary to find the N factors of the denominator of Eq. 273 in a form which will permit a partial fraction expansion containing terms for which corresponding time functions are known. For example, if $f(t) = \sin bt$, then

$$f^T(t) = [\sin bt]^T \Rightarrow F(z) = \frac{z \sin bT}{z^2 - 2 \cos bTz + 1} \quad (274)$$

but we do not know the time function corresponding to

$$F(z) = \frac{z \sin bT}{z^2 + 2 \cos bTz + 1} \quad (275)$$

which will also occur among the N factors of the denominator of Eq. 273. This situation is remedied by adding π to the argument so that $F(z)$ in Eq. 275 becomes recognizable in the time domain. For example, Eq. 275 becomes:

$$F(z) = \frac{-z \sin [b + (\pi/T)]T}{z^2 - 2 \cos [b + (\pi/T)]Tz + 1} \Rightarrow f(t) = -\sin\left(b + \frac{\pi}{T}\right)t \quad (276)$$

The reasons for adding π , when obviously $k\pi$ (k is an integer) would also work, will become apparent at a later point. Consider the denominator of Eq. 275 for the special case of $N = 2$:

$$z^4 - 2 \cos bTz^2 + 1 \equiv \left(z^2 - 2 \cos \frac{bT}{2} z + 1\right) \left(z^2 + 2 \cos \frac{bT}{2} z + 1\right) \quad (277)$$

Remove the positive coefficient of z in Eq. 277 by adding π to the argument $bT/2$:

$$z^4 - 2 \cos bTz^2 + 1 \equiv \left(z^2 - 2 \cos \frac{bT}{2} z + 1\right) \left(z^2 - 2 \cos \left[\left(b + \frac{2\pi}{T}\right) \frac{T}{2}\right] z + 1\right) \quad (278)$$

Thus, for $N = 2$, the partial fraction expansion of the output will require terms which account for not only the sine and cosine terms of the input frequency b but also for the first alias, $b + (2\pi/T)$, of the frequency b as well.

Now repeat this exercise once more, for $N = 4$. After this the result for arbitrary N will be apparent by induction.

$$z^8 - 2 \cos bz^4 + 1 = \left(z^4 - 2 \cos \frac{bT}{2} z^2 + 1\right) \left(z^4 + 2 \cos \frac{bT}{2} z^2 + 1\right) \quad (279)$$

$$= \left(z^4 - 2 \cos \frac{bT}{2} z^2 + 1\right) \left(z^4 - 2 \cos \left[\left(b + \frac{2\pi}{T}\right) \frac{T}{2}\right] z^2 + 1\right) \quad (280)$$

In turn, write

$$\begin{aligned} z^4 - 2 \cos \frac{bT}{2} z^2 + 1 &= \left(z^2 - 2 \cos \frac{bT}{4} z + 1\right) \left(z^2 + 2 \cos \frac{bT}{4} z + 1\right) \\ &= \left(z^2 - 2 \cos \frac{bT}{4} z + 1\right) \left(z^2 - 2 \cos \left[\left(b + \frac{4\pi}{T}\right) \frac{T}{4}\right] z + 1\right) \end{aligned} \quad (281)$$

and

$$\begin{aligned} z^4 + 2 \cos \frac{bT}{2} z^2 + 1 &= z^4 - 2 \cos \left[\left(b + \frac{2\pi}{T}\right) \frac{T}{2}\right] z^2 + 1 \\ &= \left(z^2 - 2 \cos \left[\left(b + \frac{2\pi}{T}\right) \frac{T}{4}\right] z + 1\right) \left(z^2 + 2 \cos \left[\left(b + \frac{2\pi}{T}\right) \frac{T}{4}\right] z + 1\right) \\ &= \left(z^2 - 2 \cos \left[\left(b + \frac{2\pi}{T}\right) \frac{T}{4}\right] z + 1\right) \left(z^2 - \cos \left[\left(b + \frac{6\pi}{T}\right) \frac{T}{4}\right] z + 1\right) \end{aligned} \quad (282)$$

Substituting Eqs. 281 and 282 into Eq. 280 gives:

$$z^8 - 2 \cos bTz^4 + 1 = \prod_{n=0}^3 \left(z^2 - 2 \cos \left[\left(b + \frac{2\pi n}{T}\right) \frac{T}{4}\right] z + 1\right) \quad (283)$$

From Eq. 283, the result for arbitrary N is apparent by induction:

$$z^{2N} - 2 \cos bTz^N + 1 = \prod_{n=0}^{N-1} \left(z^2 - 2 \cos \left[\left(b + \frac{2\pi n}{T}\right) \frac{T}{N}\right] z + 1\right) \quad (284)$$

$$= \prod_{n=0}^{N-1} \left[\left(z - \cos \left[\left(b + \frac{2\pi n}{T}\right) \frac{T}{N}\right]\right)^2 + \left(\sin \left[\left(b + \frac{2\pi n}{T}\right) \frac{T}{N}\right]\right)^2 \right] \quad (285)$$

Equation 284 is true for arbitrary N even though the development was in terms of even N .

Thus, the b rad/sec sine wave, which is actually sampled on a T interval, can be mathematically described in terms of a function having sinusoidal components at frequency b rad/sec and its first $N-1$ aliases (using a T/N interval).

D. OPEN-LOOP FREQUENCY RESPONSE — FINITE N

Consider the system of Fig. 39 where $G(s)$ represents an arbitrary transfer function and M represents an arbitrary data hold. Suppose R is a unit amplitude sine wave and we wish to sample the output with a T/N frame time.

$$C^{T/N} = (GM)^{T/N} R^T = (GM)^{T/N} \frac{z^N \sin bT}{z^{2N} - 2 \cos bTz^N + 1}, \quad z = e^{sT/N} \quad (286)$$

Expand the right-hand side of Eq. 286 in partial fractions:

$$C^{T/N} = \sum_{n=0}^{N-1} \frac{A_n z \sin \omega_n(T/N) + B_n z [z - \cos \omega_n(T/N)]}{z^2 - 2 \cos \omega_n(T/N)z + 1} + [\text{Terms due to modes of } (GM)^{T/N}] \quad (287)$$

Assume that responses in the modes of $(GM)^{T/N}$ approach zero as $t \rightarrow \infty$, i.e., that all modes are stable. In Eq. 287,

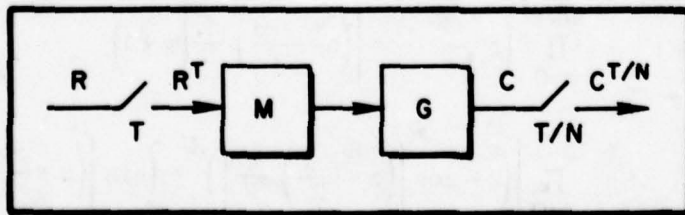


Figure 39. Open-Loop Case

$$\omega_n = b + \frac{2\pi n}{T}, \quad n = 0, 1, 2, \dots, N-1$$

For the present, we assume that $b \leq 2\pi/T$. The steady-state waveform, at the sampling instants, can be written as:

$$c(t) \Big|_{t \rightarrow \infty} = \sum_{n=0}^{N-1} (A_n \sin \omega_n t + B_n \cos \omega_n t) \quad (288)$$

To solve for A_n and B_n , multiply each side of Eq. 287 by

$$[z^2 - 2 \cos \omega_k(T/N)z + 1] \quad , \quad 0 \leq k \leq (N-1)$$

and evaluate for $z = 1 \angle \omega_k(T/N)$. Since the only term which can survive on the right-hand side occurs when $n = k$, the \sum will, of course, disappear. Then, if we so choose, the k notation can be changed back to n . To illustrate,

$$\begin{aligned} (GM)^{T/N} \frac{z^N \sin bT}{z^{2N} - 2 \cos bTz^N + 1} [z^2 - 2 \cos \omega_k(T/N)z + 1] \Big|_{z=1 \angle \omega_k(T/N)} \\ = \sum_{n=0}^{N-1} \frac{[A_n z \sin \omega_n(T/N)] + B_n z [z - \cos \omega_n(T/N)]}{z^2 - 2 \cos \omega_n(T/N)z + 1} [z^2 - 2 \cos \omega_k(T/N)z + 1] \Big|_{z=1 \angle \omega_k(T/N)} \end{aligned} \quad (289)$$

For any $n \neq k$, the right-hand side of Eq. 289 is identically zero since

$$z^2 - 2 \cos \omega_k(T/N)z + 1 = [z - \cos \omega_k(T/N)]^2 + [\sin \omega_k(T/N)]^2 \quad (290)$$

vanishes when

$$z = 1 \angle \omega_k(T/N) = \cos \omega_k(T/N) + j \sin \omega_k(T/N) \quad (291)$$

Specifically, we obtain

$$[\cos \omega_k(T/N) + j \sin \omega_k(T/N) - \cos \omega_k(T/N)]^2 + [\sin \omega_k(T/N)]^2 \equiv 0 \quad (292)$$

For $n = k$, the cancellation of the common factor guarantees the survival of an $n = k$ term. Factoring out a common z gives

$$\begin{aligned} z \{ A_k \sin \omega_n(T/N) + B_k [\cos \omega_n(T/N) - \cos \omega_n(T/N) + j \sin \omega_n(T/N)] \} \\ = (A_k + jB_k)z \sin \omega_k(T/N) \Big|_{z=1\lambda\omega_k(T/N)} \end{aligned} \quad (293)$$

Therefore, Eq. 289 becomes

$$z \sin \omega_k(T/N)(A_k + jB_k) = \frac{(G/M)^{T/N} (z^N \sin bT) [z^2 - 2 \cos \omega_k(T/N)z + 1]}{z^{2N} - 2 \cos bTz^N + 1} \Big|_{z=1\lambda\omega_k(T/N)} \quad (294)$$

At this point, let k revert to n .

$$A_n + jB_n = (GM)^{T/N} \Big|_{z=1\lambda\omega_n(T/N)} \cdot \frac{z^{N-1} \sin bT}{\sin \omega_n(T/N)} \frac{z^2 - 2 \cos \omega_n(T/N)z + 1}{z^{2N} - 2 \cos bTz^N + 1} \Big|_{z=1\lambda\omega_n(T/N)} \quad (295)$$

The last term on the right-hand side of Eq. 295 is indeterminate (0/0) when $z = 1\lambda\omega_n(T/N)$. Therefore, apply L'Hôpital's rule once and obtain

$$A_n + jB_n = (GM)^{T/N} \Big|_{z=1\lambda\omega_n(T/N)} \cdot \frac{z^{N-1} 2[z - \cos \omega_n(T/N)]}{2Nz^{N-1}(z^N - \cos bT)} \frac{\sin bT}{\sin \omega_n(T/N)} \Big|_{z=1\lambda\omega_n(T/N)} \quad (296)$$

$$A_n + jB_n = \frac{1}{N} (GM)^{T/N} \Big|_{z=1\lambda\omega_n(T/N)} \cdot \frac{[\cos \omega_n(T/N) + j \sin \omega_n(T/N) - \cos \omega_n(T/N)]}{(\cos \omega_n T + j \sin \omega_n T - \cos bT)} \frac{\sin bT}{\sin \omega_n(T/N)} \quad (297)$$

A direct substitution for $\omega_n = b + 2\pi n/T$ quickly shows that the last part of the product in Eq. 297 is unity. Therefore,

$$A_n + jB_n = \frac{1}{N} (GM)^{T/N} \left| \begin{array}{l} z = e^{sT/N} \\ z = 1 + j\omega_n(T/N) \end{array} \right| \quad (298)$$

The superscript notation in Eq. 298 is for the purpose of calling out the definition of z being used in the evaluation.

To review the situation, the system is forced with the $\sin bt$; then the steady-state output waveform, sampled with a T/N frametime, has the form

$$c^{T/N}(t) = \left(\sum_{n=0}^{N-1} A_n \sin \omega_n t + B_n \cos \omega_n t \right)^{T/N} \quad (299)$$

where

$$\omega_n = b + \frac{2\pi n}{T}, \quad n = 0, 1, 2, \dots, N-1 \quad (300)$$

The coefficients A_n and B_n are computed using Eq. 298.

For example, let

$$M = \frac{1 - e^{-sT}}{s}, \quad G(s) = \frac{a}{s + a} \quad (301)$$

so that

$$\frac{1}{N} (GM)^{T/N} = \frac{1 - e^{-aT/N}}{N(z - e^{-aT/N})} \frac{(1 - z^{-N})}{(1 - z^{-1})} \quad (302)$$

It is instructive to plot the Bode plot for Eq. 302 using N as a parameter. For the sake of clarity, we will plot versus ω rather than $\log \omega$ and, in addition, will omit the phase angle plot. Also, for reasons of clarity, the ordinate scales will be displaced for the different values of N (refer to Fig. 40). Note that, over the plotted range of 8π , the $N = 1$ case repeats itself 4 times. In a like manner, the $N = 2$ case repeats twice, whereas the $N = 4$ goes through one cycle.

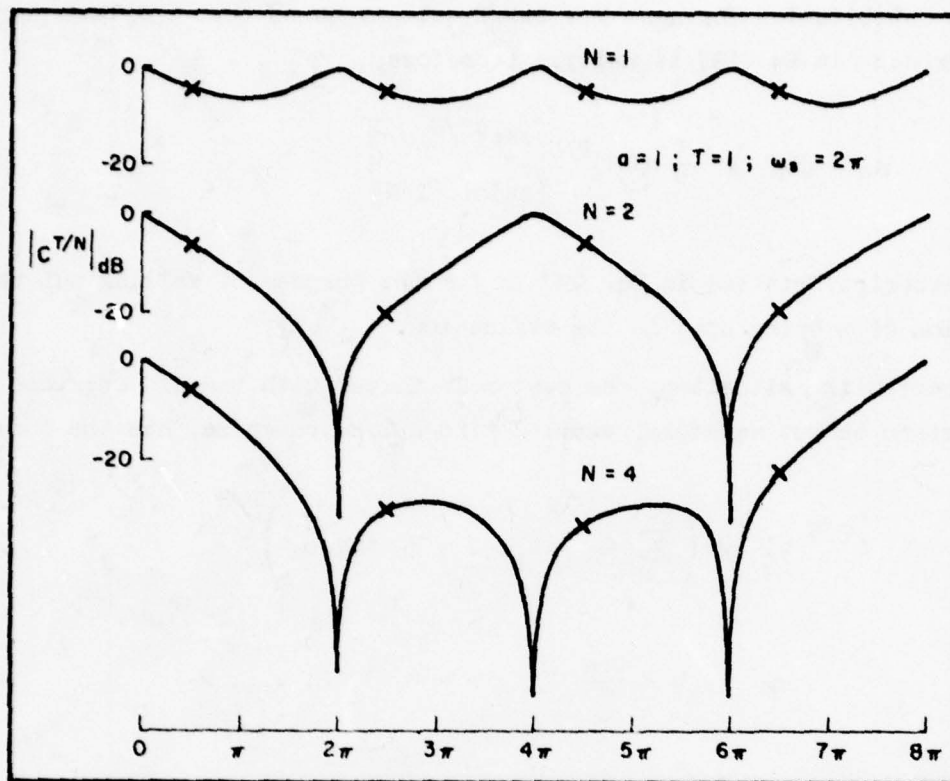


Figure 40. Magnitude Plot for $N = 1, 2, 4$

Imagine that a unit amplitude sine wave is input with a frequency of $\pi/2$. In the $N = 1$ case, our only interest is matching the sampling points with a single sine wave. The magnitude and phase angle (not shown in Fig. 40) could be read from this plot at $\omega = \pi/2, \pi/2 + 2\pi, \pi/2 + 4\pi, \pi/2 + 6\pi, \dots$; each point gives the correct values. Assume next that the input has a frequency $b = (\pi/2 + 4\pi)$. Clearly, if the objective is to match the sample points with a single sinusoid, the frequency of the output could be b plus any $2\pi/T$ multiple; the sampler cannot tell the difference. In fact, the "sub" aliases at $b - 2\pi/T, b - 4\pi/T$ will also work. These "sub" aliases are the difference terms so prominent in modulation theory.

Figure 41 depicts this situation for a steady-state response given an input frequency of $b = \pi/2$ rad/sec and assuming the system used in computing the Bode plot of Fig. 40. For the sake of clarity, only two of the many waves which fit the sample points are shown — one at $\pi/2$ rad/sec, the other at $[(\pi/2) - (2\pi/T)]$ rad/sec.

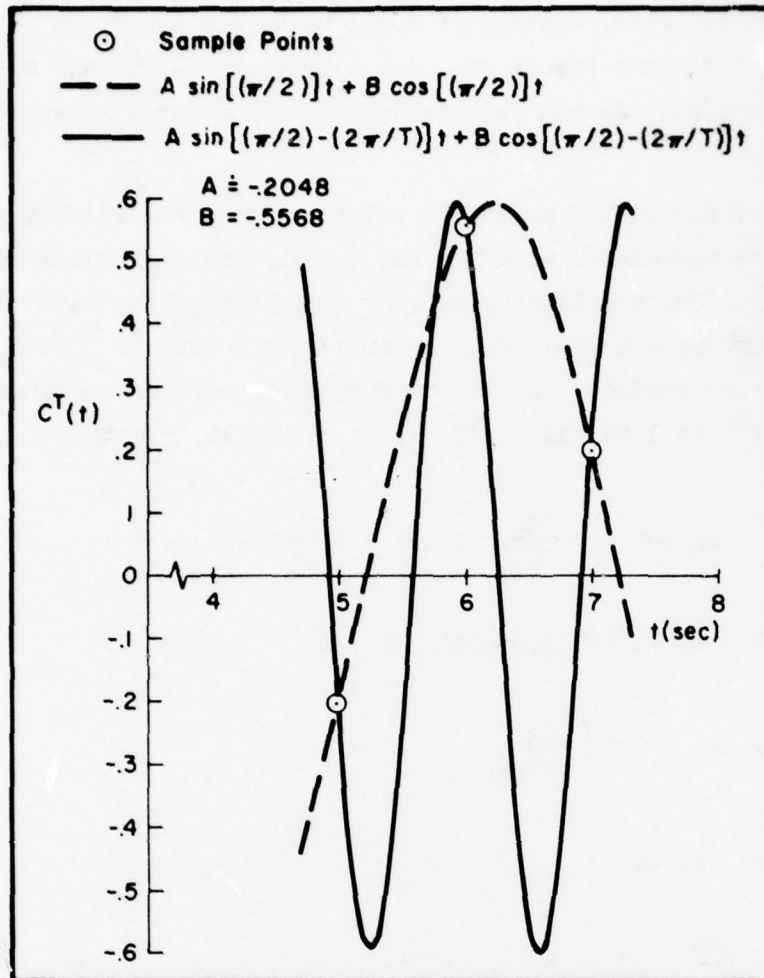


Figure 41. Two Continuous Sine Waves Which Match the Sample Points

The $N = 1$ plot in Fig. 40 corresponds to the "sampled spectrum" of sampled data control theory. Turn now to the $N = 2$ case wherein the objective is to match one inter-sample point as well as the sample points. Let the input frequency be $\pi/2$ and note that the points at $\omega = \pi/2, \pi/2 + 2\pi$ give the correct answers, as would the points $\pi/2 + 4\pi, \pi/2 + 6\pi$. Suppose next that the input frequency is $b = \pi/2 + 2\pi$. Clearly, the second required component could be read from the "first alias" at $b + 2\pi/T$ or the first sub-alias at $b - 2\pi/T$ (or, for that matter, a whole host of other frequencies).

In the $N = 4$ case, four sine waves are required to fit three inter-sample points as well as the sampled points. If the input frequency were $b = \pi/2 + 6\pi$, and if the plot of Fig. 40 with its limited range of 8π were

the only one available, clearly it would be to our advantage to use the "difference" frequency points at $\omega = b - 2\pi/T$, $b - 4\pi/T$, and $b - 6\pi/T$ to establish the magnitude and relative phase of the three remaining sine waves.

This brief discussion serves to point out that the aliases and sub-aliases can be associated with the sum and difference frequencies of modulation theory. One should not, however, think that both sum and difference components must be simultaneously present in the output. Clearly, only N components are needed. We can now remove the earlier constraint that $b \leq 2\pi/T$. If b is less than $2\pi/T$, it is certainly true that

$$\omega_n = b + \frac{2\pi n}{T}, \quad n = 0, 1, 2, \dots, N-1 \quad (303)$$

However, if $b > 2\pi/T$, let $\omega_s = 2\pi/T$ and use

$$n_0 = -\left(\frac{b}{\omega_s}\right)_{\text{INT}} \quad (304)$$

to restate Eq. 303 as

$$\omega_n = b + \frac{2\pi n}{T}, \quad n = n_0, n_0+1, \dots, 0, 1, 2, \dots, N-n_0-1 \quad (305)$$

For our previous example where $N = 4$, suppose $b = 6\pi + \pi/2$. Then

$$n_0 = -\left(\frac{6\pi + (\pi/2)}{2\pi}\right)_{\text{INT}} = -3 \quad (306)$$

Thus,

$$\omega_n = b + \frac{2\pi n}{T}, \quad n = -3, -2, -1, 0 \quad (307)$$

and we use three sub aliases. If $b = \pi/2$, then

$$n_0 = -\left(\frac{\pi/2}{2\pi}\right)_{\text{INT}} = 0$$

and we use

$$\omega_n = \frac{2\pi n}{T}, \quad n = 0, 1, 2, 3$$

the "positive" aliases.

Keep in mind that all this represents a convention which the reader may not necessarily elect to follow. What is important is a clear understanding which will permit one to pick a consistent set of N points from the Bode plot.

Of interest is the case where N is extremely large. In fact, let $N \rightarrow \infty$ after evaluating Eq. 302 at $z = 1 \pm j\omega_n(T/N)$:

$$\frac{1 - e^{-aT/N}}{N(z - e^{-aT/N})} \frac{1 - z^{-N}}{1 - z^{-1}} \bigg|_{z=1 \pm j\omega_n(T/N)} = \frac{(1 - e^{-aT/N})(1 - 1 \pm j\omega_n T)}{N[1 \pm j\omega_n(T/N) - e^{-aT/N}][1 - 1 \pm j\omega_n(T/N)]} \bigg|_{\substack{\lim \\ N \rightarrow \infty}} \quad (308)$$

An indeterminate form is obtained. Therefore, use L'Hôpital's rule twice (substitute $1 \pm j\omega_n(T/N) = \cos \omega_n(T/N) + j \sin \omega_n(T/N)$, etc.) and obtain (see Appendix I):

$$\frac{1}{N} \left(\frac{1 - e^{-sT}}{s(s+1)} \right) \bigg|_{z=1 \pm j\omega_n(T/N)} \bigg|_{\substack{\lim \\ N \rightarrow \infty}} = \frac{1 - e^{-j\omega_n T}}{j\omega_n T} \frac{1}{1 + j\omega_n} = \frac{1 - e^{-sT}}{sT} \frac{1}{s+1} \bigg|_{s=j\omega_n} \quad (309)$$

That is, as $N \rightarrow \infty$, one simply divides GM by T and evaluates the coefficients at $s = j\omega_n$. This is representative of the general result discussed in the next subsection.

E. OPEN LOOP FREQUENCY RESPONSE — CONTINUOUS OUTPUT

In the previous section it was shown that

$$A_n + jB_n = \frac{1}{N} (GM)^{T/N} \bigg|_{z=1 \pm j\omega_n(T/N)} z^{\pm 1} e^{sT/N} \quad (310)$$

To deduce the behavior for infinite N , rewrite Eq. 310 as

$$\frac{1}{T} \left\{ \frac{T}{N} (GM)^{T/N} \right\} = \frac{1}{T} \left\{ \frac{T}{N} \left[\frac{1}{T/N} \sum_{k=-\infty}^{\infty} (GM) \left(s - \frac{2\pi kN}{T} \right) \right] \right\} \quad (311)$$

The T/N 's cancel, and as N gets very large only the $k = 0$ term contributes since all the "aliased" spectra have moved to infinite frequency. Therefore,

$$\lim_{N \rightarrow \infty} \frac{1}{N} (GM)^{T/N} \Big|_{z=1} e^{sT/N} = \frac{GM}{T} \Big|_{s=j\omega_n} \quad (312)$$

$$\omega_n = b + \frac{2\pi n}{T}, \quad n = n_0, n_0 + 1, \dots$$

where

$$n_0 = - \left(\frac{b}{\omega_s} \right)_{INT}$$

The finite N example of the previous section can now be studied for the case of infinite N — therefore the "continuous" frequency response. Thus

$$A_n + jB_n = \frac{1 - e^{-sT}}{sT} \cdot \frac{1}{s + 1} \Big|_{s=j\omega_n} \quad (313)$$

This is shown in Fig. 42 where the components for input frequencies of $b = 0.1, 1.0, 4.0, 6.0$ rad/sec have been indicated with different symbols.

The interpretation of Fig. 42 is as follows. Suppose a unit sine wave at 1 rad/sec is input to the sampler. Then, if sine waves at $1, 1 + 2\pi/T, 1 + 4\pi/T, \dots$, are added together, the resultant waveform will be an exact match of the actual steady-state output waveform. One would expect this waveform to be relatively clean, since the first alias is down by something on the order of 30 dB, relative to the input component. However, the

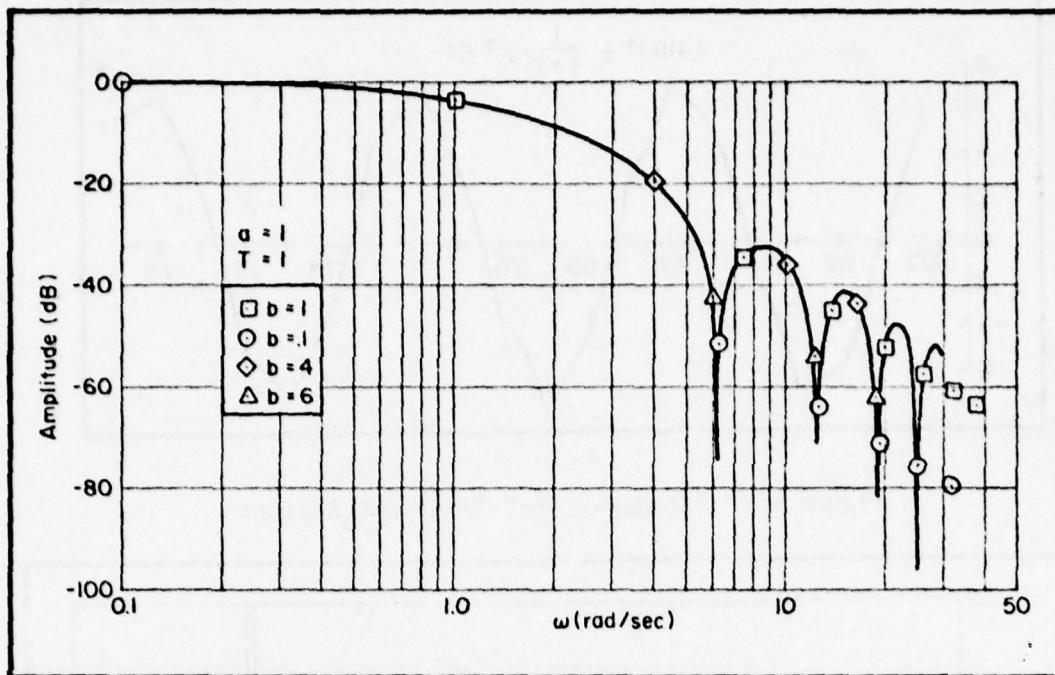


Figure 42. Frequency Response and Spectral Components of Output

transient response itself does not bear out this conjecture as can be seen in Fig. 43. The reason is that the higher terms are important. They do not represent "harmonic" terms but are rather modulation components which must add together properly in order to match conditions at the T transition points. As mentioned earlier in Section IV, it can be seen that the "steady state" does not necessarily take on the additional attribute of periodicity. This occurs only when the input frequency and the sampling frequency bear an integer relationship with respect to one another. As another example, the "frequency response" for a higher-order system is shown in Fig. 44. In this example, the sampling frequency was deliberately picked to suppress the bending mode responses.

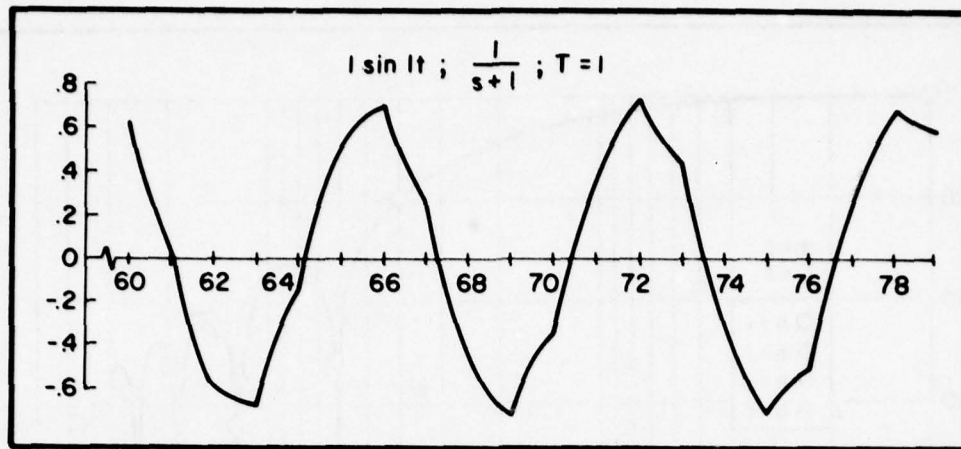


Figure 43. "Steady-State" Transient Response

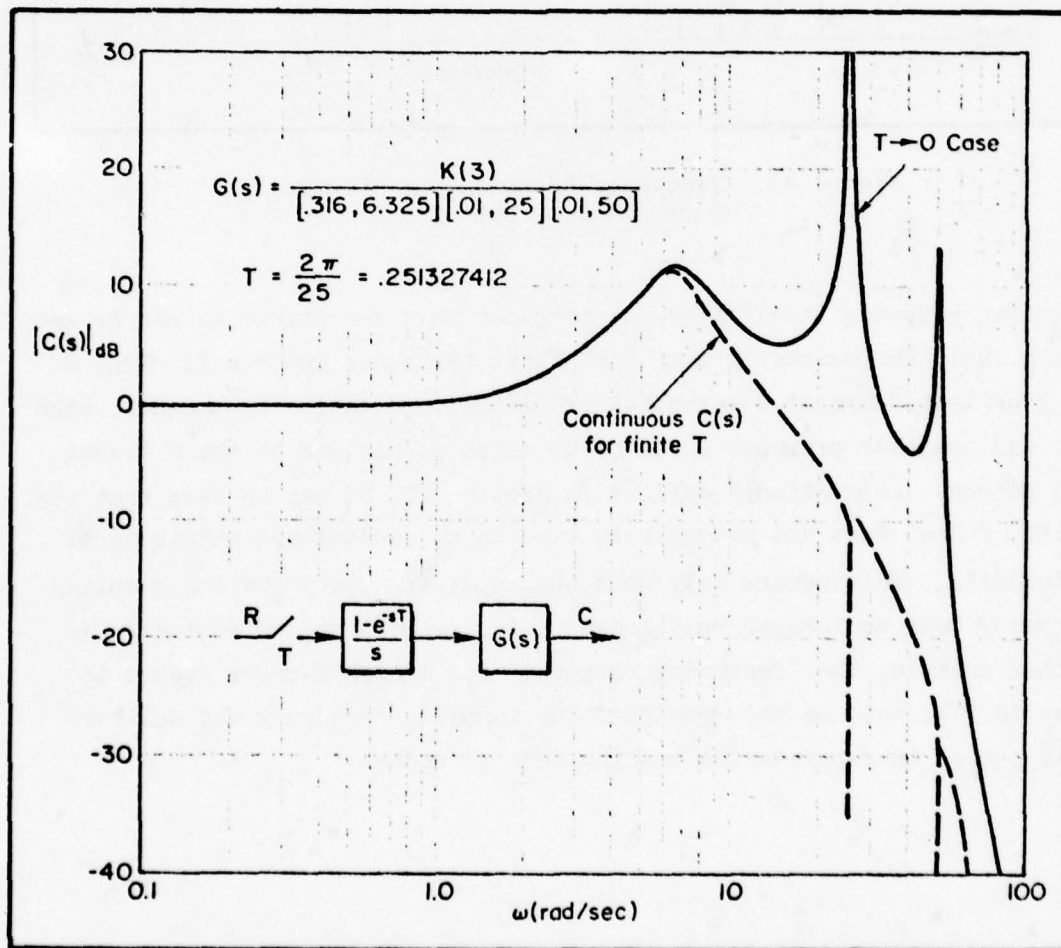


Figure 44. A More Complex Case

F. INPUT SIGNAL WITH PHASE SHIFT

If the input signal has the form

$$r(t) = k_1 \sin bt + k_2 \cos bt \quad (314)$$

the results of the previous section are changed only by a complex constant. Following exactly the procedures of Subsection D, except for using the more general input given in Eq. 314, gives (see Appendix E):

$$A_n + jB_n = \frac{1}{N} (GM)^{T/N} \left| \begin{matrix} z^{\Delta} e^{sT/N} \\ z = 1 + \Delta \omega_n(T/N) \end{matrix} \right| \cdot (k_1 + jk_2) \quad (315)$$

Limit $N \rightarrow \infty$

$$A_n + jB_n = \frac{1}{T} GM \Big|_{s=j\omega_n} \cdot (k_1 + jk_2) \quad (316)$$

G. SINGLE-RATE CLOSED-LOOP FREQUENCY RESPONSE

The closed-loop results will be configuration dependent. However, the mathematics are quite tractable and can be followed through on a case-by-case basis. Thus it is more important, for the present, to have an insight into the mathematical structure and the particular simplifications that surface in a closed-loop analysis.

Consider the (vector) system shown in Fig. 45. The procedure we now follow will be typical. First, solve for the vector component at the input of the data holds.

$$E^T = G_1^T R^T - G_1^T G_2^T (GM)^T E^T \quad (317)$$

Therefore

$$E^T = [I + G_1^T G_2^T (GM)^T]^{-1} G_1^T R^T \quad (318)$$

Next, solve for $C(s)$:

$$C = (GM) [I + G_1^T G_2^T (GM)^T]^{-1} G_1^T R^T \quad (319)$$

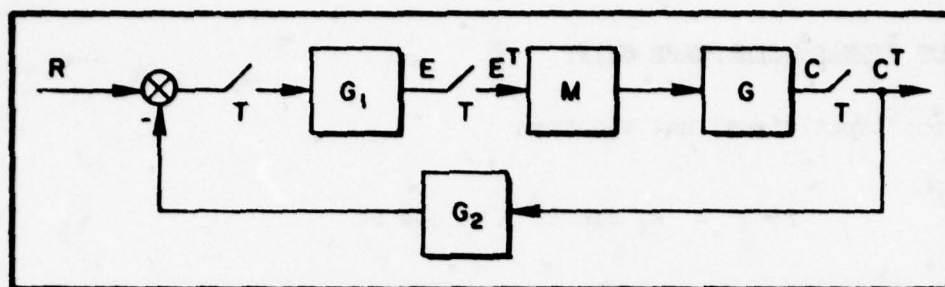


Figure 45. Illustrative Vector Closed-Loop Configuration

The spectrum of $C(s)$ is what is really of interest; we seek it by finding first the spectrum of C^T/N and going to the limiting case of $N \rightarrow \infty$.

Let the input be a sine wave at frequency b rad/sec and let the delay operator be

$$z^{-1} = e^{-sT/N} \quad (320)$$

so that

$$R^T = \frac{z^N \sin bT}{z^{2N} - 2 \cos bTz^N + 1} \quad (321)$$

Therefore

$$C^T/N = (GM)^{T/N} [I + G_1^T G_2^T (GM)^T]^{-1} G_1^T R^T \quad (322)$$

For the sake of brevity write Eq. 322 as

$$C^T/N = G_A^{T/N} G_B^T R^T \quad (323)$$

Expand the right-hand side of Eq. 323 in partial fractions:

$$\begin{aligned} C^T/N &= G_A^{T/N} G_B^T \frac{z^N}{z^{2N} - 2 \cos bTz^N + 1} \\ &= \sum_{n=0}^{N-1} \frac{A_n z \sin \omega_n(T/N) + B_n z [z - \cos \omega_n(T/N)]}{z^2 - 2 \cos \omega_n(T/N)z + 1} \\ &\quad + [\text{Terms due to modes of } G_A^{T/N} G_B^T] \end{aligned} \quad (324)$$

Assume that responses in the modes of $G_A^{T/N} G_B^T$ approach zero as $t \rightarrow \infty$, i.e., that all modes are stable. In Eq. 324,

$$\omega_n = b + \frac{2\pi n}{T}, \quad n = 0, 1, 2, \dots, N-1 \quad (325)$$

[More generally, $n = n_0, n_0 + 1, \dots, N - n_0 - 1$, where $n_0 = -(b/\omega_s)_{INT}$].

Note that Eq. 324 is exactly the same as Eq. 287, except $(GM)^{T/N}$ has been replaced by $G_A^{T/N} G_B^T$. Hence we can write a crucial result using Eq. 298:

$$A_n + jB_n = \frac{1}{N} G_A^{T/N} G_B^T \Big|_{z=1\angle\omega_n(T/N)} \quad (326)$$

But

$$G_B^T \triangleq G_B(z^N) \quad (327)$$

Therefore, using

$$\begin{aligned} [1\angle\omega_n(T/N)]^N &= 1\angle\omega_n T \\ &= \cos \omega_n T + j \sin \omega_n T \\ &= \cos [b + (2\pi n/T)]T \\ &\quad + j \sin [b + (2\pi n/T)]T \\ &= \cos bT + j \sin bT \end{aligned}$$

we obtain

$$\begin{aligned} G_B^T \Big|_{1\angle\omega_n(T/N)} &\equiv G[1\angle\omega_n(T/N)]^N \\ &\equiv G[1\angle\omega_n T] = G[1\angle bT] \end{aligned} \quad (328)$$

Thus, we can replace z^N in G_B^T with z and evaluate it at $z = 1\angle bT$. At this point we have

$$A_n + jB_n = \left(\left[\frac{1}{N} G_A^{T/N}(z) \right]_{z=1 \pm j\omega_n(T/N)} z^{\pm} e^{sT/N} \right) \left(\left[G_B^T(z) \right]_{z=1 \pm j\omega_n bT} z^{\pm} e^{sT} \right) \quad (329)$$

Equation 329 is the basic result for the finite N case. To reiterate, to find the coefficients of the N sine waves for the T/N sampled output of C , we compute the normal "T" transfer functions for

$$G_B^T = [I + G_1^T G_2^T (GM)^T]^{-1} G_1^T \quad (330)$$

and evaluate it for

$$z = 1 \pm j\omega_n bT \quad (331)$$

Next, compute the normal T/N pulsed transfer function for G_A ; evaluate it at $z = 1 \pm j\omega_n(T/N)$ where $\omega_n = b + (2\pi n/T)$.

Thus, G_B^T is periodic in $(2\pi/T)$ and it is superfluous to use $\omega_n(T/N)$; it suffices to use bT . Moreover, only the $G_A^{T/N}$ is a function of N ; this simplifies the procedure involved in the limiting case tremendously. For the case of $N \rightarrow \infty$, the continuous case, we obtain:

$$A_n + jB_n = \left(\left[\frac{M(s)G(s)}{T} \right]_{s=j\omega_n} \right) \left(\left[G_B^T(z) \right]_{z=1 \pm j\omega_n bT} z^{\pm} e^{sT} \right) \quad (332)$$

Equation 332 is the desired result for the given closed-loop configuration.* However, the mathematical ideas are what count; one can follow the details through for other configurations quite easily.

*Accurate numerical determination of $G_B^T|_{1 \pm j\omega_n bT}$ may prove difficult at high sampling rates. This is the result of small differences between large numbers which occur in the computations as poles and zeros approach the unit circle. In this event, one is well advised to carry out equivalent computations in a domain where numerical conditioning is much improved (e.g., in terms of w' or w).

H. THE "MOTIVATING" EXAMPLE REVISITED

Recall the single-rate design problem of Section IV wherein a closed-loop system was designed to have exactly the same step transient response at the sampling instants even though the open-loop parameter took on two different values. For convenience, the step response is repeated in Fig. 46.

Using the result of the previous subsection, we are now in a position to examine the frequency response. The magnitude plot is given in Fig. 47 (the magnitude is plotted against ω rather than $\log \omega$).

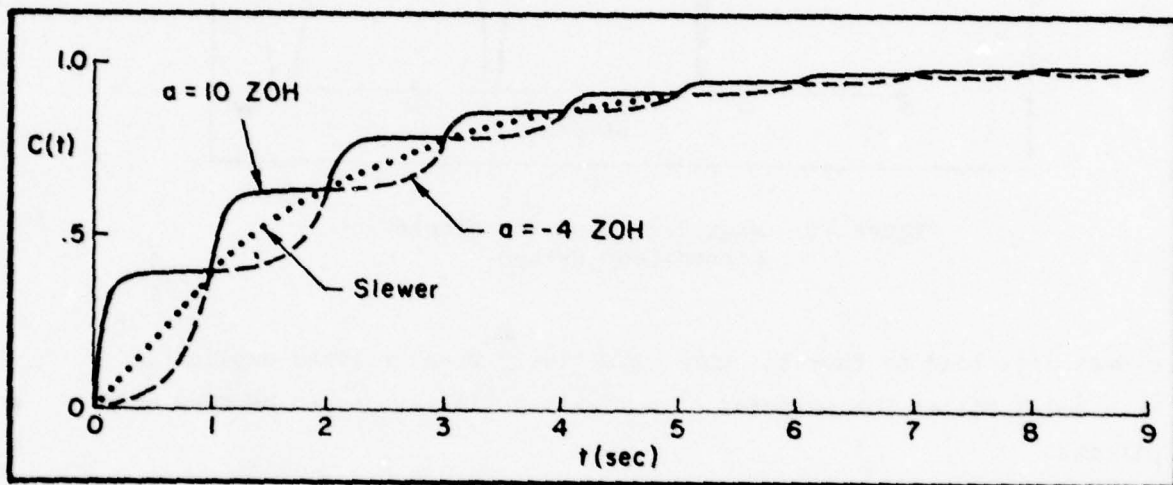


Figure 46. Closed-Loop Step Response

Note that the "sampled spectrum," the $N = 1$ case, is unable to differentiate as to whether the open-loop parameter is either $a = -4$ or $a = 10$. Moreover, the difference in the frequency content of the steady state when the ZOH is used cannot be distinguished from that when the slewer is used. Certainly (at least for this example) the classical "sampled spectrum" is of limited use. On the other hand, the continuous spectrum ($N \rightarrow \infty$ case) clearly displays the differences in the closed-loop designs. Note, in particular, the added width of the notches when the slewer is used; the ZOH notches are very sharp by comparison. Thus, one would expect the

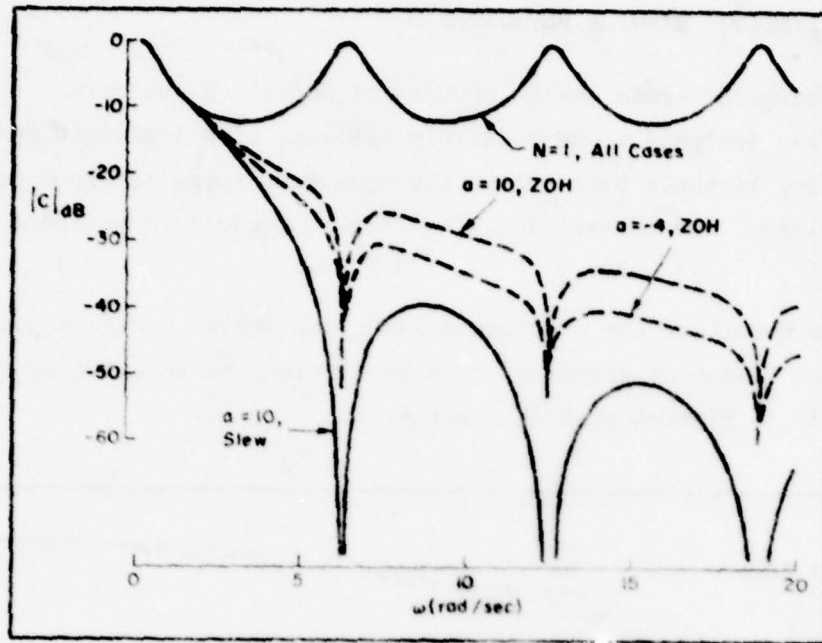


Figure 47. Magnitude Plot for Single-Rate Closed-Loop System

slewer data hold to function more effectively when utilized explicitly as a notch filter for purposes of mitigating lightly damped bending mode effects.

Before leaving this example, let us take the opportunity to solidify the meaning of the frequency response for the finite N case. Consider the $a = 10$ case and use the recursion equation to generate the continuous transient response for a unit amplitude sine wave with a frequency of $\pi/2$. This is shown in Fig. 48. According to theory we should be able to set $N = 1$ and from the Bode plot read the magnitude and phase of the single sinusoid that fits the sample points at the sample instant. This indeed proves to be the case and is shown in Fig. 49. In Fig. 49 a section of the transient response has been "copied" and overlaid with the sine wave which results from the $N = 1$ computation, namely

$$\left(c(t) \Big|_{t \rightarrow \infty} \right)^T = \left(a_0 \sin \frac{\pi}{2} t + b_0 \cos \frac{\pi}{2} t \right)^T \quad (333)$$

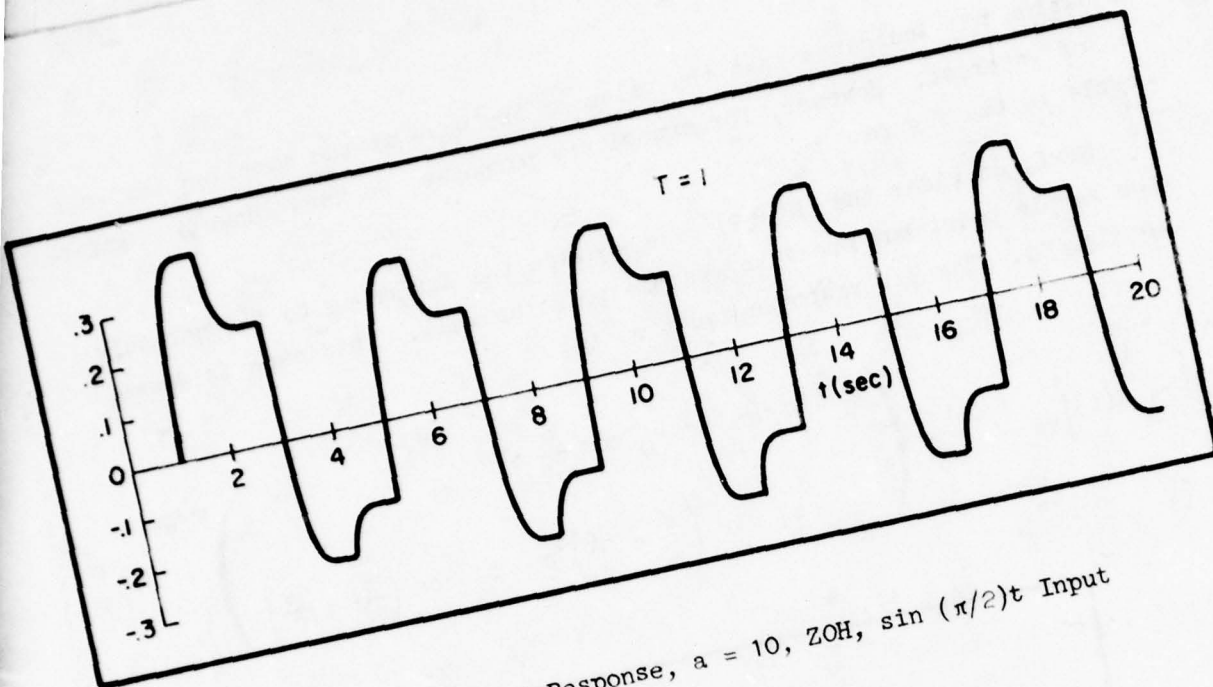


Figure 48. Transient Response, $a = 10$, ZOH, $\sin(\pi/2)t$ Input

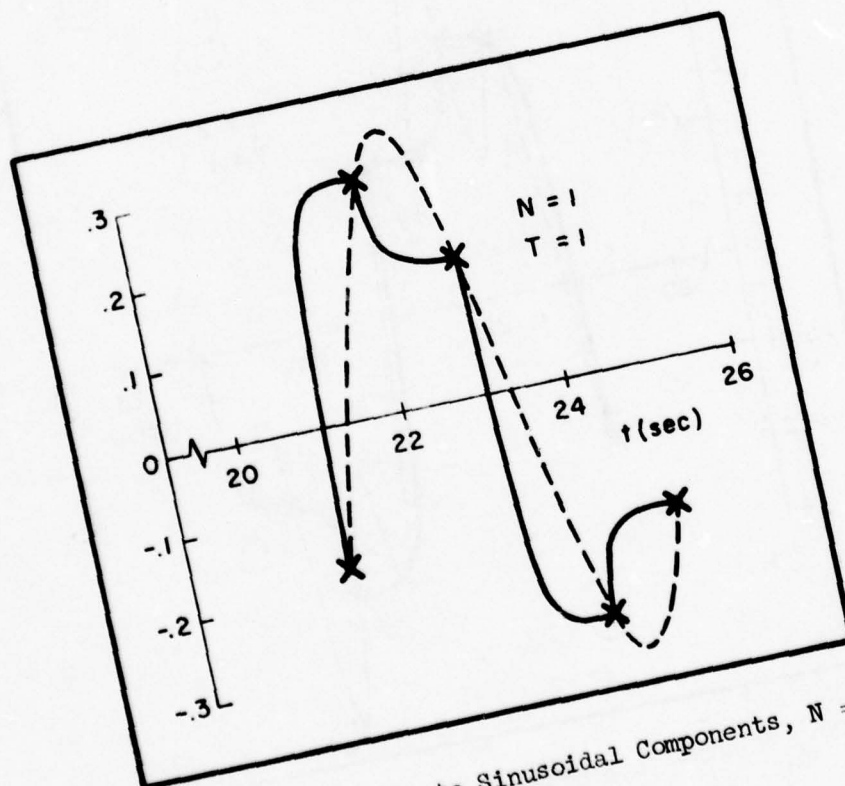


Figure 49. Steady-State Sinusoidal Components, $N = 1$

Equation 333 indicates that the value of the wave at the sampling instants is of interest. However, for expository purposes, we have shown a complete cycle in the figure.

Next, consider the ($N = 2$) case wherein the desire is to fit not only the sample point but one inter-sample point as well. This case is shown in Fig. 50. The $T/2$ response equation is

$$C(t)|_{ss}^{T/2} = \left(\begin{aligned} &a_0 \sin \frac{\pi}{2} t + b_0 \cos \frac{\pi}{2} t \\ &+ a_1 \sin \left(\frac{\pi}{2} + \frac{2\pi}{T} \right) t + b_1 \cos \left(\frac{\pi}{2} + \frac{2\pi}{T} \right) t \end{aligned} \right)^{T/2} \quad (334)$$

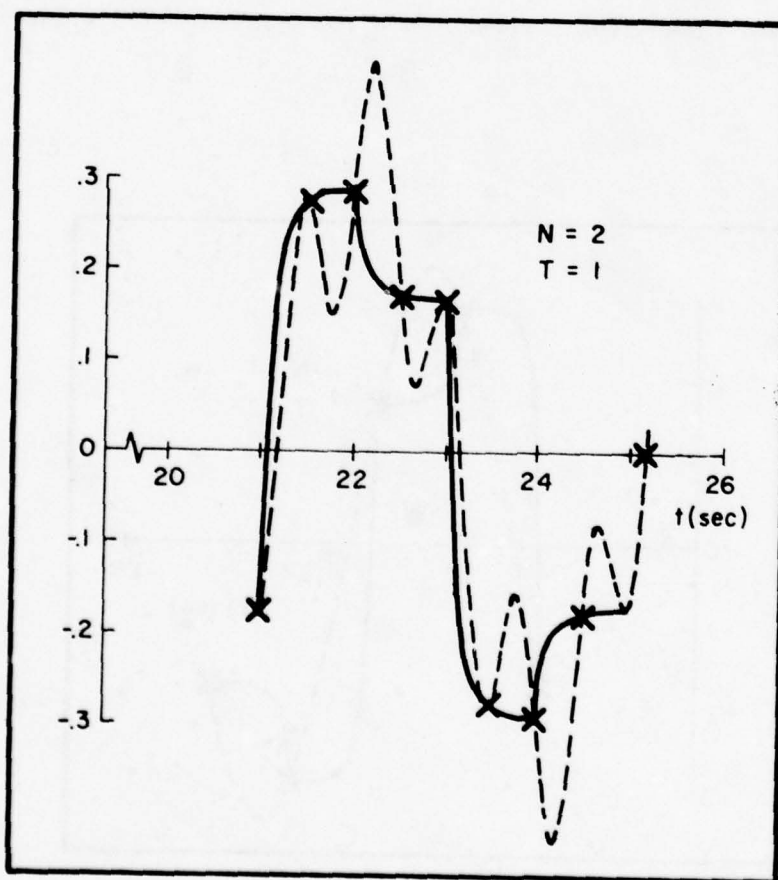


Figure 50. Steady-State Sinusoidal Components, $N = 2$

Again, for expository reasons we have shown the continuous waveform which results from sines and cosines at $\omega = \pi/2$ and its first alias at $\omega = (\pi/2) + (2\pi/T)$. A half period for the $N = 10$ case is shown in Fig. 51.

The reader is reminded that the steady-state wave of this example is periodic and free of modulation effects simply because the selected input frequency bears an integer relationship to the sampling frequency. In general, the expansion of the steady state in terms of aliases is a non-orthogonal series. For those special cases where the steady state is periodic, it is readily apparent that the $N = \infty$ case degenerates to a Fourier series.

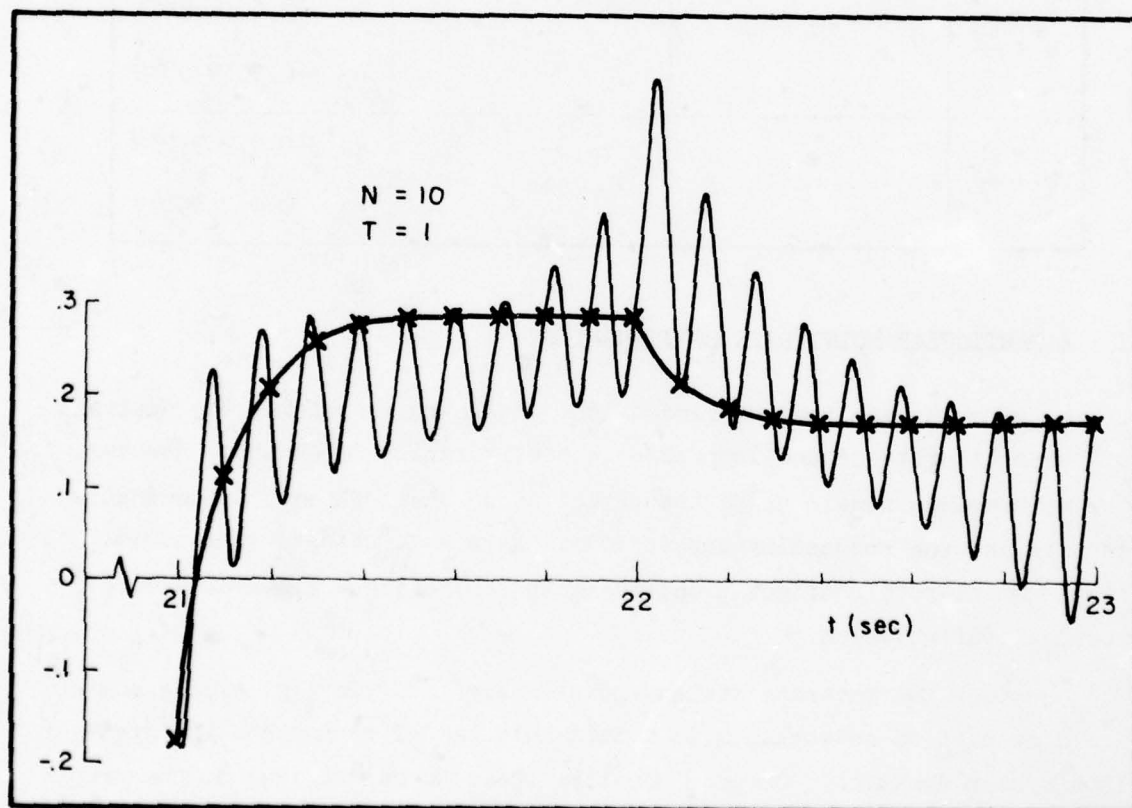


Figure 51. Steady-State Sinusoidal Components, $N = 10$, Half Period

It is also important to bear in mind that we are "matching" the sample points; thus the a_0 term for $N = 1$ will be unequal to the a_0 term for $N = 2$. This is demonstrated in Table 7 for $N = 1, 2$, and 4 (let $b = \pi/2$).

TABLE 7. COMPONENT COEFFICIENTS $N = 1, 2, 4$

	$N = 1$	$N = 2$	$N = 4$
b	a_0 -0.174468021 b_0 -0.287649137	a_0 -0.048579760 b_0 -0.306381976	a_0 0.002998683 b_0 -0.302606086
$b + \frac{2\pi}{T}$		a_1 -0.125888261 b_1 0.018732839	a_1 -0.046197029 b_1 -0.043548018
$b + \frac{4\pi}{T}$			a_2 -0.051578443 b_2 -0.003775889
$b + \frac{6\pi}{T}$			a_3 -0.079691232 b_3 0.062280857

I. A PARTICULAR MULTI-RATE CONFIGURATION

As with the analysis of closed-loop single-rate systems, the analysis of the multi-rate closed-loop case is configuration dependent. However, the mathematics remain quite tractable, as we shall attempt to demonstrate in this and the succeeding subsections. Here we consider a particularly simple multi-rate configuration; the next subsection will treat a more complex configuration.

Consider the two-rate system shown in Fig. 52. In Fig. 52, W_1 and W_2 are compensation networks, M is a data hold, and G represents the open-loop system dynamics. One may consider these to be matrices of the proper dimensions.

The objective is to find the "frequency response" for the output vector C . As in the single-rate case, we shall assume that C undergoes

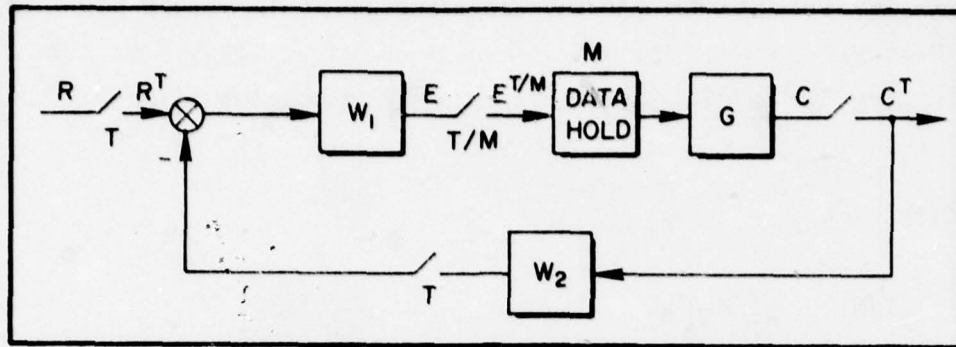


Figure 52. A Specific Two-Rate Closed-Loop Configuration

a phantom T/N sampling operation and then seek the limit as $N \rightarrow \infty$. From Fig. 52 it is seen that

$$C = GME^{T/M} \quad (335)$$

or

$$C^{T/N} = (GM)^{T/N} E^{T/M}, \quad N/M \text{ an integer} \quad (336)$$

Thus, the first task is to solve for $E^{T/M}$. This is a non-trivial task; the details must be followed with care.

$$E = W_1 R^T - W_1 W_2^T (GME^{T/M})^T \quad (337)$$

Therefore,

$$E^{T/M} = W_1^{T/M} R^T - W_1^{T/M} W_2^T (GME^{T/M})^T \quad (338)$$

Pre-multiply Eq. 338 by GM and sample at a T interval.

$$(GME^{T/M})^T = (GMW_1^{T/M})^T R^T - (GMW_1^{T/M})^T W_2^T (GME^{T/M})^T \quad (339)$$

Solve Eq. 339 for $(GME^{T/M})^T$:

$$(GME^{T/M})^T = [I + (GMW_1^{T/M})^T W_2^T]^{-1} (GMW_1^{T/M})^T R^T \quad (340)$$

Substitute Eq. 340 into Eq. 338 and clear through. The result is:

$$E^{T/M} = W_1^{T/M} \left\{ I - W_2^T [I + (GMW_1^T/M)^T W_2^T]^{-1} (GMW_1^T/M)^T \right\} R^T \quad (341)$$

For brevity, let

$$E^{T/M} = W_1^{T/M} G_A^T R^T \quad (342)$$

The evaluation of G_A^T is non-trivial; for example, the $(GMW_1^T/M)^T$ element of G_A^T will have to be computed using either switch decomposition or the phantom sampler. Via the phantom sampler,

$$(GMW_1^T/M)^T \equiv [(GM)^T/M W_1^T/M]^T \quad (343)$$

So far, the two-rate example yields:

$$C^{T/N} = (GM)^{T/N} W_1^{T/M} G_A^T R^T \quad (344)$$

and we see that the only new element added over the single-rate case is the addition of a term sampled on a T/M interval and the additional constraint that N/M be an integer.

Let

$$z = e^{sT/N} \quad (345)$$

so that a unit amplitude sinusoidal input at b rad/sec has the transform

$$R^T = \frac{z^N \sin bT}{z^{2N} - 2 \cos bT z^N + 1} \quad (346)$$

As in the single-rate case, substitute Eq. 346 into Eq. 344:

$$c^{T/N} = (GM)^{T/N} W_1^{T/M} G_A^T \frac{z^N \sin bT}{z^{2N} - 2 \cos bT z^N + 1} \quad (347)$$

Expand Eq. 347 into partial fractions*:

$$c^{T/N} = \sum_{n=0}^{N-1} \frac{A_n z \sin \omega_n(T/N) + B_n z [z - \cos \omega_n(T/N)]}{z^2 - 2 \cos \omega_n(T/N) z + 1} + \left[\begin{array}{l} \text{Terms due to} \\ (GM)^{T/N} W_1^{T/M} G_A^T \end{array} \right] \quad (348)$$

where

$$\omega_n = b + \frac{2\pi n}{T} \quad (349)$$

(Keep in mind that we can no longer pick N arbitrarily. Thus, if $M = 3$, we cannot look at c^T within the present problem structure; however, we can look at $c^{T/3}$, $c^{T/6}$, $c^{T/9}$, etc., since N/M is an integer. Thus, as we let $N \rightarrow \infty$, we would have to do so in multiples of 3.)

Assume that the terms due to $(GM)^{T/N} W_1^{T/M} G_A^T$ vanish as $t \rightarrow \infty$. Thus, the steady-state response, at the sampling instants, is given by:

$$c(t) \Big|_{t \rightarrow \infty} = \sum_{n=0}^{N-1} A_n \sin \omega_n t + B_n \cos \omega_n t \quad (350)$$

To find A_n and B_n , multiply Eqs. 347 and 348 by $[z^2 - 2 \cos \omega_k(T/N)z + 1]$ (note the dummy index).

*At this point we may fall back on the results of previous subsections and proceed directly to Eq. 358. However, it is a worthwhile exercise to complete the proof in order to gain familiarity with the notation.

$$\begin{aligned}
& (GM)^{T/N} W_1^T / M_{GA}^T \frac{z^N \sin bT[z^2 - 2 \cos \omega_k(T/N)z + 1]}{z^{2N} - 2 \cos bTz^N + 1} \\
& = [z^2 - 2 \cos \omega_k(T/N)z + 1] \sum_{n=0}^{N-1} \frac{A_n z \sin \omega_n(T/N) + B_n z [z - \cos \omega_n(T/N)]}{z^2 - 2 \cos \omega_n(T/N)z + 1} \\
& \quad + [z^2 - \cos \omega_k(T/N)z + 1] [(GM)^{T/N} W_1^T / M_{GA}^T] \quad (351)
\end{aligned}$$

Evaluate both sides for $z = \cos \omega_k(T/N) + j \sin \omega_k(T/N)$. Thus, the only term which survives in the summation on the right-hand side is when $n = k$. We may as well drop the k notation and retain n (the choice is ours).

So far,

$$\begin{aligned}
& A_n z \sin \omega_n(T/N) + j B_n z \sin \omega_n(T/N) \\
& = (GM)^{T/N} W_1^T / M_{GA}^T \frac{z^N \sin bT[z^2 - 2 \cos \omega_k(T/N)z + 1]}{z^{2N} - 2 \cos bTz^N + 1} \Big|_{z=1 \angle \omega_n(T/N)} \quad (352)
\end{aligned}$$

or

$$\begin{aligned}
A_n + j B_n & = (GM)^{T/N} W_1^T / M_{GA}^T \frac{z^{N-1} \sin bT[z^2 - 2 \cos \omega_n(T/N)z + 1]}{\sin \omega_n(T/N)(z^{2N} - 2 \cos bTz^N + 1)} \Big|_{z=1 \angle \omega_n(T/N)} \\
& \quad (353)
\end{aligned}$$

Note:

$$1 \angle \omega_n(T/N) \equiv \cos \omega_n(T/N) + j \sin \omega_n(T/N)$$

The right-hand side of Eq. 353 is indeterminate when $z = 1 \angle \omega_n(T/N)$. Therefore, use L'Hôpital's rule,

$$A_n + jB_n = (GM)^{T/N} W_1^T / M_G^T \frac{z^{N-1} \sin bT}{\sin \omega_n(T/N)} \frac{2z - 2 \cos \omega_n(T/N)}{2N(z^{2N-1} - \cos bT z^{N-1})} \Big|_{1\angle \omega_n(T/N)} \quad (354)$$

$$= (GM)^{T/N} W_1^T / M_G^T \frac{z^{N-1} \sin bT}{\sin \omega_n(T/N)} \frac{(2)[z - \cos \omega_n(T/N)]}{\cancel{2N} z^{N-1} (z^N - \cos bT)} \Big|_{1\angle \omega_n(T/N)} \quad (355)$$

$$A_n + jB_n = (GM)^{T/N} W_1^T / M_G^T \Big|_{1\angle \omega_n(T/N)} \times \frac{\sin bT [\cos \omega_n(T/N) + j \sin \omega_n(T/N) - \cos \omega_n(T/N)]}{[\sin \omega_n(T/N)] N (\cos \omega_n T + j \sin \omega_n T - \cos bT)} \quad (356)$$

Therefore,

$$A_n + jB_n = \frac{1}{N} (GM)^{T/N} W_1^T / M_G^T \Big|_{1\angle \omega_n(T/N)} \times \frac{(\sin bT) [j \sin \omega_n(T/N)]}{[\sin \omega_n(T/N)] (\cos \omega_n T + j \sin \omega_n T - \cos bT)} \quad (357)$$

but,

$$\begin{aligned} [1\angle \omega_n(T/N)]^N - \cos bT &= 1\angle \omega_n T - \cos bT \\ &= \cos \omega_n T + j \sin \omega_n T - \cos bT \\ &= \cos [b + (2\pi m/T)]T + j \sin [b + (2\pi m/T)]T - \cos bT \\ &= \cos bT + j \sin bT - \cos bT \\ &= j \sin bT \end{aligned}$$

Therefore,

$$A_n + jB_n = \frac{1}{N} (GM)^{T/N} W_1^T / M_G^T \Big|_{1\angle \omega_n(T/N)} \quad (358)$$

Next,

$$G_A^T = G_A(z^N)$$

Therefore,

$$\begin{aligned} G_A(z^N) \Big|_{1\angle\omega_n(T/N)} &= G_A[1\angle\omega_n(T/N)]^N \\ &= G_A(1\angle\omega_n T) = G_A(1\angle bT) \end{aligned} \quad (359)$$

That is, take the "T" z-transform of G_A , and evaluate at $z = 1\angle bT$. Now, the "new" element, $W_1^{T/M}$:

$$W_1^{T/M} \triangleq W_1(z^{N/M}) \quad (360)$$

Therefore,

$$W_1(z^{N/M}) \Big|_{1\angle\omega_n(T/N)} = W_1[1\angle\omega_n(T/N)]^{N/M} \quad (361)$$

$$= W_1[1\angle\omega_n(T/M)] \quad (362)$$

That is, take the "T/M" z-transform of W_1 and evaluate it at $z = 1\angle\omega_n(T/M)$.

At this point, only GM depends on N and we can go to the limit of $N \rightarrow \infty$.

$$A_n + jB_n = \frac{1}{N} \left[(GM)^{T/N} \Big|_{z=1\angle\omega_n(T/N)} \right] \left[W_1^{T/M} \Big|_{z=1\angle\omega_n(T/M)} \right] \left[G_A^T \Big|_{z=1\angle bT} \right] \left[z^{\angle e^{sT}} \right] \quad (363)$$

This is the desired result for finite N (remember $N = M, 2M$, etc.). As $N \rightarrow \infty$, the coefficients of the continuous spectrum are given by

$$A_n + jB_n = \frac{1}{T} (GM) \Big|_{s=j\omega_n} \left[W_1^{T/M} \Big|_{z=1\angle\omega_n(T/M)} \right] \left[G_A^T \Big|_{z=1\angle bT} \right] \left[z^{\angle e^{sT}} \right] \quad (364)$$

An example which illustrates the use of Eq. 364 is given in Fig. 53. This frequency response (which is plotted on a linear scale rather than $\log \omega$) can be contrasted with the single-rate results shown in Fig. 54. In each case, the design objective was to force unity DC gain and a closed-loop short period at $\Delta = (s+2)^2 + (2)^2$ when the open loop was $D = (s+2)^2 + (6)^2$.

Note that the two-rate configuration requires a significant increase in the feedback gain. Also, the first "notch" does not occur until $\omega = 100$ rad/sec.

J. A FAST INNER-LOOP, SLOW OUTER-LOOP PROBLEM

The vector configuration of Fig. 55 is typical of the "fast sampled" inner-loop, "slow sampled" outer-loop format. This type of configuration is particularly easy to analyze; closed-form analytical solutions can usually be obtained. This will be demonstrated using the configuration of Fig. 55.

$$C_1 = G_1 M_1 E^T - H G_2 M_2 C_1^{T/M} \quad (365)$$

Therefore

$$C_1^{T/M} = (G_1 M_1)^{T/M} E^T - (H G_2 M_2)^{T/M} C_1^{T/M} \quad (366)$$

or

$$C_1^{T/M} = [I + (H G_2 M_2)^{T/M}]^{-1} (G_1 M_1)^{T/M} E^T \quad (367)$$

Let

$$G_A^{T/M} = [I + (H G_2 M_2)^{T/M}]^{-1} (G_1 M_1)^{T/M} \quad (368)$$

so that

$$C_1^{T/M} = G_A^{T/M} E^T \quad (369)$$

Next, solve for E^T in terms of R^T :

$$\begin{aligned} E &= R - C \\ &= R - G_2 M_2 C_1^{T/M} = R - G_2 M_2 G_A^{T/M} E^T \end{aligned} \quad (370)$$

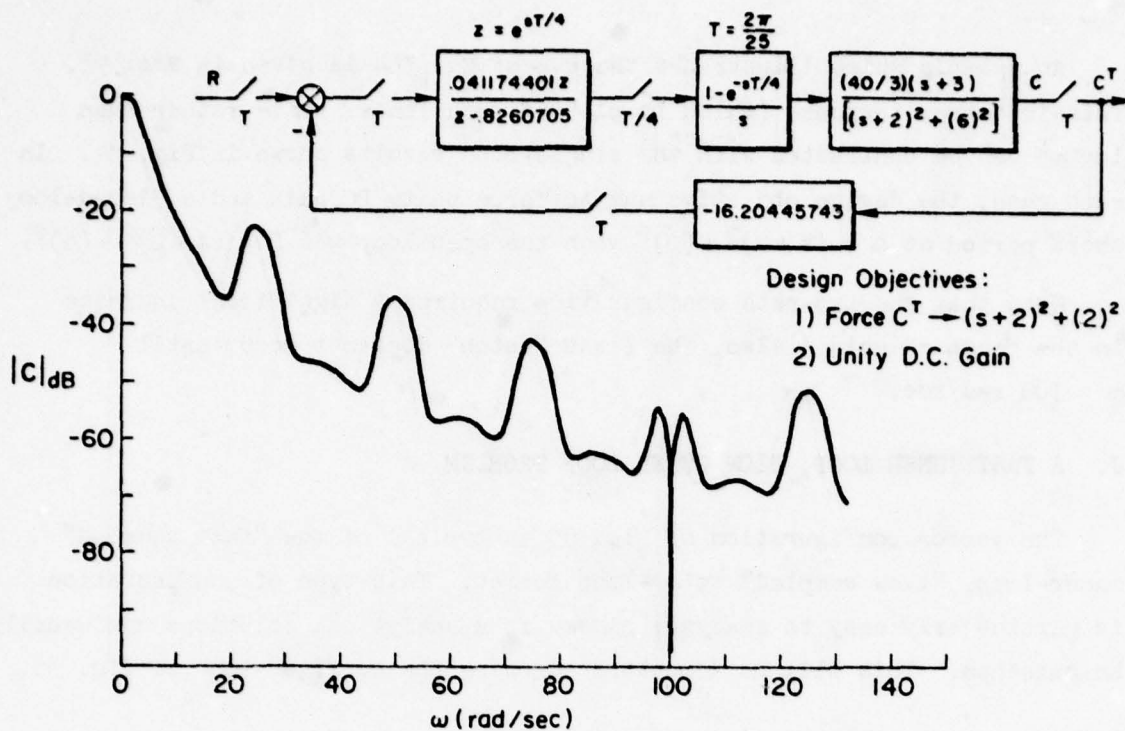


Figure 53. Magnitude Plot $T/4$, T , Closed-Loop System

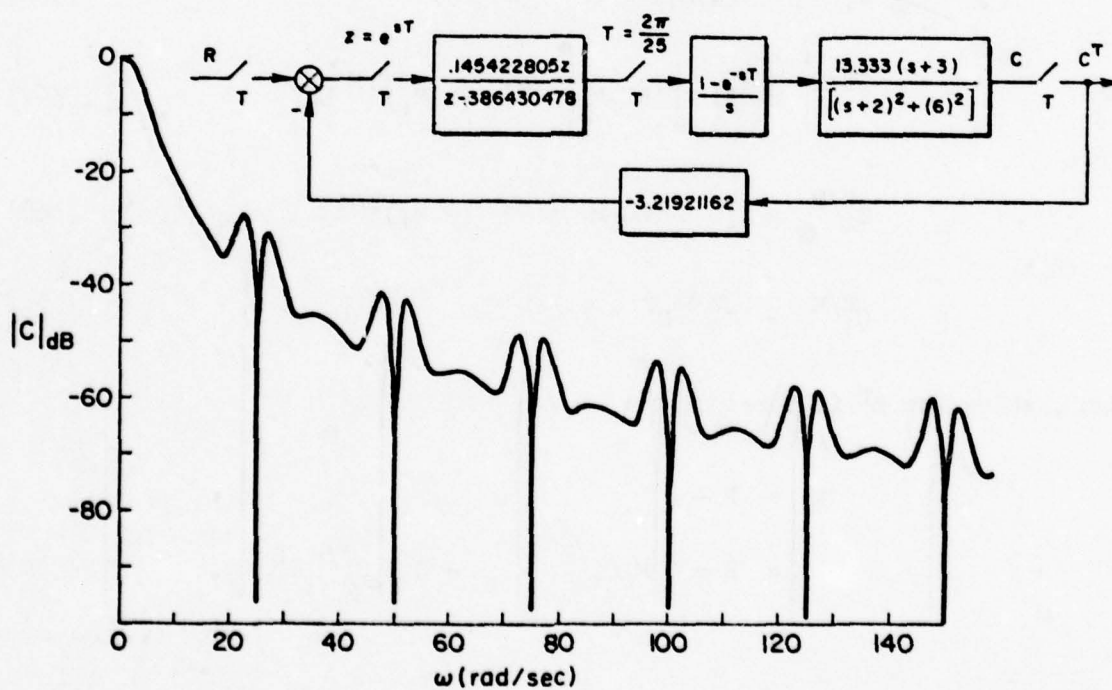


Figure 54. Magnitude Plot T , Closed-Loop System

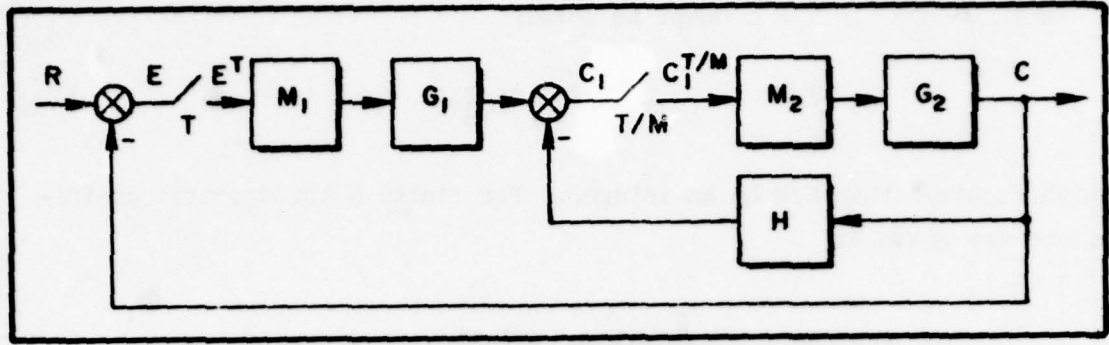


Figure 55. Fast Inner-Loop, Slow Outer-Loop Example

Therefore

$$E^T = R^T - (G_2 M_2 G_A^T/M)^T E^T$$

and we can solve for E^T

$$E^T = [I + (G_2 M_2 G_A^T/M)^T]^{-1} R^T \quad (371)$$

Since

$$C = G_2 M_2 C_1^T/M = G_2 M_2 G_A^T/M E^T \quad (372)$$

we can use Eq. 371 to obtain a closed-form analytical relationship for the continuous output vector C. The result is

$$C = G_2 M_2 G_A^T/M [I + (G_2 M_2 G_A^T/M)^T]^{-1} R^T \quad (373)$$

where G_A^T/M is defined by Eq. 368. Notice that either vector switch decomposition or the phantom sampler concept must be used to evaluate $(G_2 M_2 G_A^T/M)^T$.

Let

$$G_B^T = [I + (G_2 M_2 G_A^T/M)^T]^{-1} \quad (374)$$

so that

$$C = G_2 M_2 G_A^T/M G_B^T R^T \quad (375)$$

Next we use the T/N concept to obtain

$$C^{T/N} = (G_2 M_2)^{T/N} G_A^{T/M} G_B^{T/R} \quad (376)$$

which requires that N/M be an integer. For finite N the spectral coefficients are given by

$$A_n + jB_n = \frac{(G_2 M_2)^{T/N}}{N} G_A^{T/M} G_B^{T/R} \Big|_{z=1 \Delta (\omega_n T/N)} \quad (377)$$

where

$$\omega_n = b + \frac{2\pi n}{T} \quad (378)$$

and

$$r(t) = \sin bt \quad (379)$$

In the limit, as $N \rightarrow \infty$, we obtain the continuous signal spectrum coefficients

$$A_n + jB_n = \left[\frac{G_2 M_2}{T} \right]_{s=j\omega_n} \left[G_A^{T/M} \right]_{z=1 \Delta (\omega_n T/M)} \left[G_B^{T/R} \right]_{z=1 \Delta bT} \quad (380)$$

As usual, the notation $G_A^{T/M} \Big|_{z=1 \Delta (\omega_n T/M)}$ means compute the z-transform of G_A with respect to a T/M second frame time and evaluate it at $z = \cos \omega_n(T/M) + j \sin \omega_n(T/M)$. In a similar fashion the z-transform of G_B is computed with respect to a T frame time and evaluated at $z = \cos bT + j \sin bT$.

To this point in the development, all results apply regardless of whether Fig. 55 is a scalar or a vector block diagram.

It is worthwhile to go through a simple scalar illustrative example in order to bring the mathematical details sharply into focus.

Example

Let

$$G_2 = \frac{1}{s+1}, \quad H = -1, \quad M_2 = \frac{1 - e^{-sT/M}}{s} \quad (381)$$

$$G_1 = \frac{2}{s+2}, \quad M_1 = \frac{1 - e^{-sT}}{s} \quad (382)$$

Reviewing the equations it is seen that we must compute:

- 1) $(HG_2M_2)^{T/M}$
- 2) $(G_1M_1)^{T/M}$
- 3) $[I + (HG_2M_2)^{T/M}]^{-1}$
- 4) $G_A^{T/M} = [I + (HG_2M_2)^{T/M}]^{-1} (G_1M_1)^{T/M}$
- 5) $(G_2M_2G_A^{T/M})^T$
- 6) $G_B^T = [I + (G_2M_2G_A^{T/M})^T]^{-1}$

Let us now compute Items 1-6 noting as we go the "tricky points" that one may have a tendency to stumble over.

Item 1

$$(HG_2M_2)^{T/M} = - \left[\frac{1 - e^{-sT/M}}{s(s+1)} \right]^{T/M}$$

This is a trivial computation since the frame time of the sampling operation and the frame time of the data hold involved are the same. Let $z = e^{sT/M}$:

$$(HG_2M_2)^{T/M} = - \left[\left(\frac{z-1}{z} \right) \left[\frac{1}{s} - \frac{1}{s+1} \right] \right]^{T/M} = - \frac{1 - e^{-T/M}}{z - e^{-T/M}} \quad (385)$$

Item 2

$$(G_1M_1)^{T/M} = \left[\frac{2(1 - e^{-sT})}{s(s+2)} \right]^{T/M}$$

We proceed a little more carefully with this computation since the frame time of the sampling operation is shorter than the frame time of the data hold. Again we use $z = e^{sT/M}$.

$$\begin{aligned}
\frac{2(1 - e^{-sT})}{s(s+2)} &= \frac{z^M - 1}{z^M} \left[\frac{1}{s} - \frac{1}{s+2} \right]^{T/M} \\
&= \frac{z^M - 1}{z^M} \left[\frac{z}{z-1} - \frac{z}{z - e^{-2T/M}} \right] \\
&= \frac{z^M - 1}{z^M} \left[\frac{z(1 - e^{-2T/M})}{(z-1)(z - e^{-2T/M})} \right]
\end{aligned}$$

Therefore,

$$(G_1 M_1)^{T/M} = \frac{1 - e^{-2T/M}}{z - e^{-2T/M}} \frac{z^M - 1}{(z-1)z^{M-1}} \quad (384)$$

Item 3

$$\begin{aligned}
[I + (H G_2 M_2)^{T/M}]^{-1} &= \left[1 - \frac{1 - e^{-T/M}}{z - e^{-T/M}} \right]^{-1} \\
&= \frac{z - e^{-T/M}}{z - 1} \quad (385)
\end{aligned}$$

Item 4

$$G_A^{T/M} = \frac{z - e^{-T/M}}{(z-1)^2} \frac{z^M - 1}{z^{M-1}} \frac{1 - e^{-2T/M}}{z - e^{-2T/M}} \quad (386)$$

Steps 3 and 4 were straightforward. The next step is the "hardest." To evaluate it we resort to the phantom sampler concept.

Item 5

$$(G_2 M_2 G_A^{T/M})^T \equiv \left[(G_2 M_2)^{T/M} G_A^{T/M} \right]^T$$

Since

$$(G_{2M_2})^{T/M} = \frac{1 - e^{-T/M}}{z - e^{-T/M}}$$

we obtain

$$(G_{2M_2})^{T/M} G_A^{T/M} = \frac{(1 - e^{-T/M})(1 - e^{-2T/M})(z^M - 1)}{(z - 1)^2 z^{M-1} (z - e^{-2T/M})} \quad (387)$$

Rewrite Eq. 387 in a more illuminating form:

$$(G_{2M_2})^{T/M} G_A^{T/M} = \frac{(1 - e^{-T/M})(1 - e^{-2T/M})}{(z - 1)(z - e^{-2T/M})} \left[1 + z^{-1} + \dots + z^{-(M-1)} \right] \quad (388)$$

The incentive for rewriting Eq. 387 in the form of Eq. 388 is simply that we recognize that this system only has two poles; the other poles, z^{M-1} , have been forced on us by the difference in the frame time of the sampling operation and the frame time of the computer.

Next, recall that a function of z has a corresponding continuous time function which we can visualize as being the "generator" of the sampled function. For example, we can say that the function

$$F(z) = \frac{z(1 - e^{-2T/M})}{(z - 1)(z - e^{-2T/M})} = \frac{z}{z - 1} - \frac{z}{z - e^{-2T/M}} \quad (389)$$

was generated by sampling $f(t)$ at intervals T/M where

$$f(t) = (1 - e^{-2t})\mu(t)$$

and $\mu(t)$ is a unit step function. This insures that $f(t) \equiv 0$ for $t < 0$. We can find $[G_{2M_2})^{T/M} G_A^{T/M}]^T$ by taking advantage of this observation; simply find the continuous time "generator" for $(G_{2M_2})^{T/M} G_A^{T/M}$ and resample it using a T sampling interval! Thus we can rewrite Eq. 388:

$$\frac{(1 - e^{-T/M})(1 - e^{-2T/M})z}{(z - 1)(z - e^{-2T/M})} (z^{-1} + z^{-2} + z^{-3} + \dots + z^{-M})$$

$$= (1 - e^{-T/M}) \left[\frac{z}{z - 1} - \frac{z}{z - e^{-2T/M}} \right] (z^{-1} + \dots + z^{-M}) \quad (390)$$

If we set

$$f(t) = (1 - e^{-T/M})(1 - e^{-2t}) \quad (391)$$

the continuous "generator" to be sampled is

$$[(G_2 M_2)^{T/M} G_A^{T/M}]^T = \left[f\left(t - \frac{T}{M}\right) \mu\left(t - \frac{T}{M}\right) \right. \\ \left. + f\left(t - \frac{2T}{M}\right) \mu\left(t - \frac{2T}{M}\right) + \dots + f(t - T) \mu(t - T) \right]^T \quad (392)$$

If one prefers, Laplace transforms can be used. For example, if $M = 2$,

$$[(G_2 M_2)^{T/2} G_A^{T/2}]^T = \left[\left(\frac{1}{s} - \frac{1}{s + 2} \right) (e^{-sT/2} + e^{-sT}) \right]^T (1 - e^{-T/2}) \quad (393)$$

can be readily evaluated using a table of advanced z -transforms. To illustrate,

$$\left[\frac{e^{-sT/2}}{s} - \frac{e^{-sT/2}}{s + 2} + \frac{e^{-sT}}{s} - \frac{e^{-sT}}{s + 2} \right]^T = \left[\frac{1}{z - 1} - \frac{e^{-T}}{z - e^{-2T}} + \frac{1}{z - 1} - \frac{1}{z - e^{-2T}} \right]^T \quad (394)$$

Therefore,

$$[(G_2 M_2)^{T/2} G_A^{T/2}]^T = \frac{(1 - e^{-T/2})[(1 - e^{-T})z + (1 + e^{-T} - 2e^{-2T})]}{(z - 1)(z - e^{-2T})} \quad (395)$$

where z is understood to be $z = e^{sT}$. If we keep $e^{sT/2} = z$ as our reference, then

$$[(G_{22})^{T/2} G_A^{T/2}]^T = \frac{(1 - e^{-T/2})[(1 - e^{-T})z^2 + (1 + e^{-T} - 2e^{-2T})]}{(z^2 - 1)(z^2 - e^{-2T})} \quad (396)$$

For frequency response purposes, we can use Eq. 395 evaluated at $z = 1/\omega_n T$ or Eq. 396 evaluated at $z = 1/\omega_n(T/2)$; the answers will, of course, be the same.

Return now to the basic problem at hand. Instead of setting $M = 2$, let it be arbitrary and re-evaluate Eq. 392 as

$$[(G_{22})^{T/M} G_A^{T/M}]^T = \frac{(1 - e^{-T/M}) \left[\left(M - \frac{1 - e^{-2T}}{1 - e^{-2T/M}} \right) z + \left(\frac{1 - e^{-2T}}{1 - e^{-2T/M}} - M e^{-2T} \right) \right]}{(z - 1)(z - e^{-2T})} \quad (397)$$

To derive Eq. 397, simply write the generic term for the delayed z -transform, recognizing that the sum resulting from $(z^{-1} + \dots + z^{-M})$ can be placed in closed form since it is a geometric progression. This concludes the evaluation of Item 5; it was the most difficult step.

Item 6

$$G_B^T = [I + (G_{22} G_A^T/M)^T]^{-1} = \frac{(z - 1)(z - e^{-2T})}{z^2 + a_1 z + a_0} \quad (398)$$

where

$$a_1 = (1 - e^{-T/M}) \left(M - \frac{1 - e^{-2T}}{1 - e^{-2T/M}} \right) - 1 - e^{-2T} \quad (399)$$

$$a_0 = e^{-2T} + (1 - e^{-T/M}) \left(\frac{1 - e^{-2T}}{1 - e^{-2T/M}} - M e^{-2T} \right) \quad (400)$$

We are now ready to evaluate Eq. 380.

$$A_n + jB_n = \left[\frac{1 - e^{-sT/M}}{sT} \frac{1}{s+1} \right]_{s=j\omega_n} \left[\frac{z - e^{-T/M}}{(z-1)^2} \frac{z^M - 1}{z^{M-1}} \frac{1 - e^{-2T/M}}{z - e^{-2T/M}} \right]_{z=1 \pm j(\omega_n T/M)} \\ \times \left[\frac{(z-1)(z - e^{-2T})}{z^2 + a_1 z + a_0} \right]_{z=1 \pm j b T} \quad (401)$$

where $\omega_n = b + (2\pi n/T)$.

One must remember that the terms in Eq. 401 do not cancel. For example, the $z-1$ in the numerator of the last term does not cancel a $z-1$ in the denominator of the second term, since each bracketed term is being evaluated at a different value of z .

For comparison purposes, we can define a reference "analog" system by removing the sample and holds from Fig. 55. The transfer function would then be

$$C = G_2 [I + H G_2]^{-1} G_1 [I + G_2 (I + H G_2)^{-1} G_1]^{-1} R \quad (402)$$

For this scalar illustrative example the reference transfer function becomes

$$\frac{C}{R} = \frac{2}{s^2 + 2s + 2} \quad (403)$$

The Bode plot obtained using Eq. 403 can be compared against those obtained using Eq. 401. Some comparative results are shown in Fig. 56 for the case where $M = 2$. Note that for rates as low as 10 samples/second ($T = 0.1$) that there is no discernible difference in the magnitude plot — at least in the portion of the first fold that is shown in Fig. 56. However, the difference in the phase plots is noticeable. Of course, the difference becomes quite large when the frame time is set at 1 second ($T = 1$).

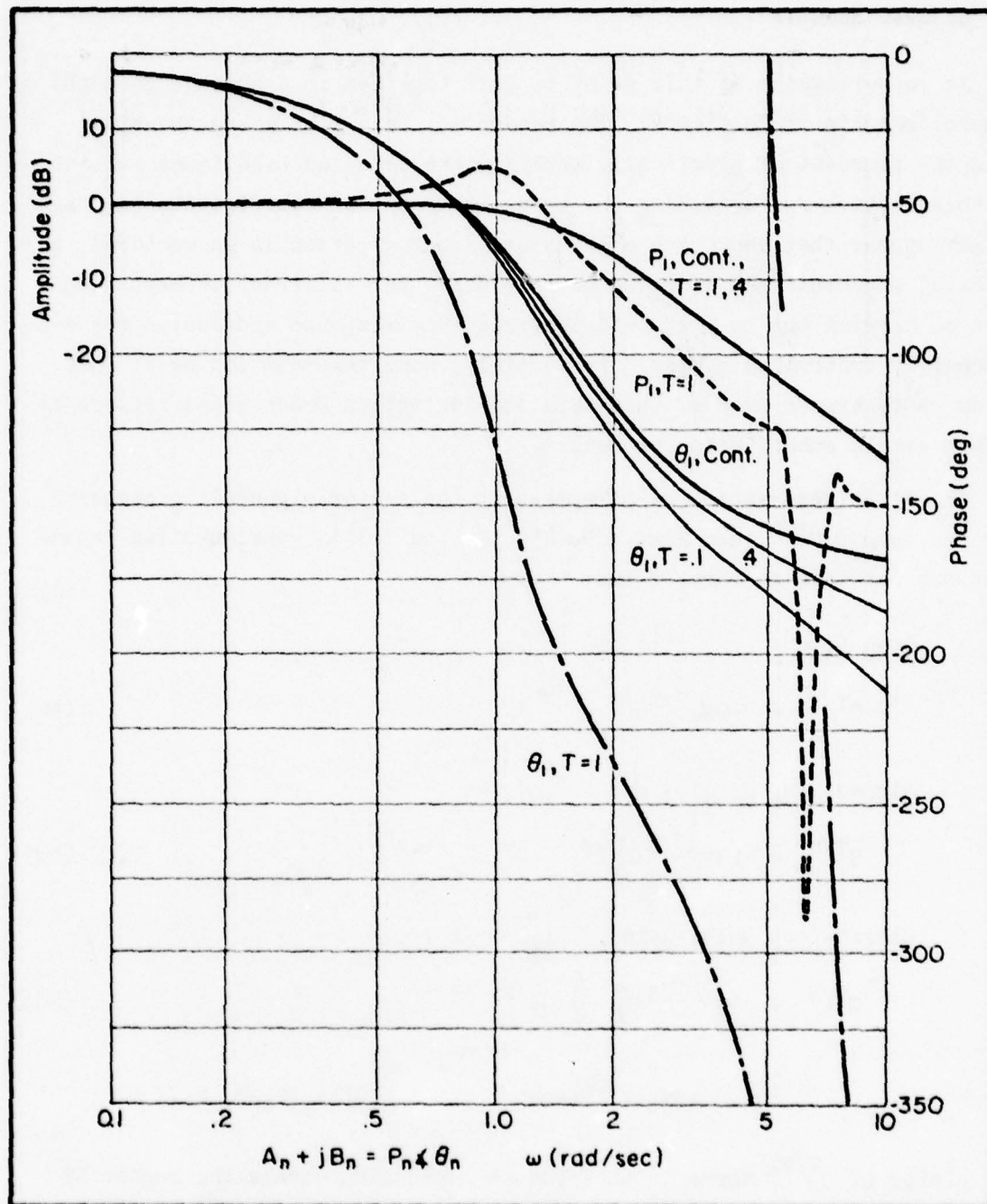


Figure 56. Bode Plot for Illustrative Example

K. GENERAL RESULTS

It is worthwhile at this point to pull together in a compact form the general results of Section V. The reader may be a little apprehensive over the prospect of practically applying the detailed techniques outlined in this section for obtaining the frequency response coefficients $(A_n + B_n j)$. It may appear that each time a new system configuration is encountered, a detailed algebraic and limiting process using partial fraction expansion must be carried out to formulate the frequency response expression for a discretely controlled system. Fortunately, some generalities exist that allow us to bypass much of this detailed derivation process and replace it with a simple substitution procedure.

The first observation we make is that the vector algebraic expression for the output $C^{T/N}$ (see Figs. 39, 45, 52, and 55) is configuration dependent but can take on three forms:

Open-Loop

$$C^{T/N} = (GM)^{T/N} R^T \quad (404)$$

Closed-Loop Single-Rate

$$C^{T/N} = (GM)^{T/N} G_A^T R^T \quad (405)$$

Closed-Loop Multi-Rate

$$C^{T/N} = (GM)^{T/N} G_A^T \prod_{k=0}^K G_k^{T/M_k} R^T \quad (406)$$

$$N/M_k = \text{Integer} \quad ; \quad k = 0, 1, 2, 3, \dots$$

The number of G_k^{T/M_k} terms in the product expression equals the number of different sampling rates in the system (excluding the "T" sampling rate). For example, if a particular system has samplers operating at T, T/10, T/20, and T/50 ($N = 100$)

$$C^{T/100} = (GM)^{T/100} G_A^T G_1^{T/10} G_2^{T/20} G_3^{T/50} R^T \quad (407)$$

With the $C^{T/N}$ expression formulated using block diagram algebra, the following identities allow the frequency response expression ($A_n + jB_n$) to be written directly from inspection of each term in the $C^{T/N}$ vector equation.

Finite N

$$(GM)^{T/N} \rightarrow \frac{1}{N} (GM)^{T/N}(z) \left| \begin{array}{l} z^{\Delta} e^{sT/N} \\ z = 1 \angle \omega_n(T/N) \end{array} \right. \quad (408)$$

$$G_A^T \rightarrow G_A^T(z) \left| \begin{array}{l} z^{\Delta} e^{sT} \\ z = 1 \angle bT \end{array} \right. \quad (409)$$

$$G_k^{T/M_k} \rightarrow G_k^{T/M_k}(z) \left| \begin{array}{l} z^{\Delta} e^{sT/M_k} \\ z = 1 \angle \omega_n(T/M_k) \end{array} \right. \quad (410)$$

$$A_n + jB_n = \left[\frac{1}{N} (GM)^{T/N}(z) \left| \begin{array}{l} z^{\Delta} e^{sT/N} \\ z = 1 \angle \omega_n(T/N) \end{array} \right. \right] \left[G_A^T(z) \left| \begin{array}{l} z^{\Delta} e^{sT} \\ z = 1 \angle bT \end{array} \right. \right] \times \\ \left[\prod_k^k G_k^{T/M_k}(z) \left| \begin{array}{l} z^{\Delta} e^{sT/M_k} \\ z = 1 \angle \omega_n(T/M_k) \end{array} \right. \right] \quad (411)$$

$N \rightarrow \infty$

$$(GM)^{T/N} \rightarrow \frac{1}{T} (GM)(s) \left| \begin{array}{l} \\ s = j\omega_n \end{array} \right. \quad (412)$$

$$G_A^T \rightarrow G_A^T(z) \left| \begin{array}{l} z^{\Delta} e^{sT} \\ z = 1 \angle bT \end{array} \right. \quad (413)$$

$$G_k^{T/M_k} \rightarrow G_k^{T/M_k}(z) \left| \begin{array}{l} z^{\Delta} e^{sT/M_k} \\ z = 1 \angle \omega_n(T/M_k) \end{array} \right. \quad (414)$$

$$A_n + jB_n = \left[\frac{1}{T} (GM)(s) \right]_{s=j\omega_n} \left[G_A^T(z) \right]_{\substack{z=e^{sT} \\ z=1\angle bT}} \times \left[\prod_k^k G_k^{T/M_k}(z) \right]_{\substack{z=e^{sT/M_k} \\ z=1\angle \omega_n(T/M_k)}} \quad (415)$$

$$\omega_n = b + \frac{2\pi n}{T}$$

$$n = n_0, n_0 + 1, \dots, 0, 1, 2, \dots, N - n_0 - 1$$

$$n_0 = - (b/\omega_s)_{\text{INT}}$$

The notation used in these identities indicates the definition of "z" to be used in calculating each z-transform expression and the subsequent evaluation performed to calculate coefficients for the fundamental and alias terms in the output waveform ($A_n + jB_n$). That is,

Take the T/N z-transform of (GM) and evaluate at $z = 1\angle \omega_n(T/N)$.

Take the T z-transform of G_A and evaluate at $z = 1\angle bT$.

Take the T/M_k z-transform of each G_k term and evaluate at $z = 1\angle \omega_n(T/M_k)$.

Then, for the (GM) term, directly calculate the normal z-transform expression via the partial fraction expansion/table lookup approach of Section II and then replace each "T" in this expression with " T/N ." Follow the same procedure for G_A and G_k with "T" replaced with " T/M_k " in the resulting z-transform expression for the G_k terms. Now with (GM) , G_A , and G_k in z-transform form, each term is individually evaluated at the appropriate value of "z" as indicated by the notation.

Even though the tables of Section II essentially assume $z = e^{sT}$, these tables can be used for any sampling period T/N , T/M_k , etc., by simply replacing "T" in these tables with T/N , T/M_k , etc. The definition of "z" is then completely arbitrary (as far as sampling rate is concerned) and must be explicitly indicated with each pulse transfer function, i.e.,

$$(GM)(z) = \text{-----}, \quad z = e^{sT/N}$$

$$G_A(z) = \text{-----}, \quad z = e^{sT}$$

$$G_k(z) = \text{-----}, \quad z = e^{sT/M_k}$$

Example:

$$C^{T/100} = (GM)^{T/100} G_A^T G_1^{T/10} G_2^{T/20} G_3^{T/50} R^T \quad (416)$$

$$A_n + jB_n = \left[\frac{1}{N} (GM)^{T/100}(z) \left| \begin{matrix} z^{\frac{1}{N}} e^{sT/100} \\ z = 1 \angle \omega_n(T/100) \end{matrix} \right| \right] \left[G_A^T(z) \left| \begin{matrix} z^{\frac{1}{N}} e^{sT} \\ z = 1 \angle bT \end{matrix} \right| \right] \left[G_1^{T/10}(z) \left| \begin{matrix} z^{\frac{1}{N}} e^{sT/10} \\ z = 1 \angle \omega_n(T/10) \end{matrix} \right| \right] \\ \times \left[G_2^{T/20}(z) \left| \begin{matrix} z^{\frac{1}{N}} e^{sT/20} \\ z = 1 \angle \omega_n(T/20) \end{matrix} \right| \right] \left[G_3^{T/50}(z) \left| \begin{matrix} z^{\frac{1}{N}} e^{sT/50} \\ z = 1 \angle \omega_n(T/50) \end{matrix} \right| \right] \quad (417)$$

$$\omega_n = b + \frac{2\pi n}{T}$$

$$n = n_0, n_0 + 1, \dots, 0, 1, 2, \dots, N - n_0 - 1$$

$$n_0 = -(b/\omega_s)_{\text{INT}}$$

Thus it is not necessary to carry out the detailed algebraic and limiting process each time a new system configuration is encountered. Once the $C^{T/N}$ expression has been determined for the system, simple substitution produces the exact frequency response expression for either the finite N case or the limiting case of $N \rightarrow \infty$. Using this expression, the coefficients $(A_n + jB_n)$ for the fundamental and its aliases present in the output waveform can then be determined. A summary of the steps required is as follows:

- Obtain the C^T/N expression using block diagram/signal flow algebra.
- Apply the identities outlined in this subsection to each term in the C^T/N expression.
- Calculate the individual z-transform expressions using the appropriate definition of "z."
- Evaluate each z-transform expression at the appropriate values of "z."

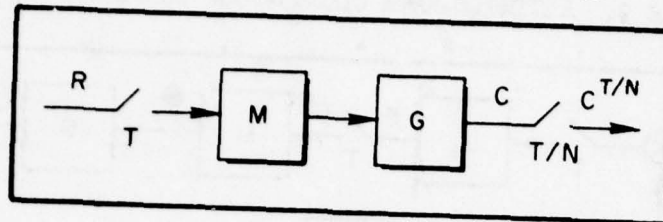
As a final remark, it should be noted that these simplifications still do not relieve us from the non-trivial nature of obtaining z-transform expressions such as $(GMW_1^T/M)^T$. This type of expression will require the use of either switch decomposition or the phantom sampler as illustrated in preceding subsections.

L. SECTION SUMMARY

The "sampled spectrum" concept of sampled data control theory is concerned with determining the simple sinusoid that fits the output samples of a single-rate system at the sampling instants. In this section, the frequency concept has been extended to encompass the continuous spectrum of the continuous variables in a discretely controlled system. Moreover, the theory considers the finite N case wherein one is concerned with the group of N sinusoids that matches the data not only at the sample points but at $N-1$ inter-sample points as well. This is an important aspect since bench validation of digital hardware is often specified in terms of an end-to-end "frequency response." Since output data are taken at a finite number of points, it will be important to compute finite N results; the coefficients will differ significantly from the continuous ($N \rightarrow \infty$) values.

The results for the closed-loop cases have been configuration dependent; however, the basic technique is relatively clear. One starts at the continuous state vector and writes the system equations back to the first input point. The next fundamental step is to convert that input into an equation which contains the sinusoidal input as the basic forcing function. Then one may always invoke the basic equations which apply to the open-loop case. The equations which summarize the cases considered in this section are given in Tables 8-11.

TABLE 8. AN OPEN-LOOP CONFIGURATION



$$r(t) = \sin bt$$

$$(C^{T/N})_{ss} = \left(\sum_{n=0}^{N-1} A_n \sin \omega_n t + B_n \cos \omega_n t \right) T/N$$

$$\omega_n = b + \frac{2\pi n}{T}, \quad n = 0, 1, \dots, N-1$$

Finite N

$$A_n + jB_n = \frac{1}{N} (GM)^{T/N} \left| \frac{z^{\frac{1}{2}} e^{sT/N}}{z = 1 \pm j\omega_n(T/N)} \right|$$

$$z = 1 \pm j\omega_n(T/N) = \cos \omega_n(T/N) + j \sin \omega_n(T/N)$$

Lim N $\rightarrow \infty$

$$A_n + jB_n = \frac{GM}{T} \Big|_{s=j\omega_n}$$

Note: If $r(t) = k_1 \sin bt + k_2 \cos bt$

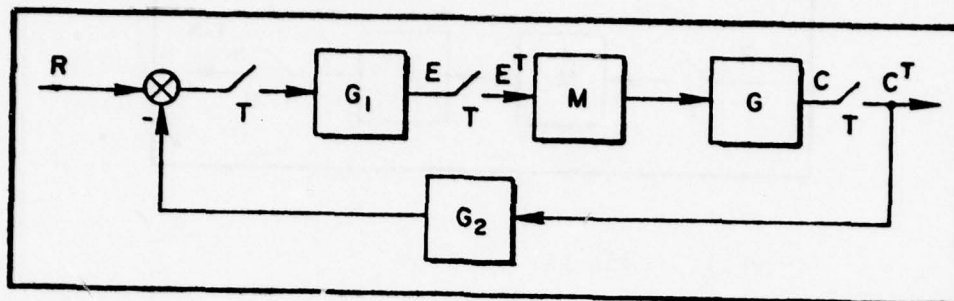
Finite N

$$A_n + jB_n = \frac{1}{N} (GM)^{T/N} \left| \frac{z^{\frac{1}{2}} e^{sT/N}}{z = 1 \pm j\omega_n(T/N)} \right| \cdot (k_1 + jk_2)$$

Lim N $\rightarrow \infty$

$$A_n + jB_n = \frac{GM}{T} \Big|_{s=j\omega_n} \cdot (k_1 + jk_2)$$

TABLE 9. A SINGLE-RATE CLOSED-LOOP CONFIGURATION



$$r(t) = \sin bt$$

$$C^T/N \Big|_{ss} = \left(\sum_{n=0}^{N-1} A_n \sin \omega_n t + B_n \cos \omega_n t \right)^{T/N}$$

$$\omega_n = b + \frac{2\pi n}{T}, \quad n = 0, 1, \dots, N-1$$

Finite N

$$A_n + jB_n = \left(\frac{1}{N} (GM)^{T/N} \right) \Big|_{z=1 \angle \omega_n (T/N)}^{z=e^{sT/N}} \cdot G_B^T \Big|_{z=1 \angle bT}^{z=e^{sT}}$$

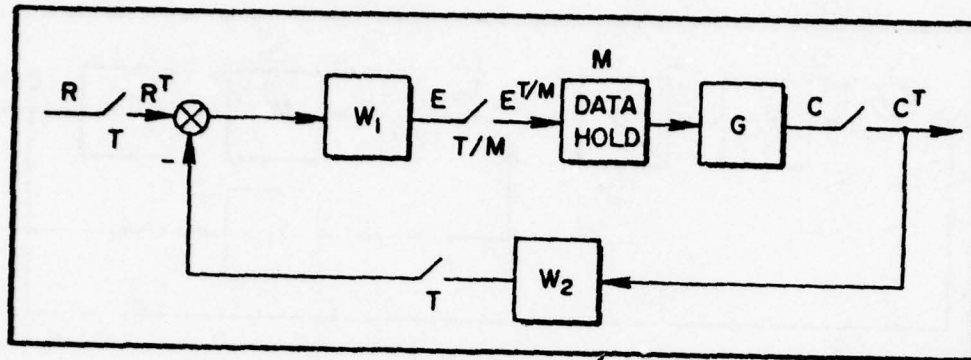
where

$$G_B^T = [I + G_1^T G_2^T (GM)^T]^{-1} G_1^T$$

Infinite N

$$A_n + jB_n = \left(\frac{GM}{T} \right)_{s=j\omega_n} \cdot G_B^T(z) \Big|_{z=1 \angle bT}^{z=e^{sT}}$$

TABLE 10. A PARTICULAR MULTI-RATE CONFIGURATION



6

$$r(t) = \sin bt$$

$$C^{T/N} \Big|_{ss} = \left(\sum_{n=0}^{N-1} A_n \sin \omega_n t + B_n \cos \omega_n t \right)^{T/N}$$

$$\omega_n = b + \frac{2\pi n}{T}, \quad n = 0, 1, \dots, N-1$$

Finite N

$$A_n + jB_n = \left(\frac{1}{N} (GM)^{T/N} \begin{vmatrix} z^{\Delta} e^{sT/N} \\ z = 1 \angle \omega_n(T/N) \end{vmatrix} \right) \left(W_1^{T/M} \begin{vmatrix} z^{\Delta} e^{sT/M} \\ z = 1 \angle \omega_n(T/M) \end{vmatrix} \right) \left(G_A^T \begin{vmatrix} z^{\Delta} e^{sT} \\ z = 1 \angle bT \end{vmatrix} \right)$$

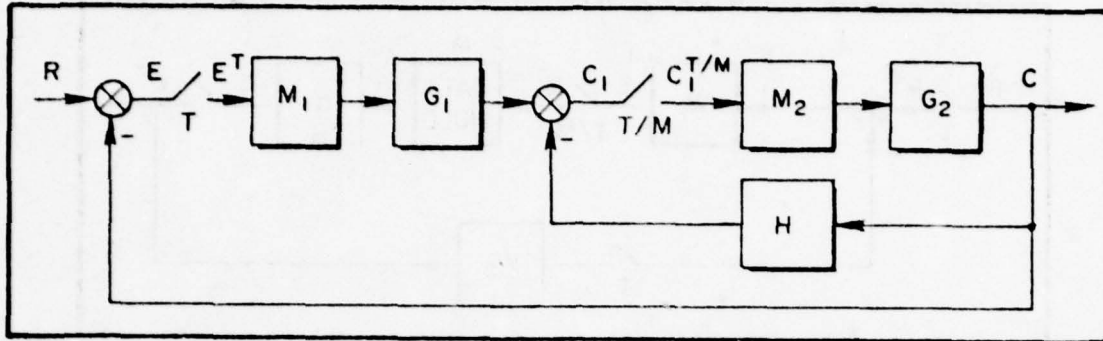
where

$$G_A = I - W_2^T [I + (GMW_1^{T/M})^T W_2^T]^{-1} (GMW_1^{T/M})^T$$

Infinite N

$$A_n + jB_n = \frac{GM}{T} \Big|_{s=j\omega_n} \cdot \left(W_1^{T/M} \begin{vmatrix} z^{\Delta} e^{sT/M} \\ z = 1 \angle \omega_n(T/M) \end{vmatrix} \right) \left(G_A^T \begin{vmatrix} z^{\Delta} e^{sT} \\ z = 1 \angle bT \end{vmatrix} \right)$$

TABLE 11. A FAST INNER-LOOP, SLOW OUTER-LOOP CONFIGURATION



$$r(t) = \sin bt$$

$$C^{T/N}|_{ss} = \left(\sum_{n=0}^{N-1} A_n \sin \omega_n t + B_n \cos \omega_n t \right)^{T/N}$$

$$\omega_n = b + \frac{2\pi n}{T}, \quad n = 0, 1, \dots, N-1$$

Finite N

$$A_n + jB_n = \left(\frac{G_2 M_2}{N} \right)^{T/N} \left[\begin{matrix} z^{\frac{1}{2}} e^{sT/N} \\ z = 1 \angle \omega_n(T/N) \end{matrix} \right] \left(G_A^{T/M} \left[\begin{matrix} z^{\frac{1}{2}} e^{sT/M} \\ z = 1 \angle \omega_n(T/M) \end{matrix} \right] \right) \left(G_B^T \left[\begin{matrix} z^{\frac{1}{2}} e^{sT} \\ z = 1 \angle bT \end{matrix} \right] \right)$$

where

$$G_A^{T/M} = [I + (HG_2 M_2)^{T/M}]^{-1} (G_1 M_1)^{T/M}$$

$$G_B^T = [I + (G_2 M_2 G_A^{T/M})^T]^{-1}$$

Infinite N

$$A_n + jB_n = \left[\frac{G_2 M_2}{T} \right]_{s=j\omega_n} \left[G_A^{T/M} \left[\begin{matrix} z^{\frac{1}{2}} e^{sT/M} \\ z = 1 \angle \omega_n(T/M) \end{matrix} \right] \right] \left[G_B^T \left[\begin{matrix} z^{\frac{1}{2}} e^{sT} \\ z = 1 \angle bT \end{matrix} \right] \right]$$

SECTION VI

FLYING QUALITIES APPLICATIONS

A. INTRODUCTION

As noted in Section I, increasingly stringent operational demands on military aircraft have forced the use of more complex stability and control augmentation systems. An augmented aircraft may have, for example, short-period characteristics that apparently satisfy the MIL-F-8785B specification and yet, because of the additional modes introduced by the flight control system, the aircraft actually responds as if it had short-period characteristics which do not meet the specification. Examples of these anomalies are given in Ref. 4, one of which is used here.

The purpose of the (specially constructed) examples in Ref. 4 was to point out possible loopholes in interpretation of the short-period frequency requirements of MIL-F-8785B (Para. 3.2.2.1.1). The problem stems from the fact that, although the specification refers to "short period response in angle of attack," the requirement was based on configurations for which this response was defined by a natural short-period mode. The specification does not consider additional modes which might be introduced by the FCS. Since the pilot senses the total response (sum of natural airframe modes plus FCS modes), specification of the short-period roots alone does not necessarily define the physical situation or insure acceptable flying qualities. Now, the trend towards the use of digital flight control systems gives the flexibility which tends to yield additional FCS modes, but also introduces additional effects due to the digital implementation.

One method proposed (e.g., Refs. 1 and 4) to treat such situations is to develop lower-order models of higher-order systems that can be compared against the MIL-F-8785B requirements as they are presently stated. To see how this method works, we will review an example from Ref. 4 which deals with the effects of FCS modes on the MIL-F-8785B requirements. This contrived example considers a tactical fighter which requires some type of flight control system (FCS) to maintain the short-period frequency within

acceptable limits at low speeds. Pitch rate feedback is intentionally used to illustrate the possible pitfalls in designing a control system to meet MIL-F-8785B requirements using an equivalent low-order system. It will become obvious that pitch rate feedback alone can not increase the effective unaugmented short-period frequency.

The subsequent digital implementation of this example from Ref. 4 will not attempt to cure the obviously inadequate analog design, but will attempt to bring into sharp focus the manner in which the equivalent low-order model should be modified in order to account for the additional artifacts introduced when the analog controller is replaced with a digital implementation. It is our intention to illustrate how the techniques developed in this report can be used to include the effects of digital implementation in the parameters of a lower-order model of airplane dynamics and not digitally design for good flying qualities. The same general flying qualities design techniques and philosophies used for analog controller design apply equally as well in a valid discrete domain synthesis such as in the w' -domain (Section III).

It is readily concluded that, to use the equivalent model concept, an exact Bode plot for the closed-loop digital system which includes all the effects of the digital artifacts (e.g., sampling, data holds, and computational delay) is needed. This can be obtained for any single-rate or multi-rate system using the digital frequency response methods of Section V. These methods are in contrast to the traditional concept of "sampled spectrum" of sampled data theory which is limited to determining the amplitude and phase of the single sinusoid that fits the output samples of a single-rate system at the sampling instants.

The example used in this section will be closed loop with a washout network in the pitch rate feedback loop. The Tustin transform is used to obtain a digital implementation of the analog washout filter to illustrate the disadvantage of this emulation procedure (i.e., the Tustin transform does not account for the phase lag introduced by the D/A conversion). The effects of throughput delay will also be incorporated into the analysis. This is done in order to indicate a procedure for modeling computational delay via vector switch decomposition (Section II) and to also indicate the effects of the delay on the closed-loop Bode plot.

Even though the washout filter is emulated for illustration purposes, it should be noted that direct digital synthesis in the w' -domain (Section III) would produce lead compensation to offset the throughput delay and nonminimum phase A/D, D/A effects. This is assuming that a match of the already established inadequate analog design is wanted. As covered in detail in Section III, direct digital design in the w' -domain is straightforward following the same procedures as an analog s -domain design. It should be noted that the power of a w' -domain direct digital design is that all effects of digital implementation (e.g., sampling, data holds, and computational delay) is directly and naturally accounted for in the resulting w' -domain control law. That is, the resulting design in the w' -domain is exact in the same sense as the analog control law is in the continuous s -domain synthesis. Then, from a practical and realistic standpoint, a complete redesign of the control law for the example in this section using different feedback schemes (e.g., angle-of-attack feedback) should be done either in the s -domain for the analog system or in the w' -domain for the digital system.

B. TACTICAL FIGHTER — ANALOG CONTROLLER

Current trends in fighter design frequently require some type of FCS to maintain the short-period frequency within acceptable limits at low speed. The airplane characteristics used in this example are typical of modern fighter aircraft in the power approach configuration. The attitude transfer function is given as:

$$\frac{\theta}{\delta e} = \frac{-1.6(0.1)(0.6)}{[0.05, 0.1][0.7, 0.5]} = \frac{-1.6(0.6)}{(s)[0.7, 0.5]} \quad (418)$$

where

$$[\zeta, \omega] \Rightarrow s^2 + 2\zeta\omega s + \omega^2 \quad ; \quad (1/T) \Rightarrow s + 1/T$$

Some type of compensation is desired because the low short-period frequency violates MIL-F-8785B and produces a sluggish pitch response. As we will see, feedback of lagged pitch rate results in an apparent increase in short-period frequency (and damping). This signal would be washed out to prevent

the pitch damper from receiving low-frequency signals which might saturate the system. The example FCS is shown in Fig. 57 along with a system survey to indicate the effect of gain (K_0) on the system. Since the phugoid frequency is only 20 percent of the short period, the two-degree-of-freedom constant-speed approximation is used for the sake of clarity. Closing the loop at $K_0 = -0.63$ results in short-period poles at 1.35 rad/sec. The augmented attitude dynamics are then given as:

$$\frac{\theta}{\delta_p} = \frac{-1.6(0.6)(0.5)(2.0)}{s(0.68)(0.2)[0.86, 1.35]} \quad (419)$$

From Fig. 57 it appears that the FCS increases the short-period undamped natural frequency and, apparently, specification compliance has been achieved. However, an equivalent lower-order system which gives approximately the same frequency response is:

$$\left(\frac{\theta}{\delta_p}\right)_{\text{eff}} = \frac{-1.47(0.5)}{s[1, 0.5]} \quad (420)$$

This effective second-order system fitted to the actual system has a natural frequency of only 0.5 rad/sec and is critically damped. Plotting the apparent augmented ω_{sp} and the "effective ω_{sp} " on the MIL-F-8785B requirement illustrates the danger in considering only the short-period pole for specification compliance when a FCS is employed (see Fig. 58). Note that even though the FCS apparently increased ω_{sp} from 0.5 to 1.35 rad/sec, the effective response indicates that pitch rate feedback only increased damping. The sluggish characteristics of the augmented airframe are indicated in the pitch rate time history to a step input of δ_p as shown in Fig. 59. Note that the time responses for the actual and effective transfer functions are in close agreement.

The above augmentation scheme is obviously unsatisfactory, making a sluggish response even worse. It still serves our purposes to consider the digital mechanization of this system.

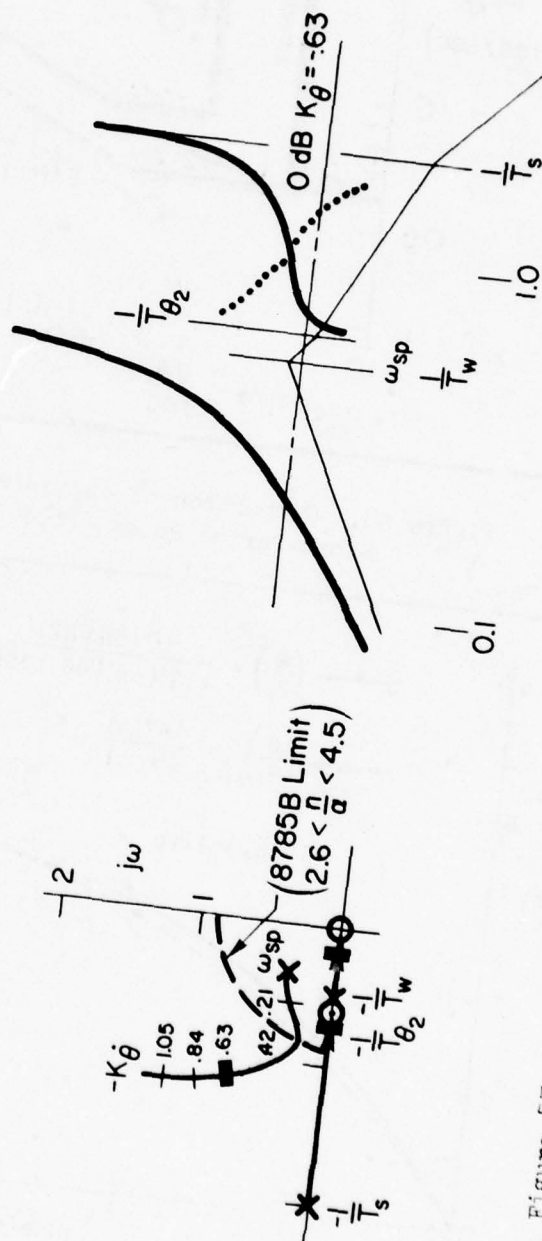
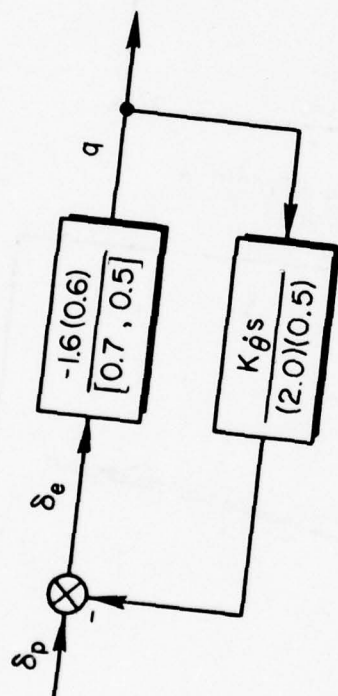


Figure 57. FCS Loop Closure for Typical Fighter Aircraft in Power Approach

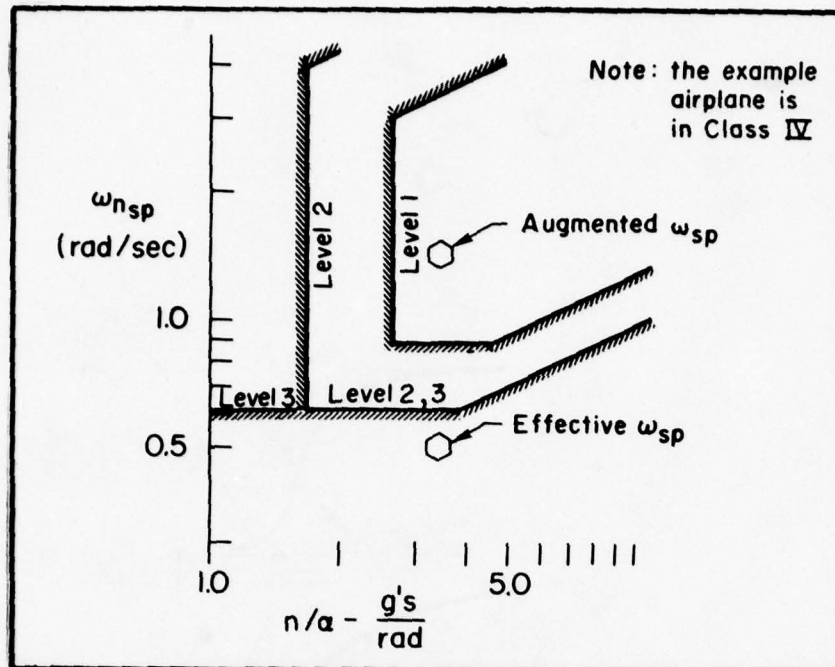


Figure 58. Comparison of Augmented and Effective Short-Period Roots (Pitch Rate FCS)

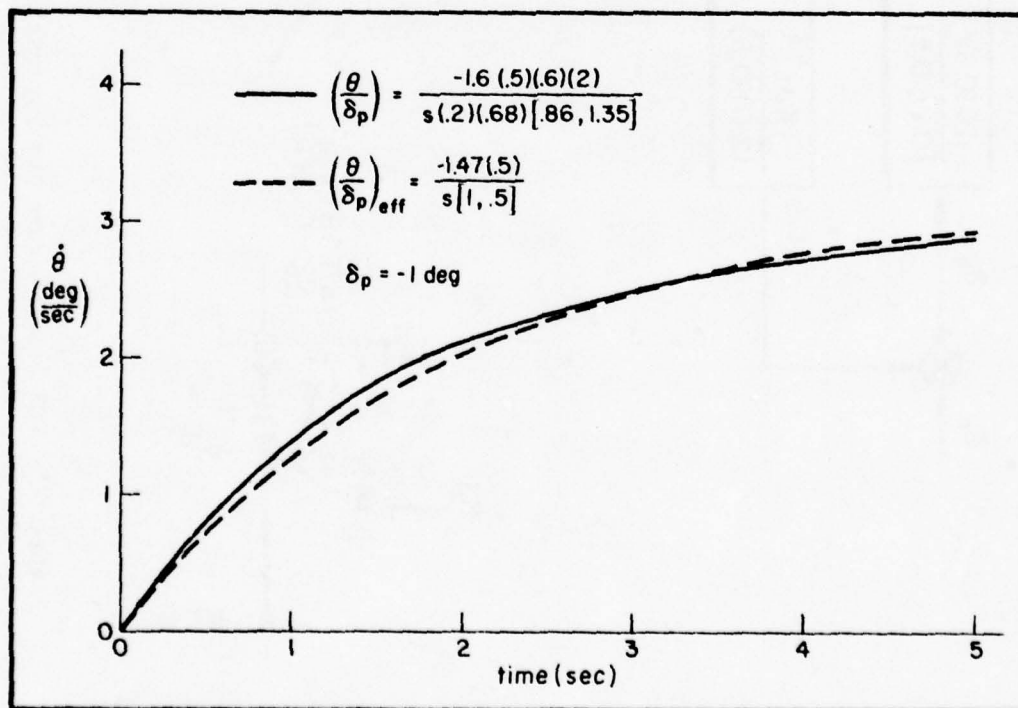


Figure 59. Comparison of Exact and Effective Time Responses

C. TACTICAL FIGHTER — DIGITAL CONTROLLER

Consider a possible model for one implementation of a digital controller for the tactical fighter shown in Fig. 60. The associated timing diagram is shown in Fig. 61.

In Fig. 61 the timing events are:

- ① δ_p is sampled and stored in buffer register; q is sampled and stored for computation of the feedback portion of the control law.
- ② Computation completed; control algorithm output to control actuator through a zero-order hold.

In Fig. 60 advantage has been taken of the fact that a sampling operation which is delayed with respect to the sampling operation of a reference sampler by T_0 seconds can be modeled by switch decomposition (refer to Appendix F) as shown in Fig. 62. From Fig. 60 the equations which pertain can be written:

$$U_1^T = (e^{sT_0} M)^T \delta_p^T - (e^{sT_0} M)^T H^T (G M e^{-sT_0})^T U_1^T \quad (421)$$

But

$$(e^{sT_0} M)^T = \left[e^{sT_0} \left(\frac{1 - e^{-sT}}{s} \right) \right]^T \quad (422)$$

and the table of advanced z-transforms (Table 4, Section II) shows that

$$\left[(1 - e^{-sT}) \left(\frac{e^{sT_0}}{s} \right) \right]^T = \frac{z - 1}{z} \frac{z}{z - 1} \equiv 1.0 \quad (423)$$

given $0 \leq T_0 < T$.

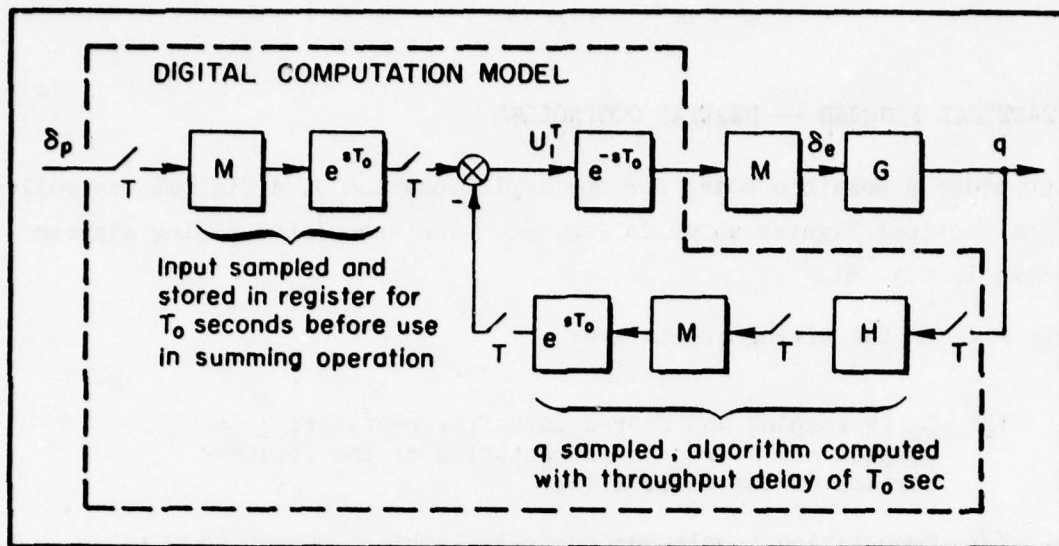


Figure 60. Digital Implementation of FCS for Tactical Fighter

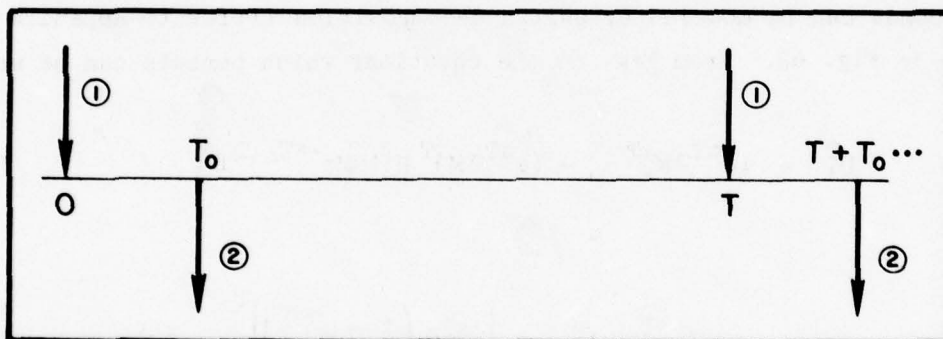


Figure 61. Digital FCS Timing Diagram

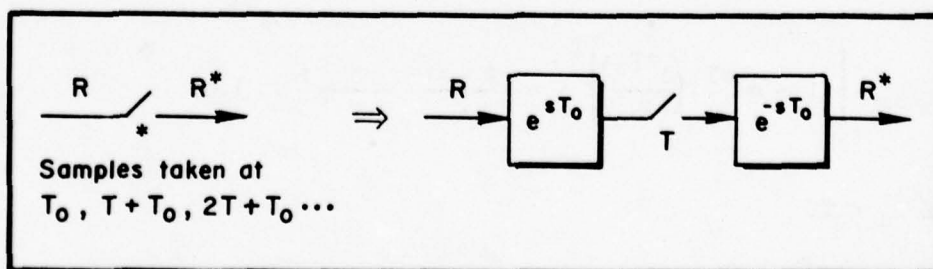


Figure 62. Model of a Non-Synchronous Sampling Operation

Equation 415 simplifies to

$$U_1^T = \delta_p^T - H^T (GMe^{-sT_0})^T U_1^T \quad (424)$$

or

$$U_1^T = \left[I + H^T (GMe^{-sT_0})^T \right]^{-1} \delta_p^T \quad (425)$$

The output is then given by

$$\begin{aligned} q &= (GMe^{-sT_0}) \left[I + H^T (GMe^{-sT_0})^T \right]^{-1} \delta_p^T \\ &= (GM)e^{-sT_0} G_A^T \delta_p^T \end{aligned} \quad (426)$$

The "continuous" spectrum, given that δ_p is a sine wave input, can be obtained (using the tools of Section V) by a limiting procedure on $q^{T/N}$.

$$q^{T/N} = (GMe^{-sT_0})^{T/N} G_A^T \delta_p^T \quad (427)$$

The spectral coefficients for the θ response, $\theta \triangleq q(s)$, can then be computed using:

$$A_n + jB_n = \frac{1}{T} \left(\frac{GMe^{-sT_0}}{s} \right) \bigg|_{s=j\omega_n} G_A^T \bigg|_{z=1\Delta bT} \quad (428)$$

The procedure is as follows:

- 1) Compute $(GMe^{-sT_0})^T$, $z \triangleq e^{sT}$.
- 2) Compute H^T via Tustin transform.
- 3) Evaluate $[I + H^T (GMe^{-sT_0})^T]^{-1} = G_A^T$.
- 4) Evaluate

$$A_n + jB_n = \frac{1}{T} \left(\frac{GMe^{-sT_0}}{s} \right) \bigg|_{s=j\omega_n} G_A^T \bigg|_{z=1\Delta bT}$$

Step 1

$$e^{-sT_0} = e^{-(1-\Delta)sT} = e^{-sT} e^{\Delta sT} ; 0 \leq \Delta \leq 1$$

$$\begin{aligned} (GMe^{-sT_0})^T &= \left\{ e^{-sT} \left(\frac{1 - e^{-sT}}{s} \right) \frac{[-1.6s - .96]e^{\Delta sT}}{s(s^2 + .7s + .25)} \right\}^T \\ &= \frac{z - 1}{z^2} \left[\frac{(-1.6s - .96)e^{\Delta sT}}{s^2(s^2 + .7s + .25)} \right]^T \\ &= \frac{z - 1}{z^2} \left[\frac{(a_1 z^2 + a_2 z + a_3)z}{(z - 1)(z^2 + b_2 z + b_3)} \right] \end{aligned}$$

or

$$(GMe^{-sT_0})^T = \frac{a_1 z^2 + a_2 z + a_3}{z(z^2 + b_2 z + b_3)} \quad (429)$$

Values for the coefficients of Eq. 429 are tabulated as a function of Δ in Table 12 [$\Delta = (T - T_0)/T$].

TABLE 12
COEFFICIENTS OF $(GMe^{-sT_0})^T$

Δ	0	0.1	0.5	0.7	0.9	1.0
a_1	0.000000000	-0.006398718	-0.031967618	-0.044736233	-0.057494098	-0.063868953
a_2	-0.063868954	-0.051224119	-0.000694195	0.024540610	0.049754926	0.062354308
a_3	0.062354309	0.056108192	0.031147168	0.018680978	0.006224527	0.000000000

Note: $b_2 = -1.971993928$; $b_3 = 0.972388367$

Step 2

The Tustin transform of the washout network is a direct substitution technique wherein one substitutes

$$s = \frac{2}{T} \frac{z - 1}{z + 1}$$

into the s-domain transfer function, $H(s)$. The result for $T = 0.04$ sec (25 samples/sec) is:

$$H(s) = -\frac{0.6s}{(s + 2)(s + 0.5)} \Rightarrow H(z) = \frac{a_0(z^2 - 1)}{z^2 + b_0z + b_1} \quad (430)$$

$$a_0 = -0.011995$$

$$b_0 = -1.903275$$

$$b_1 = 0.904798$$

Step 3

The computation of G_A^T could be carried out on a point-by-point basis since the problem being considered is a scalar. However, it is illuminating, even if somewhat disconcerting, to examine the numerical expression for G_A^T wherein polynomial coefficients are rounded to three-place accuracy:

$$\frac{z^5 - 3.875z^4 + 5.63z^3 - 3.735z^2 + 0.880z}{z^5 - 3.875z^4 + 5.63z^3 - 3.636z^2 + 0.880z}$$

Thus, even when using a sampling rate as low as 25 samples/second, it is impossible to distinguish between the characteristics of the open- and closed-loop systems with only three-place accuracy for the algorithm coefficients. This example serves to warn one of numerical roundoff problems that may be encountered in digital systems even at moderate sampling rates, and indicates the need for at least double precision computation at higher sampling rates.

Step 4

The frequency response is computed with respect to θ rather than q . Since $\theta \doteq q/s$, the computation is carried through using $(1/T)(GMe^{-sT_0}/s)$ rather than $(1/T)GMe^{-sT_0}$. The result is shown in Fig. 63. Notice at the relatively slow sample rate of 25 samples/sec that the difference between the magnitude plot for the "continuous" washout network and the discretized version only becomes significant at frequencies above 50 rad/sec. There is, however, a substantial difference between the phase angles of the continuous washout and the discretized version at frequencies above 2 rad/sec. This result is a typical one when the Tustin transform approach is used. The only recourse for decreasing the difference between the phase responses when the Tustin transform approach is used is to decrease the sampling period. This is the case because the Tustin transform does not account for the phase lag introduced by the A/D, D/A conversion process (i.e., the data holds).

The phase for the discretely controlled system is shown for three different values: $T_0 = 0$ ($\Delta = 1$), $T_0 = 0.3T$ ($\Delta = 0.7$), and $T_0 = T$ ($\Delta = 0$). Clearly, the closed-loop phase characteristic is sensitive to the throughput delay of T_0 seconds. The accuracy with which the lower-order system models the higher-order system would be improved by inclusion of a pure time delay term. However, specification of acceptable delay is not presently part of MIL-F-8785B. Therefore, further adjustments of the effective short-period damping and natural frequency in the lower-order model are required if the "digital" phase angle artifacts are to be accounted for in the format of MIL-F-8785B. The result will be an increase in the effective damping and a decrease in the effective short-period frequency. Either in this form or considering the lag shown in Fig. 63 the result is further degradation of flying qualities due to the digital mechanization.

As discussed in the introduction to this section, an exact digital implementation would require an independent direct digital design in a valid discrete domain such as the w' -domain (Section III). The resulting digital control law would in general differ from the simple Tustin transform of the analog control law, because the w' -domain synthesis would

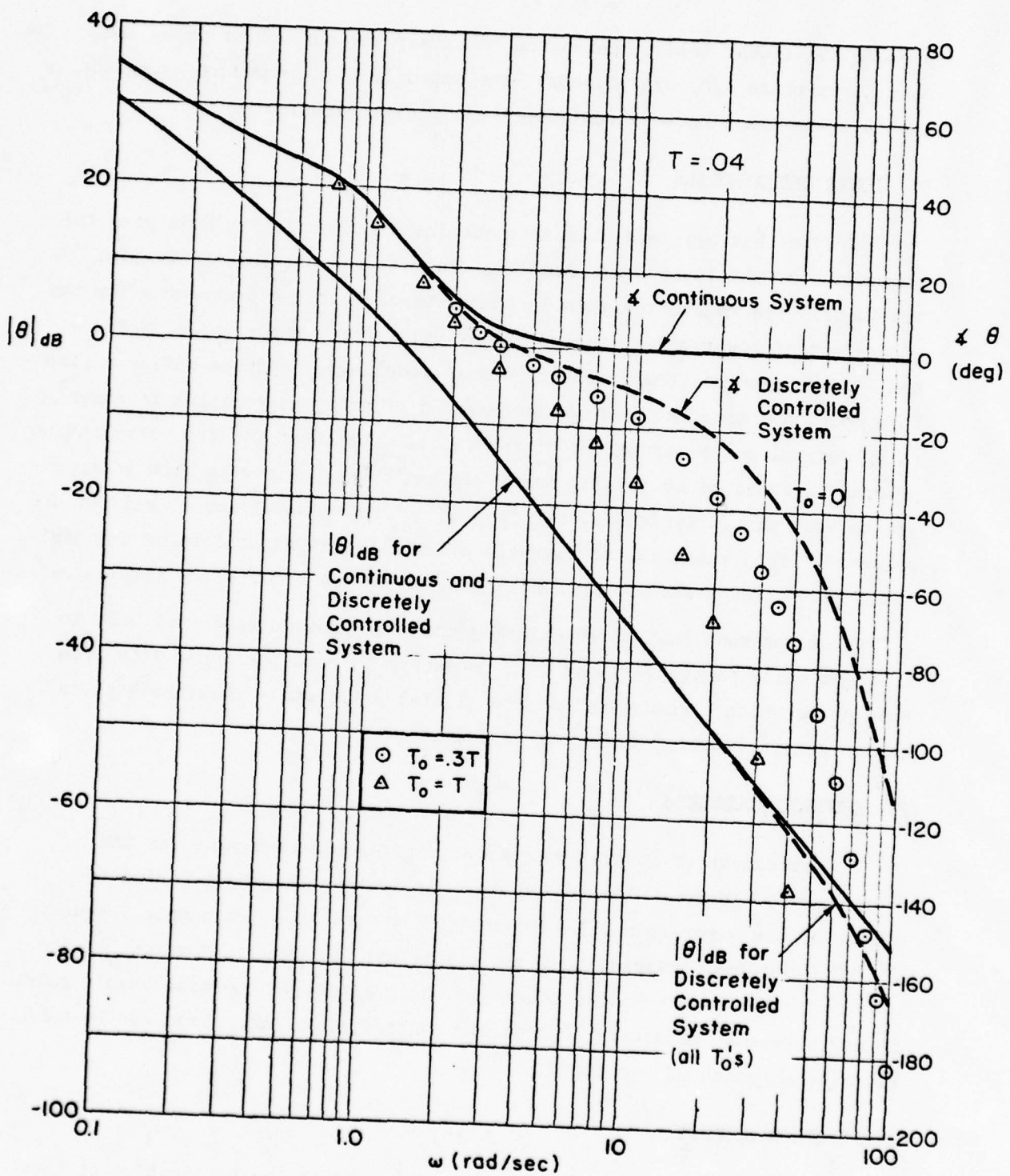


Figure 63. Fighter Attitude Dynamics (Digital Controller)

produce additional lead compensation to offset the throughput delay and nonminimum phase A/D, D/A effects. The approximation procedure using the Tustin transform cannot account for these digital artifacts.

D. LOWER-ORDER MODELS

No effort has been made herein to define a rationale for modifying the parameters of the lower-order model in order to account for the digital artifacts. The reason for this is that several modeling procedures for the generation of lower-order models already exist (see, for example, Refs. 1 and 4). In general, the frequency domain modeling procedures define a fixed-form model and then use machine-implemented "fitting" algorithms to numerically determine the parameters of the model. The input for the optimization program is obtained by reading magnitude and phase angle data from an appropriate Bode plot. Typically, ten frequencies between 0.1 and 10 rad/sec are selected. This range is, of course, well within the first fold of any digitally controlled system using sampling rates on the order of 25 samples/sec.

It is apparent that these existing modeling procedures do not have to be drastically changed. It is only necessary to read the input data from Bode plots which already include the digital artifacts. These Bode plots can be generated using the tools of Section V.

E. CONTROL ROUGHNESS

No assessment of control roughness (ripple) has been made for the illustrative example. The reason for this is that the short-period frequency of the aircraft model is considerably less than the sample frequency of 157.1 rad/sec, insuring that the ripple will be small. However, if the methods in the report had been used to their extent to minimize sample rate, it may have been necessary to consider control roughness. This can be done with the approach of Section V.

F. SECTION SUMMARY

An illustrative example was used to demonstrate the application of the digital tools developed in this report towards lower-order system modeling of aircraft and control system dynamics. This example highlights several

salient features of the digital analysis/synthesis techniques dealt with in this report:

- The Bode plots generated using the frequency response tools of Section V contain all the information required to assess the effective time delays and control roughness resulting from digital implementation. The phase plot quantifies the effective time delay and the magnitude plot the control roughness.
- For assessing MIL-F-8785B requirements, the effects of the digital artifacts on the equivalent low-order model can be accounted for exactly using the digital frequency response techniques of Section V.
- Although a single-rate example was used, the frequency response methods of Section V are also applicable to multi-rate systems. This is in contrast to the traditional concept of "sampled spectrum" of sampled data theory which is limited to single-rate systems.
- A direct digital design is needed if the phase lag introduced by the throughput delay and A/D, D/A conversion process is to be offset through proper control law design. The w -domain synthesis methods of Section III accomplish this, whereas the emulation procedure using the Tustin transform neglects these digital phase angle artifacts.
- The procedure for modeling computational delay is easily handled using vector switch decomposition coupled with the advanced z -transform methods of Section II.

SECTION VII

SUMMARY, CONCLUSIONS, AND RECOMMENDATIONS

A. SUMMARY AND CONCLUSIONS

The criteria of MIL-F-8785 presume an analog augmentation system. There is now an additional concern for response characteristics which are unique to digital augmentation systems. The purpose of this study was to identify those characteristics which are unique to the digitally controlled system, and to review the quantitative tools available which permit an assessment of the effects of these characteristics relative to the MIL-F-8785 requirements.

Two important characteristics are introduced by digital control laws:

- The effective delay introduced by the A/D and D/A process and the delay introduced by the digital algorithms and computational frame time.
- The "control roughness" or inter-sample ripple introduced when the digital computer is coupled to the control actuators using data holds.

The first characteristic is of great concern to the flying qualities community since even relatively small delays are potentially important in certain closed-loop piloting tasks involving motion cues and/or pilot-induced oscillations. The second characteristic is of concern since aircraft response resulting from control roughness is in effect an additional disturbance source.

Measures of the effective time delay introduced by the A/D computation, D/A conversion process can be computed using a variety of analytical techniques that apply at the sampling instants. For example, w' -, w -, or z -domain analyses and discrete frequency response techniques can be applied effectively to obtain both a quantitative and qualitative evaluation of the delay introduced.

The second characteristic is more difficult to assess since it involves the response of the continuous system during the inter-sample interval.

Traditional analysis tools such as the "sampled spectrum" (discrete frequency response) are of little value for this assessment because they generally ignore continuous system response between samples.

This leads to the other main objective of this study — to encourage the practicing engineer to gain working familiarity with three analytical techniques well suited for the analysis of digitally controlled systems:

- Analysis (and synthesis) in the w' -domain.
- Multi-rate transform domain analysis.
- Evaluation of continuous system frequency response to discrete excitation.

The w' -domain (Section III) is related to the well-known w -domain by a scalar transformation and to the z -domain by a bilinear algebraic transformation. We believe that those engineers skilled in frequency domain design procedures will immediately feel at home with analysis in the w' -domain, since all analog control system design technology transfers completely for digital control system design. In the w' -domain, the "analog" control system designer is transformed instantly into a "digital" control system designer.

The second item deals with a multi-rate transform domain approach that we developed (Section IV) into an effective tool for analyzing not only multi-rate sampled closed-loop systems (Section IV), but also the transient inter-sample response of discretely excited systems (Section V). That is, it yields recursion equations describing the inter-sample performance to any degree of fineness desired without increasing computer storage requirements.

The latter use is a departure point (Section V) to extend frequency response concepts to include the continuous frequency response of a discretely controlled system. The discrete frequency response concept has not been particularly productive for the analysis of discretely controlled systems, since it is limited to determining the amplitude and phase of the single sinusoid that fits the output samples of a single-rate system at the sampling instants. Development proceeded by first removing this restriction

for open-loop systems and then extending the results to single-rate closed-loop systems. Finally, the solution for the multi-rate closed-loop case was developed using the results of Section IV.

B. RECOMMENDATIONS

There are two specific recommendations. First, there is a need for portable, general purpose software to support the frequency response analysis of Section V. The basic requirements for one implementation are:

- 1) Compute the matrix of open-loop transfer functions, in the s -domain, given equations in either a state variable or degree-of-freedom format.
- 2) Partial fraction expand each element(s) of this matrix, compute the advanced z -transform of each term, and then combine the individual terms to obtain a polynomial in z . The result is a matrix of transfer functions in z for the discretized system.
- 3) Given the matrix of transfer functions in z , compute the w' -matrix of transfer functions.

An alternate implementation might replace the transform domain computations in Items 1 and 2 with state transition computations which produce equivalent results. These requirements are easily satisfied. It is primarily a matter of integrating existing codes in a manner which will permit easy interaction between the user and program.

The second recommendation deals with the application of switch decomposition to model data skewness and throughput delay effects in digital computations. This approach to modeling multi-rate, multiple order, throughput delay and data skewness effects has vast potential for the effective analysis of complex systems exhibiting these phenomena. Only a hint of the power switch decomposition teamed with the continuous frequency response concept is given by the simple illustrative example of Section VI. Specifically, the switch decomposition/frequency response techniques in combination can (and should) be developed into an analytical approach for pinpointing error sources that arise because of digital effects in the control and simulation of continuous systems.

REFERENCES

1. Hodgkinson, J., W. J. LaManna, and J. L. Heyde, "Handling Qualities of Aircraft with Stability and Control Augmentation Systems — A Fundamental Approach," Aeron. J., Vol. 80, No. 782, Feb. 1976, pp. 75-81.
2. Brady, C. C., J. Hodgkinson, and R. K. Wilson, "The New Military Flying Qualities Specification — A Valid Design Tool?" AIAA Paper 71-766, presented at AIAA 3rd Aircraft Design and Operations Meeting, Seattle, 12-14 July, 1971.
3. "Flying Qualities of Piloted Airplanes," MIL-F-8785B(ASG), 7 Aug. 1969.
4. Stapleford, R. L., D. T. McRuer, R. H. Hoh, et al., Outsmarting Mil-F-8785B(ASG), The Military Flying Qualities Specification, Systems Technology, Inc., TR-190-1, Aug. 1971.
5. Kalman, R. E., and J. E. Bertram, "A Unified Approach to the Theory of Sampling Systems," J. Franklin Inst., Vol. 267, No. 5, May 1959, pp. 405-436.
6. Kranc, G. M., "Input-Output Analysis of Multi-Rate Feedback Systems," IRE Trans. on Automatic Control, Vol. PG AC-3, Nov. 1957, pp. 21-28.
7. Ragazzini, J. R., and G. F. Franklin, Sampled-Data Control Systems, New York, McGraw-Hill, 1958.
8. Tou, J. T., Digital and Sampled-Data Control Systems, New York, McGraw-Hill, 1959.
9. Aseltine, J. A., Transform Method in Linear System Analysis, New York, 1958.
10. Goff, K. W., "Dynamics in Direct Digital Control, Part I," ISA J., Vol. 13, No. 11, Nov. 1966, pp. 45-49; "Part II," Vol. 13, No. 12, Dec. 1966, pp. 44-54.
11. Fryer, W. D., and W. C. Schultz, "A Survey of Methods for Digital Simulation of Control Systems," Cornell Aeronautical Laboratory, Buffalo, N.Y., XA-1681-E-1, July 1964.
12. Madwed, A., "Number Series Method of Solving Linear and Nonlinear Differential Equations," MIT Instrumentation Lab., Cambridge, Mass., 6445-T-26, Apr. 1950.
13. Tustin, A., "A Method of Analyzing the Behavior of Linear Systems in Terms of Time Series," Proceedings of the IEE, Vol. 94, Pt. IIA, No. 1, 1947, pp. 130-142.

14. Borow, M. S., R. O. Gaabo, R. C. Hendrick, et al., "Navy Digital Flight Control Development," Honeywell, Inc., 21857-FR, Dec. 1972.
15. "Tactical Aircraft Guidance System Development Program Flight Test Phase Report," Army Air Mobility Research and Development Lab., USAAMRDL-TR-73-89A and -89B, Apr. 1974.
16. Bailey, D. G., and K. Folkesson, "Software Control Procedures for the SAAB JA-37 Digital Automatic Flight Control System," Proceedings of the AIAA Guidance and Control Conference, American Institute of Aeronautics and Astronautics, Aug. 1976, pp. 122-129.
17. Stapleford, R. L., "Digital Flight Control Design Procedures," Systems Technology, Inc., Memorandum, 20 Aug. 1974.
18. Franklin, G. F., and J. D. Powell, "Digital Control, Notes Prepared for E207," Stanford University, Jan. 1976, pp. 5.19-5.22.
19. McRuer, D. T., I. L. Ashkenas, and H. R. Pass, Analysis of Multiloop Vehicular Control Systems, ASD-TDR-62-1014, Mar. 1964.
20. Saucedo, R., and E. E. Schiring, Introduction to Continuous and Digital Control Systems, New York, Macmillan, 1968.
21. Kuo, B. C., Digital Control Systems, Champaign, Ill., SRL, 1977.

APPENDIX A

PROPERTIES OF THE LAPLACE TRANSFORM

INTRODUCTION

Some of the more important properties of the Laplace transform that were not discussed in Section II will be reviewed here. Of particular interest are the properties of "translation in time" and "periodic functions."

LAPLACE TRANSFORM OF THE DERIVATIVE OF A TIME FUNCTION

The definition of the Laplace transform of a time function $f(t)$ is

$$\mathcal{L}[f(t)] \triangleq F(s) = \int_0^{\infty} f(t)e^{-st} dt \quad (A-1)$$

Given $F(s)$, the transform of $df(t)/dt$ is found using integration by parts.

Let

$$u = e^{-st}, \quad dv = \frac{df}{dt} dt \quad (A-2)$$

so that

$$\int u dv = uv - \int v du \rightarrow f(t)e^{-st} \Big|_0^{\infty} + s \int_0^{\infty} f(t)e^{-st} dt \quad (A-3)$$

Therefore

$$\mathcal{L}\left[\frac{df}{dt}\right] = sF(s) - f(0) \quad (A-4)$$

giving the pair

$$\frac{df}{dt} \iff sF(s) - f(0) \quad (A-5)$$

INITIAL AND FINAL VALUE THEOREM

The pair given in Eq. A-5 can be now used to prove the equalities

$$\lim_{t \rightarrow 0} f(t) = f(0) = \lim_{s \rightarrow \infty} sF(s) \quad (\text{A-6})$$

$$\lim_{t \rightarrow \infty} f(t) = f(\infty) = \lim_{s \rightarrow 0} sF(s) \quad , \quad \begin{array}{l} \text{poles of } sF(s) \\ \text{in LHP} \end{array} \quad (\text{A-7})$$

Since

$$\int_0^{\infty} \frac{df}{dt} e^{-st} dt = sF(s) - f(0) \quad (\text{A-8})$$

we may write

$$sF(s) - f(0) = \lim_{t \rightarrow \infty} \int_0^t \frac{df}{du} e^{-su} du \quad (\text{A-9})$$

so that letting $s \rightarrow \infty$ immediately gives

$$\lim_{s \rightarrow \infty} sF(s) - f(0) = 0 \quad (\text{A-10})$$

which proves Eq. A-6.

Next, let $s \rightarrow 0$ in Eq. A-9, giving

$$\lim_{s \rightarrow 0} sF(s) - f(0) = \lim_{t \rightarrow \infty} \int_0^t \frac{df}{du} du = \lim_{t \rightarrow \infty} [f(t) - f(0)] \quad (\text{A-11})$$

proving Eq. A-7.

The existence of the limit as $s \rightarrow 0$ requires the restriction on the poles of $sF(s)$. The limiting procedure of Eq. A-7 may give a "nonsense" answer if this restriction is not observed. For example,

$$\sin bt \iff \frac{b}{s^2 + b^2} \quad (\text{A-12})$$

so that

$$f(\infty) = \lim_{s \rightarrow 0} sF(s) = \lim_{s \rightarrow 0} \frac{sb}{s^2 + b^2} = 0 \quad (\text{A-13})$$

Since the poles of $sF(s)$ are not in the left-half plane (they are on the imaginary axis), the restriction is not satisfied, and the result of Eq. A-13 is meaningless. This is as it should be, since no one knows the value that the sine wave, although bounded by ± 1 , takes on when $t = \infty$.

HIGHER DERIVATIVES

The results of the second article in this appendix, page 171 are sufficient for finding the transform of higher derivatives. Consider

$$\mathcal{L} \left[\frac{d^2g}{dt^2} \right] = \mathcal{L} \left[\frac{dg}{dt} \right] \quad (\text{A-14})$$

where $g(t)$ is set equal to df/dt . Therefore,

$$\frac{dg}{dt} \iff sG(s) - g(0) \quad (\text{A-15})$$

which gives, upon substitution for g ,

$$\frac{dg}{dt} = \frac{d^2f}{dt^2} \iff s[sF(s) - f(0)] - \frac{df}{dt} \Big|_{t=0} \quad (\text{A-16})$$

or

$$\frac{d^2f}{dt^2} \iff s^2F(s) - sf(0) - f'(0) \quad (\text{A-17})$$

For example,

$$\mathcal{L}\left[\frac{d^3 f}{dt^3}\right] = s\mathcal{L}\left[\frac{d^2 f}{dt^2}\right] - f''(0) = s^3 F(s) - s^2 f(0) - sf'(0) - f''(0) \quad (A-18)$$

and

$$\begin{aligned} \mathcal{L}\left[\frac{d^4 f}{dt^4}\right] &= s\mathcal{L}\left[\frac{d^3 f}{dt^3}\right] - f'''(0) = s^4 F(s) - s^3 f(0) - s^2 f'(0) \\ &\quad - sf''(0) - f'''(0) \end{aligned} \quad (A-19)$$

As an application, consider the time domain differential equation

$$\ddot{x} + 6\ddot{x} + 11\dot{x} + 6x = 0 \quad (A-20)$$

where

$$x(0) = 2, \quad \dot{x}(0) = -6, \quad \ddot{x}(0) = 20$$

This transforms into an algebraic function of s

$$\begin{aligned} [s^3 X(s) - s^2 x(0) - s\dot{x}(0) - \ddot{x}(0)] \\ + 6[s^2 X(s) - sx(0) - \dot{x}(0)] + 11[sX(s) - x(0)] + 6X(s) = 0 \end{aligned} \quad (A-21)$$

or

$$\begin{aligned} [s^3 + 6s^2 + 11s + 6]X(s) &= s^2 x(0) + s[\dot{x}(0) + 6x(0)] \\ &\quad + [\ddot{x}(0) + 6\dot{x}(0) + 11x(0)] \end{aligned} \quad (A-22)$$

Substituting the initial conditions and dividing through by the characteristic equation gives

$$X(s) = \frac{2s^2 + 6s + 6}{s^3 + 6s^2 + 11s + 6} = \frac{2s^2 + 6s + 6}{(s+1)(s+2)(s+3)} \quad (A-23)$$

Partial fraction expansion gives

$$X(s) = \frac{1}{s+1} - \frac{2}{s+2} + \frac{3}{s+3} \quad (\text{A-24})$$

so that the time solution, via table lookup, is

$$x(t) = (e^{-t} - 2e^{-2t} + 3e^{-3t}) u(t) \quad (\text{A-25})$$

TRANSLATION IN TIME

Given $f(t) u(t)$, the transform of the translated function can be easily found:

$$\mathcal{L}[f(t-a)u(t-a)] = \int_0^{\infty} f(t-a) u(t-a) e^{-st} dt \quad (\text{A-26})$$

$$= \int_a^{\infty} f(t-a) e^{-st} dt, \quad a \geq 0 \quad (\text{A-27})$$

Let $x = t-a$ so that

$$\int_0^{\infty} f(x) e^{-s(x+a)} dx = e^{-as} \int_0^{\infty} f(x) e^{-sx} dx = e^{-as} F(s) \quad (\text{A-28})$$

Thus,

$$f(t-a) u(t-a) \iff e^{-as} F(s) \quad (\text{A-29})$$

Given that $a \geq 0$, the application of Eq. A-29 is neat and straightforward for finding the transform of a delayed time function. However, given $a \geq 0$, the transform of an advanced time function must be treated with greater care. Using the same procedures as above one finds:

$$\mathcal{L}[f(t+a)u(t)] = \int_0^{\infty} f(t+a)e^{-st} dt \quad (\text{A-30})$$

Let $t+a = x$, so that $dx = dt$ and $t = x-a$. Substituting into Eq. A-30 gives:

$$\begin{aligned}\mathcal{L}[f(t+a)u(t)] &= \int_a^\infty f(x)e^{-s(x-a)} dx \\ &= e^{as} \int_0^\infty f(x) u(x-a)e^{-sx} dx \\ &\triangleq e^{as} \mathcal{L}[f(t)u(t-a)]\end{aligned}\tag{A-31}$$

Comparing Eq. A-31 with Eq. A-29, we see that the advantage of using the translation theorem has disappeared. Namely, in Eq. A-29 we need not recompute the transform of the delayed time function. It is sufficient to know the transform of the unshifted function since a simple multiplication by e^{-as} gives the desired result. However, in Eq. A-31, a premultiplication by e^{as} does not remove the necessity for recomputing the transform. Indeed, we may as well use Eq. A-30 directly when computing the transforms of time advanced functions, since no advantage accrues from the use of Eq. A-31.

PERIODIC FUNCTIONS

By definition, a function satisfying

$$f(t) = f(t + T)\tag{A-32}$$

is periodic with period T . This definition is adequate even if $f(t) \equiv 0$ for $t < 0$. Begin by defining a function equal to $f(t)$ in its first period and zero elsewhere (see Fig. A-1).

$$f_1(t) = \begin{cases} f(t) & 0 \leq t \leq T \\ 0 & \text{Elsewhere} \end{cases}\tag{A-33}$$

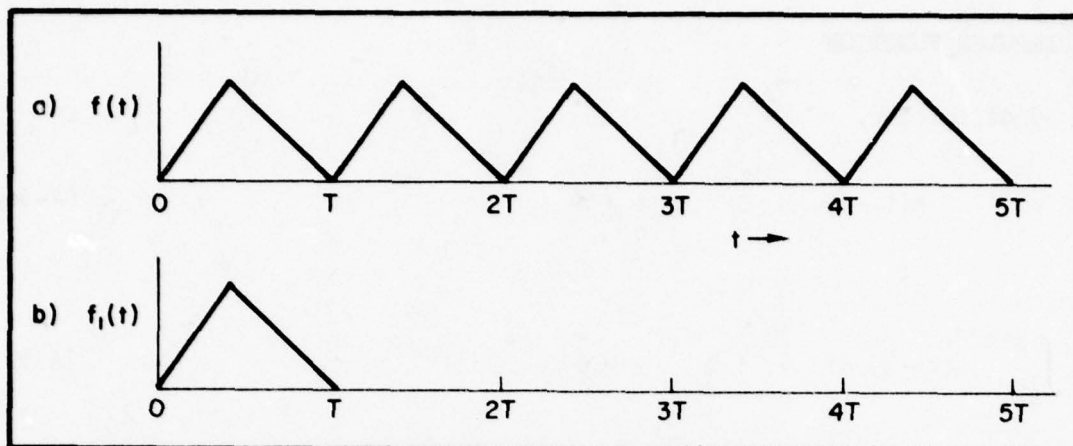


Figure A-1. A Periodic Function

From Fig. A-1 we see that $f(t)$, Fig. A-1a, can be described in terms of $f_1(t)$, Fig. A-1b,

$$f(t) = f_1(t) u(t) + f_1(t-T) u(t-T) + \dots \quad (\text{A-34})$$

Taking the transform of Eq. A-34 gives

$$F(s) = F_1(s) + F_1(s)e^{-sT} + F_1(s)e^{-s2T} + \dots \quad (\text{A-35})$$

$$= F_1(s)[1 + e^{-sT} + e^{-s2T} + \dots] \quad (\text{A-36})$$

$$F(s) = \frac{F_1(s)}{1 - e^{-sT}} \quad (\text{A-37})$$

In using Eq. A-37, it is important to develop the transform of $F_1(s)$ over its entire first period, taking careful note of the "0 elsewhere" restriction in Eq. A-33. We defer making an application of Eq. A-37 until the Laplace of the impulse function has been introduced.

THE IMPULSE FUNCTION

By definition,

$$\delta(t-a) \equiv 0 \quad t \neq a \quad (\text{A-38})$$

and

$$\int_{a-\epsilon}^{a+\epsilon} \delta(t-a) dt = 1.0 \quad \epsilon > 0 \quad (\text{A-39})$$

Therefore

$$\begin{aligned} \mathcal{L}[\delta(t-a)] &= \int_0^{\infty} \delta(t-a) e^{-st} dt \\ &= \int_0^{a-\epsilon} () dt + \int_{a-\epsilon}^{a+\epsilon} () dt + \int_{a+\epsilon}^{\infty} () dt \end{aligned} \quad (\text{A-40})$$

Therefore

$$\mathcal{L}[\delta(t-a)] = \int_{a-\epsilon}^{a+\epsilon} e^{-st} \delta(t-a) dt \Big|_{\epsilon \rightarrow 0} \quad (\text{A-41})$$

But, as $\epsilon \rightarrow 0$, $e^{-st} \rightarrow e^{-as}$ and can be removed from underneath the integral sign. Therefore,

$$\mathcal{L}[\delta(t-a)] = \int_{a-\epsilon}^{a+\epsilon} e^{-as} \delta(t-a) dt \quad (\text{A-42})$$

$$= e^{-as} \int_{a-\epsilon}^{a+\epsilon} \delta(t-a) dt$$

$$= e^{-as} \quad (\text{A-43})$$

We observe the convention that $\delta(t) = \lim_{a \rightarrow 0} \delta(t-a)$ and is therefore included within the limits of integration. Specifically,

$$\delta(t) \iff 1 \quad (\text{A-44})$$

An example is given in conjunction with the previous subsection. We wish to find the transform of the "periodic" string of δ functions shown in Fig. A-2. Since the Laplace transform of a periodic function is

$$F(s) = \frac{F_1(s)}{1 - e^{-sT}} \quad (\text{A-45})$$

it is only necessary to find the transform over one period. With the notation

$$f(t) = \delta_+(t) + \delta_+(t-T) + \delta_+(t-2T) + \dots \quad (\text{A-46})$$

to indicate a limiting process towards the left in time,

$$F_1(s) = 1$$

and we have

$$F(s) = \frac{1}{1 - e^{-sT}} \quad (\text{A-47})$$

as the transform of a "comb" of δ functions.

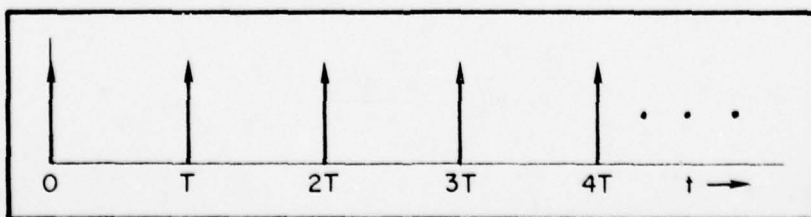


Figure A-2. The Dirac Delta Comb Function

AD-A067 177

SYSTEMS TECHNOLOGY INC HAWTHORNE CALIF
ANALYSIS OF DIGITAL FLIGHT CONTROL SYSTEMS WITH FLYING QUALITIE--ETC(U)

F/G 1/3

SEP 78 R F WHITBECK, L G HOFMANN

F33615-77-C-3026

UNCLASSIFIED

STI-TR-1101-1-VOL-2

AFFDL-TR-78-115-VOL-2

NL

3 OF 3

AD
A067177



END
DATE
FILMED
6-79
DDC

THE TRANSFORM OF TIME PRODUCTS

The inversion integral for Laplace transforms is

$$f(t) = \mathcal{L}^{-1}[F(s)] = \frac{1}{2\pi j} \int_{c-j\infty}^{c+j\infty} F(s)e^{st} ds \quad (\text{A-48})$$

To find the Laplace transform of the product of two time functions proceed as follows:

$$\mathcal{L}[f_1(t)f_2(t)] = \int_0^\infty f_2(t)e^{-st} \left\{ \frac{1}{2\pi j} \int_{c_1-j\infty}^{c_1+j\infty} [F_1(p)e^{pt} dp] \right\} dt \quad (\text{A-49})$$

Interchange the order of integration and adjust the contour

$$\mathcal{L}[f_1f_2] = \frac{1}{2\pi j} \int_{c-j\infty}^{c+j\infty} F_1(p) dp \int_0^\infty f_2(t)e^{-(s-p)t} dt \quad (\text{A-50})$$

Therefore

$$\mathcal{L}[f_1(t)f_2(t)] = \frac{1}{2\pi j} \int_{c-j\infty}^{c+j\infty} F_1(p)F_2(s-p) dp \quad (\text{A-51})$$

For example, let $f_1(t) = e^{-at}$ and let $f_2(t)$ be the Dirac δ comb function of the previous section, so that the product of f_1f_2 has the general appearance shown in Fig. A-3. The periodic property gives

$$F_2(s) = \frac{1}{1 - e^{-sT}} \quad (\text{A-52})$$

and since

$$F_1(s) = \frac{1}{s + a} \quad (\text{A-53})$$

Eq. A-51 gives

$$\mathcal{L}[f_1f_2] = \frac{1}{2\pi j} \int_{c-j\infty}^{c+j\infty} \frac{F_1(p)}{1 - e^{-T(s-p)}} dp = \frac{1}{2\pi j} \int_{c-j\infty}^{c+j\infty} \frac{dp}{(p+a)[1 - e^{-T(s-p)}]} \quad (\text{A-54})$$

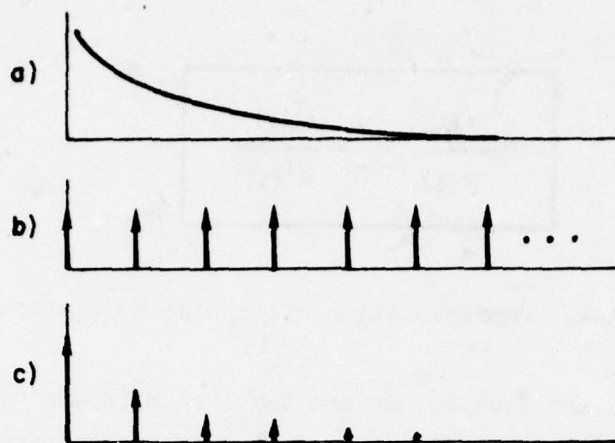


Figure A-3. Product of e^{-at} with Comb Function

Closing the contour to the left gives (see next subsection)

$$\mathcal{L}[f_1 f_2] = \frac{1}{1 - e^{-T(s+a)}} \quad (\text{A-55})$$

and we see that the use of the Laplace transform of a product, taken in conjunction with the Laplace transform of a particular periodic function, is a sufficient tool for finding the transform of an impulse modulated waveform. The next subsection reviews some of the fundamentals for evaluating Eq. A-51 when one of the time functions in the product is the Dirac delta comb function.

REVIEW COMMENTS ON CONTOUR INTEGRATION

The properties of sampled systems have been developed directly in terms of the delay operator z^{-1} in Section II. It has now been shown that the Laplace transform properties associated with periodic functions and with the product of two time functions can be used to develop an alternative frequency domain description (by letting one of the product functions be the Dirac delta comb). Representation of the product of a continuous time function with a Dirac delta comb is cast as an equivalent "impulse modulation" model in Fig. A-4. It has already been shown that

$$R^T(s) = \frac{1}{2\pi j} \int_{c-j\infty}^{c+j\infty} \frac{R(p) dp}{1 - e^{-T(s-p)}} \quad (\text{A-56})$$

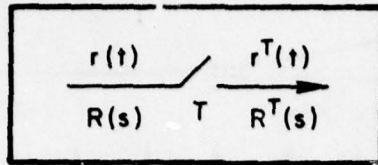


Figure A-4. Representation of Impulse Modulation

If the poles of $R(s)$ are finite, one can say that $R^T(s)$ is the summation of the residues of $R(p)$ by closing the contour of integration to the left. On the other hand, if the contour is closed to the right, enclosing the poles of the Dirac delta comb, one obtains

$$R^T(s) = \frac{1}{T} \sum_{n=-\infty}^{\infty} R\left(s - \frac{2\pi nj}{T}\right) \quad (\text{A-57})$$

Equations A-56 and A-57 are useful in investigating the properties of multi-rate systems, and it is thus worthwhile to gain some insight into the "mechanics" of evaluating Eq. A-56.

First, some review points. If a pole is enclosed with a counterclockwise contour giving a residue k_1 , then a clockwise enclosure gives the residue $-k_1$. That is, a counterclockwise contour gives a value equal to $2\pi j \sum \text{Res}$, whereas a clockwise contour gives a value of $-2\pi j \sum \text{Res}$. Also, if the integrand is represented as the ratio of two polynomials, $N(p)/D(p)$, then the residue for any simple factor $(p-p_0)$ is given by

$$\text{Res} \Big|_{p=p_0} = \frac{N(p_0)}{D'(p_0)} \quad (\text{A-58})$$

where the prime denotes differentiation with respect to p . In the interest of brevity, the discussion will be restricted to systems containing simple poles (no multiple poles). Frequent use will be made of the identity

$$\sum_{n=-\infty}^{\infty} \frac{1}{X - 2\pi nj} = \frac{1}{1 - e^{-X}} \quad (\text{A-59})$$

Given the integral vanishes on the infinite contour C_1 (see Fig. A-5) enclosing the poles of $R(p)$, we may say that $R^T(s)$ is equal to the sum of the residues of $R(p)$. If the path is closed to the right, the infinite

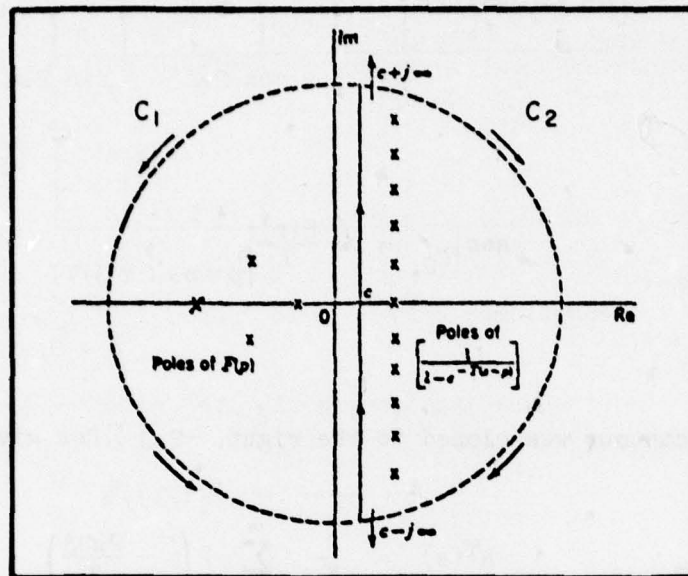


Figure A-5. The Complex p Plane

set of poles at $p = s - 2\pi nj/T$, $n = 0, \pm 1, \pm 2, \dots$, of $1 - e^{-T(s-p)}$ are enclosed. First, complete the contour to the right, enclosing the singularities at $p = s - 2\pi nj/T$. Let

$$\frac{N(p)}{D(p)} = \frac{R(p)}{1 - e^{-T(s-p)}} = \frac{N_1(p)}{D_1(p)[1 - e^{-T(s-p)}]} \quad (\text{A-60})$$

where it is assumed that $R(p)$ is a proper rational polynomial in p .

$$\text{Res}|_{C_2} = \frac{N(p)}{D'(p)} = \frac{N_1(p)}{D_1'(p)[1 - e^{-T(s-p)}] - TD_1(p)e^{-T(s-p)}} \quad (\text{A-61})$$

But,

$$\begin{aligned} 1 - e^{-T(s-p)} \Big|_{p=s-(2\pi j/T)} &= 1 - e^{-T(2\pi j/T)} \\ &= 1 - \cos 2\pi + j \sin 2\pi \equiv 0 \end{aligned} \quad (\text{A-62})$$

so that

$$\begin{aligned} \text{Res}|_{C_2} &= - \frac{R(p)}{T} \Big|_{p=s-(2\pi j/T)} \\ n &= 0, \pm 1, \dots \end{aligned} \quad (\text{A-63})$$

Since the contour was closed to the right, $-2\pi j \sum \text{Res}$ gives

$$R^T(s) = \frac{1}{T} \sum_{n=-\infty}^{\infty} R\left(s - \frac{2\pi j n}{T}\right) \quad (\text{A-64})$$

which was to be shown. We therefore have the identities

$$\begin{aligned} R^T(s) &= \frac{1}{2\pi j} \int_{c-j\infty}^{c+j\infty} \frac{R(p)}{1 - e^{-T(s-p)}} dp \\ &= \frac{1}{T} \sum_{n=-\infty}^{\infty} R\left(s - \frac{2\pi j n}{T}\right) \end{aligned} \quad (\text{A-65})$$

For example, let $R(s) = 1/(s+a)$ and close the contour C_1 .

$$\begin{aligned} R^T(s) &= \frac{1}{2\pi j} \int_{c-j\infty}^{c+j\infty} \frac{dp}{(p+a)[1 - e^{-T(s-p)}]} = \text{Res} \Big|_{p=-a} \\ &= \frac{1}{1 - e^{-T(s-p)}} \Big|_{p=-a} = \frac{1}{1 - e^{-T(s+a)}} \end{aligned} \quad (\text{A-66})$$

Note that the substitution $z = e^{sT}$ then gives

$$R(z) = R^T(s) = \frac{z}{z - e^{-aT}}$$

Equation A-66 was arrived at using conventional residue theory. The $N(p)/D'(p)$ approach also works, since $N(s) = 1$ and (again closing the contour on C_1) gives

$$\begin{aligned} R^T(s) &= \left. \frac{N}{D'} \right|_{p=-a} = \frac{1}{[1 - e^{-T(s-p)}] + (p+a)(-T)e^{-T(s-p)}} \\ &= \frac{1}{1 - e^{-T(s+a)}} \end{aligned} \quad (\text{A-67})$$

as before.

This result can also be obtained with the C_2 contour,

$$D'(p) = [1 - e^{-T(s-p)}] + (-T)(p+a)e^{-T(s-p)} \Big|_{p=s-(2\pi j/T)} \quad (\text{A-68})$$

Therefore, taking due account of the clockwise contour, we obtain

$$R^T(s) = \sum_{n=-\infty}^{\infty} \frac{1}{T(s+a) - 2\pi j n} = \frac{1}{1 - e^{-T(s+a)}} \quad (\text{A-69})$$

where Eq. A-59 has been used to place the infinite summation in closed form.

APPENDIX B

THE PULSE TRANSFER FUNCTION

INTRODUCTION

The identities

$$R^T(s) = \frac{1}{2\pi j} \int_{c-j\infty}^{c+j\infty} \frac{R(p) dp}{1 - e^{-T(s-p)}} = \frac{1}{T} \sum_{n=-\infty}^{\infty} R\left(s - \frac{2\pi nj}{T}\right) \quad (B-1)$$

were derived in Appendix A. In this appendix, use will be made of Eq. B-1 in order to deduce the properties of the two-rate system shown in Fig. B-1.

We were reluctant to introduce Eq. B-1 in the main text since its use would not be in keeping with the elementary and/or review flavor of Section II. However, its use here will serve to clear up some notational problems that surface in the multi-rate sections, as well as to provide insight into multi-rate systems. We first investigate the single-rate system.



Figure B-1. An Open-Loop Two-Rate System

SINGLE-RATE PULSE TRANSFER FUNCTION

In Fig. B-1, let $T_1 = T_2 = T$ and write

$$\begin{aligned} C^T &= [G(s) R^T(s)]^T = \frac{1}{2\pi j} \int_{c-j\infty}^{c+j\infty} \frac{G(p) R^T(p) dp}{1 - e^{-T(s-p)}} \\ &= \frac{1}{T} \sum_{n=-\infty}^{\infty} G\left(s - \frac{2\pi nj}{T}\right) R^T\left(s - \frac{2\pi nj}{T}\right) \end{aligned} \quad (B-2)$$

Now, let us look at $R^T[s - (2\pi j/T)]$, via Eq. B-1,

$$R^T\left(s - \frac{2\pi j}{T}\right) = \frac{1}{2\pi j} \int_{c-j\infty}^{c+j\infty} \frac{R(p) dp}{1 - e^{-T[s-p-(2\pi j/T)]}} \quad (B-3)$$

$$= \frac{1}{2\pi j} \int_{c-j\infty}^{c+j\infty} \frac{R(p) dp}{1 - e^{-T(s-p)} e^{2\pi j}} \quad (B-4)$$

But, $e^{2\pi j} = (\cos 2\pi - j \sin 2\pi) = 1$ for n , an integer. Therefore,

$$R^T\left(s - \frac{2\pi j}{T}\right) = R^T(s) \quad (B-5)$$

Substituting Eq. B-5 into the right-hand side of Eq. B-2 gives

$$\frac{1}{T} \sum_{n=-\infty}^{\infty} G\left(s - \frac{2\pi j}{T}\right) R^T\left(s - \frac{2\pi j}{T}\right) = \left[\frac{1}{T} \sum G\left(s - \frac{2\pi j}{T}\right) \right] R^T(s) = G^T(s) R^T(s) \quad (B-6)$$

Since $R^T(s)$ factors out of the summation, we see that the remaining term is the transform of the $g(t)$ "impulse" response. Therefore, it has been proven that

$$C^T(s) = [G(s) R^T(s)]^T = G^T(s) R^T(s) \quad (B-7)$$

At this point, it is convenient to discuss (using Eq. B-1) two other points occurring in Sections IV and V which the reader may find troublesome. The first concerns the use of the notation $R^T(s)$ rather than $R(z)$.

SUPERSCRIPT NOTATION

The superscript notation has been adopted as a matter of convenience since at times it will be expedient to redefine the delay operator z^{-1} . For example, it will often be to our advantage to define

$$e^{-sT/N} = z^{-1} \quad (\text{B-8})$$

so that

$$e^{-sT} = e^{-(sT/N)N} = (e^{-sT/N})^N = z^{-N} \quad (\text{B-9})$$

Equation B-1 offers a rationale for the superscript notation, given that we desire to keep our options open on the definition of z . To demonstrate, we seek the pulse transfer function of $1/(s+a)$ using Eq. B-1 (closing the contour to the left):

$$\begin{aligned} \left[\frac{1}{s+a} \right]^T &= \frac{1}{2\pi j} \int_{c-j\infty}^{c+j\infty} \frac{dp}{(p+a)[1-e^{-T(s-p)}]} \\ &= \frac{1}{1-e^{-T(s-p)}} \end{aligned} \quad (\text{B-10})$$

Note that Eq. B-10 contains no " z 's"; the only "sampling parameter" is T itself. Only with the subjective decision to define $z = e^{sT}$ can Eq. B-10 be written as:

$$G(z) = \frac{z}{z - a^{-aT}}, \quad z = e^{sT} \quad (\text{B-11})$$

If z had been defined according to

$$z = e^{sT/N} \quad (\text{B-12})$$

then

$$\left[\frac{1}{s+a} \right]^T = \frac{1}{1-e^{-T(s+a)}} = \frac{z^N}{z^N - e^{-aT}} \quad (\text{B-13})$$

Next, suppose one seeks the pulse transfer function of $1/(s+a)$ with respect to a T/N frametime. Then,

$$\left[\frac{1}{s+a} \right]^{T/N} \triangleq \frac{1}{2\pi j} \int_{c-j\infty}^{c+j\infty} \frac{dp}{(p+a)[1-e^{-(s-p)T/N}]} = \frac{1}{1-e^{-(s+a)T/N}} \quad (\text{B-14})$$

so that defining $z = e^{sT/N}$ gives

$$\left[\frac{1}{s+a} \right]^{T/N} = \frac{z}{z - e^{-aT/N}}, \quad z = e^{sT/N} \quad (\text{B-15})$$

In the text the prevailing definition of z will be omitted when it is felt that the meaning is clear.

The implications of Eqs. B-11, B-13, and B-15 are as follows. Proceeding according to the partial fraction/table lookup approach of Section II essentially assumes

$$z = e^{sT} \quad (\text{B-16})$$

8

since the table was written with that definition in mind. However, use of Eq. B-1 gives answers in terms of e^{sT} or $e^{sT/N}$ (whichever is appropriate), so that one can assign z at his convenience. If we wish to continue to use the tables of Section II, and yet keep the definition of z an option, then one proceeds as follows. Suppose that it is convenient to define $z = e^{sT/N}$. Then $G^{T/N}$ is computed directly from the tables using partial fraction expansion. Simply replace (mentally) T in the tables with T/N . On the other hand, G^T is computed, by table lookup/partial fraction expansion in the usual manner, retaining the T in the transform table. When the overall pulse transfer function has been computed, one simply changes z to z^N .

THE MULTI-RATE CASE

A logical point has now been reached to derive a particular relationship, pertaining to multi-rate systems, that will be of value in Sections II, IV, and V. Consider the two-rate system of Fig. B-1. Write

$$C(s) = G(s) R^{T1}(s) \quad (\text{B-17})$$

so that

$$C^{T_2}(s) = [G(s) R^{T_1}(s)]^{T_2} \quad (B-18)$$

Using Eq. B-1, one may derive a relationship between T_1 and T_2 which, when satisfied, permits the simplification

$$C^{T_2}(s) = [G(s) R^{T_1}(s)]^{T_2} = G^{T_2}(s) R^{T_1}(s) \quad (B-19)$$

Applying Eq. B-1 to Eq. B-18 gives

$$\begin{aligned} [G(s) R^{T_1}(s)]^{T_2} &= \frac{1}{2\pi j} \int_{c-j\infty}^{c+j\infty} \frac{G(p) R^{T_1}(p)}{1 - e^{-T_2(s-p)}} dp \\ &= \frac{1}{T_2} \sum_{n=-\infty}^{\infty} G\left(s - \frac{2\pi nj}{T_2}\right) R^{T_1}\left(s - \frac{2\pi nj}{T_2}\right) \end{aligned} \quad (B-20)$$

Now, take a close look, via Eq. B-1, at $R^{T_1}(s - 2\pi nj/T_2)$. By definition,

$$\left[R\left(s - \frac{2\pi nj}{T_2}\right) \right]^{T_1} = \frac{1}{2\pi j} \int_{c-j\infty}^{c+j\infty} \frac{R(p) dp}{1 - e^{-T_1[s - (2\pi nj/T_2) - p]}} \quad (B-21)$$

$$= \frac{1}{2\pi j} \int_{c-j\infty}^{c+j\infty} \frac{R(p) dp}{1 - e^{-T_1(s-p)} e^{-2\pi nj T_1/T_2}} \quad (B-22)$$

But

$$e^{2\pi nj T_1/T_2} \equiv 1 \quad \text{if } T_1/T_2 \text{ is an integer} \quad (B-23)$$

Let T_1/T_2 be an integer,

$$R^{T_1}\left(s - \frac{2\pi nj}{T_2}\right) \equiv R^{T_1}(s) \quad (B-24)$$

Equation B-20 becomes

$$C^{T_2} = \left[\frac{1}{T_2} \sum G\left(s - \frac{2\pi nj}{T_2}\right) \right] R^{T_1}(s) = G^{T_2}(s) R^{T_1}(s) \quad (B-25)$$

It has thus been proven that

$$C^{T_2} = [G(s) R^{T_1}(s)]^{T_2} = G^{T_2}(s) R^{T_1}(s), \quad T_1/T_2 = \text{integer} \quad (B-26)$$

giving the "rule" that the outer sampling operator moves through the inner one when the ratio of the inner to the outer is an integer.

For example, let

$$R(s) = \frac{1}{s+a}, \quad G(s) = \frac{1}{s+b} \quad (B-27)$$

When T_1/T_2 is an integer, we expect

$$C^{T_2} = \frac{1}{[1 - e^{-T_2(s+b)}][1 - e^{-T_1(s+a)}]} \quad (B-28)$$

as can be verified using Eq. B-1.

$$C^{T_2} = \frac{1}{2\pi j} \int_{c-j\infty}^{c+j\infty} \frac{dp}{(p+b)[1 - e^{-T_1(p+a)}][1 - e^{-T_2(s-p)}]} \quad (B-29)$$

Therefore,

$$\frac{N}{D'} = \frac{1}{[1 - e^{-T_1(p+a)}][1 - e^{-T_2(s-p)}] + T_1(p+b)e^{-T_1(p+a)}[1 - e^{-T_2(s-p)}] + (p+b)[1 - e^{-T_1(p+a)}](-T_2)e^{-T_2(s-p)}} \quad (B-30)$$

Closing the contour to the right, enclosing the singularities at $p = s - (2\pi nj/T_2)$, gives

$$c^{T_2} = \frac{1}{T_2 e^{-T_2(2\pi nj/T_2)} [1 - e^{-T_1[s+a-(2\pi nj/T_2)]}] [s+b-(2\pi nj/T_2)]} \quad (B-31)$$

$$n = 0, \pm 1, \pm 2, \dots$$

But

$$e^{-T_2(2\pi nj/T_2)} = 1, \quad e^{T_1(2\pi nj/T_2)} = 1 \quad (B-32)$$

so that we are left with

$$c^{T_2} = \frac{1}{[1 - e^{-T_1(s+a)}]} \sum_{n=-\infty}^{\infty} \frac{1}{T_2(s+b) - 2\pi nj} \quad (B-33)$$

Using Eq. A-59 gives

$$c^{T_2} = \frac{1}{[1 - e^{-T_1(s+a)}] [1 - e^{-T_2(s+b)}]} \quad (B-34)$$

If T_1/T_2 is not an integer, we are stopped at

$$c^{T_2} = \sum_{n=-\infty}^{\infty} \frac{1}{[1 - e^{-T_1(s+a)}] e^{2\pi nj T_1/T_2} [T_2(s+b) - 2\pi nj]} \quad (B-35)$$

If T_2/T_1 is an integer, an answer can be obtained by closing the contour to the left. Doing this encloses the singularities in Eq. B-29 at $p = -b$ and $p = -a - (2\pi nj/T_1)$ [poles of $1 - e^{-T_1(s+a)}$]. At $p = -b$, using Eq. B-30 gives

$$\text{Res}|_{p=-b} = \frac{1}{[1 - e^{-T_1(a-b)}] [1 - e^{-T_2(s+b)}]} \quad (B-36)$$

The Res at $p = -a - (2\pi nj/T_1)$ is

$$\text{Res} \Big|_{p = -a - (2\pi nj/T_1)} = \frac{1}{T_1(b-a - (2\pi nj/T_1)) [1 - e^{-T_2(s+a + (2\pi nj/T_1))}]} \quad (\text{B-37})$$

$n = 0, \pm 1, \pm 2, \dots$

Since

$$1 - e^{-T_2[s+a + (2\pi nj/T_1)]} = 1 - e^{-T_2(s+a)} e^{-2\pi njT_2/T_1} = 1 - e^{-T_2(s+a)} \quad (\text{B-38})$$

if T_2/T_1 is an integer,

$$\frac{1}{1 - e^{-T_2(s+a)}} \sum_{n=-\infty}^{\infty} \frac{1}{T_1(b-a) - 2\pi nj} = \frac{1}{1 - e^{-T_2(s+a)}} \cdot \frac{1}{1 - e^{-T_1(b-a)}} \quad (\text{B-39})$$

The final result is

$$C^{T_2} = \frac{1/[1 - e^{-T_1(a-b)}]}{1 - e^{-T_2(s+b)}} + \frac{1/[1 - e^{-T_1(b-a)}]}{1 - e^{-T_2(s+a)}} \quad (\text{B-40})$$

Equation B-40 highlights the fact that it is not really necessary to use the phantom sampler approach when T_2/T_1 is an integer; a direct evaluation via contour integration is feasible.

APPENDIX C

ILLUSTRATIVE EXAMPLE — METHODS FOR FINDING THE CONTINUOUS RESPONSES OF DISCRETELY EXCITED SYSTEMS

INTRODUCTION

An example is used to demonstrate various techniques for finding both the discrete and continuous response of a discretely excited system. The example is a scalar one and hence will not make the dimensionality considerations associated with, for example, the state transition approach overly clear. However, our objective is to expose the reader (or remind him) of the large number of methods available for computing transient responses. All the methods demonstrated can be applied equally as well when the system description is in a matrix format.

ILLUSTRATIVE EXAMPLE MODEL

The model for the illustrative example is given in Fig. C-1. For numerical convenience let

$$r(t) = e^{-bt} \quad , \quad e^{-bT} = 0.5 \quad , \quad T = 0.5$$

and

$$e^{-aT} = 0.25$$

so that

$$a = 2.772588722$$

$$b = 1.386294361$$

Although the tables used in the "lookup" process will be in terms of e^{-bnT} , etc., for convenience of presentation, we ask the reader to keep in mind that $e^{-bnT} = (e^{-bT})^n = 0.5^n$.

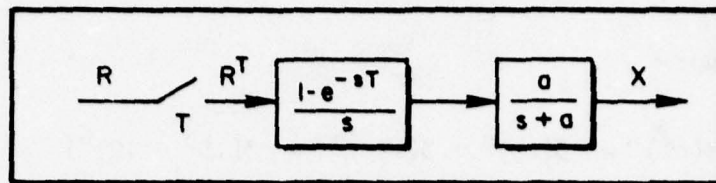


Figure C-1. Illustrative Example

The fundamental equations describing the responses are

$$X = \left(\frac{a}{s + a} \right) \left(\frac{1 - e^{-sT}}{s} \right) R^T \quad (C-1)$$

$$X^T = \left[\frac{a(1 - e^{-sT})}{s(s + a)} \right]^T R^T = \frac{.75}{z - .25} \left(\frac{z}{z - .5} \right) \quad (C-2)$$

First we enumerate six methods for finding the discrete time response, $X(nT)$.

DISCRETE TIME RESPONSE

Method I, Partial Fraction Expansion

This is an "analytical" method, in that the response is given in closed form for all values of n . The technique is basically partial fraction expansion coupled with table lookup.

Expand Eq. C-2 in partial fractions:

$$\frac{.75z}{(z - .25)(z - .5)} = \frac{Az}{z - .5} + \frac{Bz}{z - .25}$$

$$A = \left. \frac{.75}{z - .25} \right|_{z=.5} = 3$$

$$B = \left. \frac{.75}{z - .5} \right|_{z=.25} = -3$$

(C-3)

$$X(z) = \frac{3z}{z - .5} - \frac{3z}{z - .25}$$

Via table lookup:

$$X(nT) = 3(.5)^n - 3(.25)^n = 3[.5^n - .25^n] \quad (C-4)$$

Method II, The Inversion Integral

The inversion integral approach is essentially a residue theory method which eliminates the need for table lookup. For all intents and purposes, this method is identical to Method I in that the solution is defined for arbitrary values of n . Using the relationship:

$$f(nT) = \frac{1}{2\pi j} \int z^{n-1} f(z) dz = \sum \text{Residues} \quad (C-5)$$

we obtain

$$\frac{1}{2\pi j} \int \frac{z^{n-1} \cdot .75z}{(z - .25)(z - .5)} dz = \frac{.75(.5)(.5)^{n-1}}{.5 - .25} + \frac{.75(.25)(.25)^{n-1}}{.25 - .5}$$

or

$$X(nT) = 3[.5^n - .25^n] \quad (C-6)$$

Method III, Continued Fraction Expansion

In this approach, write $X(z)$ as a ratio of polynomials in z and divide the denominator into the numerator, interpreting the negative powers of z as suitably shifted delta functions in time. To demonstrate:

$$\begin{aligned} X(z) &= \frac{.75z}{(z - .5)(z - .25)} = \frac{.75z}{z^2 - .75z + .125} \\ &= .75z^{-1} + .5625z^{-2} + .328125z^{-3} + .17578125z^{-4} + \dots \end{aligned}$$

Therefore

$$X(t) = .75\delta(t-T) + .5625\delta(t-2T) + .328125\delta(t-3T) + \dots \quad (C-7)$$

Method IV, Recursion [R(z) Given Analytically]

Suppose a closed form is given for R(z), as in Eq. C-2. Then we may write

$$(z^2 - .75z + .125)X_1(z) = .75z \quad (C-8)$$

or

$$X(nT) = .75X[n-1)T] - .125X[n-2)T] + .75\delta(n-1) \quad (C-9)$$

Method V, Recursion [R(z) in Symbolic Form]

Suppose we retain the input as R(z) without taking $e^{(-bt)^T}$. Then, again from Eq. C-2, one may write

$$X^T = \frac{.75}{z - .25} R^T$$

or

$$X[n+1)T] = .25X(nT) + .75R(nT) \quad (C-10)$$

Method VI, State Transition

State transition can be used to find the total response. Using state transition concepts we may write (refer to Fig. C-2):

$$\begin{bmatrix} \dot{x}_1 \\ \dot{x}_2 \end{bmatrix} = \begin{bmatrix} -a & a \\ 0 & 0 \end{bmatrix} \begin{bmatrix} x_1 \\ x_2 \end{bmatrix} + \begin{bmatrix} 0 \\ 0 \end{bmatrix} R(nT) = Ax + BR$$

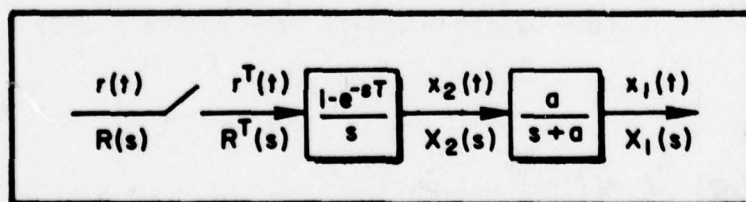


Figure C-2. Illustrative Example Relabeled

Let

$$\varphi(\tau) = \mathcal{L}^{-1}[\mathbf{IS} - \mathbf{A}]^{-1} = \begin{bmatrix} e^{-a\tau} & 1 - e^{-a\tau} \\ 0 & 1 \end{bmatrix}$$

so that

$$\mathbf{x}(nT + \tau) = \varphi(\tau) \mathbf{x}(nT) + \int_0^\tau \varphi(\xi) \mathbf{B} d\xi R(nT) \quad (\text{C-11})$$

gives, for the \mathbf{x}_1 component (Note: $\mathbf{x}_2(nT) = R(nT)$)

$$x_1(nT + \tau) = (1 - e^{-a\tau}) R(nT) + e^{-a\tau} x_1(nT), \quad 0 < \tau \leq T$$

Let $\tau = T$ and obtain the difference equation

$$x_1[(n+1)T] = (1 - e^{-aT}) R(nT) + e^{-aT} x_1(nT) \quad (\text{C-12})$$

or

$$x_1[(n+1)T] = .75R(nT) + .25 x_1(nT) \quad (\text{C-13})$$

Equation C-13 is, of course, in agreement with Eq. C-10.

SUMMARY OF DISCRETE RESPONSE METHODS

Method I, Partial Fraction Expansion

$$X(z) = \frac{.75z}{(z - .25)(z - .5)} = \frac{3z}{z - .5} - \frac{3z}{z - .25}$$

Therefore

$$X(nT) = 3[(.5)^n - (.25)^n]$$

Method II, Inversion Integral

$$\begin{aligned}X(nT) &= \frac{1}{2\pi j} \int \frac{z^{n-1} (.75z)}{(z - .25)(z - .5)} dz \\&= 3(.5)(.5)^{n-1} - 3(.25)(.25)^{n-1} \\&= 3[.5^n - .25^n]\end{aligned}$$

Method III, Continued Fraction Expansion

$$X(z) = \frac{.75}{(z - .5)(z - .25)} = .75z^{-1} + .5625z^{-2} + \dots$$

Method IV, Recursion [R(z) Given Analytically]

$$(z^2 - .75z + .125)X(z) = .75z$$

Therefore

$$X(nT) = .75X[(n-1)T] - .125X[(n-2)T] + .75\delta(n-1)$$

Method V, Recursion [R(z) in Symbolic Form]

$$X(z) = \frac{.75}{(z - .25)} R(z)$$

Therefore

$$X[(n+1)T] = .75R(nT) + .25X(nT)$$

Method VI, State Transition

Evaluate the state transition equation at $\tau = T$ to get discrete transition equation:

$$X(nT + \tau) = (1 - e^{-a\tau})R(nT) + e^{-a\tau}X(nT), \quad 0 \leq \tau \leq T$$

$$\begin{aligned}X[(n+1)T] &= (1 - e^{-aT})R(nT) + e^{-aT}X(nT) \\&= .75R(nT) + .25X(nT)\end{aligned}$$

Summary Table of Time Response

Using any of the six approaches we arrive at the summary table given in Table C-1.

TABLE C-1. DISCRETE TRANSIENT RESPONSE

<u>n</u>	<u>X(nT)</u>	<u>n</u>	<u>X(nT)</u>
0	0	6	.046142578
1	.75	7	.023254395
2	.5625	8	.011672974
3	.328125	9	.005847931
4	.17578125	10	.002926826
5	.090820313		

CONTINUOUS RESPONSE

We will illustrate two basic methods for finding the continuous response of a discretely excited system:

- I. State Transition
- II. Continued Fraction Expansion

A third method, the T/N approach, is treated in the text.

Method I, State Transition

The state transition equation is

$$X(nT + \tau) = (1 - e^{-a\tau}) R(nT) + e^{-a\tau} X(nT) \quad , \quad 0 \leq \tau \leq T \quad (C-14)$$

This is, in a strict sense, a recursion equation. That is, we must know $R(nT)$ and $X(nT)$ in order to compute $X(nT + \tau)$ where $0 \leq \tau \leq T$. However, if $R(nT)$ is given analytically (as in this example), then one may use the "closed form" discrete results in conjunction with Eq. C-14 to

"jump ahead" in time and compute the continuous response for $nT \leq t \leq (n+1)T$. To illustrate, a "normal" application of Eq. C-14, starting at $t = 0$, would give the results shown in Table C-2.

TABLE C-2. CONTINUOUS RESPONSE

t	$X(nT + \tau)$
0	0
.1	.24214177
.2	.425650823
.3	.564724718
.4	.670123022
.5	.75
.6	.689464571
.7	.643587294
.8	.608818821
.9	.582469245
1.0	.5625

Now, if desired, we could skip ahead to, for example, $t = 4.5$ since

$$t = nT = 9(.5) = 4.5 \text{ sec}$$

$$R(9T) = (.5)^9$$

$$X(9T) = 3[.5^9 - .25^9]$$

Therefore

$$\begin{aligned} X(9T + \tau) &= (1 - e^{-a\tau})(.5)^9 + e^{-a\tau}[3(.5)^9 - (.25)^9] \\ &= (1 - e^{-a\tau})(.001953125) + e^{-a\tau}(.005847931) \end{aligned} \quad (C-15)$$

This gives Table C-3.

TABLE C-3

CONTINUOUS RESPONSE — "JUMPING AHEAD"

<u>t</u>	<u>X(nT + τ)</u>
4.5	.005847931
4.6	.004904836
4.7	.004190104
4.8	.003648438
4.9	.003237932
5.0	.002926826

Method II, Continued Fraction Expansion

The continued fraction expansion method is easily extended to cover the continuous response of a discretely excited system. Consider Eq. C-1:

$$X = \frac{a}{s+a} \frac{1 - e^{-sT}}{s} R^T \quad (C-16)$$

which has the form

$$X = F_1(s) F_2(z) \quad (C-17)$$

Expand $F_2(z)$ in a continued fraction expansion:

$$X = F_1(s) [a_0 + a_1 z^{-1} + a_2 z^{-2} + \dots] \quad (C-18)$$

Therefore

$$x(t) = a_0 f_1(t) u(t) + a_1 f_1(t-T) u(t-T) + a_2 f_1(t-2T) u(t-2T) \dots \quad (C-19)$$

For our example

$$\begin{aligned} X &= \left[\frac{a}{s(s+a)} \right] \frac{z-1}{z} \frac{z}{z-.5} \\ &= \left[\frac{a}{s(s+a)} \right] [1 - .5z^{-1} - .25z^{-2} - \dots - (.5)^n z^{-n} - \dots] \end{aligned}$$

Therefore

$$\begin{aligned} x(t) = & (1 - e^{-at}) u(t) - .5[1 - e^{-a(t-T)}] u(t - T) \\ & - .25[1 - e^{-a(t-2T)}] u(t - 2T) - \dots \end{aligned} \quad (C-20)$$

Equation C-20 gives the same numerical values shown in Tables C-2 and C-3.

SUMMARY

There are a variety of methods for finding the continuous response of a discretely excited linear time invariant system. They can be roughly cataloged as:

- State transition.
- Continued fraction expansion.
- Higher rate sampling in conjunction with either:
 - Partial fraction expansions.
 - Recursion equations.

APPENDIX D PARTIAL FRACTION COEFFICIENTS FOR SECOND-ORDER REAL POLES

Expressions for finding the partial fraction coefficients for real second-order poles, in terms of the numerator and denominator polynomials (and their higher derivatives), are derived. If

$$F(s) = \frac{N}{D} = \frac{A}{(s+a)^2} + \frac{B}{(s+a)} + \dots \quad (D-1)$$

the A coefficient is found by multiplying each side of the equation by $(s+a)^2$ and applying L'Hôpital's rule twice. Thus

$$A = (s+a)^2 \frac{N}{D} \Big|_{s=-a} = \frac{0}{0} \quad (D-2)$$

is indeterminate if $(s+a)^2$ is not explicitly factored out of the denominator and canceled with the numerator factor of $(s+a)^2$. Applying L'Hôpital's rule once gives

$$\frac{2(s+a)N + N'(s+a)^2}{D'} = \frac{0}{0} \quad (D-3)$$

Applying the rule only once leaves an indeterminate form, since each numerator term contains free $(s+a)$ factors and the denominator, D' , now contains only a simple pole at $s = -a$.

Using L'Hôpital's rule a second times gives

$$A = \frac{2(s+a)N' + 2N + (s+a)^2N'' + 2(s+a)N'}{D''}$$

Therefore

$$A = \frac{2N}{D''} \Big|_{s=-a} \quad (D-4)$$

will give the correct value for the A coefficient, since D" is now free of the double singularity at $s = -a$. This verifies the result stated in Section II.

To find B, subtract $A/(s+a)^2$ from each side of Eq. D-1 and use L'Hôpital's rule three times:

$$\frac{N}{D} - \frac{A}{(s+a)^2} = \frac{N(s+a)^2 - AD}{D(s+a)^2} = \frac{B}{s+a} + \dots \quad (D-5)$$

Multiply by $(s+a)$ and evaluate the result for $s = -a$:

$$B = \frac{N(s+a)^2 - AD}{D(s+a)} = \frac{0}{0} \quad (D-6)$$

Since D contains $(s+a)^2$, both numerator terms are zero (as is the denominator) when $s = -a$. Using L'Hôpital's rule for the first time gives

$$\left. \frac{2(s+a)N + N'(s+a)^2 - AD'}{D'(s+a) + D} \right|_{s=-a} = \frac{0}{0} \quad (D-7)$$

since every term in the numerator still contains a free $(s+a)$, as does each term of the denominator. Use the rule for the second time:

$$\left. \frac{4(s+a)N' + (s+a)^2N'' + (2N - AD'')}{D''(s+a) + 2D'} \right|_{s=-a} = \frac{0}{0} \quad (D-8)$$

Again, each term of both the numerator and denominator is zero when $s = -a$ by virtue of containing a free $(s+a)$ or the definition of A itself. That is, the last term in the numerator of Eq. D-8 is identically zero at $s = -a$ because:

$$2N - AD'' \Big|_{s=-a} = 2N - \frac{2N}{D''} D'' \equiv 0 \quad (D-9)$$

Using the rule for the third time gives:

$$\begin{aligned}
 B &= \frac{4N''(s+a) + 4N' + 2N'' + (s+a)^2 N''' + 2(s+a) N'' - AD'''}{D'''(s+a) + 3D''} \Big|_{s=-a} \\
 &= \frac{6N' - AD'''}{3D''} = \frac{2N'}{D''} - \frac{AD'''}{3D''} \quad (D-10)
 \end{aligned}$$

which verifies the result stated in Section II.

APPENDIX E

SINE WAVE INPUT OF ARBITRARY PHASE

INTRODUCTION

The frequency response of a discretely excited system was developed, in Section V, for a "zero phase" sine wave input. However, it is a straightforward exercise to extend the development to encompass a sine wave input of arbitrary phase. This will be done first for the finite N case followed by the limiting process ($N \rightarrow \infty$) which gives the continuous results.

FINITE N CASE

In Fig. E-1, let the input be

$$r(t) = k_1 \sin bt + k_2 \cos bt \quad (E-1)$$

with the s -plane representation

$$R(s) = \frac{k_1 b}{s^2 + b^2} + \frac{k_2 s}{s^2 + b^2} \quad (E-2)$$

Using $z = e^{sT/N}$ gives the z -plane representation

$$R^T = \frac{k_1 z^N \sin bT + k_2 z^N (z^N - \cos bT)}{z^{2N} - 2 \cos bT z^N + 1} \quad (E-3)$$

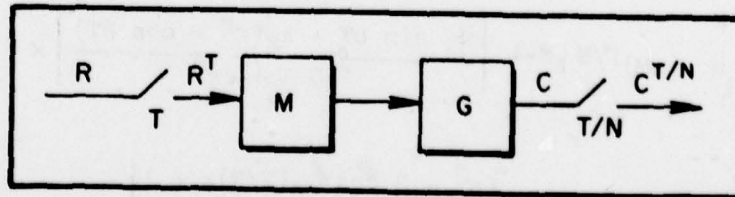


Figure E-1. Open-Loop System

so that

$$\begin{aligned}
 c^{T/N} &= (GM)^{T/N} \frac{k_1 z^N \sin bT + k_2 z^N (z^N - \cos bT)}{z^{2N} - 2 \cos bT z^N + 1} \\
 &= \sum_{n=0}^{\infty} \frac{A_n z \sin \omega_n(T/N) + B_n z [z - \cos \omega_n(T/N)]}{z^2 - 2 \cos \omega_n(T/N) z + 1} \\
 &\quad + \left[\begin{array}{c} \text{Terms due to} \\ \text{the modes of} \\ (GM)^{T/N} \end{array} \right] \quad (E-4)
 \end{aligned}$$

In Eq. E-4,

$$\omega_n = b + \frac{2\pi n}{T}, \quad n = 0, 1, 2, \dots, N-1 \quad (E-5)$$

so that the "steady state" output waveform is given by

$$\left[c(t) \right]_{t \rightarrow \infty}^{T/N} = \left(\sum_{n=0}^{N-1} [A_n \sin \omega_n t + B_n \cos \omega_n t] \right)^{T/N} \quad (E-6)$$

We can now follow the same procedure as in Section V in order to define the partial fraction coefficients A_n and B_n in terms of the system GM. First, multiply each side of Eq. E-4 by $(z^2 - 2 \cos \omega_k(T/N)z + 1)$ and evaluate for $z = 1 \angle \omega_k(T/N)$. As in Section V, the only surviving term on the right-hand side of Eq. E-4 occurs when $n = k$. Therefore, we obtain (letting k revert to n):

$$\begin{aligned}
 A_n + jB_n &= (GM)^{T/N} z^{N-1} \left[\frac{k_1 \sin bT + k_2 (z^N - \cos bT)}{\sin \omega_n(T/N)} \right] \times \\
 &\quad \left[\frac{z^2 - 2 \cos \omega_n(T/N)z + 1}{z^{2N} - 2 \cos bT z^N + 1} \right]_{z = 1 \angle \omega_n(T/N)} \quad (E-7)
 \end{aligned}$$

The last term on the right-hand side of Eq. E-7 is indeterminate at $z = 1 \pm j\omega_n(T/N)$, so that L'Hôpital's rule has to be used once:

$$A_n + jB_n = (GM)^{T/N} z^{N-1} \left[\frac{k_1 \sin bT + k_2(z^N - \cos bT)}{\sin \omega_n(T/N)} \right] \times \left[\frac{2z - 2 \cos \omega_n(T/N)}{2Nz^{N-1}(z^N - \cos bT)} \right]_{z = 1 \pm j\omega_n(T/N)} \quad (E-8)$$

$$A_n + jB_n = \frac{(GM)^{T/N}}{N} \left[\frac{k_1 \sin bT + k_2(\cos \omega_n T + j \sin \omega_n T - \cos bT)}{\sin \omega_n(T/N)} \right] \times \left[\frac{\cos \omega_n(T/N) + j \sin \omega_n(T/N) - \cos \omega_n(T/N)}{\cos \omega_n T + j \sin \omega_n T - \cos bT} \right] \quad (E-9)$$

$$= \frac{(GM)^{T/N}}{N} \frac{k_1 \sin bT + k_2 j \sin \omega_n T}{\sin \omega_n(T/N)} \cdot \frac{j \sin \omega_n(T/N)}{j \sin \omega_n(T/N)} \quad (E-10)$$

$$A_n + jB_n = \frac{(GM)^{T/N}}{N} \left. \frac{z^N e^{sT/N}}{z = 1 \pm j\omega_n(T/N)} \right|_{z = 1 \pm j\omega_n(T/N)} (k_1 + jk_2) \quad (E-11)$$

CONTINUOUS CASE

As in Section V, let $N \rightarrow \infty$ and obtain

$$A_n + jB_n = \frac{1}{T} GM \left|_{s = j\omega_n} (k_1 + jk_2) \right. \quad (E-12)$$

APPENDIX F

NON-SYNCHRONOUS SAMPLING

Non-synchronous sampling is a basic tool that can be used to model distributed computation architecture, data skewness in the A/D and D/A conversion processes as well as the internal computational delay of the digital computer. By definition, non-synchronous sampling occurs when all the systems' sampling operations are repeated at the same rate but occur at different instants of time. This is depicted in Fig. F-1.

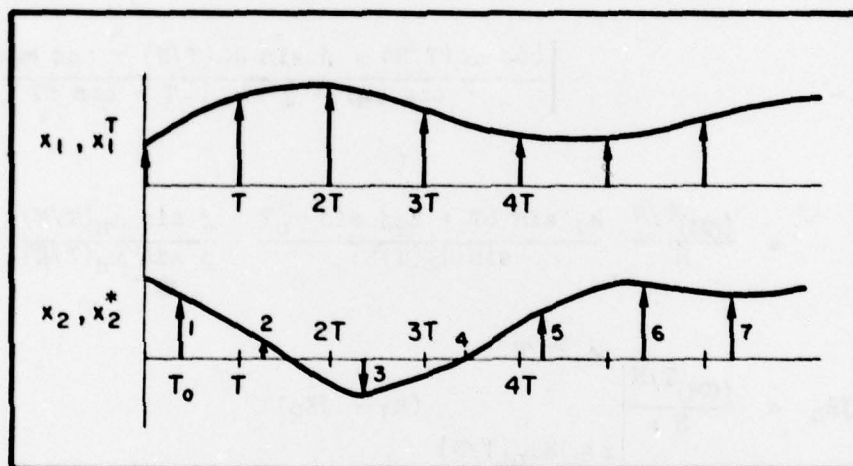


Figure F-1. A Set of Non-Synchronously Sampled Signals

In Fig. F-1 both continuous signals, x_1 and x_2 , are sampled at $1/T$ samples/second, but the x_2 sampler is "out of sync" with the x_1 sampler by T_0 seconds. The sampling operation for x_1^T is depicted symbolically in Fig. F-2a and for x_2^* in Fig. F-2b (* notation on x_2 indicates that an "unconventional" sampling operation is being carried out).

In Fig. F-2b we indicate that the non-synchronous sampler can be modeled by a synchronous sampler if we precede the sampler with the operation W_* followed by the operator W . That is,

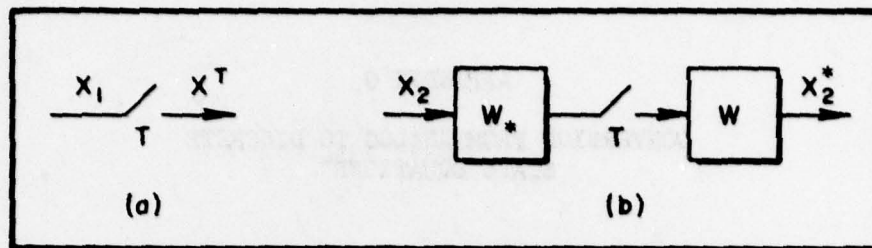


Figure F-2. Sampling Notation

$$x_2^* = W(W_*x_2)^T \quad (F-1)$$

where

$$W = e^{-sT_0} \quad , \quad W_* = e^{sT_0} \quad (F-2)$$

If we proceed according to Eq. F-2, one advances x_2 by T_0 seconds, samples at the $1/T$ rate, and then delays $(W_*x_2)^T$ by T_0 seconds to obtain the desired time sequence. This is demonstrated in Fig. F-3. Note that the non-synchronous sampling operation on x_2 can be modeled in terms of a scalar factor; thus the dimension of the equivalent single-rate sampled signal, $(W_*x_2)^T$, is not increased.

This model readily extends to the case where x is a vector.

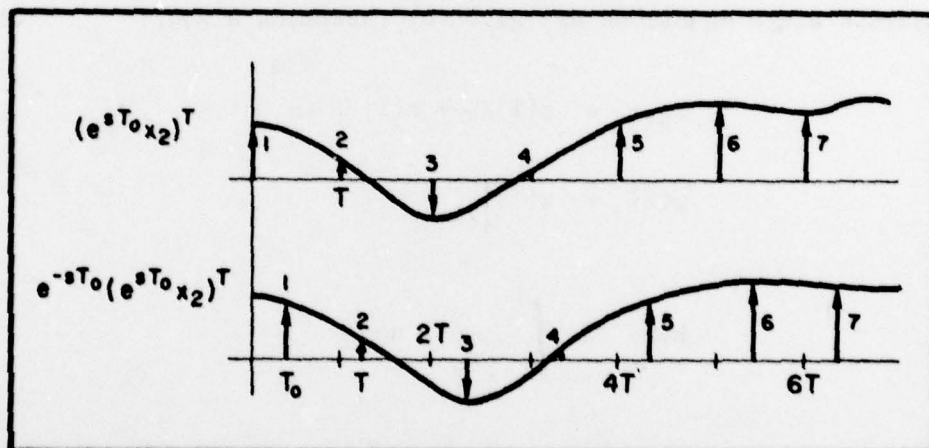


Figure F-3. Advance, Sample, Delay

APPENDIX G **CONVERSION FROM ANALOG TO DISCRETE** **STATE EQUATIONS***

The development of Eq. 193 in Section III is outlined using a combined frequency and time domain approach (page 648, Ref. 20; page 154, Ref. 21). This method assumes that the discrete input to the continuous element is reconstructed using a zero-order hold (ZOH).

Consider the simplified aircraft model of Eq. G-1:

$$\begin{bmatrix} \dot{q} \\ \dot{\alpha} \end{bmatrix} = \begin{bmatrix} -1 & -37 \\ 1 & -3 \end{bmatrix} \begin{bmatrix} q \\ \alpha \end{bmatrix} + \begin{bmatrix} -50 \\ 0 \end{bmatrix} \delta_e + \begin{bmatrix} -37 \\ -3 \end{bmatrix} a_g \quad (G-1)$$

The continuous state equations exist in the form:

$$\dot{x} = Ax(t) + Bu(t) \quad (G-2)$$

$$y = C^T x(t) + Du(t) \quad (G-3)$$

The discrete state equations are given by (assuming a ZOH):

$$X_{k+1} = \varphi(T)X_k + h(T)U(k) \quad (G-4)$$

$$\varphi(T) = \varphi(t) \Big|_{t=T} \quad (G-5)$$

$$h(T) = \int_0^T \varphi(\alpha)B \, d\alpha \quad (G-6)$$

*This appendix was prepared by Capt. Dennis G. J. Didaleusky.

The continuous state transition matrix, $\varphi(t)$, is an $n \times n$ matrix describing the fundamental characteristics of the continuous aircraft model (Eq. G-1) and is not influenced by the inputs to the system. The state transition matrix is obtained via the s -domain by

$$\begin{aligned}\varphi(t) &= \mathcal{L}^{-1}\{[sI - A]^{-1}\} \\ &= \mathcal{L}^{-1}\left\{\frac{\text{adj}(sI - A)}{\det(sI - A)}\right\}\end{aligned}\quad (\text{G-7})$$

For Eq. G-1,

$$\varphi(t) = \mathcal{L}^{-1}\left\{\frac{\begin{bmatrix} s+3 & -37 \\ 1 & s+1 \end{bmatrix}}{(s+2)^2 + (6)^2}\right\}\quad (\text{G-8})$$

Rearranging produces

$$\varphi(t) = \mathcal{L}^{-1}\left\{\frac{\begin{bmatrix} (s+3) + (1/6)(6) & -(37/6)(6) \\ (1/6)(6) & (s+2) - (1/6)(6) \end{bmatrix}}{(s+2)^2 + (6)^2}\right\}\quad (\text{G-9})$$

Equation G-9 is now in a form that enables us to use Table 1 in Section II directly. Taking the inverse Laplace transform of Eq. G-9 produces:

$$\varphi(t) = \left[\begin{array}{c|c} e^{-2t} \cos 6t + (1/6)e^{-2t} \sin 6t & -(37/6)e^{-2t} \sin 6t \\ \hline (1/6)e^{-2t} \sin 6t & e^{-2t} \cos 6t - (1/6)e^{-2t} \sin 6t \end{array} \right]\quad (\text{G-10})$$

For a sampling period of $T = 0.1$, the transition matrix becomes

$$\varphi(T)\Big|_{T=0.1} = \left[\begin{array}{c|c} 0.752776010 & -2.850789305 \\ \hline 0.077048360 & 0.598679290 \end{array} \right]\quad (\text{G-11})$$

$$\varphi(t)B = \left[\begin{array}{c|c} -50e^{-2t} \cos 6t - (50/6)e^{-2t} \sin 6t & -37e^{-2t} \cos 6t + (74/6)e^{-2t} \sin 6t \\ \hline -(50/6)e^{-2t} \sin 6t & -(34/6)e^{-2t} \sin 6t - 3e^{-2t} \cos 6t \end{array} \right] \quad (G-12)$$

Integrating produces ($T = 0.1$):

$$h(T) = \left[\begin{array}{c|c} -4.490576594 & -2.850789304 \\ \hline -0.212719538 & -0.401320710 \end{array} \right] \quad (G-13)$$

$\varphi(t)$ and $h(T)$ can be obtained alternatively by making numerical evaluations of the Taylor series expansions for e^{AT} and for $\int_0^T e^{A(T-\alpha)} B d\alpha$. The discrete state equations can now be directly written using Eqs. G-4, G-11, and G-13.

$$\begin{aligned} \begin{bmatrix} X_{1k+1} \\ X_{2k+1} \end{bmatrix} &= \begin{bmatrix} 0.752776010 & -2.850789305 \\ 0.077048360 & 0.598679290 \end{bmatrix} \begin{bmatrix} X_{1k} \\ X_{2k} \end{bmatrix} \\ &+ \begin{bmatrix} -4.490576594 & -2.850789304 \\ -0.212719538 & -0.401320710 \end{bmatrix} \begin{bmatrix} s_{ek} \\ a_{gk} \end{bmatrix} \end{aligned} \quad (G-14)$$

Taking the z-transform of this first-order set of difference equations gives:

$$\begin{aligned} \begin{bmatrix} z - .752776009 & 2.850789304 \\ \hline -0.07704836 & z - .59867929 \end{bmatrix} \begin{bmatrix} x_1(z) \\ x_2(z) \end{bmatrix} \\ = \begin{bmatrix} -4.490576597 & -2.850789304 \\ \hline -0.212719539 & -0.401320710 \end{bmatrix} \begin{bmatrix} s_e \\ a_g \end{bmatrix} \end{aligned} \quad (G-15)$$

Notice that Eq. G-15 reproduces Eq. 193 in Section III.

APPENDIX H

A PARTICULAR DESIGN PROCEDURE

Several closed-loop designs were presented in the text without detailed comment on the manner in which the compensation networks were synthesized. For the most part, a pole assignment technique was adequate to meet the design requirements posed in these simple illustrative examples. The use of the pole assignment procedure will be outlined using the "motivating" example of Section IV-G.

From Fig. 36, we may write the output equation as

$$C = (GM)[I + G_1^T G_2^T (GM)^T]^{-1} G_1^T R^T \quad (H-1)$$

One design objective was to force a closed-loop response, at the sampling instant, dictated by

$$\det[I + G_1^T G_2^T (GM)^T] \propto z + a \quad (H-2)$$

where a is determined by the s -plane pole at $s = -0.5$.

The second requirement, a unity steady-state response to a step input, was forced by applying the final value theorem to Eq. H-1. These two conditions are sufficient to determine the free parameters of G_1 and G_2 .

APPENDIX I

THE LIMITING FORM FOR A PARTICULAR EXAMPLE

The steps in obtaining the limiting form given in Eq. 309 are contained in this appendix. Specifically, we show

$$\frac{1}{N} \left[\frac{(1 - e^{-sT})a}{s(s+a)} \right]^{T/N} \Big|_{z = 1 \angle \omega_n(T/N)} \Big|_{N \rightarrow \infty} = \frac{1 - e^{-sT}}{sT} \frac{a}{s+a} \Big|_{s=j\omega_n} \quad (I-1)$$

For the example we wish to evaluate

$$\frac{(GM)^{T/N}}{N} = \frac{1}{N} \left[\frac{(1 - e^{-sT})a}{s(s+a)} \right]^{T/N} = \frac{1}{N} \frac{1 - e^{-aT/N}}{z - e^{-aT/N}} \frac{1 - z^{-N}}{1 - z^{-1}} \quad (I-2)$$

at $z = 1 \angle \omega_n(T/N) = \cos \omega_n(T/N) + j \sin \omega_n(T/N) = e^{j\omega_n(T/N)}$.

$$\frac{(GM)^{T/N}}{N} = \frac{(1 - e^{-aT/N})(1 - e^{-j\omega_n T})}{N[e^{j\omega_n(T/N)} - e^{-aT/N}][1 - e^{-j\omega_n(T/N)}]} \quad (I-3)$$

For the sake of brevity, let $1/N = u$, so that $u \rightarrow 0$ as $N \rightarrow \infty$, and consider

$$F = \frac{N}{D} = \frac{u(1 - e^{-aTu})}{[e^{j\omega_n Tu} - e^{-aTu}][1 - e^{-j\omega_n Tu}]} \quad (I-4)$$

Here F represents the part of $(GM/N)^{T/N}$ which is "troublesome" as $u \rightarrow 0$. Clearly, F becomes indeterminate as $u \rightarrow 0$; therefore, use L'Hôpital's rule (for the first time):

$$\frac{dN/du}{dD/du} = \frac{(1 - e^{-aTu}) + aTe^{-aTu}}{(j\omega_n T) e^{j\omega_n Tu} + aTe^{-aTu} - T(j\omega_n + a)e^{-Tu(j\omega_n + a)}} \quad (I-5)$$

As $u \rightarrow 0$, the form remains indeterminate; therefore, use L'Hôpital's rule for the second time:

$$\begin{aligned} \frac{d^2N/du^2}{d^2D/du^2} &= \frac{aTe^{-aTu} + aTe^{-aTu} + u[-(aT)^2 e^{-aTu}]}{(j\omega_n T)^2 e^{j\omega_n Tu} - (aT)^2 e^{-aTu} + T^2(j\omega_n + a)^2 e^{-Tu(j\omega_n + a)}} \Big|_{u=0} \\ &= \frac{2aT}{(j\omega_n T)^2 - (aT)^2 + T^2(j\omega_n + a)^2} \end{aligned} \quad (I-6)$$

$$\begin{aligned} &= \frac{2aT}{T^2[(j\omega_n)^2 - a^2 + (j\omega_n)^2 + 2aj\omega_n + a^2]} \\ &= \frac{2aT}{2T^2 j\omega_n [j\omega_n + a]} = \frac{a}{j\omega_n T [j\omega_n + a]} \end{aligned} \quad (I-7)$$

Finally, reintroduce the $(1 - e^{-j\omega_n T})$ term to obtain

$$\frac{1 - e^{-j\omega_n T}}{j\omega_n T} \frac{a}{j\omega_n + a} \equiv \frac{1 - e^{-sT}}{sT} \frac{a}{s + a} \Big|_{s=j\omega_n} \quad (I-8)$$

This verifies, after setting $a \equiv 1$, Eq. 309 of Section V.